Iron Limitation in *Mycobacterium tuberculosis*: Studies on Iron-Regulated Envelope Proteins & Catalase-Peroxidases

A Thesis
Submitted to the University of Hyderabad for the Degree of

Doctor of Philosophy

in the

Department of Animal Sciences
School of Life Sciences
University of Hyderabad
Hyderabad - 500 046
India

By

CHAITANYA VEENA YERUVA

March 2009

DEPARTMENT OF ANIMAL SCIENCES
SCHOOL OF LIFE SCIENCES
UNIVERSITY OF HYDERABAD
HYDERABAD 500 046

CERTIFICATE

This is to certify that I, Ms Chaitanya Veena Yeruva have carried out the research embodied in the present thesis for the full period prescribed under Ph.D ordinances of the University.

I declare to the best of my knowledge that no part of this thesis was earlier submitted for the award of research degree of any University.

(Signature of the candidate)
Name:
Enrollment No:

Signature of the Supervisor

Head
Department of Animal Sciences

Dean
School of Life Sciences

Acknowledgements

I express my deepest sense of gratitude towards my supervisor Prof. Manjula Sritharan, for her guidance, constant encouragement, inspiring suggestions and critical discussions throughout my doctoral studies. Throughout my thesis-writing period, she provided encouragement, sound advice, good teaching, and lots of good ideas. I also thank her for her patience and kindness. Her dedication to work and perfectionism will have a far-reaching impact on my life, academic and beyond.

I am extremely thankful to Prof. S. Dayananda, Head, Department of Animal Sciences and Prof. Aparna Dutta-Gupta, former Head, Department of Animal Sciences for their help and for providing necessary facilities for the research work.

I express my sincere thanks to Prof. M. Ramanadham, Dean, School of Life Sciences and Prof. A. S. Raghavendra, former Dean, School of Life Sciences, for extending facilities available in the School for my research work.

I would like to thank my doctoral committee members, Prof. S. Dayananda and Prof. Appa Rao Podile for their valuable suggestions and guidance throughout my doctoral studies.

I am grateful to all the faculty members of the School for their help and co-operation.

My special thanks to Dr. V. Lakshmi, NIMS for allowing me to work in her lab. I extend my thanks to Dr. S.J. Patil, Sateesh, all other the faculty members and technical staff for helping me in the collection of human clinical isolates and sera.

I would like to thank Dr. Sesikeran, Dr. Madhavan, Nair NIN and his student Vasupradha for allowing and helping me to do ligand –binding studies.

My special thanks to Dr. Niyaz Ahmed for helping me in analyzing phylogeny of HupB protein.

I thank Dr. Sritharan for constant support and suggestions through out my work.

My heartfelt thanks to my colleagues, Dr. Sundaram, Dr. Swapna, Dr. Sridevi, Dr. Sridhar, Dr. Priya, Suneel, Pandey, Raman, Subha and Poornima for their cooperation and courtesy extended during my research work and for creating cheerful work atmosphere. I wish them all success and happiness in their lives.

I would also like to thank Chandram and Srinu for their assistance in the lab.

I am thankful to my friends and all the research scholars in the School for their timely help and co-operation during my stay in the University.

I wish to thank my childhood friends, UG friends from TJPS college Guntur and especially all my MSc friends from Sourastra University, Gujarat for all the support, entertainment they provided.

I wish to thank the non-teaching staff of Dept of Animal Sciences, Mr. Ankineedu, Mr. Jagan, Mr. Gopi, Mrs. Jyothi, Mr. Narasimha and Mr. Babu Rao and CIL staff for their support and assistance.

I am grateful to AP-NL, ILS, UPE and ICMR for providing me financial support through out my work.

I thank AP-NL, DBT, CSIR, ICMR, UGC and DST providing financial support to the lab. .

The DST - FIST funding to the Department of Animal Sciences and the UGC - SAP to School of Life Sciences are gratefully acknowledged.

I am thankful to PURSE grant for providing financial support to attend ASM conference at Massachusetts, USA.

I thank my aunts, uncles, sisters and brothers Nargarjuna and Venkat for their blessings, affection and for providing me loving environment.

There are no words to describe my thanks to my brother Mr. Y.S.C. Kesav Reddy for his immense support and caring attitude. I thank my sisiter-in law Lakshmi and sweet little Mahith for their love.

I express my gratitude to my in-laws Sambi Reddy and Suguna, my sister-in-law Sridevi and brother-in-law Kiran and co-sister Rohini for their blessings.

I thank sweet little Teja and Yaash for their love and for providing me loving environment.

I wish to thank my husband S. Srinivasa Reddy for his love, support, humor, and liveliness that has given me strength in life.

My special thanks to my sweetest Son Abhinav for his co-operation, love and affection all the time.

Last, but certainly not least, I wish to express my sincere gratitude and respect to my parents Mr. Rami Reddy and Mrs. Vijaya Lakshmi for their unconditional love, support and eager to know about every advancement in my work.

Finally, I would like to dedicate this work to all my teachers and my family.

CHAITANYA VEENA YERUVA

CONTENTS

CHAPTER 2

Materials and Methods

CHAPTER 3

Results

LIST OF ABBREVIATIONS

Ag	Antigen
ATP	Adenosine triphosphate
ATT	Anti-Tuberculosis-Treatment
BCG	Bacille Calmette Guérin
BLAST	Basic Local Alignment Search Tool
Bp	Base pair
CDS	Coding sequences
CMb	Carboxymycobactin
Fur	Ferric uptake-regulator
IREP	Iron-regulated envelope protein
IRMP	Iron-regulated membrane protein
IdeR	Iron-dependant regulator
kb	kilobase pair
kDa	kilo dalton
kV	kilo Volt
Mb	Mycobactin
MS	Mass spectra
µM	Micromolar
mg	Milligram
mL	Milliliter
mM	Millimolar
NCBI	National Center for Biotechnology Information
O / N	Overnight
O.D	Optical density
ORF	Open reading frame
PBS	Phosphate buffered saline
PCR	Polymerase chain reaction
RT	Room temperature
TBS	Tris buffered saline
TMB-H_2O_2	Tetramethyl benzidine-hydrogen peroxide

Abstract

Mycobacterium tuberculosis is the causative agent of tuberculosis in humans. Despite several advances in the control of the disease, tuberculosis remains a public concern globally. A better understanding of host-pathogen interaction is required for effective control measures including diagnosis and development of new and better vaccines. Iron is one of the contributing factors to the virulence of the pathogen.

Mycobacteria have adapted to iron deprivation by elaboration of two siderophores, the intracellular mycobactin and extra cellular carboxymycobactin / exochelin and their receptors, the iron-regulated envelope proteins (IREPS). IREPS were first demonstrated in *M. smegmatis*, with a 29 kDa protein shown to be the ferric-exochelin receptor. Though iron-regulated proteins were identified in *M. tuberculosis*, no specific envelope proteins were identified upon iron limitation. The genome of *M. tuberculosis* shows the presence of at least four iron regulators, of which IdeR and FurA are experimentally verified. Though studies with *ideR* mutants confirmed the role of the IdeR in iron homeostasis, it appears that it is not the sole regulator and that iron-regulation is more complex than envisaged in mycobacteria. FurA, encoded by *furA*, located immediately upstream of *katG* encoding catalase-peroxidase controls the expression of KatG, though the association with iron levels remains to be ascertained.

The focus of the present study was to understand the effect of iron deprivation in *M. tuberculosis* and covered two major objectives. First, the effect of iron deprivation on the iron acquisition machinery was analysed and second, the influence of iron levels on catalase-peroxidase was studied. Growth of *M. tuberculosis* under low iron conditions showed the coordinate expression of both the siderophores and a 28 kDa cell wall-associated iron-regulated protein (Irep-28). Sequence analysis identified Irep-28 as the DNA-binding HU homologue HupB protein (*hupB* [Rv2986c]). HupB, though it showed similarity with other bacterial histone-binding proteins in the N-terminal region, was unique to mycobacteria in that it possessed a novel C-terminal end. Variations in this region were observed in the protein from different mycobacterial species. The cell surface association of the protein was demonstrated in *M. bovis* BCG by confocal microscopy. The association of HupB with siderophores was studied by ligand-binding studies with ^{59}Fe-labeled siderophores and by spectrofluorimetry. Of importance is the

detection of anti-HupB antibodies in the sera of human patients with tuberculosis, implying the *in vivo* expression of HupB.

Iron levels influenced the activities of catalase and peroxidase; both the enzyme activities were decreased, notably the latter upon iron limitation. A direct correlation of the peroxidase activity and the activation of the pro-drug isoniazid (INH) were demonstrated in the study. The observations were extended to viability testing of high and low iron grown organisms to INH. In correlation with the cell-free system, the low iron organisms survived the effect of the drug while high iron organisms, expressing peroxidase were susceptible to low concentration of the drug. The study was extended to clinical isolates of *M. tuberculosis* that were characterized as INH resistant and compared to drug sensitive organisms. The influence of nutrient alteration on the efficacy of anti-tubercular drugs is discussed.

CHAPTER 1

REVIEW OF LITERATURE

1.1. Introduction

Tuberculosis is a disease of great public concern globally as it is one of the leading causes of death. There are 2-3 million deaths every year and latent tuberculosis persist in over a billion individuals worldwide (WHO report 2009). In addition, the emergence of multi drug-resistant tuberculosis (MDRTB) is of great concern. This can be attributed to the human immunodeficiency virus (HIV) epidemics as well as demographic and socio-economic factors such as poverty and malnutrition, which have served to maintain the reservoir of potential infections (Bloom & Murray, 1992). This alarming rise led the WHO to declare TB **'a global emergency'** in 1993**.**

Robert Koch first identified *Mycobacterium tuberculosis* as the causative organism of tuberculosis in 1882; it was however referred to as Koch's bacillus till Lehmann and Neumann gave the generic name *Mycobacterium* (meaning fungus bacterium) due to the mould-like growth of the bacillus in liquid medium (Lehmann & Neumann, 1896). *Mycobacterium tuberculosis* is thus the etiologic agent of tuberculosis in humans and the closely related *Mycobacterium bovis* causes disease in cattle and livestock. These two species, along with the *M. marinum*, *M. canettii* and *M. africanum* comprise the *M. tuberculosis* complex. Other mycobacterial species, including *M. avium-intracellulare* complex (Girard *et al.,* 2005) *and M. kansasii* (Canueto-Quintero *et al*., 2003) that are not normally the causative organisms in human tuberculosis, have been demonstrated to cause disease in immune-compromised individuals, as seen in HIV-infected people.

1.2 Classification of mycobacteria

Mycobacteria belongs to

Kingdom	Bacteria
Phylum	Actinobacteria
Order	Actinomycetales
Family	Mycobacteriaceae
Genus	*Mycobacterium*

Mycobacteria are classified based on the production of pigments, they can be classified as scotochromogens (produce yellow pigment in the dark) for example *M.*

scrofulaceum, M. gordonae; photochromogens (produce an orange pigment in the light) for example *M. kansasii*, *M. marinum* and achromogens (do not produce any pigment) for example *M. avium*, *M. intracellularae* and *M. ulcerans*. The cultivable members of the genus can be divided into two main groups on the basis of growth rate, they can be grouped into fast growers, which include *M. fortuitum*, *M. kansasii, M. smegmatis* and slow growers, comprising mostly the pathogenic mycobacteria, including *M. tuberculosis, M. bovis and M. leprae.*

1.3. Features of mycobacteria

Bacteria of the genus *Mycobacterium* are aerobic, non-motile and non-sporulated rods. Their genome show high G + C content (61-71%) and their cell wall shows unique features with notably high lipid content. *Mycobacterium* and other closely related genera (i.e. *Corynebacterium*, *Nocardia* and *Rhodococcus*) have similar cell wall compounds and structure, and hence show some phenotypic resemblance (Gordon, 1966). Unique property of mycobacteria is the presence of lipid-rich cell wall. It can be stained with basic dyes such as carbol fuchsin and cannot be decolourised with acid-alcohol. This unique property is termed "acid-fastness" and is the basis of the Ziehl-Neelsen staining technique for the identification of mycobacteria.

The lipid rich cell envelope of mycobacteria is composed of three major constituents, the plasma membrane, the cell-wall core, and the extractable non-covalently linked glycans, lipids and proteins. The structure of the cell envelope is illustrated in Fig. 1.1 (Kaiser, 2008). External to the membrane is peptidoglycan in covalent attachment to arabinogalactan, which in turn is attached to the mycolic acids with their long mero-mycolate and shorter alkyl-chains. This portion is termed the cell-wall core, the mycolyl arabinogalactan-peptidoglycan complex (MAPc). The mycolic acids unique to mycobacteria are long-chain fatty acids that are covalently bound to the arabinogalactan-peptidoglycan co-polymer; they are implicated in the formation of the inner layer of an asymmetric outer membrane while other lipids constitute the outer leaflet (Brennan & Crick, 2007, Brennan & Nikaido, 1995) (Fig. 1.1). The mycolic acids extend perpendicular to the arabinogalactan / peptidoglycan while other cell wall-associated glycolipids intercalate into the mycolic acid layer to form a 'pseudo' lipid bilayer. The

free lipids comprise the extractable material, which include the phthiocerol-containing lipids, the phosphatidylinositol mannosides, lipomannan, lipoarabinomannan, trehalose dimycolate (cord factor), trehalose monomycolate, and the diacyl- and polyacyl-trehaloses presumably intercalating with the alkyl-branches and mero-mycolate chains of the mycolic acids (Russell, 2007). When the cell wall is subjected to treatment with various solvents, the free lipids and proteins are solubilised and the MAPc remains as an insoluble residue. Hence it was considered that these lipids, proteins, and lipoglycans are the signaling effector molecules in the disease process, whereas the insoluble core is essential for the viability of the cell (Deres *et al*., 1989).

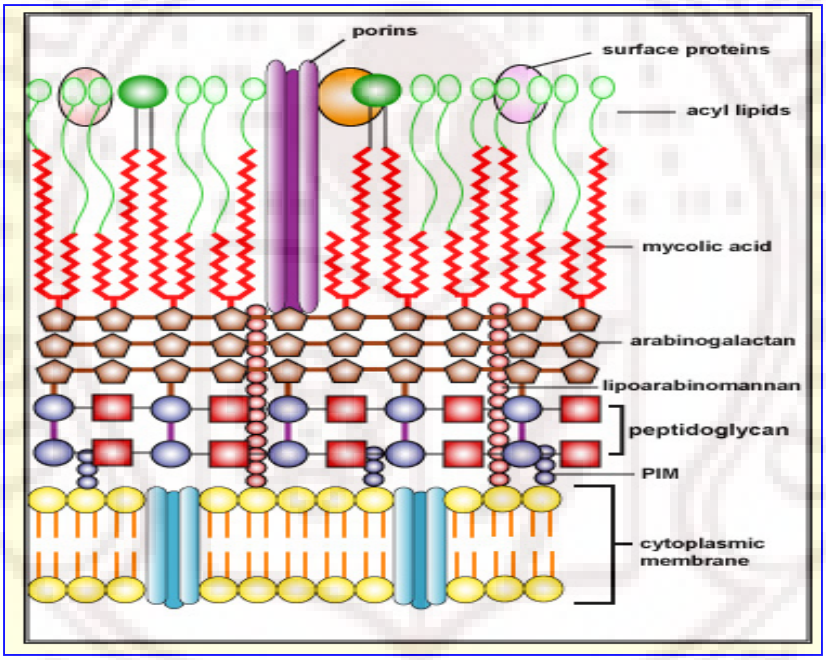

(Kaiser, 2008)

Fig 1.1. Schematic representation of the cell envelope of *Mycobacterium tuberculosis.* Peptidoglycan, arabinogalactan and mycolic acids are covalently linked together and form 60% of cell wall

1.4. Epidemiology of tuberculosis

Globally, there were an estimated 9.27 million cases of tuberculosis in the year 2007. This is an increase from 9.24 million cases in 2006, 8.3 million cases in 2000 and 6.6 million cases in 1990 (WHO report, 2009). Fig. 1.2 illustrates the estimated tuberculosis incidence rate worldwide. It has been estimated that one-third of the world's

population is infected with *M. tuberculosis* and roughly 10% of these individuals will develop active tuberculosis within their lifetime. With the rise in HIV infections, tuberculosis has been on the rise and death due to tuberculosis in HIV-infected people is two-fold higher in individuals with only HIV infection.

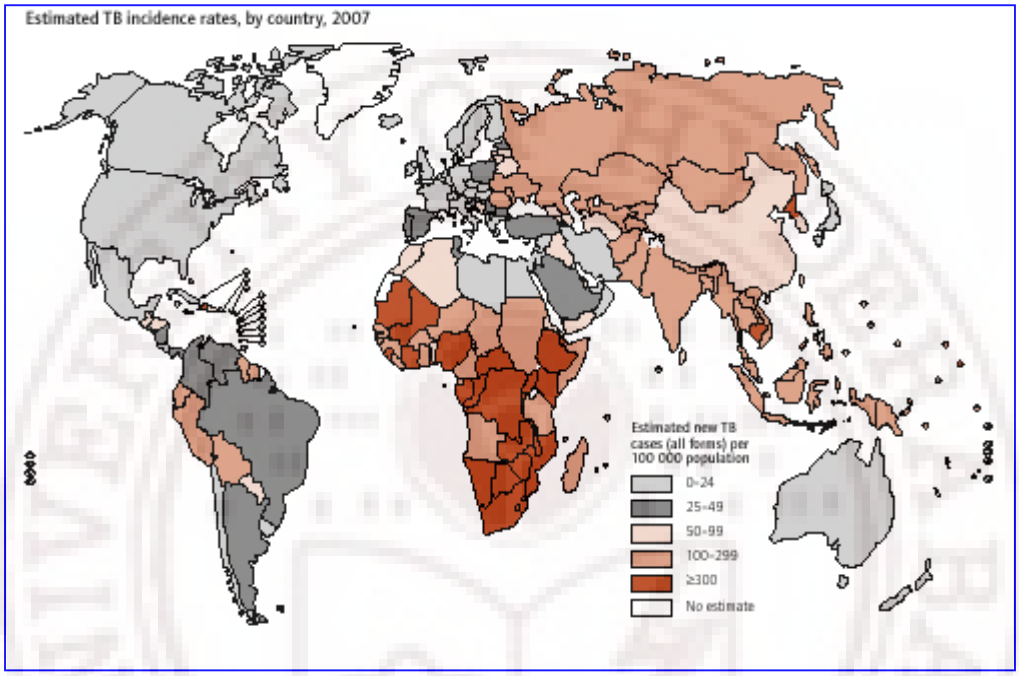

Fig. 1.2. Estimated tuberculosis incidence rate (WHO report 2009)

In addition, about one third of human population is estimated to suffer from latent tuberculosis, which can be reactivated even after several decades (Glassroth, 2005). It is estimated that, between 2000 and 2020 nearly one billion new cases will be identified and the active disease will affect 200 million, with about 35 million deaths, if control measures are not significantly improved (WHO report, 2009). India is classified along with the sub-Saharan African countries with high burden tuberculosis. It ranks first in the five most tuberculosis prevalent countries from the estimated numbers of cases in the year 2007. India accounts for one-third of the global TB burden, with 1.8 million developing the disease each year and nearly 0.4 million dying due to TB annually (Chouhan, 2003).

Tuberculosis is not only a disease of humans, but also has a devastating effect on cattle and livestock. Bovine tuberculosis caused by *M. bovis* is a significant public health

problem and it causes great economic losses in countries with infected livestock. Despite the control measures, the incidence of bovine tuberculosis in some countries for example in New Zealand, United Kingdom and Republic of Ireland has remained the same or increased due to the presence of endemic wildlife reservoirs (Olsen & Anderson, 2003). Also, bovine tuberculosis remains a significant problem in developing countries; indeed more than 94% of the world population live in countries in which the control of bovine tuberculosis is either limited or completely absent (Vordermeier *et al*., 2006).

1.5. Pathogenesis of pulmonary tuberculosis

The development of pulmonary tuberculosis from its onset on its various clinical manifestations can be viewed as a series of battles between the host and the invading pathogen. The mode of infection of *M. tuberculosis* involves a sequence of events (Fig. 1.3). It begins with the inhalation of tubercle bacilli as droplets, released into the atmosphere from an infected individual / animal. Alveolar resident macrophages are the primary cells involved in the initial uptake of *M. tuberculosis*. Dendritic cells and monocyte-derived macrophages also take part in the phagocytic process (Henderson *et al*., 1997). The bacilli are taken up by receptor-mediated phagocytosis using a variety of macrophage receptors including CR3, CR4 and mannose receptors. The inhaled bacilli may multiply or it may be estimated by alveolar macrophages before any lesion is produced.

In lungs, the infected macrophages induce a localized proinflammatory response that leads to the recruitment of mononuclear cells from neighbouring blood vessels. These cells are the building blocks for the granuloma, or tubercle, which is the signature of tuberculosis. Small caceous lesions may progress or may heal or stabilize before they are detectable by radiograph. The granuloma consists of a kernel of infected macrophages, surrounded by foamy macrophages and other mononuclear phagocytes, with a mantle of lymphocytes in association with a fibrous cuff of collagen and other extracellular matrix components that delineates the periphery of the structure (Russell, 2007) (Fig. 1.3). Larger caceous lesions may grow locally and shed bacilli into the blood and lymph. The outcome of an infection in the new host depends on the balance between

(i) host immune response and effective killing of the invading pathogen (ii) the extent of tissue necrosis, fibrosis, and regeneration (Van Crevel *et al*., 2002).

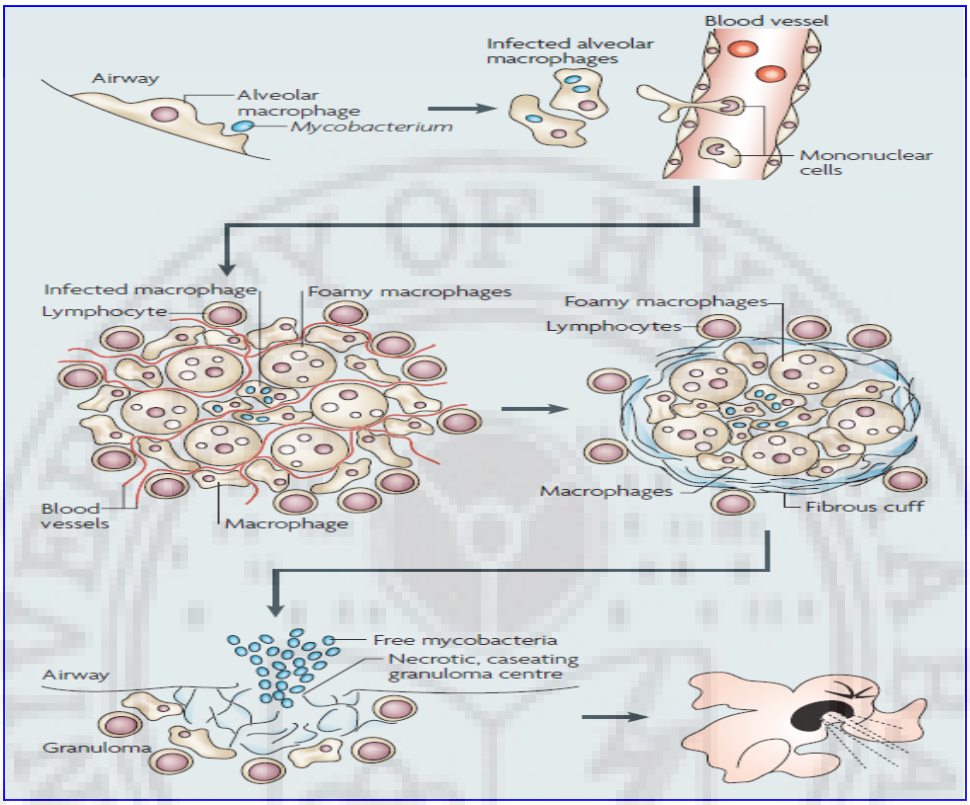

(Russell, 2007)

Fig. 1.3. Infection with *Mycobacterium tuberculosis* follows a relatively well-defined sequence of events.

The host-pathogen interactions are dominated by the ability of the pathogen to prevent phago-lysosome biogenesis (Vergne *et al*., 2004), by modulating the phagosomal compartment and preventing its fusion with acidic lysosomal compartments and actively excluding vesicular proton ATP-ases, resulting in an elevated pH of 6.3–6.5 (compared to the normal lysosomal pH of 4.5). The granuloma formation typifies the 'containment' phase of the infection in which there are no overt signs of disease and the host does not transmit the infection to others. Containment usually fails when the immune status of the host changes, which could be associated with essentially any condition that reduces the number, or impairs the function, of $CD4^+$ T cells as seen in old age, malnutrition or co-infection with HIV. Following such a change in the immune status, the granuloma caseates (decays into a structure-less mass of cellular debris), ruptures and spread within

the lungs (active pulmonary TB) and even to other tissues via the lymphatic system and the blood (miliary or extrapulmonary TB), which leads to the development of the disease and requires antibiotic therapy for survival (Dannenberg, 1994).

The uncontrolled growth of *M. tuberculosis* inside the human host leads to infection. Human tuberculosis is divided in to pulmonary and extra pulmonary tuberculosis based on the site of infection. Pulmonary tuberculosis is caused by infection of lungs and may also spread to other organs. The symptoms include cough, breathlessness, fatigue, fever and unintentional weight loss. Extra pulmonary tuberculosis is a disseminated infection occurs after the primary infection due to the immune status and nutritional deficiency of the individual. The granuloma caceates, ruptures and bacilli infects different parts of the body like lymphatic system through blood stream causing military tuberculosis and to the brain causing tubercular meningitis.

1.6. Control measures

Control measures for tuberculosis include timely diagnosis, chemotherapy and preventive measures by vaccination.

1.6.1. Diagnosis

Existing diagnostic methods can detect up to 60% of tuberculosis cases but tuberculosis management is difficult as the existing diagnostic methods are time consuming. Clinical examination by radiological testing, chest X-ray, AFB, tuberculin skin test (Mantoux test) and biopsies are routinely done in several labs globally. AFB testing of sputum samples taken on three consecutive days are taken as confirmatory evidence. Culture confirmation is the "gold standard" for tuberculosis diagnosis as it is specific and sensitive. However, it is time-consuming and can take even 4-6 weeks as *M. tuberculosis* has a long generation time. Today, culture confirmation by radiometric BACTEC system MB / Bact Alert system take only a week and are superior to the conventional culture methods; however the cost and the lack of economic viability does not allow its use in all hospitals in developing countries.

Other diagnostic methods are being developed that offer the hope of fast and more accurate testing. These include PCR amplification of the insertion element IS*6110*, and QuantiFERON TB Gold and T SPOT-TB assays based on cell-mediated immune

response monitored by measurement of the stimulation indices and / or production of IFN-γ in response to mycobacterial proteins such as ESAT-6. These tests are more expensive and not affected by immunization or environmental mycobacteria, inturn generate fewer false positive results. The development of a specific, sensitive, rapid and inexpensive diagnostic test would be particularly valuable in the developing world.

1.6.2. Chemotherapy

Tuberculosis can be cured by chemotherapy in 95% of patients with active, drug sensitive pulmonary TB (Spigelman & Gillepsie, 2006). It involves multi-drug therapy with a combination of three frontline drugs, isoniazid, rifampicin and pyrazinamide and one or more of the second-tier antibiotics including streptomycin, aminoglycosides kanamycin and amikacin, the polypeptide capreomycin, PAS, cycloserine, the thioamides ethionamide and prothionamide and several fluoroquinolones such as moxifloxacin, levofloxacin and gatifloxacin. The treatment strategy for the complete elimination of active and dormant bacilli involves two phases; in the initial intensive phase, three or more drugs (isoniazid, rifampicin, pyrazinamide and streptomycin) are used for two months, and allow a rapid killing of actively dividing bacteria and the continuation phase, in which fewer drugs (usually isoniazid and rifampicin) are used for 4 to 7 months, aimed at killing any residual bacilli to prevent, not only the recurrence of the disease bot also prevent the development of drug resistant organisms.

1.6.2.1. Mode of action of Front line drugs

(a) Isoniazid

INH or isonicotinic acid hydrazide, was synthesized in the early 1900s but its anti-tubercular action was first detected in 1952 (Middlebrook, 1952; Bernstein *et al.,* 1952). Both *M. tuberculosis* and *M. bovis* are susceptible to isoniazid in the range of 0.02 / 0.05 µg / mL (Heifets, 1994; Youatt, 1969). Isoniazid is bactericidal anti-tubercular drug and the most commonly prescribed for active infection and prophylaxis. INH enters the pathogen as a pro-drug and is activated by the catalase-peroxidase expressed by the pathogen. The peroxidase activity of the enzyme is necessary to activate INH to the active drug in the bacterial cell (Zhang *et al*., 1992) that blocks mycolic acid

biosynthesis, thereby disrupting the cell wall synthesis (discussed in detail in section 1.13.2).

(b) Rifampicin

Rifampicin, one of the front line drugs obtained from culture filtrates of *Streptomyces mediterranei,* was introduced in 1972 as an anti-tubercular drug (Woodley *et al.,* 1972). Rifampicin is extremely effective against *M. tuberculosis,* (MIC 0.1-0.2 pg / mL) and its rapid bactericidal activity (Mitchison, 1985; Heifets, 1994) in combination with the other front line drugs helped to shorten the course of treatment against drug-susceptible infections. Rifampicin binds to the β-subunit of DNA-dependent RNA polymerase and blocks transcription, thereby killing the organism.

(C) Pyrazinamide

Pyrazinamide, a nicotinamide analog, was first discovered to have anti-tubercular activity in 1952 (Kushner *et al*., 1952). The MIC for pyrazinamide varies from 8 to 60 pg / mL depending on the assay method and media, and the drug is most active against cultures of *M. tuberculosis* at pH values below 6. It targets an enzyme involved in fatty-acid synthesis and is responsible for killing persistent tubercle bacilli in the initial intensive phase of chemotherapy (Somoskovi *et al*., 2001). However, during the first two days of treatment, it has no bactericidal activity against rapidly growing bacilli (Zhang & Mitchison, 2003). Pyrazinamide is a pro-drug, which is converted to its active form, pyrazinoic acid by the pyrazinamidase elaborated by the pathogen. The activity of PZA is highly specific for *M. tuberculosis,* as it has no effect on other mycobacteria.

(d) Ethambutol

Ethambutol is a front line drug used in combination with other drugs and is specific to mycobacteria. It inhibits arabinosyl transferase used for the synthesis of arabinogalactan involved in cell wall biosynthesis (Takayama & Kilburn, 1989). The inhibition of arabinogalactan biosynthesis by ethambutol could account for the accumulation of mycolic acids and their trehalose esters and affects the permeability of cell wall.

(e) Streptomycin

Streptomycin, an aminocyclitol glycoside, is an alternative first line anti-tubercular drug recommended by the WHO (Cooksey *et al.,* 1996). It interacts with the 16S rRNA and S12 ribosomal protein (Escalante *et al*., 1998 & Finken *et al*., 1993), resulting in the misreading of the mRNA and inhibition of protein synthesis.

Due to the emergence of drug resistant organisms attributed mainly due to the inconsistency in the administration of the drugs, WHO initiated "directly observed therapy short-course" (DOTS). This is currently being adopted in 119 countries including all 22 high burden countries that contain 80% of all estimated cases (Collins & Kaufmann, 2001). India has the second largest DOTS programme in the world in population coverage. However, India's DOTS programme is the fastest expanding programme, and the largest in the world in terms of patients initiated on treatment, placing more than 100,000 patients on treatment every month and about 70%case detection is achieved (RNTCP report, 2009).

Subsequently, DOTS-Plus program included second tier anti-tubercular drugs in the treatment strategy (WHO report, 2006). The recent aim of the Stop TB Partnership's Global Plan to Stop TB program (WHO report, 2009) includes six major components, pursue high-quality DOTS expansion and enhancement; address TB / HIV, MDR-TB and the needs of poor and vulnerable populations; contribute to health system strengthening based on primary health care; engage all care providers; empower people with TB and communities through partnership; and enable and promote research.

1.6.3. Vaccines: BCG as a vaccine

Mycobacterium bovis BCG derived, as an attenuated organism from the virulent *M. bovis* is the only vaccine available for tuberculosis. The efficacy of this vaccine is controversial as there are varied reports on the protection afforded by BCG. It is given to infants soon after birth in countries where tuberculosis is endemic. The efficacy of BCG vaccination in preventing adult pulmonary tuberculosis was found to be low, as concluded from the extensive 10-year follow-up trial in Chingleput (Tamil Nadu, India).

In the developed countries like USA and UK, mass immunization with BCG is not implemented, as it is believed to interfere with the interpretation of the tuberculin test.

1.7. Advances in mycobacterial research: Development of genetic tools to manipulate mycobacteria and Whole genome sequencing

Until recently, the progress in mycobacterial metabolism was slow as it was difficult to genetically manipulate the bacteria. However, significant advances have been made in the genetic manipulation of mycobacteria. Also, whole genome sequencing of several mycobacterial genomes has been done after the first genome sequencing of the pathogenic *M. tuberculosis* H37Rv (Cole *et al*., 1998). They include the sequencing of *M. bovis* (Garnier *et al*., 2003), *M. bovis* BCG (not published), *M. leprae* (Cole *et al*., 2001), the comparative genomics study, may provide an insight into their virulence.

The genome of *M. tuberculosis* (Fig. 1.4) comprises of 4, 411, 529 bp, contains 3924 genes (Cole *et al.,* 1998). The general classification of *M. tuberculosis* annotated genes is presented in Table 1.1. The *M. tuberculosis* genome has some unusual features like the number of genes involved in fatty acid metabolism and the presence of unrelated PE and PPE families of acidic, glycine rich proteins.

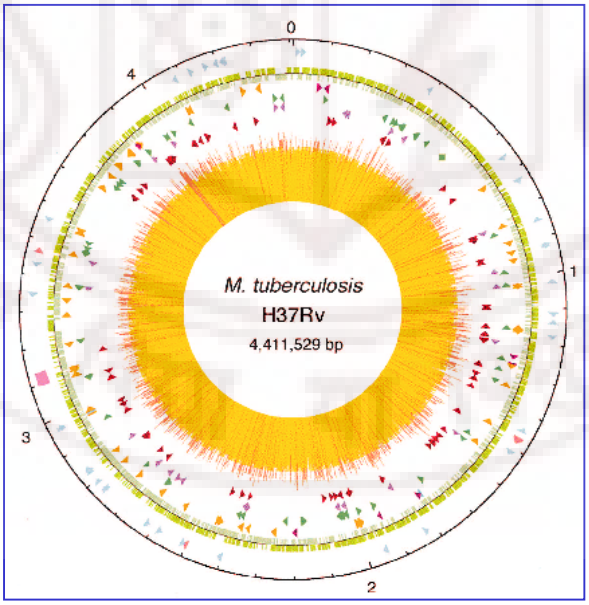

(Cole *et al.,* 1998)

Fig. 1.4. Circular map of the chromosome of *M. tuberculosis* H37Rv. The outer circle shows the scale in mega bases, with 0 representing the origin of replication. The first ring from the exterior denotes the positions of stable RNA genes (tRNAs are blue, and others

are pink) and the direct-repeat region (pink cube); the second ring shows the coding sequence by strand (clockwise, dark green; anticlockwise, light green); the third ring depicts repetitive DNA (insertion sequences, orange; 13E12 REP family, dark pink; prophage, blue); the fourth ring shows the positions of the PPE family members (green); the fifth ring shows the positions of the PE family members (purple, excluding PGRS); and the sixth ring shows the positions of the PGRS sequences (dark red). The histogram (center) represents the G+C content, with <65% G+C in yellow and >65% G+C in red.

Table 1.1. General classification of annotated *M. tuberculosis* genes

Function	No. of genes annotated	% of total genes	% of total coding capacity
Lipid metabolism	225	5.7	9.3
PE & PPE proteins	167	4.2	7.1
Cell wall & cell process	517	13	15.5
Information pathways	877	22	24.6
Regulatory proteins	188	4.7	4.0
Virulence, detoxification and adaptation	91	2.3	2.4
IS elements and bacteriophages	137	3.4	2.5
Conserved hypothetical function	911	22.9	18.4
Unknown function	607	15.3	9.9
Stable RNAs	50	1.3	0.2

Comparative sequence analysis of orthologous genes (genes that perform the same function) from different bacteria is the basis of evolutionary relatedness. However, species' phylogenies based on the comparison of single genes are often inconsistent. This is due to the high rate of horizontal gene transfer in bacteria (Sassetti & Rubin, 2002). Comparative genomics presents an attractive tool for evolutionary analysis of strain relatedness, as whole genomes can be examined rather than just individual genes (Gordon *et al.,* 1999).

1.8. Comparative genomics of the *M. tuberculosis* complex

The *M. tuberculosis* complex contains 5 pathogenic species that share identical 16S rRNA sequences and over 99.9% nucleotide identity (Sreevatsan *et al.,* 1997; Garnier *et al.,* 2003). They include *M. tuberculosi*s, *M. africanu*m, *M. microti,M. canetti* and *M. bovi*s. The members of *M. tuberculosis* complex differ in terms of their host range, phenotype and virulence for humans (Brosch *et al.,* 2000a).

Comparative genomics has identified at least 18 variable regions ranging from 0.3 kb to 12.7 kb, which are present in *M. tuberculosis* and not in BCG (Fig. 1.5). RD1 is the only region that is absent from all BCG strains but present in virulent *M. bovis* and *M. tuberculosis* strains (Brosch *et al.,* 2000; Gordon *et al.,* 1999; Mahairas *et al.,* 1996). RD2, another variable region (Rv1978- Rv1988c) is a recent deletion restricted to BCG strains derived since 1927, and includes genes coding for a variety of functions including methyl transferases, permeases, ribonucleotide reductase, a regulatory protein and a secreted protein, namely MPT64. The RD3 locus is a prophage (phiRv1) and RD4 encodes enzymes involved in the biosynthesis of lipopolysaccharides and both are absent from *M. bovis* and *M. bovis* BCG strains. RD5 contains eight ORFs, three of them encode phospholipase C enzymes (*plc*A, *plc*B, *plc*C), and the remaining five encode proteins, belonging to the Esat-6 and PPE families respectively (Gordon *et al.,* 1999). The RD6 region varies with the *M. tuberculosis* complex members and essentially consists of PPE proteins and IS1532. The RD7 region contains one of the 4 *mce* operons that encode invasin-like proteins required for *M. tuberculosis* (Arruda *et al.,* 1993). The effect of the loss of *mce3* on virulence is not known, but it was suggested that the remaining three *mce* operons could balance for any lost activity (Gordon *et al.,* 1999). The RD8 region contains genes belonging to the ESAT-6 family, PE and PPE families and an *ephA* gene that encodes epoxide hydrolase (Brosch *et al.,* 2000; Gordon *et al.,* 1999). The RD9 contains genes encoding for an export protein, oxidoreductase, and a pre-corrin methyltransferase that is involved in cobalamin biosynthesis (Gordon *et al.,* 1999).

The RD10 encompasses the genes encoding for an enoyl CoA hydratase and an aldehyde dehydrogenase. RD 11, 12 and 13 were absent in both *M. bovis* and *M. bovis* BCG, while the RD 14, 15 and 16 were restricted to few members of BCG (Brosch *et al.,* 2002). These regions can be accessed for the potential to differentiate between *M.*

tuberculosis and *M. bovis / M. bovis* BCG. Though the role of these deletions in strain differentiation is unclear, they can be applied to propose a new evolutionary scenario for the members of the *M. tuberculosis* complex (Brosch *et al.*, 2002). The authors analysed the distribution of the 20 variable regions in a total of 100 strains belonging to *M. tuberculosis*, *M. africanum*, *M. canetti*, *M. microti*, *M. bovis* and *M. bovis* BCG. Their study showed that *M. bovis* had undergone several deletions compared to *M. tuberculosis* (Fig. 1.5) (Brosch *et al.*, 2001). The characteristic deletions among the BCG strains are represented on Table 1. 2.

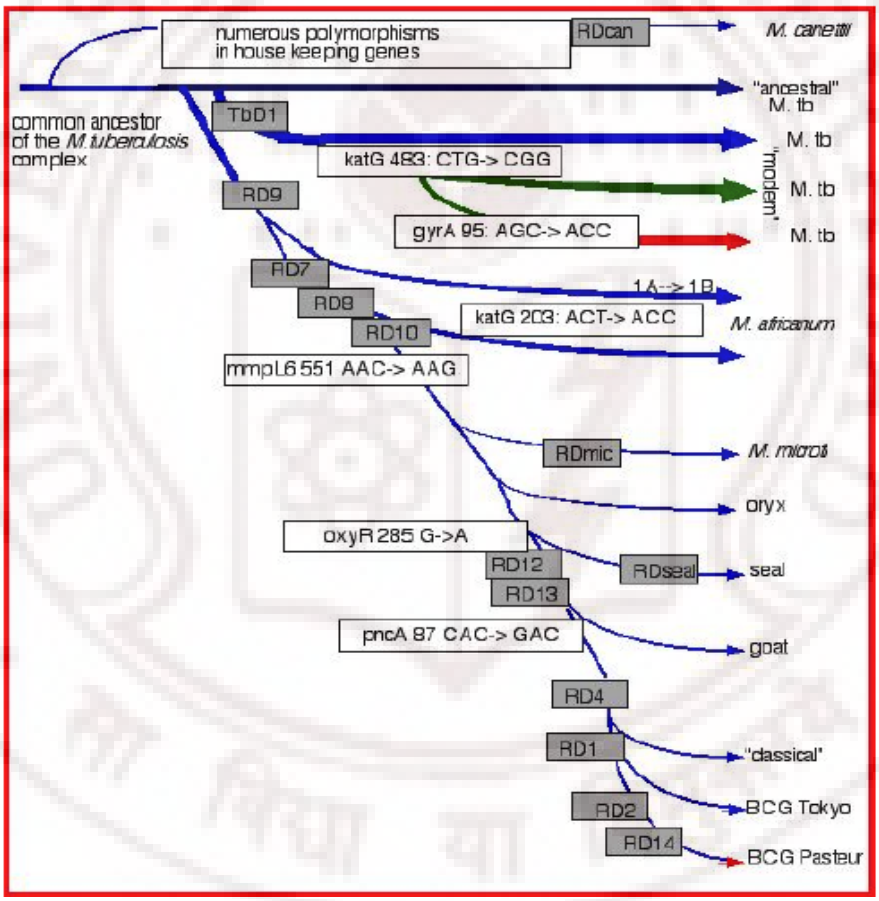

(Brosch *et al.*, 2002)

Fig. 1.5. Scheme of the proposed evolutionary pathway of the *M. tuberculosis:* illustrating successive loss of DNA in certain lineages.

Table 1.2. Characteristics of deletions from BCG (Mostowy *et al.*, 2003)

BCG strain	Deleted regions
Russia	RD1, RD Russia
Moreau	RD1, RD1
Japan	RD1
Sweden	RD1
Birkhaug	RD1
Prague	RD1, RD2
Glaxo	RD1, RD2, RD Denmark / Glaxo
Denmark	RD1, RD2, RD Denmark/ Glaxo
Tice	RD1, RD2, nRD18
Connaught	RD1, RD2, nRD18, RD8
Frappier	RD1, RD2, nRD18, RD8, RD Frappier
Phipps	RD1, RD2, nRD18
Pasteur	RD1, RD2, nRD18, RD14

1.8.2. Classification of BCG strains

Genetic variations among the BCG strains were due to the changes occurred during the continuous passages of pathogenic strain *M. bovis* (Behr & Small, 1997) and also lack of standardized growth storage procedures that gave rise to several BCG strains, found today in several geographical locations worldwide (Osborn, 1983). Based on the genetic variations among the BCG strains, they are classified into two major groups. BCG Japan, Moreau, Russia, and Sweden secrete large amounts of the MPB70 gene, have two copies of the insertion sequence IS6110, and contain methoxymycolate and MPB64 genes. In contrast, BCG Pasteur, Copenhagen, Glaxo and Tice secrete little MPB70, have a single copy of the insertion sequence IS6110, and do not contain the methoxymycolate and MPB64 genes (Ohara, 2001) (Fig. 1.6).

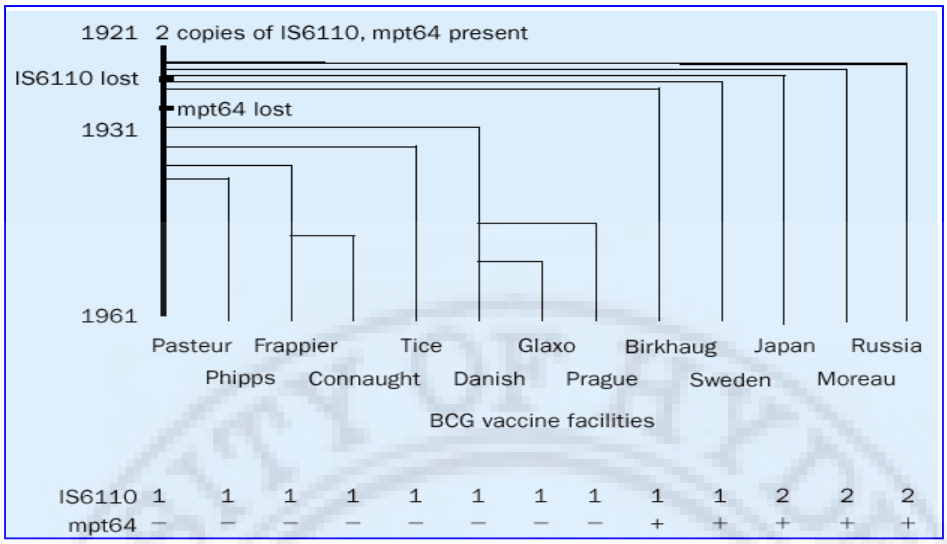

Fig. 1.6. Genealogy of BCG vaccine strains based on historical data (Behr MA, 2002). The results of analysis for the *mpt64* gene and the number of IS6110 copies are shown at the bottom. This analysis could suggest that the original BCG had *mpt64* and 2 copies of IS6110; one copy of IS6110 was lost around 1925, and mpt64 was lost between 1927 and 1931 (Behr, 2002).

1.9. Host-pathogen interactions with specific reference to iron acquisition

Iron is the second most abundant metal after aluminum and the fourth most abundant element in the earth's crust. It is an important micronutrient for all bacteria except lactobacilli, is a co-factor for several enzymes involved in vital cellular functions ranging from respiration to DNA replication (Sritharan, 2000). It exists in the two oxidation states, Fe^{3+} and Fe^{2+}, with the oxidation-reduction potential for the Fe^{2+} / Fe^{3+}couple varying between +300 mV to –500 mV, which enables it to serve as a carrier molecule in the electron transport chain. However, it is insoluble at biological pH and exists as insoluble ferric hydroxides and oxyhydroxides. At physiological pH 7.0, the major form of iron is $Fe(OH)_2^+$ (and not $Fe(OH)_3$ as thought earlier) with a solubility of approximately 1.4 X 10^{-9} M (Chipperfield & Ratledge, 2000) that is too low to support the growth of microorganisms (requiring 10^{-7} M iron).

Nature has perhaps made iron highly insoluble, as excess iron is toxic, due to its catalytic role in the Fenton reaction, resulting in the formation of free radicals (Sritharan, 2000). Pathogenic bacteria face additional iron deprivation as 99.9% iron is held as protein-bound iron within the mammalian host; it is held by transferrin and lactoferrin (extracellular fluids) and by ferritin (storage) (Bullen & Griffiths, 1999). The ability of a

pathogen to acquire iron from the mammalian host determines the outcome of an infection; the balance between the ability of a mammalian host to withhold iron from the invading microorganisms and the ease with which the latter can acquire this iron from the host is critical. Limitation of this essential nutrient is one of the innate immune defense mechanisms of the mammalian host and is refereed to as 'nutritional immunity' by Kochan (1976).

1.9.1. Bacterial adaptations to iron-limitation

Microorganisms, including mycobacteria have adapted to conditions of iron-limitation by the elaboration of novel iron acquisition machineries (Ratledge and Dover 2000; Sritharan, 2000; Ratledge, 1999; De Voss *et al*., 1999). They are well studied in E. coli and several gram-negative organisms. Two common mechanisms of iron acquisition include (a) siderophore-mediated acquisition and (b) direct acquisition via specific receptors from host iron-containing molecules like hemin, transferrin and lactoferrin etc.

a. Siderophore mediated iron acquisition machinery

Siderophores are low molecular weight (500-1000 Da) Fe^{3+}-specific high affinity molecules with binding affinity constant K_s ranging from 10^{22} to 10^{50} and can remove iron from the insoluble $Fe(OH)_3$ and from host-iron binding compounds, but not from heme proteins. As the Fe^{3+}-siderophore complex is greater than 600 Da, uptake of these molecules is a receptor-mediated process. Many of these iron transport receptors are multi-functional and mediate the transport of other molecules that include vitamin B12 and certain colicins. A vast majority of bacteria elaborate this mechanism of iron acquisition and mycobacteria also employ siderophores to acquire iron.

b. Direct acquisition

Bacteria can acquire protein-bound iron by elaborating specific cell surface receptor proteins for transferrin, lactoferrin, heme and haemoglobin (Braun & Killmann, 1999). Lactoferrin and transferrin receptors have been demonstrated in pathogenic *Neisseria* (Genco & Desai, 1996), *Pasteurella* spp. (Gray-Owen & Schryvers, 1996), *Haemophilus influenzae* (Herrington & Sparling, 1985), *Pseudomonas aeruginosa* (Sriyosachati *et al*., 1986), *Bordetella* spp. (Redhead *et al*., 1987), *Helicobacter pylori*

(Husson *et al*., 1993), *Staphylococcus aureus* (Park *et al*., 2005), and *Candida albicans* (Knight *et al*., 2005).

1.9.2. Iron-regulated membrane proteins (IRMPs)

Siderophores and their receptors, the iron-regulated membrane proteins (IRMPs) are extensively studied in *E. coli* (Griffiths & Chart, 1999). Six siderophore-mediated iron-transport systems have been demonstrated; FhuA, FepA and FecA functioning as receptors for ferrichrome, ferric enterobactin and ferric citrate respectively have been crystallized and uptake of Fe^{+3} via these receptors are well studied. Some of the IRMPs demonstrated in other bacterial system are represented in Table 1.3.

Table 1.3. Bacterial siderophores and their receptors, the iron-regulated membrane proteins (IRMPs)

Organism	Siderophore	Iron-regulated membrane proteins	
		Protein	Size (kDa)
Escherichia coli	Ferrichrome	FhuA (Coulton *et al*., 1983)	78
	Enterobactin	FepA (McIntosh & Earhart, 1977)	81
	Ferricitrate	FecA (Wagegg & Braun, 1981)	80.5
	Aerobactin	CirA (Curtis *et al*., 1988)	74
Yersinia enterocolitica	Yersiniabactin	FyuA (Rakin *et al*., 1994)	71.4
Pseudomonas aeruginosa	Pyochelin	Ferri-pyochelin receptor (Sokol & Woods, 1983)	14
	Pyoverdin	Ferri-pyoverdin receptor (Meyer *et al*., 1990)	80
Vibrio cholerae	Vibriobactin	ViuA (Butterton *et al*., 1992)	74
Burkholderia cepacia	Ornibactin	OrbA (Sokol *et al*., 2000)	81
Bordetella spp.	Alcaligin	FauA (Brickman & Armstrong, 1999)	79

1.9.3. Regulation by iron at the molecular level

Intracellular iron regulates the expression of the components of the iron-acquisition machinery, as demonstrated in *E. coli* (Griffiths & Chart, 1999). A 17 kDa regulator molecule Fur (Ferric Uptake Regulator encoded by '*fur*' gene) and the Fur – Fe^{2+} complex binds to a region called the 'Fur' or iron box (consensus sequence 5'-GATAATGATAATCATTATC -3') located upstream of the start point of the genes encoding the iron acquisition machinery (Braun *et al*., 1998). When iron is limiting, the repressor molecule, on its own does not bind to the iron box, thereby resulting in the induction of expression of components of the iron acquisition machinery (Fig. 1.7). The Fur repressor has been identified as a member of Gram-negative bacteria, including *Bordetella spp*., *Haemophillus influenza*, *Legionella*, *Neisseria* spp., *Pseudomonas spp*., *Vibrio spp*., etc. The corresponding homologue of Fur in Gram-positive bacteria is DtxR and was first identified in *C. diphtheriae* (Boyd *et al*., 1990). DtxR is slightly larger than Fur, approximately 25 kDa to 17 kDa and they have very less amino acid homology. DtxR and Fur also differ in the specificities of interaction with different of operators. The DtxR homologue identified in mycobacteria is IdeR and has been demonstrated in *M. smegmatis* and *M. tuberculosis.*

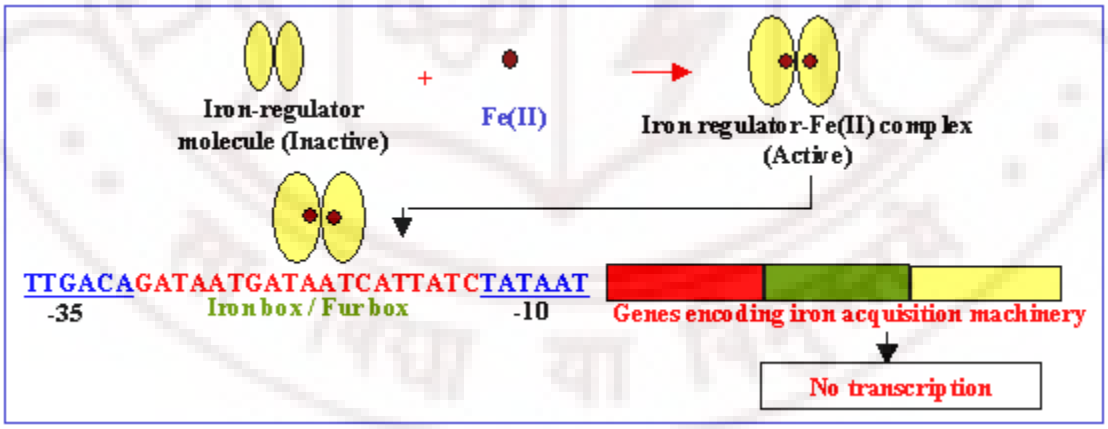

Fig. 1.7. Iron as a regulatory molecule. When iron is plentiful, the inactive repressor binds to the co-repressor Fe^{2+} and the resulting complex binds as a dimer, thereby blocking transcription.

1.9.4. Siderophore-mediated iron acquisition machinery in mycobacteria

Mycobacteria are unique in that they produce two kinds of siderophores, namely the intracellular mycobactins and the extracellular carboxymycobactins / exochelins. Pathogenic mycobacteria express mycobactin and carboxymycobactin while the saprophytic mycobacteria express mycobactin and exochelin predominantly though carboxymycobactin have been identified in small concentrations in *M. smegmatis* (Ratledge & Ewing, 1996). Mycobactin is hydrophobic and is located in the cell wall, while the more polar carboxymycobactin is released into the medium (Ratledge, 1999), Based upon the type of siderophore(s) expressed, mycobacteria can be classified into four groups, namely those

1. expressing mycobactin and carboxymycobactin, eg. *M. tuberculosis.*
2. expressing mycobactin, carboxymycobactin and exochelin, eg. *M. smegmatis*.
3. expressing only the exochelins and no mycobactin, e.g. *M. vaccae*.
4. that do not produce any siderophores and require the addition of exogenous mycobactin for *in vitro* growth e.g. *M. paratuberculosis*.

1.9.4.1. Mycobactins

Mycobactins are intracellular hydrophobic siderophores localized in the lipid-rich cell wall. They have high affinity for Fe^{+3} (Ks of ca. 10^{36}) with low binding to Fe^{+2}. They belong to the mixed ligand type; wherein they have two hydroxamate groups and the third pair being provided by an oxygen atom on the aromatic residue and nitrogen in the oxazoline moiety. Snow (1970) elucidated the structure of mycobactin and performed extensive analyses of mycobactin from different mycobacterial species and showed that they can be used as chemotaxonomic markers. The yield of mycobactin varies among the species, with *M. smegmatis* expressing up to 10% of the cell dry weight while *M. kansasii* produces only about 0.05% of the cell dry weight.

All mycobactins have the same core nucleus that consists of a 2-hydroxyphenyloxazoline moiety linked by an amide bond to an acylated ε-N-hydroxylysine residue (Fig. 1.8). The second ε-N-hydroxylysine is cyclised to form the seven-membered lactam and is attached to β-hydroxyacid via an amide bond. This, in turn is connected to the α-carboxyl of the first lysine residue. Within this core, a methyl

group may or may not be present at the 6th position of phenolic ring and the 5′ position of the oxazoline (Gobin *et al*., 1995). The variation in the structure occurs in the alkyl substituents of the hydroxyacids (R3 and R4) and the acyl moiety R5. In general, the R5 group is a long chain fatty acid that is unsaturated and with an unusual *cis* double bond conjugated to the carbonyl group. Variation in R groups of mycobactins from different mycobacterial species is represented in the Table 1.4.

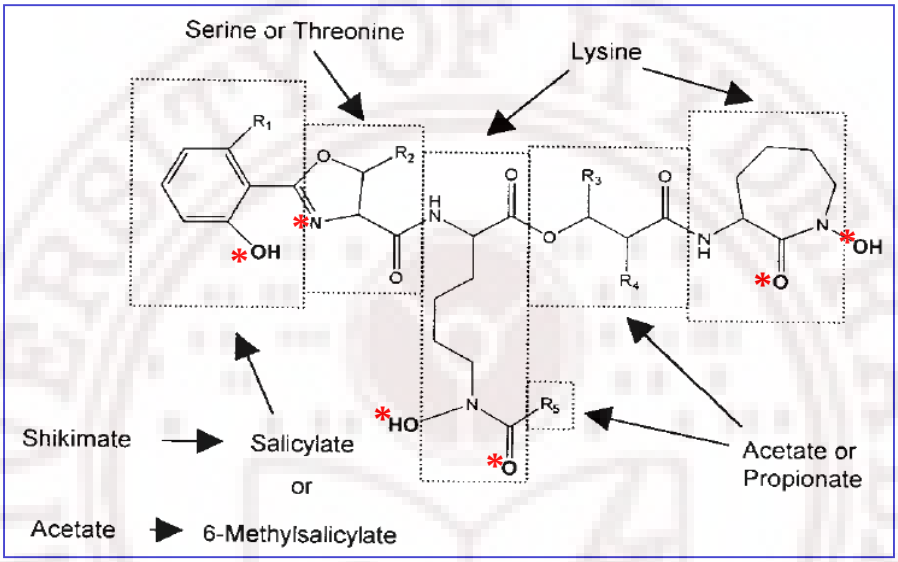

(Devoss *et al*., 1999)

Fig. 1.8. General structure of mycobactins. Three pairs of iron chelating sites are represented in red colour. Variations in the R groups among the mycobacterial species are represented in the table below.

Table 1.4. Variations among the mycobactins produced by different mycobacterial species

Organism	Mycobactin	Substituents				
		R1	R2	R3	R4	R5
M. aurum	A	CH_3	H	CH_3	H	C_{13}
M. fortuitum	F	CH_3 / H	CH_3	CH_3	H	$C_{9\text{-}17}$
M. fortuitum	H	CH_3	CH_3	CH_3	H	$C_{17\text{-}19}$
M. marinum	M	H	CH_3	$C_{15\text{-}18}$	CH_3	C_1
M. marinum	N	H	CH_3	$C_{15\text{-}18}$	CH_3	C_2
M. phlei	P	CH_3	H	CH_2CH_2	CH_3	$C_{15\text{-}19}$
M. smegmatis	S	H	H	CH_3	H	$C_{9\text{-}19}$
M. tuberculosis	T	H	H	CH_3	H	$C_{17\text{-}20}$
M. avium	Av	H	CH_3	CH_3CH_2	CH_3	$C_{11\text{-}14,\ 18}$

1.9.4.2. Carboxymycobactins

The carboxymycobactins are structurally related to mycobactins. The lipophilicity of the mycobactins due to the long chain acyl group at R5 is replaced either by –COOH / -$COOCH_3$ thus rendering it water-soluble. These are produced mainly by the pathogenic mycobacterial species (Gobin *et al.,* 1999), but they also have been detected in small quantities in the non-pathogenic *M. smegmatis* (Ratledge & Ewing, 1996).

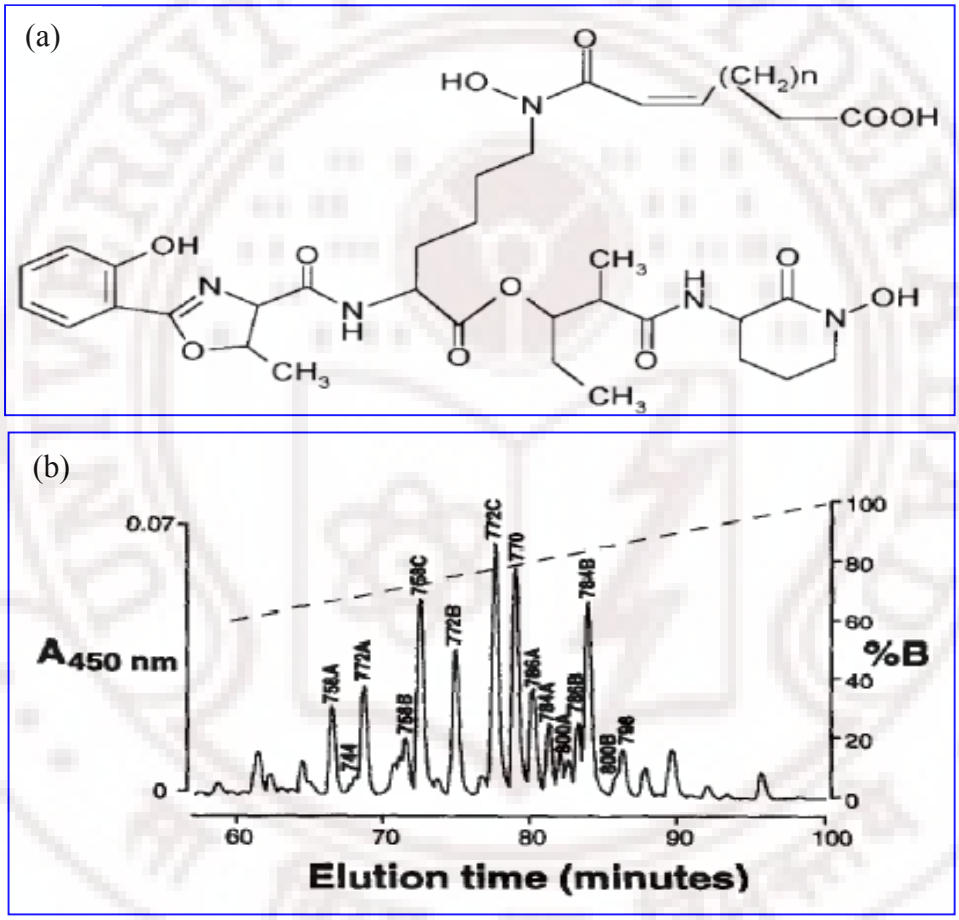

Fig. 1.9. (a). Structure of carboxymycobactin of *M. tuberculosis* (Gobin *et al.,* 1995). (b) HPLC purification of carboxymycobactins from culture supernatant of *M. tuberculosis* (Gobin & Horwitz, 1995).

Their structures have been elucidated in *M. avium* (Lane *et al.,* 1995), *M. tuberculosis* (Gobin *et al.,* 1995; Wong *et al.,* 1996), *M. bovis* and *M. bovis* BCG (Gobin

et al., 1999). They differ from the mycobactin in the side chain at the R positions (R positions as represented in Table 1.4. Mycobactins (Ratledge & Ewing, 1978) and carboxymycobactins (Lane *et al*., 1995) are usually a mixture of closely related molecules that differ in the length of the acyl groups at R5; for example, 17 different mycobactins from *M. smegmatis* was demonstrated by HPLC analysis. They are expressed as a family of related molecules (Fig. 1.9b) and differ marginally from each other, due to varying levels of esterification of the COOH group, as evident by HPLC analysis (Barclay *et al.,* 1986).

1.9.4.3. Exochelins

Exochelins are water-soluble, peptide siderophores produced by non-pathogenic mycobacteria and well characterized in *M. smegmatis* and *M. neoaurum* (Sharman *et al*., 1995a & 1995b). They are small peptides (5-10 a.a) consisting of D-amino acids, predominantly ornithine and do not contain conventional peptide bonds (Ratledge & Dover, 2000).

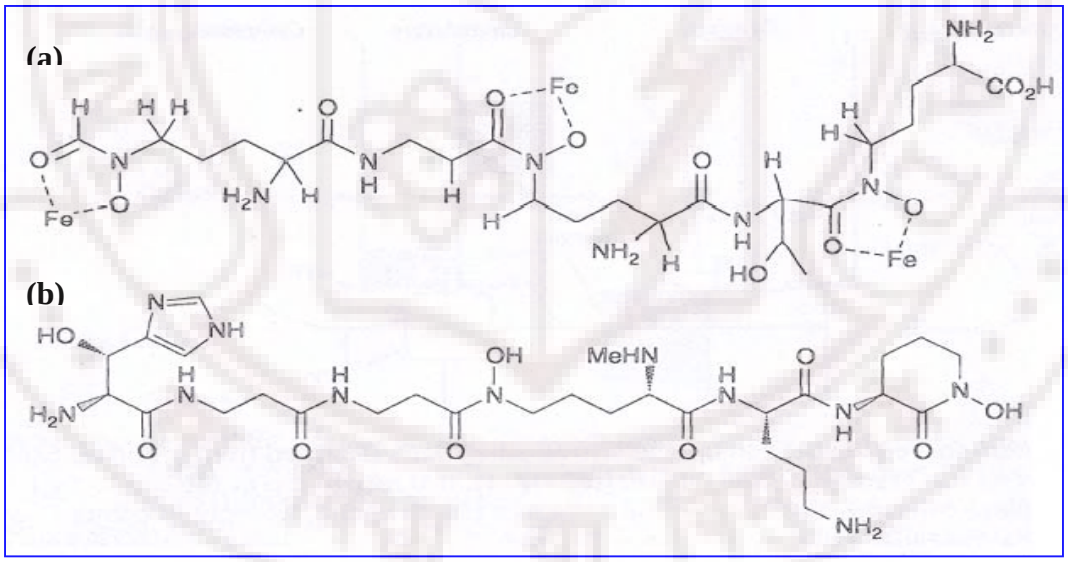

(Sharman *et al*., 1995a & b)

Fig. 1.10. **Structure of exochelins MS and MN.** Exochelin MS (a), from *M. smegmatis* is formyl-D-ornithine 1 β-alanine-D-ornithine 2-D-allo threonine-L-ornithine-3 and exochelin MN (b) from *M. neoaurum* is L-threonine-β-hydroxy histidine-β alanine- β alanine-L-α methyl ornithine-L-ornithine-L-(cyclo)ornithine.

The coordination center with Fe^{3+} is hexa-dendate; it is held in an octahedral structure involving the three-hydroxamic acid groups donated by ornithine. The exochelin MS from *M. smegmatis* is a formylated pentapeptide derived from three molecules of δ-N-hydroxyornithine, β-alanine and threonine (Fig. 1.10a). Exochelin MN from *M. neoaurum* is a hexapeptide with two δ-N-hydroxyhistidines (providing the coordination center for iron chelation), two β-alanine residues and an ornithine (Fig. 1.10 b). Till date, there are no reports on the expression of exochelins by pathogenic bacteria.

1.9.4.4. Biosynthesis of mycobactin / carboxymycobactin

Mycobactins are synthesised by the polyketide synthase / non-ribosomal peptide synthetases (NRPs) strategy. The different enzymes involved in mycobactin and carboxymycobactin synthesis are encoded with the genes in the *mbt* operon in the *M. tuberculosis* genome (Cole *et al*., 1998). The *mbt* operon (Fig. 1.11) includes a cluster of 10 genes (*mbt A-J*) referred to as *mbt*-1 cluster (Quadri *et al*., 1998) involved in the synthesis of mycobactin core and the *mbt*-2 cluster which includes 4 genes *mbt K-N* shown to be Rv1347c, Rv1344, *fadD3*3, and *fadE1*4 respectively (Krithika *et al*., 2006), which is involved in the incorporation of lipophilic aliphatic chain. However most of the aspects of the biosyntheses of mycobactin and carboxymycobactin out lined remain to be experimentally explored and validated.

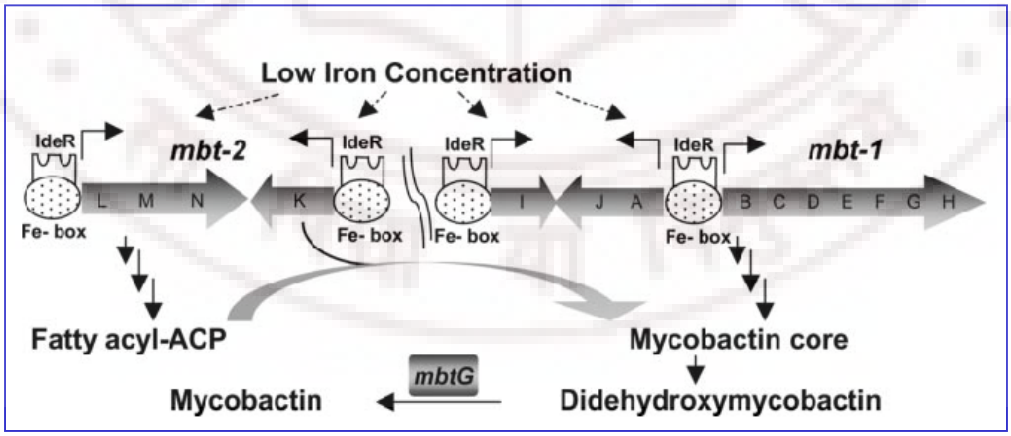

(Krithika *et al*., 2005)

Fig. 1.11. Organisation of *mbt* operon in *M. tuberculosis* H37Rv genome. Contains *mbt*-1 cluster and *mbt-2* cluster involved in the biosynthesis of mycobactin and carboxymycobactin.

The proposed biosynthetic sequence followed the predicted pathway of assembly of mycobactin starting with the synthesis of salicylic acid. The *mbt*-1 cluster includes the genes for the enzymes that synthesize didehydroxymycobactin, the salicyl-capped non-ribosomal peptide-polyketide core scaffold of mycobactin and carboxymycobactin from the building blocks salicylic acid, serine or threonine, lysine, acetyl CoA and malonyl CoA. The salicylate moiety in *M. smegmatis* is synthesised by the shikimate pathway, while the 6-methyl salicylate in *M. tuberculosis*, is a polyketide metabolite synthesized by the condensation of four acetate units by the enzyme isochorismate synthase recently shown to be salicylate synthase (MbtI) (Hudson *et al*., 1970). MtbB, a NRPs is believed to activate serine, condense it with the salicylate moiety, and cyclize this product to a hydroxyphenyloxazoline. There are two other NRPSs, encoded by *mbtE* and *mbtF* that have the appropriate activation, condensation, and peptide carrier domains for donation of the two lysine-derived moieties of MB. Also in the gene cluster are *mbtC* and *mbtD*, which encode proteins that are homologous to polyketide synthases. The encoded proteins appear to contain the appropriate modules to produce the required β-hydroxybutyrate. Additionally, *mbtG* encodes a protein that is homologous to known ornithine and lysine oxygenases, performs the N6-hydroxylation step to generate functionally important hydroxamate moieties. MbtF has a terminal domain that was assigned a role as either an epimerization domain or as a thioesterase responsible for releasing the MB from the enzyme by lactamization of the terminal hydroxy-lysine residue.

Thus, these seven genes, *mbtA* to *mbt*G, appear to encode sufficient activities for the biosynthesis of the core of the MBs (Fig. 1.12). There are two other proposed gene products, MbtH and MbtJ, to which no clear biochemical role has been assigned. The loaded building blocks are bound to their corresponding enzymes by a thioester linkage to the phosphopantetheinyl group, which would be added to the carrier protein domains by PptT (Quadri *et al*., 1998, Chalut *et al*., 2006). MbtK protein of *mbt-2* cluster showed exclusive specificity to acylate at the ε-amino position, and the amino group at α-position was not readily modified. Interestingly, this protein was able to acylate the δ-position of ornithine amino acid and also catalyzed transfer of acyl chains on to two ornithine

residues (Krithika *et al*., 2006, Card *et al*., 2006) to yield mycobactin and carboxymycobactin. The unsaturation of the lipidic chain is produced by acyl-acyl carrier protein (ACP) dehydrogenase (MbtN) (Krithika et al., 2006). MbtG has a five-fold preference for acetylated lysine over lysine (Krithika *et al*., 2006) and didehydroxymycobactin has recently been isolated from *M. tuberculosis* (Moody *et al*., 2006) suggesting that hydroxylation takes place after didehydroxymycobactin assembly and release.

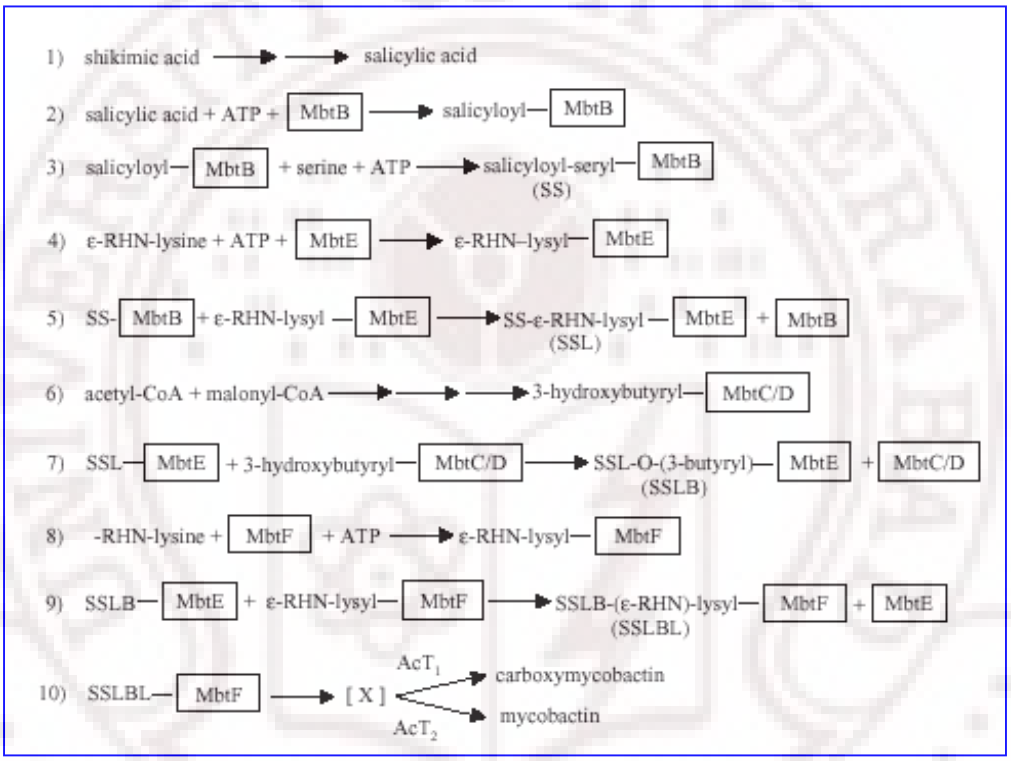

(Ratledge, 2004)

Fig. 1.12. Proposed scheme for mycobactin and carboxymycobactin biosynthesis. Proposed biosynthetic cascade for mycobactin and carboxymycobactin catalyzed by Mbt locus.

De Voss and coworkers (2000) made a knock out mutant of *mbtB* that was unable to produce either mycobactin or carboxymycobactin. Failure to synthesize the siderophores resulted in drastic decrease in growth both under iron deficient medium and in macrophages giving the relevance of both the siderophores involved in the bacterial multiplication in iron limiting conditions and also intracellularly. It is also proposed that the structure of MbtI, a salicylate synthase is used to design the inhibitors of mycobactin

biosynthesis, which may be useful in the production of anti-tuberculosis drugs (Harrison *et al*., 2006).

1.9.4.5. Biosynthesis of Exochelin

The genes involved in the production of exochelin MS were first identified by Fiss *et al*. (1994). An exochelin-deficient strain of *M. smegmatis* was obtained by UV mutagenesis. The gene FxbA, encodes a protein with homology to formyl transferases was obtained by compliment analysis. The complementing fragment contains additional ORFs *fxuA*, *fxuB* and *fxuC* bearing homology to FepG, FepC and FepD of *E. coli* that are ferric-enterobactin permeases; the mycobacterial proteins are presumed to be associated with transport of exochelin. Yu and his group (1998) identified a 30 kb complementing fragment with a total of nine ORFs along with *fxbA.* The locus composed of (i) *orf1* and *orf2*, encoding proteins homology to ABC transporters; (ii) *fxbB* and *fxbC* encoding proteins homology to nonribosomal peptide synthetases; (iii) *fxuD*, encoding a protein homology to periplasmic siderophore receptors, (iv) *orf3,* encodes proteins with an ATP-binding domain and (v) *orf4* and *orf5*, encoding proteins with multiple transmembrane-spanning segments. Presumptively, all the genes would be responsible for the complete assemblage of the exochelin molecule by sequential attachment of ornithine to β-alanine, then to ornithine and on to the attachments of threonine and the final ornithine molecule. Based on the structural information available it was proposed that the exochelin MS was synthesised non-ribosomally via the multiple-carrier thiotemplate mechanism. Zhu *et al.* (1998) also reported the genetic organization of exochelin MS locus of *M. smegmatis* and identified *exiT*, encoding the protein proposed to be involved in secretion of exochelin. In addition *fxbB* and *fxbC* were identified. Much remains to be understood about exochelin biosynthesis.

1.9.4.6. Uptake of ferri siderophore in mycobacteria

A. Uptake of ferri-exochelin

Uptake of ferri-exochelin has been well studied in *M. smegmatis* (Ratledge, 2004). It is thought to be an active transport process, inhibited by energy poisons and uncouplers of oxidative phosphorylation (Macham *et al.,* 1975). Uptake involves the

complete transfer of the molecule along with the metal ligand (Stephenson and Ratledge, 1979). Several proteins are involved in the uptake process that includes a 29 kDa ferri-exochelin receptor (Hall *et al.,* 1987). After recognition by the receptor, the ferri-siderophore complex is taken up by the FxuD protein and then transferred through the cytoplasmic membrane proteins FxuA, FxuB and FxuC (Fig. 1.13), which share amino acid sequence homology with FepG, FepC and FepD, which are involved in the uptake of ferri-enterochelin in *E. coli* (Ratledge, 2004). The release of iron involve reduction of the ferric iron to ferrous iron involving an appropriate reductase (ferri-mycobactin reductase may represent a non-specific NAD(P)H-dependent siderophore reductase). The exochelin, after releasing its iron into the cytoplasm, is transferred back into the extracellular environment of the cells using a specific exiting protein, ExiT (Zhu *et al.,* 1998) operating in conjunction with other proteins and involving the input of energy (Pavelka, 2000).

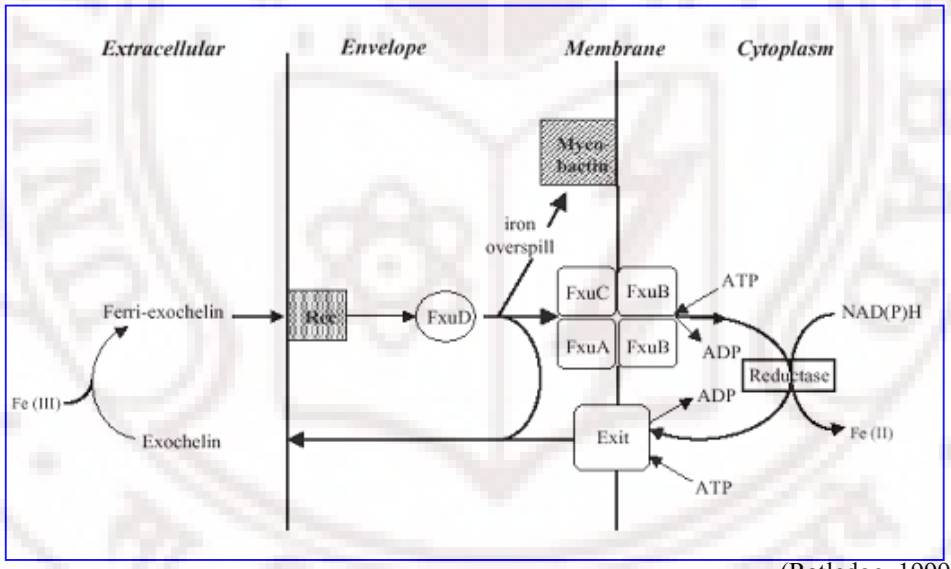

(Ratledge, 1999)

Fig. 1.13. Proposed mechanism for uptake of iron by *M. smegmatis* via ferri-exochelin.

B. Uptake of ferri - carboxymycobactin

The mechanism of uptake of carboxymycobactin is not known completely. It is thought that it might traverse the cell envelope either by diffusion, by virtue of its hydrophobicity (Rodriguez & Smith, 2006), or it is transported via a porin-like molecule (Fig. 1.14). The hypothesis involving porins is supported by the size of the inner diameter

of the porin molecule, which is about 2.2 nm, and the diameter of the carboxymycobactin may be equivalent to the mycobactin *i.e.* 1.1-1.4 nm (Trias & Benz, 1992). Calder and Horwitz, (1998) identified two iron-regulated proteins Irp10 and Mta72 from *M. tuberculosis*, which is hypothesized to be involved in the uptake of ferri-carboxymycobactin across the envelope and directly to a ferri-reductase. These two proteins, by their close homology to metal-transporting P-type ATPases and may function as a two-component metal transport system. Iron would be released from mycobactin by the same reductase. This is contradictory to the previous reports of Stephenson and Ratledge (1980), who showed that it does not require energy.

Recent studies have suggested the involvement of two IdeR - regulated ABC transporter proteins Rv1348 and Rv1349, also known as IrtA and IrtB respectively, in carboxymycobactin mediated iron acquisition (Rodriguez & Smith, 2006).

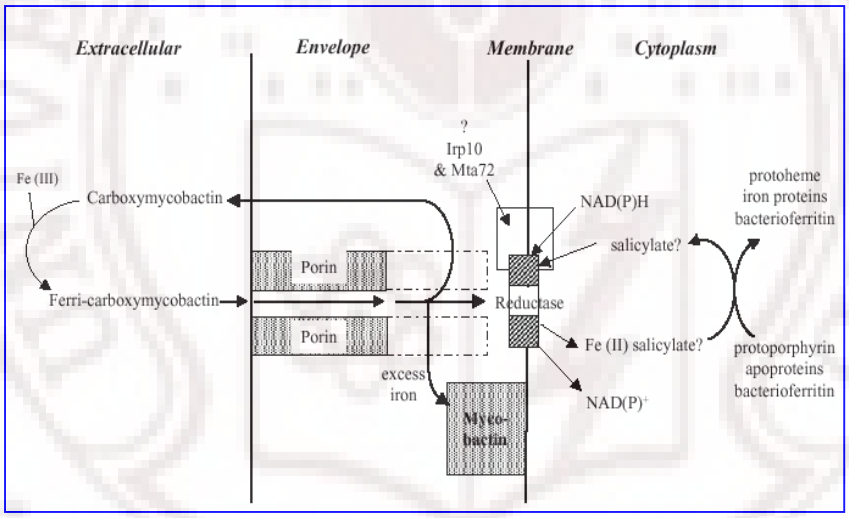

(Ratledge, 2004)

Fig. 1.14. Proposed mechanism for uptake of iron as mediated by carboxymycobactin.

1.9.4.7. Iron-regulated envelope proteins (IREPs) in mycobacteria

Hall *et al*., (1987) first demonstrated the expression of IREPs in *M. smegmatis.* The authors compared the protein profile of cell wall and membrane of *M. smegmatis* grown in the presence of 4 µg Fe / mL (high iron) and 0.02 µg Fe / mL (low iron) and demonstrated several iron regulated envelope proteins. Among them, a 29 kDa IREP was

shown as a potential receptor for the exochelin MS by specifically blocking its uptake using monospecific antibodies against the 29 kDa protein. This was further substantiated by the specificity of this protein as a receptor by Dover & Ratledge (1996). In *M. neoaurum* (Sritharan & Ratledge, 1989), a 21 kDa IREP was shown to be coordinately regulated with the siderophores mycobactin and exochelin MN. IREPs were identified in other mycobacterial species not only under defined lab conditions of established iron status but also under *in vivo* conditions (Sritharan & Ratledge, 1990). IREPs of 180, 29, 21, 14 kDa were identified in *M. avium* isolated from infected C57 black mice, while the 21 kDa IREP was demonstrated in the cell wall fraction of *M. leprae* obtained from infected armadillo liver. It is worth mentioning here that M. leprae was able to acquire iron from ferri-exochelin MN and not from other ferri-siderophores, whether this reflects the presence of the 21 kDa IREP in both the organisms is a possibility. Table 1.5 lists the IREPs identified in mycobacteria.

Studies on the effect of iron limitation in *M. tuberculosis* include the identification of several proteins influenced by iron levels as analysed by two-dimensional gel electrophoresis combined with mass spectrometry (Wong *et al.,* 1999). A putative cation transporting ATPase, a mycobacterial homologue of PEPCK (phosphoenolpyruvate carboxykinase) and an NADP-dependent dehydrogenase were identified in iron-limited organism. On the other hand, FurA (homologous to Fur protein), a homologue of a translational factor EF-Tu and aconitase were synthesized in higher amounts in bacteria grown in iron-rich medium.

The expression of 153 proteins was altered upon transcriptional profiling of *M. tuberculosis* grown under iron-regulated conditions (Rodriguez *et al.,* 2002). About one third of these proteins were IdeR dependant, while iron levels alone regulated the IdeR-independent proteins. Among the proteins identified, two-thirds of these were up regulated by iron limitation, half of which are of unknown function. The other half includes iron acquisition genes such as *mbt-1* cluster, the *mbt-2* cluster and the *irtAB* operon in addition to genes encoding membrane proteins, members of the glycine-rich PE / PPE protein family, putative transporters and several genes encoding proteins involved in basic metabolism (Rodriguez *et al.,* 2002). High iron levels in the culture medium results in induction of genes including *bfrA* and *bfrB,* which encode putative iron-storage

proteins (i.e. bacterioferritin and ferritin, respectively) and *katG*, which encodes a catalase-peroxidase.

Table 1.5. Iron-regulated envelope proteins in mycobacteria grown *in vitro* and *in vivo* (Sritharan, 2000).

Organism	Expression of IREPs of size (kDa) with reference to iron status									
	Low iron							High iron		
	180	84	29	25	21	14	11	250	240	12
Defined iron status (*in vitro*-derived mycobacteria)										
M. smegmatis	+	+	+	+	-	+	-	+	+	-
M. neoaurum	+	-	+	-	+	+	-	+	+	+
ADM 8563	-	-	+	-	-	+	+	?	?	-
M. avium	+	-	+	-	+	+	-	+	+	-
Undefined iron status (in vivo-derived mycobacteria)										
M. avium	+	-	+	-	+	+	-	+	+	-
M. leprae	-	-	+	-	+	+	-	+	+	-
+ and - denote the presence or absence of the protein										
? denotes a very faint band.										

1.10. Iron regulation at molecular level in mycobacteria

Intracellular iron levels operate at molecular level and regulate the expression of the components of iron acquisition machinery. The well-characterized iron regulator in mycobacteria is IdeR (iron dependant regulator) homologous to DtxR of gram-positive bacteria. Iron-regulation is probably more complex in mycobacteria, as additional iron regulators have been identified from whole genome sequencing, namely the FurA and FurB (Fur family) and SirR (DtxR family).

1.10.1. IdeR

IdeR is present in both pathogenic as well as non-pathogenic mycobacteria. It is a 230-amino acid protein sharing 90% homology with DtxR proteins in the first 180 amino acids (Schmitt *et al.,* 1995). It functions as a homodimer and each monomer has three functional domains with two metal-binding sites. In addition to iron, IdeR can also bind

other divalent metal ions such as Mn, Zn, Co, Ni, and Mg (Pohl *et al.*, 1999). From the crystal structure of IdeR (Feese *et al*., 2001), four IdeR monomers form two functional dimers, as observed previously in DtxR (Qiu *et al*., 1995). Metal binding activates the protein's DNA-binding ability by causing a conformational change in the DNA-binding domains. This change is mediated by amino acids at the amino-terminal that also participate in metal binding and therefore link the DNA- and metal-binding domains.

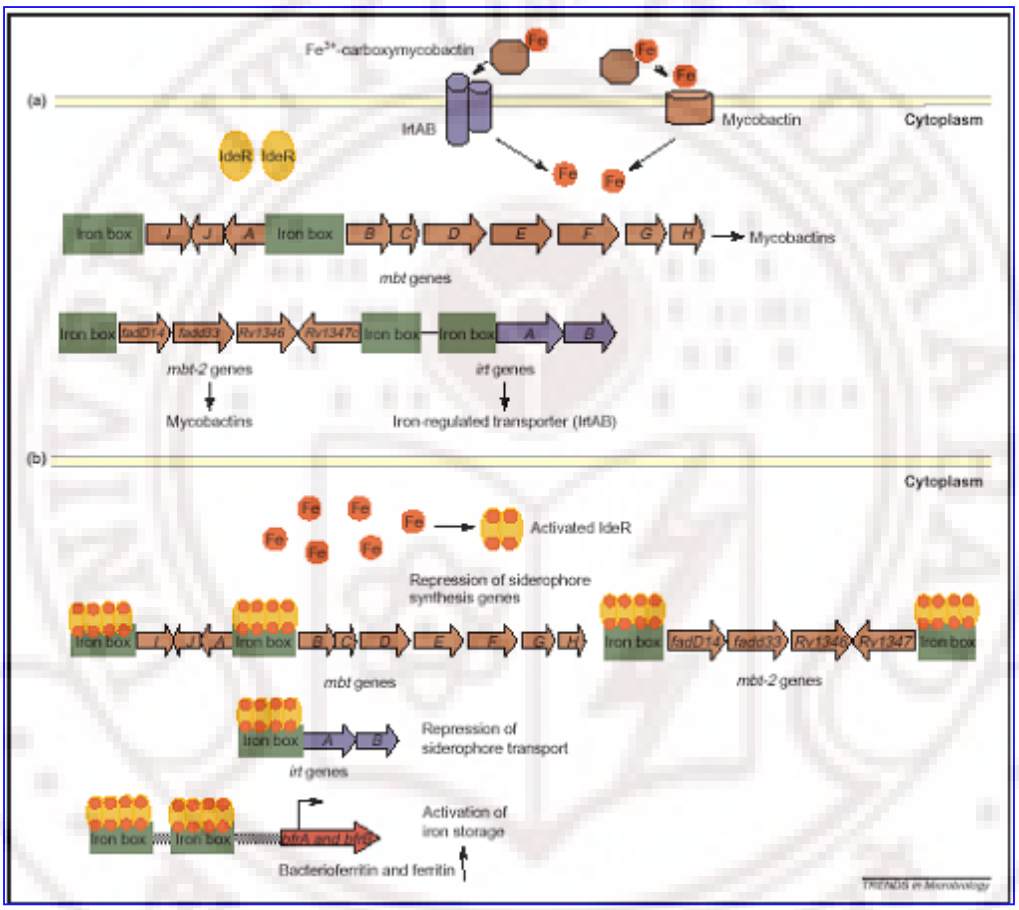

(Rodriguez, 2006)

Fig. 1.15. Regulation of iron metabolism in *Mycobacterium tuberculosis*. (a) Under low iron condition, IdeR present in the cytoplasm lacks iron and is inactive for binding to the promoters of iron-regulated genes. Consequently, genes that are negatively regulated by IdeR like the *mbt* clusters and the *irtAB* operon required for iron uptake are actively transcribed, whereas the iron-storage genes *bfrA* and *bfrB* that are positively regulated by IdeR are not transcribed. (b) When intracellular iron levels increase, IdeR combines with Fe^{2+} and binds to specific sequences (iron boxes) in the promoter region of iron-regulated genes modulating their transcription.

IdeR can be activated *in vitro* by several metals but iron (the natural cofactor) is the optimal metal for IdeR function. In the presence of iron, IdeR binds to a 19 bp (5'-TTAGGTTAGGCTAACCTAA-3') sequence called the IdeR box in the vicinity of promoter region of iron-regulated genes. It is a dual function regulator; under high iron conditions it represses siderophore biosynthesis and induces iron-storage proteins bacterioferritin and ferritin (BfrA and BfrB) (Gold *et al.,* 2001). In the presence of Fe^{2+}, IdeR-Fe^{2+} complex binds to the iron box, upstream of *mbt* genes and *bfrA* and *bfrB* genes but it affects their expression in opposite ways (Fig. 1.15). It represses transcription of the former genes and activates the latter. In low-iron conditions, the IdeR–Fe^{2+} complex is not formed, and IdeR-repressed genes are transcribed while iron storage genes are not expressed (Rodriguez and Smith, 2003). Transcriptional profiling of organisms grown under iron-defined conditions showed that IdeR controls genes encoding putative transporters, transcriptional regulators, proteins involved in general metabolism, members of the PE / PPE family of conserved mycobacterial proteins and the virulence determinant MmpL4 (Camacho *et al*., 1999).

The essential nature of *M. tuberculosis ideR* contrasted with the dispensability of *ideR* reported in *M. smegmatis* (Dussurget *et al*., 1996). In *M. smegmati*s the inactivation of *ideR* resulted in iron-independent production of siderophores (Dussurget *et al*., 1996) and salicylic acid (Adilakshmi *et al*., 2000). A direct role for IdeR as a repressor of siderophore production was supported by the presence of putative IdeR binding sites in the promoter regions of exochelin synthesis and transport genes (Yu *et al*., 1998; Dussurget *et al*., 1999).

In *M. smegmati*s, the ideR mutations resulted in the decreased levels of catalase and the major superoxide dismutase, SodA (Dussurget *et al*., 1996), as IdeR is required for the full expression of *katG* and *sod*A. However, this effect is not direct, as there are no IdeR binding sites in the promoters of these genes (Dussurget *et al*., 1998). Whereas in *M. tuberculosi*s, the inactivation of *ideR* results in increased sensitivity to oxidative stress is not well understood and no difference was found in the expression of genes involved in oxidative stress protection between the *ideR* mutant and the wild-type strains (Rodriguez *et al*., 2002). It is possible that there is an increase in a redox-reactive iron pool in the

ideR mutant, and this, combined with decreased expression of bacterioferritin and ferritin, may result in increased sensitivity to oxidative stress.

1.10.2. FurA (Ferric uptake regulator)

FurA regulates the expression of catalase-peroxidase encoded by KatG (Pym *et al*., 2001). The *furA-katG* is expressed as an operon (Fig. 1.16), with FurA auto-regulating its own expression by binding to a unique sequence upstream of the *furA* gene (Sala *et al*., 2003) called *pfurA* and has been reported in *M. tuberculosis*, *M. smegmatis* and *M. bovis* BCG (Milano *et al*., 2001). *pfurA* is negatively controlled by the mycobacterial FurA protein, which binds upstream of the *furA* gene and in turn auto regulates its own expression.

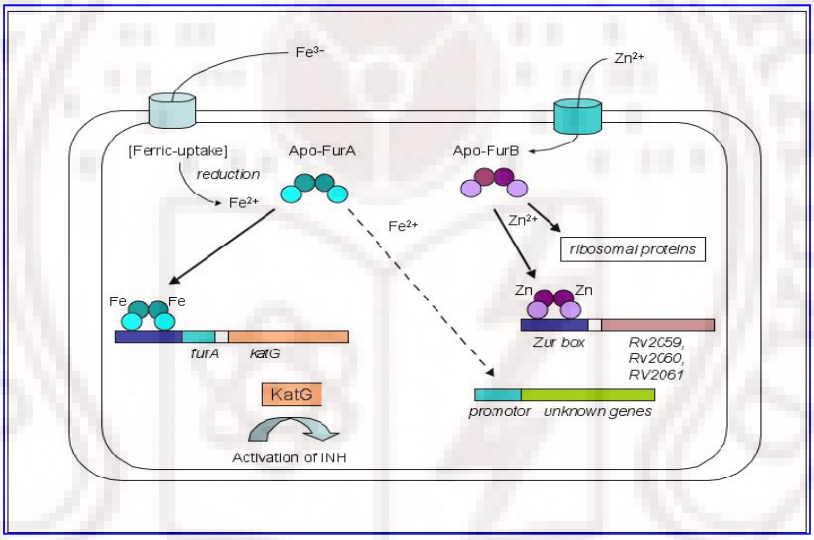

(Lucarelli *et al*., 2008)

Fig. 1.16. Schematic representation of the regulatory functions of *M. tuberculosis* FurA and FurB.

In *M. tuberculosis* (Pym *et a*l., 2001) and *M. smegmatis* (Zahrt *et a*l., 2001), FurA negatively regulates the expression of *kat*G, thereby modulating the response to oxidative stress. This effect, however, is iron-independent in *M. smegmatis* (Pym *et a*l., 2001). It was proved by Pym *et al*. (2001) that FurA is not the principle regulator for siderophore production. Where as FurB acts as a Zinc uptake regulator (Zur) in *M. tuberculosis* and it is co-transcribed with its upstream gene (Rv2358), which encodes another zinc-dependent regulator. SirR present *Staphylococcus epidermidis* is an additional iron-

dependant regulator belonging to the DtxR family. The function of SirR homologue in *M. tuberculosis* is yet to be determined.

1.11. Iron-regulated expression of virulence determinants

The intracellular iron levels regulate not only the iron acquisition machinery but also the expression of virulence factors / toxins in several bacterial systems (Salyers & Whitt, 1994). This was first demonstrated in *C. diphtheriae* in which iron levels control the expression of '*tox*' gene (Boyd *et al*., 1990). When Fe^{2+} binds to DtxR as a co-repressor molecule, the DtxR - Fe binds to the –10 region upstream of transcription start site of the *tox* gene encoding diphtheria toxin, thus blocking its transcription by RNA polymerase. Thus under low iron conditions, the toxin production is increased. Iron regulates the expression of Shiga toxin in *Shigella* spp., exotoxinA in *P. aeruginosa*, haemolytic toxin of *V. cholerae,* vero-cytotoxin of enterohaemorrhagic *E. coli* and α-hemolysin in *E. coli* (Litwin & Calderwood, 1993; Sritharan, 2000). The relationship between iron and bacterial virulence has also been demonstrated in experimental animals using *S. aureus* (Gladstone & Walton, 1970), *V. cholerae* (Ford & Hayhoe, 1976) and *Y. enterocolitica* (Robins-Brown & Prpic, 1985). The virulence of the organisms and their multiplication increased significantly upon injection of exogenous iron into these animals, while reducing the iron availability helped to control the growth of the pathogen and thus the infection.

Pathogenic mycobacteria are facultative intracellular bacteria with the ability to survive and proliferate inside the phagolysosomes of macrophages. One of the bactericidal mechanisms of macrophages is the production of reactive oxidative intermediates (ROI) such as superoxide anion ($O2^{-}$), hydrogen peroxide (H_2O_2), hydroxyl radical (•OH) and singlet oxygen ($^1O2$). These oxygen species are extremely toxic to microorganisms (Edwards *et al*., 2001). Mycobacteria produce enzymes like catalase-peroxidase (KatG), superoxide dismutase (SOD), alkyl hydroperoxidase (AhpC) that provide defence against the ROI.

DeVoss and his coworkers (2000) reported that the deletion of the peptide synthetases gene *mbtB* of the *mbt* cluster of *M. tuberculosis* resulted in a mutant unable to produce either mycobactin or carboxymycobactin. Further the mutant showed a decreaseI n growth both in low iron conditions and inside macrophages. Manabe *et al*. (1999) established the relevance of proper IdeR-dependant regulation for the virulence of *M. tuberculosis*, by the construction of *M. tuberculosis* strain expressing an iron-independent positive dominant corynebacterial *dtxR* and proved that the wild type IdeR controlled events influenced the virulence in a murine model of infection. In *M. smegmatis* Dussurget *et al.* (1996) demonstrated the role of IdeR in oxidative stress response in addition to iron metabolism and showed an increase in sensitivity to hydrogen peroxide in IdeR mutants due to the decreased activity of catalase-peroxidase (KatG) and superoxide dismutase (SodA) activity, implying that IdeR is most likely to play a central role in oxidative stress.

1.12. Mycobacterial catalase-peroxidases

Within the genus *Mycobacterium* three different types of catalase-peroxidases have been identified: they include the T, M and A catalases. The heat-labile, H_2O_2-inducible KatG catalase-peroxidase (T-catalase) is a member of the HPI group of catalases. The heat-stable, non-inducible KatE catalase-peroxidase (M-catalase) belongs to the HPII group. The HPI KatG catalase-peroxidase is resistant to aminotriazole, while the HPII KatE catalase-peroxidase is sensitive. The third type of catalase (A-catalase) was identified and described in strains of *M. avium* and *M. intracellulare*. It is similar to the mycobacterial KatE HPII catalase, but has greater resistance to high temperature, has a different charge, is more hydrophobic, and fails to react with antibody to KatE (Wayne and Diaz, 1988). *M. tuberculosis* expresses only a single catalase, the KatG, heat-labile, H2O2-inducible, HPI type catalase- peroxidase (Wayne & Diaz, 1982). Different types of catalase-peroxidases identified in different mycobacterial species are represented in the Table. 1.6.

Table 1.6. Catalase-peroxidases in different mycobacterial species (Bartos *et al.*, 2004).

Mycobacterial species	Catalase-peroxidase		Authors
	HPI-type	HPII-type	
M. asiaticum	Kat *G*	Kat *E*	Wayne & Diaz, 1986
M. aurum	Nd	Kat *E*	Quemard *et al*., 1991
M. avium	Kat *G*	Kat *E*	Wayne & Diaz, 1986, Mayer & Falkinham, 1986; Milano *et al*., 1996
M. bovis	Kat *G*	Nd	Wilson *et al*., 1995
M. intracellulare	Kat *G*	Kat *E*	Wayne & Diaz, 1982; 1986; 1988; Mayer & Falkinham, 1986; Sherman *et al*., 1996
M. gordonae	Kat *G*	Kat *E*	Wayne & Diaz, 1986
M. kansasii	Kat *G*	Kat *E*	Wayne & Diaz, 1986
M. leprae	Nd	Nd	Wheeler & Gregory, 1980
M. lepraemurium	Nd	Nd	Ichihara *et al*., 1977
M. phlei	Nd	Nd	Chikata *et al*., 1975
M. scrofulaceum	Kat *G*	Kat *E*	Wayne & Diaz, 1986; Mayer & Falkinham, 1986
M. smegmatis	Kat *G*	Nd	Kusunose *et al*., 1976b; Marcinkeviciene *et al.,* 1995
M. terrae	Nd	Kat *E*	Wayne & Diaz, 1986
M. tuberculosis	Kat *G*	Nd	Middlebrook & Cohn, 1953;, Kusunose *et al*., 1976b; Wayne & Diaz, 1986; Zhang *et al*., 1993
M. xenopi	Kat *G*	Nd	Wayne & Diaz, 1982

Nd =not detected – identification of the enzyme in organism was not described so far

1.13. Structure of catalase-peroxidase KatG of *M. tuberculosis*

The *M. tuberculosis* catalase-peroxidase is a multifunctional heme-dependent enzyme. Bertrand *et al*. (2004) crystallized the enzyme and reported its crystal structure refined to 2.4-Å resolution. The study reveals the dimeric assembly of the protein (Fig. 1.17a) of about 80 kDa, with each subunit of ~ 40 kDa. Each monomer (Fig. 1.17b) is composed of two domains that are mainly α-helical and display a common core structure shared by members of the bacterial and plant peroxidase families including yeast

cytochrome c peroxidase. The N-terminal domain contains the active site of the enzyme, which includes the heme *b* prosthetic group. The fold of the C-terminal domain of the enzyme is similar to that of the N-terminal domain, consistent with the proposal that the enzyme arose from a gene duplication event. No heme is observed in this domain.

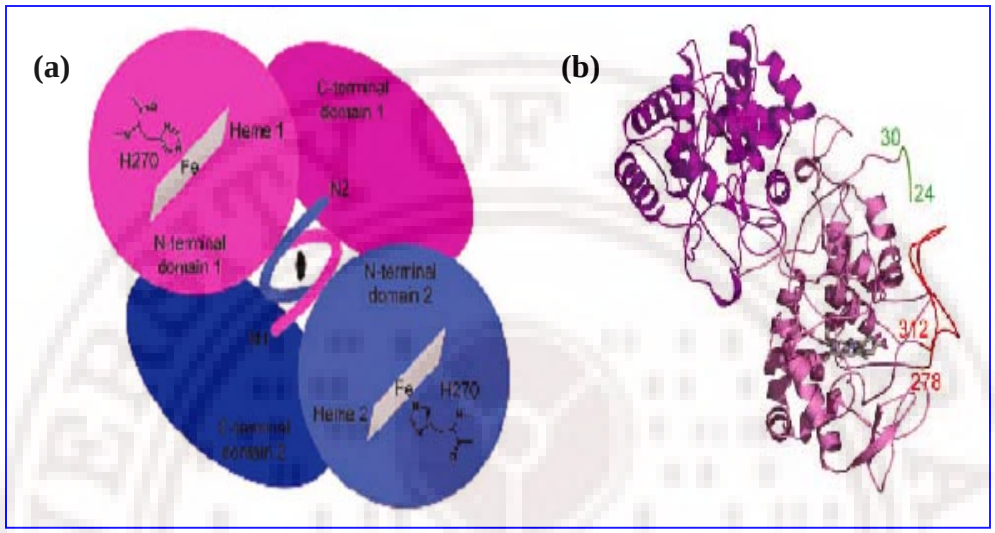

(Bertrand *et al*., 2004)

Fig. 1.17. Structure of *Mycobacterium tuberculosis* catalase- peroxidase. (a). Schematic representation of the homodimer. N-terminal residues of each monomer subunit form interlocking hooks via hydrophobic interactions. (b). A monomer. The N-terminal domain is shown in light pink, and C-terminal domain is shown in dark pink. The heme is shown in gray. N-terminal residues 24–30 are highlighted in green. Residues 278–312 are highlighted in red.

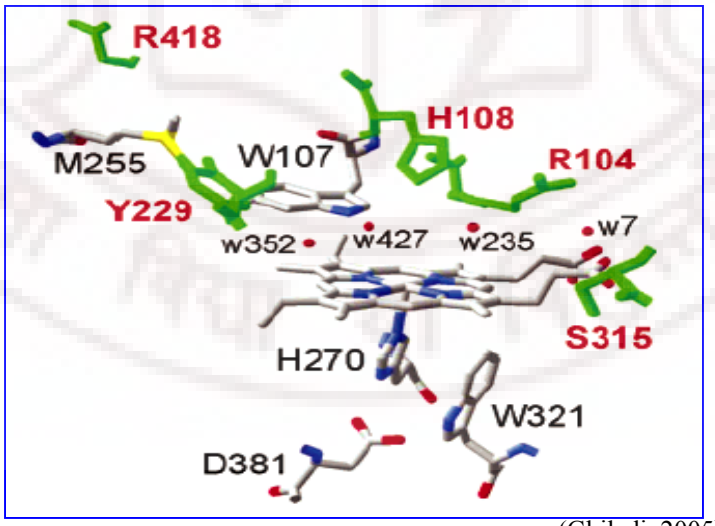

(Ghiladi, 2005)

Fig. 1.18. Heme environment of *M. tuberculosis* KatG. Active site residues (R418, Y229, R104, H108, and S315) are displayed in green

KatG from *M. tuberculosis* is particularly important due to its role in the activation of the drug INH. Considerable interest lies in understanding how the catalytic site has the enzyme that can bind and the drug. Studies have focused on the determination of those residues that are involved in this interaction. Among the several observations on mutations in the katG gene, resulting in a non-functional molecule, Ser-315 is found to be the most commonly occurring (Bertrand *et al*., 2004), resulting in up to a 200-fold increase in the minimum inhibitory concentration for the drug. Ser-315 has reported to be mutated to asparagine, isoleucine, arginine, and glycine, although the most frequently occurring mutation is to threonine. It has been postulated that Ser-315 forms hydrogen bonds to one of the heme propionate groups and that mutation to threonine would, therefore, modify the heme pocket, altering INH binding. Asp-137 is another amino acid residue that is thought to play a key role in the binding and activation of INH, as this residue appears to be a catalase-peroxidase specific proton donor in the enzyme-catalyzed activation pathway.

1.14. KatG and activation of isoniazid

INH is active against growing tubercle bacilli but not resting bacilli. Oxygen plays an important role in INH activation since INH has no activity against *M. tuberculosis* under anaerobic conditions. The work of several researchers (Lei e*t al*., 2000; Nguyen *et al.,* 2002) has shed light on the mechanism of action of INH. INH is activated by KatG to generate a range of reactive (oxygen and organic) species, which then attack multiple targets in the tubercle bacilli. One of these species, the isonicotinic acyl radical attacks the nicotinamide group of NAD^+ to form an INH-NAD adduct (Fig. 1.19). These adducts have been shown to occur in different isomeric forms including the open isomeric forms and it is not clear which of them is the active species. Adduct inhibits the InhA which is NADH-specific enoyl acyl carrier protein (NAD reductase) which is encoded by *inhA*. InhA is part of the fatty acid synthase type-II (FAS-II). This explains the earlier observation by Takayama *et al*. (1973) who showed that inhibition of mycolic acid led to the characteristic distribution of membrane and the cell death. The blocking of the FAS-II pathway leads the accumulation of the FAS I products that blocks the synthesis of the cell wall. The KatG mediated INH activation can also achieved with

manganese, which enhances the production of the INH-NAD adduct formation (Nguyen *et al.,* 2002). Mdluli *et al*., (1993a) demonstrated the involvement of β-ketoacyl ACP synthase KasA, also a part of the FAS-II system was a target of INH.

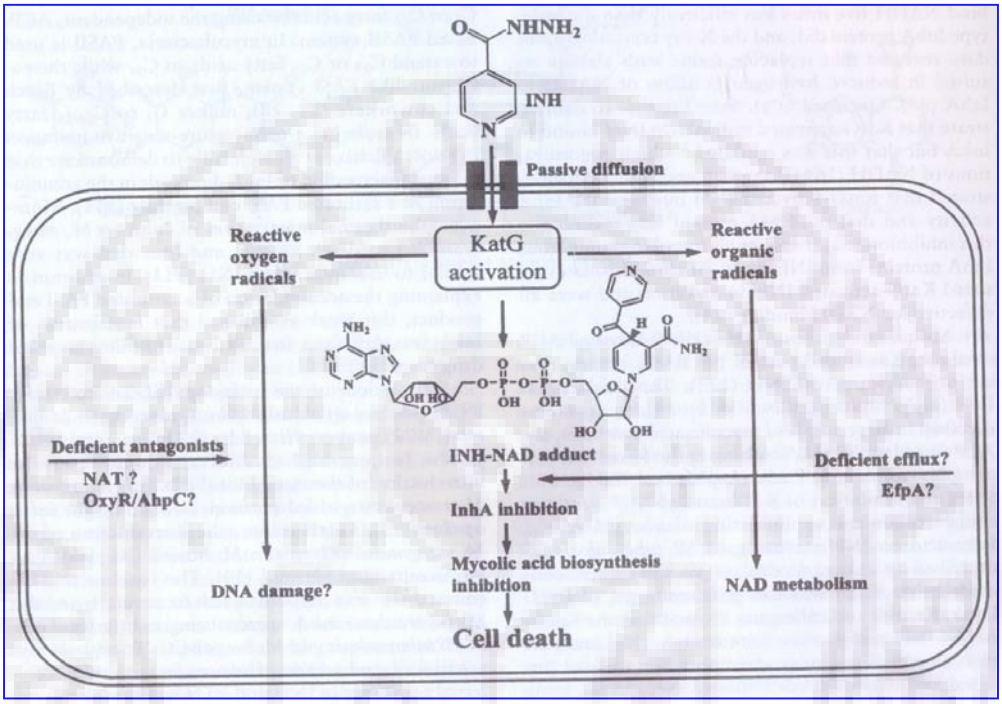

Fig. 1.19. Schematic representation of KatG mediated INH activation and its mechanism of action (Zhang *et al.*, 2005)

1.15. INH resistance: Alterations in *katG* as a contributing factor

Middlebrook (1952) first demonstrated catalase-peroxidase as a virulence determinant. He reported spontaneous INH resistant mutations of *M. tuberculosis* in *in vitro* culture and showed that these mutants lacked catalase activity and became attenuated in guinea pigs. Based on several reports world wide on INH resistant strains it is now evident that *katG* deletions and more commonly the *katG* point mutations are encountered. Lack of KatG due to alterations in the *katG* gene, reduces the ability KatG to activate INH thus leading to INH resistance. Between 20-80% of INH resistant *M. tuberculosis* showed a mutation in the *katG* gene depending upon the geographical location. Among these mutations the Ser 315 Thr is the most common and occurs in 50-93% of INH resistant isolates. These mutations reduces the catalase and peroxidase

activity by 50% and increases the MIC of these organisms to 5-10 µg / mL. This mutation affects the binding of INH to KatG.

Other genes, which are potentially involved in INH resistance, include *kasA*, *inhA*, *mdh* (NADH encoding type-II enzyme). Another candidate is the efflux protein EfpA that is induced by INH (Colangeli *et al*., 2005). It is also a possibility that aryl amine N-acetyl transferase (Nat), which is presents in humans as two isoforms NatI and NatII and acetylate aryl amine and hydrazine and can inactivate INH could be a candidate for INH resistance. The Nat homologues are seen in *M. tuberculosis* and *M. smegmatis* on the purified enzyme to convert INH to N-acetyl INH.

1.16. Relevance of studying the role of iron in pathogenic mycobacteria

There are several reports stating that the iron levels contribute to the pathogenesis of *M. tuberculosis*. Anemia is frequently encountered in tuberculosis patients, indicating that this is one of the mechanisms of the mammalian host to lower the bioavailability of this essential nutrient. The iron-withholding ability of the host, as manifested through the transferrin and lactoferrin proteins is vital as a defense mechanism against infection and, if this is compromised by the administration of iron, then the consequences can indeed be dire for the patient as the iron will preferentially feed the pathogen and not the patient (Ratledge, 2004). Though there is increasing evidence that pathogenic mycobacteria, specifically *M. tuberculosis* grows under conditions of iron limitation *in vivo*, the influence of iron levels on the host-pathogen interactions is yet to be understood fully. This will help in the identification of candidate antigens that can be exploited as potential drug targets.

Objectives of the study

I. Studies on the iron acquisition machinery in *Mycobacterium tuberculosis*

1. Establishment of conditions of iron-limitation for the growth of mycobacteria.
2. Analysis of IREPs in *M. tuberculosis.*
3. Studies on the characterization of the iron-regulated HupB protein.

II. Effect of iron deprivation on mycobacterial catalase-peroxidases and the implications on the efficacy of the anti-tubercular drug isoniazid on *Mycobacterium tuberculosis*.

CHAPTER 2

MATERIALS & METHODS

2.1. Sources of chemicals

Culture media Middle brook 7H9 / 7H10 / 7H11, supplements OADC / ADC, Bactec 12B vials, p-nitro-alpha-acetyl amino-beta-hydroxy propiophenone (NAP) vials, Lowenstein Jensen base and iron free chemicals were purchased from Becton & Dickinson, USA Hi-Media and Alfa AESAR respectively. All fine chemicals, including hexadecyltrimethyl ammonium bromide (HDTMA), Chrome azurol sulphonate (CAS) and anhydrous piperazine, cocktail protease inhibitor, Bovine serum albumin (BSA), Nitro Blue Tetrazolium (NBT), 3,3'-Diaminobenzidine tetra hydrochloride hydrate (DAB), acrylamide, Ponceau S, agarose, ethidium bromide, isopropyl β-D-1-thiogalactopyranoside (IPTG), Coomassie Brilliant blue R - 250 and bicinchoninic acid (BCA) protein estimation kit were purchased from Sigma Aldrich Pvt. Ltd, USA. Nitrocellulose membrane and 0.2 μm syringe filters were purchased from Sartorius, GmbH, Gottingen. 5-bromo-4-chloro-3-indolyl phosphate / nitroblue tetrazolium (BCIP – NBT), tetra-methyl benzidine/ hydrogen peroxide (TMB H_2O_2) and anti-IgG alkaline phosphatase (ALP) and fluorescent isothiocyanate (FITC) secondary antibodies were purchased from Bangalore Genei Pvt. Ltd, India. Bacterial grade media components, other chemicals, acids, analytical reagents and organic solvents were purchased from Qualligen / Sisco Research Laboratories / Hi-media / Bangalore Genei Pvt. Ltd. Bug Buster Ni-NTA His-bind purification kit was purchased from Novagen, USA. DNA gel extraction kit was purchased from Biogene Reagents Inc. CA, USA. Oligo nucleotide primers were synthesized from Imperial BioMedics, France. DNA restriction enzymes, RNaseA, dNTPs, DNA and protein molecular weight markers were purchased from MBI Fermentas, Lithuvania. Microtitre plates were purchased from Tarsons, India. Mycotest strips were from GVK Biosciences, India.

2.2. Source of bacterial strains and plasmid vectors

The mycobacterial strains used in the study are *Mycobacterium tuberculosis* (ATCC 27294), *M. bovis* (ATCC 27289), *M. kansasii* (ATCC 12478), *M. smegmatis* mc^2155, *M. fortuitum* and *M. vaccae* (National Mycobacterial Repository at JALMA Institute, Agra, India) and strains of *M. bovis* BCG - Denmark, Birkhaug, Moreau, Phipps, Sweden, Russia, and Pasteur (a kind gift from Dr. Peter Small, Stanford

University, USA). *Escherichia coli* strain DH5α was from our lab collection, *Escherichia coli* strain BL21 (DE3) and pET-28a (+) vector were purchased from Novagen, USA.

2.2.1. Source and collection of clinical isolates

Patients attending the Tuberculosis Clinic at Nizam's Institute of Medical Sciences, Hyderabad with signs and symptoms of pulmonary tuberculosis were clinically examined. Based on the provisional clinical diagnosis of tuberculosis, the relevant investigations, including chest X-ray, Ziehl Neelson (ZN) staining and culture by BACTEC of pulmonary samples such as sputum, bronchial wash and pleural fluid were performed.

The culture positive samples were tested for *Mycobacterium tuberculosis* complex (MTBC) by performing NAP (p-nitro-alpha-acetylamino-beta-hydroxy propiophenone) test. In this study, a total number of 40 definite cases of MTBC positive human clinical isolates sensitive to the front line drugs; Streptomycin, Isoniazid, Rifampicin and Ethambutol (SIRE) and resistant to Isoniazid (INH) were chosen based upon the BACTEC drug sensitivity test.

Group I: Isolates susceptible to anti- tuberculosis drugs (20 isolates) (Table 1)

Group II: Isolates resistant to INH (20 isolates) (Table 2)

Table 2.1. List of clinical isolates susceptible to anti- tuberculosis drugs (SIRE)

S.No.	Lab no.	Age/Sex	Sample	AFB	X-ray	Culture
1	A236-07	35 / M	Bronchial wash	Negative	Positive	Positive
2	A887-07	48 / M	Sputum	Positive	Positive	Positive
3	A1165-07	20 / F	Sputum	Positive	Positive	Positive
4	A1748-07	46 / M	Bronchial wash	Negative	Positive	Positive
5	PM053-06	17/ M	Sputum	Positive	Positive	Positive
6	PM052-06	19 / F	Sputum	Positive	Positive	Positive
7	A3229-08	28 / F	Sputum	Positive	Positive	Positive
8	A2600-08	72 / M	Sputum	Negative	Positive	Positive

9	A2835-08	54 / M	Bronchial wash	Negative	Positive	Positive
10	A2556-08	30 / M	Sputum	Positive	Positive	Positive
11	A2468-08	36 / F	Sputum	Positive	Positive	Positive
12	A2419-08	16 / F	Bronchial wash	Negative	Positive	Positive
13	A2220-08	55 / M	Sputum	Negative	Positive	Positive
14	A2272-08	40 / M	Bronchial wash	Negative	Positive	Positive
15	A2489-08	54 / M	Sputum	Negative	Positive	Positive
16	A2498-08	76 / M	Sputum	Positive	Positive	Positive
17	A2830-08	55 / M	Sputum	Positive	Positive	Positive
18	A2913-08	36 / M	Sputum	Positive	Positive	Positive
19	A2780-08	40 / M	Sputum	Positive	Positive	Positive
20	PM056-06	38 / M	Sputum	Positive	Positive	Positive

Table 2.2. List of clinical isolates resistant to INH

S.No.	Lab no.	Age/Sex	Sample	AFB	X-ray	Culture
1	A2765-07	23 / M	Sputum	Positive	Positive	Positive
2	PM 028-06	30 / F	Sputum	Positive	Positive	Positive
3	PM049-06	15 / M	Sputum	Positive	Positive	Positive
4	PM047-06	32 / M	Sputum	Positive	Positive	Positive
5	PM034-06	24 / F	Sputum	Negative	Positive	Positive
6	PM015-06	24 / M	Sputum	Negative	Positive	Positive
7	A5197-06	46 / M	Bronchial wash	Positive	Positive	Positive
8	A2751-08	54 / M	Sputum	Negative	Positive	Positive
9	A5351-06	53 / M	Bronchial wash	Positive	Positive	Positive
10	A3025-08	38 / F	Sputum	Negative	Positive	Positive
11	A4969-08	40 / M	Pleural fluid	Negative	Positive	Positive
12	A4787-08	26 / M	Bronchial wash	Positive	Positive	Positive
13	A4891-06	50 / M	Sputum	Positive	Positive	Positive
14	A2828-08	48 / M	Sputum	Positive	Positive	Positive

15	PM003-06	24 / M	Sputum	Positive	Positive	Positive
16	PM031- 06	19 / F	Sputum	Positive	Positive	Positive
17	A4200-07	40 / M	Sputum	Positive	Positive	Positive
18	A4416-06	55 / F	Bronchial wash	Negative	Positive	Positive
19	PM033-06	42 / M	Sputum	Negative	Positive	Positive
20	PM 024-06	26 / M	Sputum	Positive	Positive	Positive
21	PM051 - 06	16 / F	Sputum	Positive	Positive	Positive

2.3. Sources of serum samples

Serum samples from human patients with clinical symptoms of tuberculosis were collected at Nizam Institute of Medical Sciences (NIMS), Hyderabad. Serum samples from normal healthy volunteers were collected at University of Hyderabad, Hyderabad.

2.4. Media preparation

2.4.1. Lowenstein Jenson (LJ) egg-based solid medium

5.8 gms of LJ base, 1.8 mL of Tween-80 and 2 mL of glycerol were dissolved in a final volume of 90 mL of DDW and autoclaved at 15 lbs / sq. inch pressure for 30 min. 100 mL of egg homogenate was prepared in a sterile 500 mL conical flask, previously autoclaved with glass beads and the contents of the eggs were added and shaken vigorously to form a uniform homogenate. Then the prepared egg homogenate and 1 mL of 2% malachite green solution were added in to the autoclaved LJ base medium and mixed thoroughly. The medium was filtered and approximately 6-8 mL was aliquoted into 30 mL McCartney bottles. The slants were coagulated by inspissation at 80°C for 90 min for three successive days.

2.4.2. Middlebrook - enrichment media

0.47 g of 7H9 Middlebrook base, 0.1 g of bacto casitone and 0.2 mL of glycerol was dissolved in 90 mL of pre- autoclaved double distilled water in a 250 mL conical flask and autoclaved at 15 lbs / sq. inch pressure for 30 min. Then 10 mL of ADC

enrichment was added under aseptic conditions and stirred well and stored at 4°C for future use.

For preparing 7H11 Middlebrook solid medium, 2.1 g of 7H11 Middlebrook base, 0.5 mL of glycerol was dissolved in 90 mL of pre-autoclaved double distilled water in a 250 mL conical flask and autoclaved at 15 lbs / sq. inch pressure for 30 min. Then 10 mL of OADC enrichment was added under aseptic conditions and stirred well. Slants were made using 5-7 mL of medium in McCartney bottles and stored at 4 °C till future use.

2.4.3. Iron-free Proskauer and Beck medium

All glassware used for preparation of medium was made iron free by soaking with 2% methanolic KOH overnight (O/N) followed by soaking in 8N HNO_3 O/N and subsequent washes with glass double distilled water. Proskauer and Beck medium was prepared by dissolving 5 g of L-asparagine, 5 g of potassium dihydrogen orthophosphate and 20 mL of glycerol in 900 mL of glass double distilled water. The pH was adjusted to 6.8 with 10 N NaOH and the medium was made up to 1 L. Alumina (6 g) was added and autoclaved at 121°C at 15 lbs / $inch^2$ for 30 min. The media was cooled and filtered using Whatman grade 541 filters to remove the alumina. The media was aliquoted as 100 mL volume in 250 mL conical flasks and re-autoclaved.

Before inoculation, added 1 mL of salt solution containing (16.8 mM Mg^{2+}, 5.01 µM Mn^{2+} and 17 µM Zn^{2+}) to 100 mL medium. Iron was added at 8 µg Fe / mL (144 µM of Fe) and 0.02 µg Fe / mL (0.36 µM of Fe) for high and low iron media respectively.

2.4.4. Luria - Bertani (LB) media

1 g of tryptone, 0.5 g of yeast extract and 0.5 g of NaCl were dissolved in 100 mL double distilled water and the pH was adjusted to 7.2. The medium was autoclaved at 15 lbs / sq. inch pressure for 15 min and stored at 4ºC for future use. For preparing solid agar, a 1.5 g of bacteriological agar was added to the above ingredients before autoclaving.

2.5. Growth of *Mycobacterium tuberculosis* under high and low iron conditions

Mycobacterium tuberculosis and *M. bovis* BCG strains, maintained as glycerol stocks at -80°C / LJ slants at 4°C were revived in 7H9 Middlebrook medium supplemented with ADC enrichment. The revived cultures were used to inoculate 100 mL of iron-free Proskauer and Beck medium supplemented with 1 mL of salt solution and 8 µg Fe / mL for high iron conditions and 0.02 µg Fe / mL for low iron conditions.

A homogenous suspension of the organisms grown in 7H9 medium was prepared by vortexing the sample in the presence of glass beads, diluted to McFarland 4 and 1 mL was used as the inoculum. The organisms were maintained at 37°C with shaking at 150 rpm for 14 days. The cells were separated by centrifugation at 6000 rpm for 15 minutes and the spent growth medium and the cell pellet were used for further studies. Growth was measured by determination of the cell dry weight.

2.5.1. Growth of *M. tuberculosis* with varying concentrations of iron

Mycobacterium tuberculosis was grown as above in medium supplemented with iron at 0.02, 0.05, 0.1, 0.2, 0.4, 1, 4, 8 and 12 µg Fe / mL respectively and grown for 14 days as mentioned above.

2.5.2. Time-dependant growth of *M. tuberculosis*

Mycobacterium tuberculosis was inoculated separately into 5 flasks each of high (8 µg of Fe/mL) and low iron (0.02 µg Fe / mL) media respectively and grown as mentioned above. The organisms were harvested on days 4, 8, 12, 16, 20 and 24 respectively.

2.6. Assay of CMb and Mb

CMb and Mb were assayed in the culture filtrate and the cell pellet respectively. CMb was assayed by Universal CAS assay and Mb was assayed by measuring the absorbance of the ferri-Mb at 450 nm.

2.6.1. Assay of CMb by Universal CAS assay (Schwyn and Neilands, 1987)

Preparation of reagents

Solution A

6 mL of hexadecyltrimethyl ammonium bromide (HDTMA) from 10 mM stock (3.645 g / L of DDW) was pipetted in a standard flask and diluted with 10 mL of DDW. To this, 1.5 mL of a freshly prepared 1 mM ferric chloride taken from 10 mM stock (0.1622 g / L) in 10 mM HCl and 7.5 mL of 2 mM Chrome azurol sulphonate (CAS) (1.211 g / L) were added slowly.

Solution B

Anhydrous piperazine (4.3 g) was dissolved in a minimum volume of water and 7.25 mL of concentrated HCl was added. All the above solutions were made in iron-free glassware. To prepare working CAS assay solution, solution B was added slowly to solution A and made up to 100 mL with iron free DDW.

Procedure

2 mL of CAS assay solution was added to 2 mL of water (blank) and 2 mL of culture filtrate (test), incubated for 30 min at RT and the absorbance read at 630 nm. The absorbance is converted to siderophore units, using the equation below:

$$\text{Siderophore Unit (SU)} = (A_b - A_t / A_b) \text{ X } 100$$

(A_b: $OD_{630\ nm}$ of blank and A_t: $OD_{630\ nm}$ of test).

Ferric-CMb was expressed as siderophore units per 100 mg cell dry weight.

2.6.2. Extraction of ferric-CMb (Gobin *et al*., 1995)

To the 100 mL of spent culture filtrate, approximately 1 mL of saturated aqueous ferric chloride was added drop wise, till it forms a precipitate. It was centrifuged at 6,000 rpm for 15 min and to the clear supernatant one and half volumes of chloroform was added to extract the ferri-CMb. The concentration of ferric-CMb was measured by reading the absorbance of the clear supernatant at 450 nm ($E\%_{450nm}$ of ferric-CMb = 48).

2.6.3. Extraction of ferric-Mb ((Ratledge & Ewing, 1996)

Ferric-Mb was extracted as follows. To the cell pellet from 100 mL culture, 10 mL of absolute ethanol was added, left at RT for O/N, followed by centrifugation at 6000

rpm for 15 min. To the cell-free supernatant, 1 mL of saturated ferric chloride (in ethanol) was added and left for 30 min at RT. The ferric-Mb was extracted with 10 mL of chloroform, washed thrice with water and the concentration was determined by reading at 450 nm using chloroform as blank. Ferri-Mb was expressed as OD_{450} units per g dry weight. ($E\%_{450nm}$ of ferric-Mb = 43).

2.7. Isolation of Iron-regulated envelope proteins (IREPs) from *M. tuberculosis*: analysis of cell wall and membrane proteins by SDS-PAGE (Hall *et al.*, 1987)

Preparation of solutions

1. Wash buffer: 10 mM Tris-HCl, pH 7.8

2. Pre-condensation of Triton X-114 (Bordier, 1981): 1 mL of Triton X-114 was mixed with 500 mL of 10 mM Tris-HCl (pH 7.4) containing 150 mM NaCl. After complete dissolution at 4ºC for O/N, the clear solution was incubated for 1 h at 37ºC. Condensation of detergent occurred and mixture separated into aqueous and detergent phases. The aqueous phase was discarded and replaced by same volume of above buffer. Condensation was repeated thrice and stored at 4ºC.

3. Dissolving buffer (100 mL): 25mM Tris pH 8.8 (2.5 mL of 1 M Tris pH 8.8), 75 mM glycine (0.18 g), 2% SDS dissolved in DDW and made up to 100 mL.

2.7.1. Isolation of cell wall and cell membrane fractions

The cells grown in high and low iron condition were harvested at 6000 rpm for 15 min. The supernatant was removed and cells were washed and resuspended in 6 mL of wash buffer and subjected to sonication (time 20 min at 30 s pulse with 30 s interval, amplitude 40 Hz, at probe temperature of 4ºC in Sonics Vibra cell sonicator). The sonicate was centrifuged at 6000 rpm at 4ºC for 15 min to remove cell debris and the supernatant was centrifuged at 18,000 rpm for 40 min at 4 ºC to pellet the cell wall; the supernatant was again subjected to ultra centrifugation at 45,000 rpm for 2 h 30 min to pellet the cell membrane. Both the cell wall and cell membrane pellets were washed twice with 1mL of wash buffer, to remove the unbound debris.

2.7.2. Solubilisation of cell wall and membrane using Triton X-114 (Sinha *et al.*, 2002)

The cell wall and cell membrane pellets were solubilised by adding an appropriate volume of 5% pre-condensed Triton X-114 and incubating at 4ºC overnight with rocking. The detergent and aqueous phases were separated by incubating in 37ºC water bath for an hour followed by centrifuging at 3000 rpm for 15 min at RT. The left over pellet was again extracted with 5% pre-condensed Triton X-114 and the aqueous and the detergent phases were separated as described previously. After three suitable washes of both aqueous and the detergent phases, the proteins were precipitated by adding 5 volumes of chilled acetone and left overnight at -20ºC. The precipitated proteins were centrifuged at 12,000 rpm for 20 min, supernatant was discarded and the pellets were resuspended in 2 mL of chilled acetone and again centrifuged at 12000 rpm for 10 min. Later the protein pellets were dried and dissolved in minimal amount of dissolving buffer and then subjected to 5-20% gradient SDS-PAGE.

2.7.3. Protein estimation

Total protein concentration in the sample was estimated by BCA protein assay reagent kit as per manufacturer's instructions.

2.8. Sodium dodecyl sulphate polyacrylamide gel electrophoresis (SDS-PAGE) (Laemmli, 1970)

Stock solutions

Acrylamide and N, N'-bisacrylamide mix (30:0.8): 30 g of acrylamide and 0.8 g of bisacrylamide were dissolved in 60 mL of water and made upto 100 mL.

Resolving gel buffer: Tris-HCl (1.5 M, pH 8.8) with 0.4% SDS.

Stacking gel buffer: Tris-HCl (0.5 M, pH 6.8) with 0.4% SDS.

Ammonium per sulfate (APS): 10% APS solution was prepared fresh in double distilled water.

Sample buffer (2X): 0.125 M Tris-HCl (pH 6.8) containing 4% SDS, 20% glycerol and 0.002% bromophenol blue.

Running buffer: Tris-glycine buffer (25 mM Tris, 250 mM glycine and 0.1% SDS), pH 8.8.

Staining solution: 0.25% Coomassie Brilliant Blue in 50% methanol and 10% glacial acetic acid.

Destaining solution: 20% Methanol and 10% glacial acetic acid in DDW.

Table 2.3. Preparation of resolving gel mix

Ingredients	Volume of the ingredients (mL)		
	Gradient gel		10%
	5%	20%	
Acrylamide: Bisacrylamide	2.75	10.60	10.60
Resolving gel buffer	4.00	4.00	8.00
Double distilled water	9.162	1.312	13.232
Ammonium persulphate	0.08	0.08	0.16
TEMED	0.008	0.008	0.008
Total volume	16.000	16.000	32.000

The resolving gel was prepared as 5 - 20% gradient gel or 10% gel using the recipe as given above. The gradient was prepared using a gradient maker. The resolving gel was allowed to polymerize and then the stacking gel was poured over it after appropriately positioning the comb.

Table 2.4. Preparation of 5% stacking gel mix

Components	Volume (mL)
Acrylamide: Bisacrylamide	1.5
Stacking gel buffer	2.5
Double distilled water	6.0
Ammonium persulphate	0.03
TEMED	0.01
Total	10.04

About 40 µg of protein was loaded on to minigels and 50 µg of protein was used for gradient standard gels. Equal volumes of the protein samples and 2X sample buffer were mixed, boiled for 10 min and centrifuged for 10 min at 10,000 rpm to remove any

insoluble material. The clear supernatant was loaded onto gel and electrophoresis was carried out at 25 mA constant current using Hoefer electrophoresis unit (SE600 series). The electrophoresis was allowed to run until the tracking dye was run out of the gel, followed by electrophoresis for an additional 5 min. The gel was stained with Coomassie Blue for 2 - 4 h and then destained O/N.

2.9. Western blotting analysis (Towbin *et al*., 1979)

Preparation of stock solutions

Transblot buffer (10X): Stock solution was prepared by dissolving 250 mM Tris and 1.3 M glycine in 400 mL of double distilled water. Working solution was prepared by mixing 200 mL of 10X stock solution and 400 mL of methanol in 1.4 L of double distilled water.

Tris buffer saline (TBS): 50 mM Tris HCl (pH 8.0) containing 150 mM NaCl in 1.0 L of double distilled water.

Tris buffer saline – Tween solution (TBS-T): TBS containing 0.05% Tween – 20.

Ponceau S stain: Ponceau S, trichloroacetic acid and sulfosalicylic acid were mixed in 2:30:30 (w/v) ratio and the final volume was made up to 100 mL with double distilled water. One part of stock solution was diluted with 9 parts of deionized water to make a working solution.

The proteins resolved on polyacrylamide gel were electrophoretically transferred on to nitrocellulose membrane at 30 V constant voltage O/N, employing transblot buffer using Broviga transfer apparatus (Balaji Scientific). After the transfer, proteins were visualized by Ponceau S stain to check the efficiency of protein transfer and for marking the protein molecular weight marker. The membrane was then blocked 2 h using 5% non-fat milk solution (NFM) dissolved in TBS-T. The membrane was washed thrice with TBS and incubated O/N with appropriate antiserum (1:2000 for anti-HupB antibodies and 1: 250 clinical serum samples) diluted in TBS-T containing 1% NFM at 4°C. Later, the membrane was washed 4 times with TBS and incubated in 1:500 dilution of anti-IgG alkaline phosphotase conjugate in TBS-T containing 1% NFM at room temperature for 1½ h. Then, the blot was washed thoroughly with TBS and developed using ready to use 5-bromo-4-chloro-3-indolyl phosphate / nitroblue tetrazolium (BCIP – NBT).

2.10. Purification of Irep-28

Preparation of solutions

1) Elution buffer: 25 mM Tris-HCl (pH 8.8) buffer containing 5% glycerol, 1% SDS and 0.24 mM glycine.

Purification of Irep-28 was done by excising of 28kDa protein bands from a 10% preparative SDS-PAGE from cell wall detergent phase protein fraction of *M. tuberculosis* grown under low iron conditions. The excised slices were crushed with the help of a gel crusher and protein was eluted using elution buffer and subsequent incubations at 37°C. Five volumes of acetone was added to the elute and the protein was precipitated. Later the protein pellets were dried and dissolved in minimal amount of dissolving buffer and then the purity of the eluted protein was confirmed using 5-20% gradient SDS- PAGE (detailed protocol refer 2.8).

2.11. Sequence analysis of Irep-28

The purified Irep-28 sample was digested in-gel, S - alkylated, and the tryptic peptides were separated by liquid chromatography and analyzed by tandem mass spectrometry (MS/MS) on a Waters Q-TOF Ultima Global as described earlier (done in the lab of Dr. F. Altmann, Universitaet fuer Bodenkultur, Austria).

2.12. Antibodies against Irep-28

Antibodies against the cell wall associated Irep-28 (shown to be HupB) was used to immunize rabbit subcutaneously and intramuscularly with 100 µg of purified HupB mixed with Freund's incomplete adjuvant. The secondary immunization was done using 50 µg of purified HupB mixed with Freund's incomplete adjuvant. The rabbit was bled 2 weeks after secondary immunization and serum was separated and stored in - 80ºC in separate aliquots for further use.

2.13. *In silico* analysis

Nucleotide and amino acid sequences were analyzed using standard SWISS-PROT bioinformatics and proteomics tools. BLASTN and BLASTX were used to search the genome of *M. tuberculosis*. CLUSTALW was used for multiple sequence alignment.

Sequence analysis and construction of phylogenetic tree for proteins was done using CLUSTALw and CLC bio programs. SMART software was used to identify the functional partners of HupB and the functionality prediction of HupB was done using TB PRED soft ware.

2.14. Evaluation of clinical significance of HupB

2.14.1. Study group: Selection of tuberculosis patients

Study group include, patients attending the Tuberculosis Clinic at Nizam's Institute of Medical Sciences (Hyderabad, India), with signs and symptoms of pulmonary or extra-pulmonary tuberculosis were examined. Based on the provisional clinical diagnosis of tuberculosis, the relevant investigations, including chest X-ray, ZN staining and culture by BACTEC and L-J of pulmonary/ extra-pulmonary were performed. In this study, a total number of 44 definite cases of tuberculosis (confirmed clinically and by lab testing) were chosen. Serum samples were collected from all these patients and were tested for antibodies against Irep-28. The serum was also tested by commercial lateral flow device (Mycotest, GVK BioSciences, India).

2.14.2. Immunoreactivity of serum samples with HupB

Preliminary analysis included immunoreactivity of serum sample by western blotting analysis of the solubilised wall and membrane proteins was done using serum from selected tuberculosis patients at a dilution of 1:250 using standard protocols. All serum samples were subjected to dot blot analysis against the purified HupB antigen. 2.5 µg of HupB was spotted on nitrocellulose membrane. After blocking the membrane with 5% non-fat milk powder in TBS-T, human serum (1:250 dilution) was added and incubated overnight. After suitable washes anti-human IgG ALP- conjugate (1:500 dilution) was added, followed by development of the blot with the ready-to-use BCIP - NBT substrate (Bangalore Genei, India) as per manufacturer's instructions.

2.14.3. Testing of serum samples with the commercial lateral flow device Mycotest

All serum samples were tested by the commercial Mycotest (marketed by GVK Biosciences, India), which is a lateral flow device coated with recombinant antigens for

secretory proteins specific for *M. tuberculosis* (with a sensitivity and specificity of 87% and 90% respectively, as per manufacturer's information). 80-100 µL of serum was added and the detection of a pink band in addition to the control band within 15 minutes after addition of serum was considered positive for tuberculosis.

2.15. Molecular biology studies for cloning and expression of *hupB*

Cloning and expression studies were done following standard molecular biology protocols (Sambrook *et al*., 1989). pET-28a (+) vector system (Fig.), *E. coli* DH5α were used for cloning and *E. coli* BL21 (DE3) was used as host for expression studies.

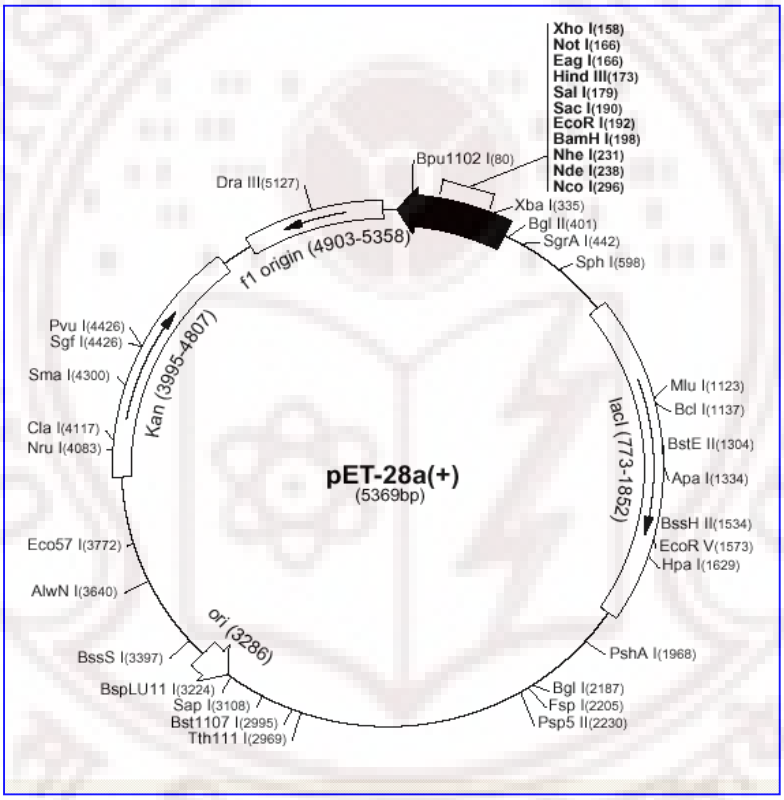

Fig. 2.1. pET-28a (+) expression vector

2.15.1. Genomic DNA Isolation (van Soolingen *et al.*, 1994)

Preparation of solutions

1) TE buffer: 10 mM Tris-HCl; pH 8.0 containing 1 mM EDTA

2) Lysozyme (10 mg / mL stock): Dissolved 50 mg of lysozyme in 5 mL double distilled water, aliquoted and stored at - 20°C.

3) Proteinase K (10 mg / mL stock): Dissolved 50 mg of proteinase K in 5 mL double distilled water, aliquoted and stored at - 20°C.

Mycobacterium tuberculosis genomic DNA was isolated by using the standard detergent-proteinase K lysis protocol. Two loopful of mycobacterial cells were taken and washed three times in TE buffer (100 mM Tris / HCl, pH 8.0 and 100 mM EDTA), re-suspended into 600 µL of TE buffer and heat killed at 80^{o}C for 30 min. the cells were treated with 50 µL lysozyme (stock solution 10 mg / mL) for 1 h at 37^{o}C. The clear solution was then treated with 6 µL proteinase K (stock solution 10 mg / mL) and 70 µL SDS (10%) and the mixture were incubated in a water bath at 60^{o}C for 10 min with mild shaking. The sample was brought to room temperature and to this equal volume of phenol: chloroform: isoamylalcohol (25:24:1) was added and further incubated for 20 min at room temperature (25^{o}C-28^{o}C) with mild shaking. The sample was centrifuged at 12, 000 g for 15 min at room temperature. The upper phase was separated and mixed with 1 / 100 volume of RNase A stock solution (10 mg / mL), and incubated at 37^{o}C for 30 min. The above phenol: chloroform: isoamylalcohol was repeated again. The DNA was precipitated with 0.6 volumes of isopropanol at room temperature for 30 min. The DNA pellet was washed with cold 70% ethanol. The DNA pellet was air dried overnight and dissolved in an appropriate volume of sterile TE buffer and stored at 4^{o}C. The concentration and purity of DNA was determined by measuring the absorbance at 260 and 280 nm respectively.

2.15.2. Agarose gel electrophoresis

Preparation of reagents

1) Tris-acetate-EDTA (TAE) buffer: Dissolved 4.84 g Tris, 1.14 mL glacial acetic acid and 20 mL 0.5 M EDTA in 1 L of double distilled water and pH was adjusted to 8.0.

2) Ethidium bromide: 1 mg / mL stock solution was prepared and added to the gels to give a final concentration of 0.1 µg / mL.

3) Gel loading buffer: 0.25% bromophenol blue, 0.25% xylene cyanol FF, and 40% (w/v) of sucrose in water.

Genomic DNA and PCR amplified products were subjected to electrophoretic separation using 0.8% and 1.2% agarose gels, respectively. The gels were prepared by

adding appropriate amounts of agarose into TAE buffer and subsequent boiling in a microwave for complete dissolution. The DNA samples were prepared by adding 6X gel loading buffer (6:1 - DNA: loading buffer) and loaded onto the gel. The DNA size standards loaded onto gel included 8 µL of 1 kb ladder or λ DNA, *EcoRI-HindIII* double digest (0.5 µg / µL stock). Samples were subjected to electrophoresis at 100 V and the DNA was visualised in a UV transilluminator.

2.15.3. PCR amplification

PCR amplification of the full-length *hupB* gene was done using genomic DNA of *M. tuberculosis* H37Rv as template. PCR was performed in a final volume of 20 µL, using 50 – 100 ng of template DNA. The reaction mixture contained 2 µL of 10X Taq buffer with KCl, 200 µM of each dNTP, 0.5 U Taq DNA polymerase, 0.15 mM $MgCl_2$, and 100 ρmoles of primers L1 (with an NdeI site; 5' GGG AAT TCC ATA TGA ACA AAG CAG AGC TCA T 3') and L2 (with an Hind III site; 5' CCC AAG CTT CTA TTT GCG ACC CCG CCG AG 3'). A negative control without template DNA was included. PCR was done in a PTC-200 thermal cycler (MJ research, USA). The program consisted of an initial denaturation step (5 min, 95°C) followed by 30 cycles of amplification (1 min at 60°C, 1 min at 72°C and 1 min at 94°C) with a final extension for 6 min at 72°C. The *hupB* (645 bp) product was visualized after separation in 1% agarose gel. It was gel purified using Biogene DNA gel extraction kit according to manufacturer's recommendations and kept at - 20°C.

2.15.4. Cloning and expression of *hupB*

a) Restriction digestion of vector and *hupB* amplicon

1 µg of pET-28a (+) plasmid DNA and *hupB* amplicon were individually subjected to double digestion with *NdeI* and *HindIII* in a reaction mixture of 50 µL and incubated at 37°C for O/N. After heat inactivation at 65°C for 10 min, they were purified using mini-elute reaction clean up kit (Qiagen, Germany).

b) Ligation

Ligation was done using vector and insert DNA in molar ratio of 3:1 using the following formula.

$$\text{Concentration of the insert (ng)} = \frac{\text{ng of the insert x Size of the insert (kb)}}{\text{Size of the vector (kb)}} \times \text{Molar ratio}$$

The ligation reaction was carried out in a total reaction volume of 10 µL containing 100 ng of vector DNA, 35 ng of *hupB*, 1 µL of 10X ligase buffer, 1 µL of T4 DNA ligase (5 U / µL) and made up to 10 µL with sterile double distilled water. The reaction mixture was incubated at 16°C O/N. After heat inactivation at 65°C for 10 min, the reaction mixture was stored at - 20ºC or used for transformation immediately.

2.15.5. Transformation (Sambrook *et al.*, 1989)

E. coli competent cells were prepared as follows; a single colony of *E. coli* DH5α was picked with a sterile inoculation loop and inoculated into 5 mL of LB broth under aseptic conditions. The culture was incubated O/N at 37ºC in an orbital shaker. This was added to 100 mL of LB medium and when the cell density reached 0.6 ($OD_{600\ nm}$), the cells were harvested by centrifugation at 3,000 rpm for 10 min at 4°C. The cell pellet was re-suspended in 15 mL of 0.1 M $CaCl_2$ and incubated in ice for 30 min. The cell suspension was centrifuged (3,000 rpm for 10 min) and the competent cells were re-suspended in 1 mL of 0.1 M $CaCl_2$.

10 µL of ligation mixture was added to 200 µL of competent cells, mixed gently and incubated on ice for about 30 min. The cells were then subjected to heat shock at 42°C in a water bath for 90 sec and transferred to ice for 2 min. 800 µL of LB broth was added to the mixture and cells were incubated at 37°C for 1 h in a shaking incubator at 225 rpm. The cells were plated out on LB agar plates supplemented with kanamycin (50 µg / mL). The plates were incubated at 37°C O/N.

The colonies grown were picked serially, streaked on LB agar plate having kanamycin and allowed to grow for O/N. The isolated colonies were used for colony PCR. The positive clones were picked and tested for the presence of insert by plasmid preparation followed by restriction digestion.

2.15.6. Screening of recombinants

Plasmid DNA preparation: Miniprep method of Birnboim & Doly, 1979.

Preparation of solutions

Solution I: 50 mM glucose was dissolved in 50 mL of 25 mM Tris HCl (pH 8.0) containing 10 mM EDTA. The pH was adjusted to 8.0 and stored at 4°C.

Solution II: 0.2 N NaOH solution containing 1.5% SDS was prepared fresh.

Solution III: Prepared by mixing 5M potassium acetate (pH 5.2), glacial acetic acid and double distilled water in ratio of 60.0:11.5:28.5 (v/v).

A single colony was inoculated into 5 mL of LB medium with kanamycin (50 µg / mL) and incubated overnight with shaking at 37°C. 1.5 mL of the culture was centrifuged for 5 min at 6,000 rpm at 4°C in an eppendorf tube. The supernatant was removed by aspiration. The pellet was re-suspended in 100 µL of Solution I by vortexing and incubated on ice for 5 min. 200 µL of freshly prepared Solution II was added, the contents were mixed well, and incubated on ice for 5 min. The solution was neutralized by adding 150 µL of ice-cold Solution III, mixed by inversion for five times and after incubation in ice for 5 min., centrifuged at 10,000 rpm for 10 min at 4°C. The supernatant was carefully transferred to a fresh tube and DNase free RNase was added to a final concentration of 10 µg / mL and incubated at 37°C for 30 min. The plasmid DNA was extracted into the aqueous phase by the addition of equal volume of phenol:chloroform (1:1) subsequently followed by centrifugation at 12,000 rpm for 10 min. The plasmid DNA was precipitated with 2 volume of isopropanol at room temperature for 10 min and centrifuged at 12,000 rpm for 15 min. The plasmid pellet was washed with 70% ethanol, air-dried, and dissolved in 20 µL of TE buffer and stored at –20°C.

The presence of *hupB* insert was identified by restriction digestion of 1 µg recombinant plasmid with *NdeI* and *HindIII* in a reaction mixture of 20 µL and incubated at 37°C for O/N. After heat inactivation at 65°C for 10 min, the release of insert was identified using 1.2% agarose gel electrophoresis.

2.15.7. Expression of recombinant HupB protein in *E. coli*

Recombinant plasmid from a positive clone was isolated and transformed into *E. coli* BL21 (DE3) cells for expression studies. A single colony was inoculated in 5 mL of LB medium supplemented with kanamycin and incubated at 37°C for O/N in an orbital shaker. The 5 mL of O/N culture was inoculated in to 95 mL of LB medium supplemented with kanamycin and incubated at 37°C until the $OD_{600\ nm}$ of the culture reached 0.6. An aliquot of culture representing un-induced cells was transferred to a new tube and 1 mM IPTG was added to the remaining culture and allowed to grow for an additional two hours. Both un-induced and induced cells were harvested by centrifugation at 10,000 rpm for 15 min at 4°C, washed thrice and subjected to sonication for 5 min (20 sec pulse in Vibra Cell sonicator). The pellet and supernatant separated by centrifugation at 10,000 rpm for 20 min were analyzed by SDS-PAGE using a 10% gel.

2.15.8. Purification of rHupB protein

rHupB was obtained as insoluble inclusion bodies and low level of expression was observed in the soluble fraction as deduced by 10% SDS-PAGE. Purification of rHupB from the insoluble fraction was done using gel elution procedure (refer to 2.10).

2.16. Surface localization of HupB protein by confocal microscopy

Preparation of reagents

Anti-HupB anti-bodies

Propidium iodide solution: 50 µg of propidium iodide was dissolved in 5 mL of double distilled water and stored in aliquots at 4ºC.

PBS-T: 10mM PBS pH 7.2 containing 0.05% Tween-20.

Confocal microscopy was performed with a Leica TCS SP2 AOBS instrument, based on the published protocol (Asuthkar *et al*., 2007). Briefly, mycobacteria were harvested at 8,000 rpm for 20 min, washed twice with PBS, and re-suspended in PBS with 2.5% BSA to a cell density equivalent to McFarland standard of 1. A thin smear was prepared on a slide, allowed to air dry, and then heat fixed by quickly passing the slide through the flame of a Bunsen burner twice. The smear was then treated with 4% paraformaldehyde at RT for 30 min and then blocked with 5% BSA for 1.5 h. Anti-HupB

immunoglobulins were added at a dilution of 1:100 to the fixed mycobacteria and incubated overnight at 4°C. After four washes with PBS with 0.05% Tween 20, the slide was incubated with a 1:500 dilution of goat anti-rabbit fluorescein isothiocyanate (FITC) conjugate (Bangalore Genei) for 1.5 h at room temperature and then subjected to four washes with PBS to remove the unbound conjugate. Propidium iodide (10 μg / mL) was applied as a counter stain. A drop of 90% glycerol was added to the slide to keep it moist and sealed after overlying with a cover slip. The FITC fluorescence was visualized at 535 nm after excitation at 500 nm, while the excitation and emission wavelengths for propidium iodide are 600 and 732 nm, respectively.

2.17. Ligand-binding studies: binding of HupB with ferric-Mb and ferric-CMb from *M. tuberculosis*

2.17.1. Purification of ferric-Mb and ferric-CMb by HPLC

Purification of both ferric-Mb and ferric-CMb was done from *M. tuberculosis* grown under low iron by HPLC using published protocols (Ratledge & Ewing, 1996).
The chloroform extracts of both ferric-Mb and ferric-CMb were taken in a separating funnel, washed thrice with water to remove the excess ferric chloride and the excess water was removed. The sample was dried by rotary evaporation and the residue was dissolved in minimal quantity of chloroform and filtered though Nylon membrane filter to remove any insoluble material.

2.17.1.1. Separation by HPLC (Lane *et al.*, 1998, Barclay *et al.*, 1986)

Both ferric-Mb and ferric-CMb were separated by reverse phase HPLC on Water's C18 column (150 mm x 4.6 mm id) at a flow rate of 1 mL / min for 35 min and monitored continuously at 450 nm. The hydrophobic ferric-Mb was separated using a gradient (Table 5) of 0 to 100 % with buffer A (0.09% formic acid / 90% acetonitrile) and buffer B (0.1% formic acid in 60% acetonitrile) and 40% methanol. The ferric-CMb was separated using a gradient of 0 to 100% with buffer A (0.1% formic acid) and buffer B (0.09% formic acid in 90% acetonitrile).

Table 2.5. HPLC gradient for purification of ferric-Mb and ferric-CMb

Time (min)	Buffer A %	Buffer B %
2	100	0
32	0	100
33	0	100
35	100	0

Fractions with maximal absorbance at 450 nm were collected, concentrated by Speed vac system and then subjected to mass spectrometry. The purity of the concentrated sample was determined by performing spectral scan ranging from 250 nm-600 nm by using chloroform as blank. The concentration of ferric complexes of siderophores was determined by using their extinction coefficients.

2.17.1.2. Preparation of desferri-Mb and desferri-CMb (Sharman *et al*., 1995, Macham *et al*., 1977)

16 μM of Mb and 20 μM of CMb (= 100 μL) of HPLC purified ferric-siderophore was diluted to 1 mL with de-ionized water, mixed with 5.8 mg (1 μmol) of 8–hydroxyquinolone in 1 mL of HPLC grade methanol, and stirred for 20 min at room temperature and then incubated at 22˚C for 2 h for the complete formation of dark green coloured ferri-8-hydroxyquinoline. The colourless desferri-siderophores were extracted into redistilled chloroform (100 μL). All the glassware used for preparing desferri-siderophores was made iron free to prevent the reformation of ferri-complex. The purity of the desferri-siderophores was confirmed by spectral scan ranging from 250 nm-600 nm using chloroform as blank and compared with the spectral scan of ferri-siderophores.

2.17.1.3. Titration of iron and desferri-CMb / desferri-Mb

Preparation of solutions

250 μM of Fe in $FeCl_3$ stock solution: 400 mg of anhydrous $FeCl_3$ was dissolved in 1 mL of acetonitrile (HPLC grade) and then diluted 10 times with acetonitrile.

The iron binding capacity of the siderophores was determined by titrating 2 mL of des-ferri siderophores (100 µL of extracted desferri-CMb / desferri-Mb (16 µg) in 1900 µL of chloroform) with 1 µL of $FeCl_3$ stock solution stepwise. The complex formation was measured until the relative A_{450nm} of the siderophore became constant. The concentration of the iron bound to the siderophore was calculated from the titration curve.

2.17.1.4. Labeling of des-ferri siderophores with ^{59}Fe (Dover and Ratledge, 1996)

For labeling of siderophores, from a stock solution of 7.175 µ moles solution of ^{59}Fe (specific activity of 5.77 Ci / g) in acetonitrile, 36 n moles was added to 2 mL of desferri – siderophores and incubated for 2 h at RT. Sufficient amount of non-radioactive $FeCl_3$ (1.728 µ moles) in water was added to the mixture to 95% saturate the siderophore with iron. The mixture was held at 4˚C O/N and the unbound iron was removed by centrifuging at 5000 rpm for 15 min. The ^{59}Fe bound siderophore counts were measured in β-counter (Tricarb-2100TR) using 5 mL of Bray's mixture comprising POP (2 g), POPOP (0.1 g), naphthalene (30 g), methanol (50 mL), ethylene glycol (10 mL) and made up to 500 mL with 1, 4-dioxane.

2.17.2. Transblot analysis for the isolation of HupB protein

To demonstrate the interaction of HupB with the ferri-siderophores, HupB was prepared from the cell wall detergent fraction of *M. tuberculosis* by Triton X-114 phase separation (detailed procedure refer section 2.7.2) and 50 µg of protein fraction without SDS was separated by native preparative gel electrophoresis (7% resolving gel and 5% stacking gel), followed by transfer on to nitrocellulose membrane. Proteins were visualized by Ponceau S stain and the 28 kDa HupB protein band (approx. 25 µg) was excised from the membrane, blocked for 2 h in 20% NFM in TBS-T and used for the ^{59}Fe-siderophore uptake studies.

2.17.3. Radiolabeled studies for the binding of siderophores to HupB

2.17.3.1. Dose dependant binding of ^{59}Fe labeled siderophores to HupB

Dose-dependant binding of 25 µg of cell wall purified HupB with ^{59}Fe labeled siderophores was done by incubating the *M. tuberculosis* HupB with varying

concentration of ^{59}Fe-CMb ranging from 0, 25, 50, 75, 100 and 126 nmoles of iron and to ^{59}Fe-Mb ranging from 0, 26, 52, 78, 104 and 131 nmoles of iron in 1 mL of TBS for 3 h at RT. The unbound ligand was washed with TBST and the HupB bound ^{59}Fe-CMb and ^{59}Fe-Mb respectively was counted using 5 mL of Bray's mixture.

2.17.3.2. Specific binding of HupB with the siderophores

a. Blocking studies with anti-HupB antibodies

Specific binding of siderophore to 25 µg of cell wall purified HupB was verified by inhibition of binding of labeled siderophore to HupB by blocking of HupB sites with anti-HupB antibodies (1:200 dilution) for 2 h at RT with shaking. After suitable washes to remove the unbound antibody, the membranes were incubated with ^{59}Fe-CMb (74 n moles) and ^{59}Fe-Mb (74 n moles) respectively for 3 h at RT with shaking. The bound siderophore(s) was measured by taking the counts after the addition of 5 mL of Bray's mixture.

b. Displacement studies

Specific binding of siderophores to 25 µg of cell wall purified HupB was also verified by displacement studies. HupB immobilized on the nitrocellulose membranes were incubated with 143 n moles of ^{59}Fe-CMb and 147 nmoles of ^{59}Fe-Mb for 3 h at RT with shaking. After suitable washes with TBST, the bound ^{59}Fe - siderophores was displaced by the addition of cold ferric-Mb and ferric-CMb at concentrations of 0, 3, 9 and 14 nmoles and incubated for 2 h at RT with shaking. The unbound was washed thrice with TBST and counted using 5 mL of Bray's mixture.

2.17.4. Spectrofluorimetric studies of interaction of HupB with mycobactin and carboxymycobactin

Spectrofluorimetric analysis, performed in Cary Eclipse fluorescence spectrophotometer, USA, was done with purified rHupB (25 µg) protein in 3 mL of TBS. The sample was subjected to excitation at 280 nm, and the emission spectra were obtained from 200 nm to 600 nm. Slit widths of 10 and 5 nm for excitation and emission respectively were used and the integration time was set at 0.1 s. Ferric form of CMb and Mb from a stock solution of 160 µM and 200 µM respectively were added from 0.4 µM

to16 μM stepwise and the emission spectrum was recorded after each addition. The data obtained was fitted to Wolf's equation to calculate the binding constant. The intrinsic binding constant (Kb) was determined from the plot of Bound (I_o-I) / ligand (μM) *vs.* Bound (I_o-I) where [ligand] is the concentration of ferric carboxymycobactin / ferric mycobactin (μM) and I corresponds to fluorescence intensity at a particular concentration and Io corresponds to fluorescence intensity in free form. The intercept/slope gives the binding constant value.

The data were fitted to

$$\text{Bound } (I_o\text{-I}) / \text{ligand} = \text{Bound } (I_o\text{-I}) / \text{ligand} + 1/ \text{Kb } (I_o\text{-I})$$

Each set of data, when fitted to the above equation, gave a straight line with a slope of 1/ (I_o-I) and a y-intercept of 1/ Kb (I_o-I). Kb was determined from the ratio of the slope to intercept. An in-house non-linear least square analysis program or the Micro Cal Origin software package was used for curve fitting the data (Arounaguiri *et al.,* 2000).

2.18. Effect of iron levels on mycobacterial catalase-peroxidases

2.18.1. Mycobacterial strains and growth conditions

Slow growers such as *Mycobacterium tuberculosis* (ATCC 27294), *M. bovis* (ATCC 27289) and *M. bovis* BCG Danish strain and fast growers such as *M. kansasii* (ATCC 12478), *M. smegmatis* mc^2155, *M. fortuitum* and *M. vaccae* (JALMA) were used in this study. All the mycobacterial species were grown under high and low iron conditions as described earlier (for detailed procedures refer methodologies 2.5 & 2.6).

2.18.2. Preparation of cell-free cell extracts

The mycobacterial cells grown under high and low iron conditions were harvested, washed and re-suspended in phosphate buffer (0.05 M, pH 7.2). Then the cells were sonicated in a Vibra Cell sonicator (12 pulses with each pulse for 20 s with 20 s interval at 40 Hz) and centrifuged at 8000 rpm for 20 min to obtain the cell-free extract, which was stored at -80°C till further use.

2.18.3. Protein estimation

Total protein concentration in the cell-free extract was estimated by BCA protein assay reagent kit as per manufacturer's instructions.

2.18.4. Native-PAGE and activity staining in non-denaturing native gel (Wayne and Diaz, 1986)

All the stock solutions for native PAGE was prepared as mentioned in Section 2.8 with out SDS.

Table 2.6. Preparation of resolving gel mix for 7.5% acrylamide gel

Components	Volume (mL)
Acrylamide: Bisacrylamide	2
Resolving gel buffer	2
Double distilled water	4
10% Ammonium persulphate	0.04
TEMED	0.004

The resolving gel was allowed to polymerize and then the stacking gel was poured over it after appropriately positioning the comb.

Table 2.7. Preparation of 5% stacking gel mix

Components	Volume (µL)
Acrylamide: Bisacrylamide	750
Stacking gel buffer	750
Double distilled water	1350
10% Ammonium per sulfate	30
TEMED	4

About 40 µg of protein was loaded on to gels. Equal volumes of the protein samples and 2X sample buffer were mixed and centrifuged for 10 min at 10,000 rpm to remove any insoluble material. The clear supernatant was loaded onto gel and electrophoresis was carried out at constant voltage of 40V at 4°C. The electrophoresis was allowed to run

until the tracking dye was run out of the gel. The in-gel staining for catalase-peroxidase was done as described below.

2.18.5. Analysis of catalase and peroxidase activities

2.18.5.1. Dual Staining for catalase and peroxidase in-gels (Wayne and Diaz, 1986)

The gel was washed with 100 mM phosphate buffer (pH 7.2) three times at intervals of 10 minutes and finally incubated in 100 mL of freshly prepared phosphate buffer (100 mM, pH 7.2) containing 10 µL of H_2O_2 and 50 mg of 3, 3'-diamino benzidine (DAB) for 20 min. After the gel was washed thrice with double distilled water, it was incubated in 100 mL of DDW containing 50 µL of 30% H_2O_2 for 10 min. After incubation, the gel was washed with increasing amounts of DDW. Then the gel was transferred in to a freshly prepared mixture of 30 mL of potassium ferricyanide (2%) and 30 mL of anhydrous ferric chloride (2%) and the reaction was stopped with water.

2.18.5.2. Spectrophotometric assay for catalase

Catalase activity was determined spectrophotometrically (Beers and Sizer, 1952) by measuring the decrease in H_2O_2 concentration by reading the absorbance at 240 nm (E_{240} = 0.0435 $mM^{-1}cm^{-1}$). The assay was performed in a quartz cuvette by the addition of 1 mL of reaction mix containing 40 µg of sample, 100 mM phosphate buffer (pH 7.2) and the reaction was started by the addition of 30 mM 30% H_2O_2. The decrease in the absorbance at 240 nm for 1 min was calculated and the specific activity of catalase was expressed as micromoles of H_2O_2 decomposed per min per mg of total protein.

2.18.5.3. Spectrophotometric assay for peroxidase (Marcinkeviciene *et al*., 1995)

Peroxidase assay was performed in a microtitre plate. 40 µg of mycobacterial cell free sonicate was taken in a volume of 100 µL in 0.1 M phosphate buffer (pH 7.2), 100 µL of phosphate buffer was used as blank. To this 100 µL of substrate 1x TMB / H_2O_2 (Bangalore Genei) in 50 mM citrate buffer (pH 5.5) was added. The plate was incubated for 15 minutes in dark at room temperature. The reaction was stopped by the addition 50 µL of 1.25 N H_2SO_4 to each well. Absorbance was measured at 450 nm in ELISA reader. The peroxidase activity was expressed as A_{450nm} per mg total protein.

2.18.5.4. Isoniazid (INH)-mediated reduction of nitro blue tetrazolium (NBT) (Joanis *et al*., 1999)

Peroxidase-mediated activation of INH was assayed by the reduction of nitroblue tetrazolium (NBT) both spectrophotometrically and by activity staining in native gels (Saint-Joanis *et al*., 1999). In the spectro-photometric assay, the reaction mixture consist of 40 µg of total protein in 1 mL of solution containing NBT (600 µg) and INH (2.04 mg) in 50 mM sodium phosphate buffer, pH 7.2 (prepared by dissolving 30 mg of NBT and 102 mg of INH in 50 mL of 50 mM of sodium phosphate buffer, pH 7.2) and 30 mM of H_2O_2. After 1 h of incubation, 100 µL of isopropanol was added and the absorbance read at 570 nm.

For the activity staining of gels, essentially the same protocol (except the addition of isopropanol) was applied after electrophoretic separation of 40 µg of total protein under non-denaturing conditions.

2.18.5.5. Microplate Alamar Blue Assay (MABA) for determining the viability of mycobacteria in the presence of INH

The microplate version of the Alamar Blue Assay (MABA) (Franzblau *et al*. 1998) was used to assess the mycobacterial susceptibility to INH. High and low iron cells of *M. tuberculosis*, *M. bovis*, *M. bovis* BCG and *M. fortuitum* were adjusted to a cell density corresponding to McFarland 1 (equivalent to 1.5 x10^8 cells / mL). In a microtitre plate, a sterile solution of INH (stock solution of 8 mg / mL in water was diluted to get a working solution of 4 µg / mL) was serially diluted from 4 µg / mL to 0.0125 µg / mL. To two such separate sets of the drug dilutions, 100 µL of high and low cell suspensions were added respectively. Controls included wells containing the respective organisms minus the drug. The microplate was incubated in an atmosphere of 5% carbon dioxide at 37ºC for 5 days. Then 50 µL of Alamar Blue, prepared by mixing equal volumes of Alamar Blue with 10% Tween 80 was added to each well. The color changes were recorded visually after 30 min and 2 h after addition of the dye.

2.18.6. Analysis of the clinical isolates for catalase-peroxidase activity

Clinical isolates were obtained from Nizam's Institute of Medical Science (NIMS, Hyderabad; cultures were kindly provided by Dr. V. Lakshmi Head, Microbiology). Fig. 2.2 shows the detailed processing of the clinical isolates. The clinical isolates were categorized as sensitive (SIRE) to Streptomycin, Isoniazid, Rifampicin and Ethambutol and Isoniazid resistant based on the drug sensitivity testing. The cultures were revived from the BACTEC 12B vials into 7H9 / ADC medium. They were subcultured in Proskauer and Beck liquid medium under high (8 µg Fe / mL) and low (0.02 µg Fe / mL) iron conditions. *Mycobacterium tuberculosis* (ATCC 27294) strain was used as positive control (refer 2.5).

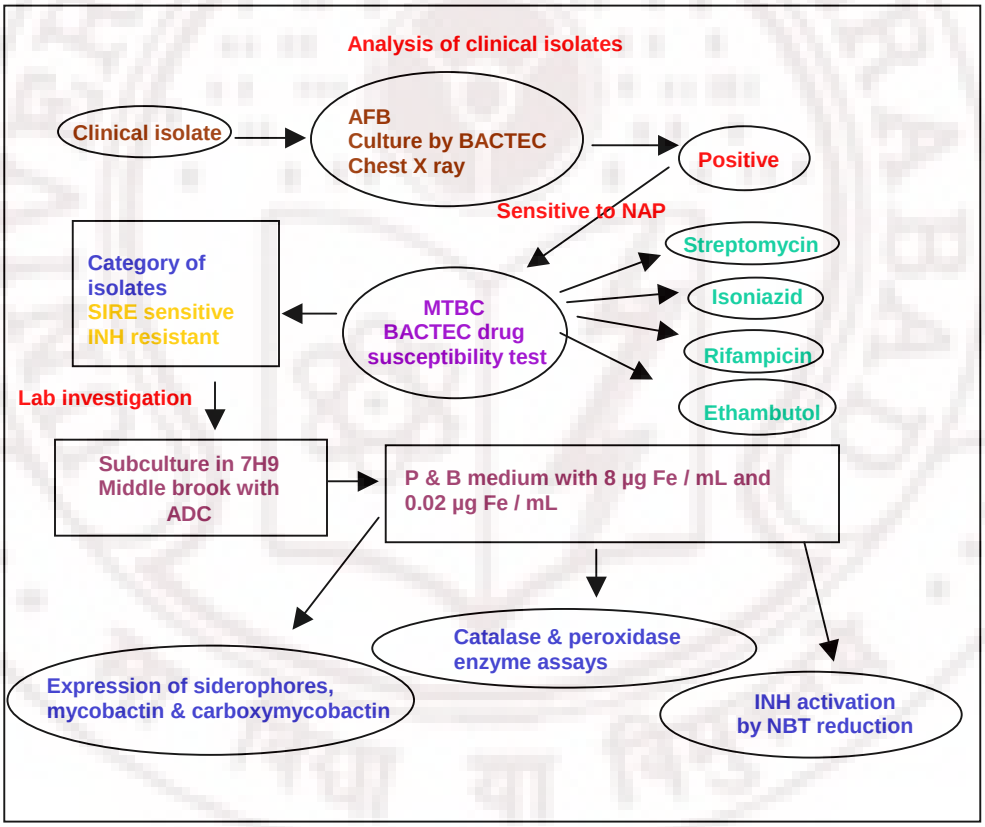

Fig. 2.2. Analysis of clinical isolates

The clinical isolates were assayed for catalase, peroxidase as described for the reference strains (for detailed protocols refer to methodologies 2.18.2, 2.18.4, 2.18.5 respectively).

CHAPTER 3

EXPERIMENTAL RESULTS

3.1. Studies on the effect of iron limitation in *M. tuberculosis*

3.1.1. Influence of iron levels on the expression of mycobactin and carboxymycobactin

Mycobacterium tuberculosis was grown in Proskauer and Beck medium with iron added to a final concentration of 0.02, 0.05, 0.1, 0.2, 0.4, 1, 4, 8 and 12 µg Fe / mL respectively. A five-fold increase in the expression of both mycobactin (Mb) and carboxymycobactin (CMb) was seen at 0.02 µg Fe / mL (Fig. 3.1) when compared to 8 and 12 µg Fe / mL respectively. There was a steady decrease in the levels of both these siderophores with increasing iron concentration in the growth medium. The cut-off point was 0.4 µg Fe / mL, above which there was repression of both Mb and CMb synthesis.

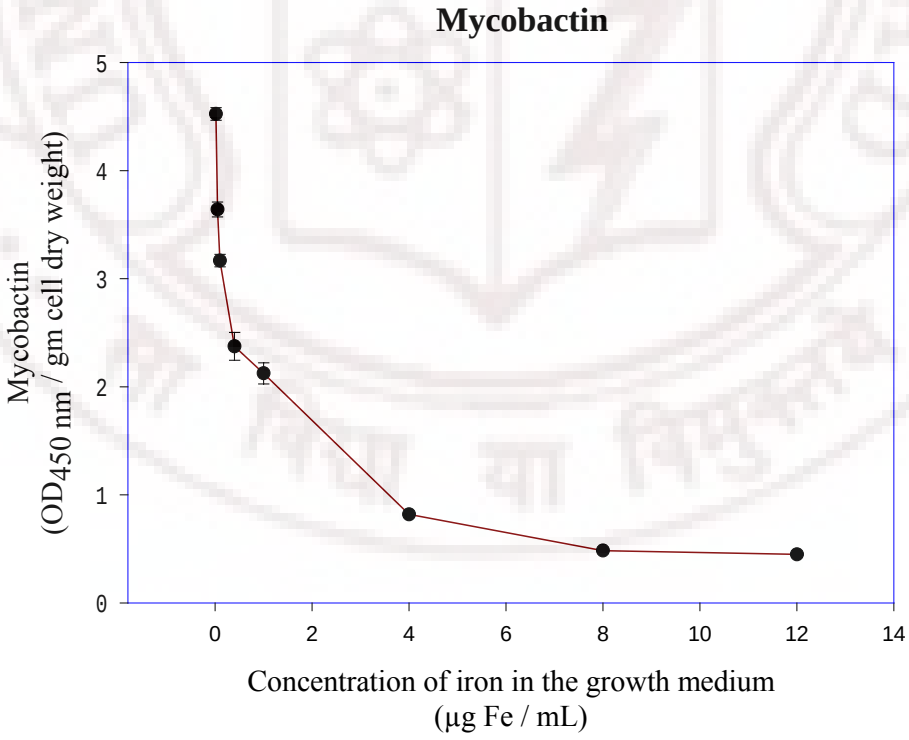

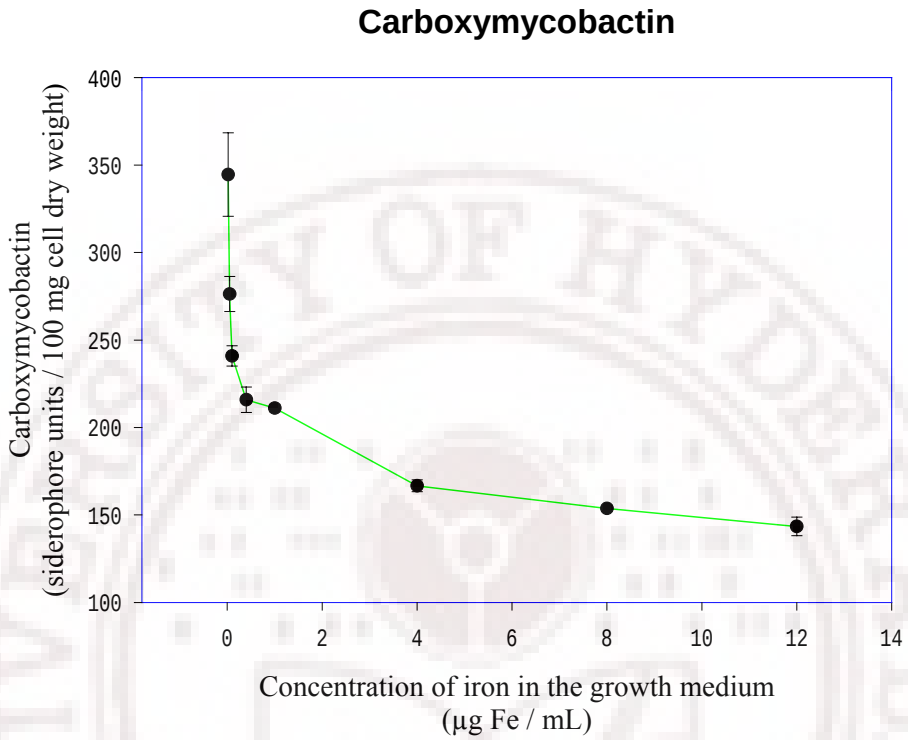

Fig. 3.1. Effect of iron levels on the expression of Mb and CMb. *Mycobacterium tuberculosis* was grown with 0.02, 0.05, 0.1, 0.2, 0.4, 1, 4, 8 and 12 µg Fe / mL respectively and the siderophores were assayed as described in Methods. Mb is expressed as OD450 nm units / gm cell dry weight and CMb is expressed as SU / 100 mg cell dry weight. The vertical bars represent the standard deviation of the mean from three independent experiments.

3.1.2. Identification of iron-regulated envelope proteins (IREPs): coordinated expression of Irep-28 with Mb and CMb

As described in the methods, the cell wall and cell membrane, obtained by differential centrifugation was solubilised by Triton X-114. Figure 3.2 shows the SDS-PAGE protein profile of the detergent and aqueous phases of cell wall and cell membrane proteins. A 28 kDa protein (henceforth called Irep-28) in the cell wall detergent fraction was found to be influenced by iron levels; maximal expression was seen in cells grown with 0.02 µg Fe / mL in the medium with the level decreasing with increasing iron until at 12 µg Fe / mL, there was complete repression of protein (Fig. 3.2 A). There was coordinate regulation of Irep-28 with Mb and CMb; high level of expression of all these

three components were seen at concentrations below 1 µg Fe / mL with almost complete repression above 8 µg Fe/ mL.

Several other iron-regulated proteins were also identified. In the cell wall aqueous phase, a 130 kDa protein (Irep-130) was seen under high iron conditions, with expression up-regulated in organisms grown with 0.4 µg Fe / mL to 12 µg Fe / mL (Fig. 3.2 b, lanes 4-8). A 54 kDa protein (Irep-54) was seen in the cell membrane aqueous phase upon iron limitation (Fig. 3.2 d), with the expression seen in organisms grown in 0.02 µg Fe / mL to 1 µg Fe / mL (lanes 1-5). An interesting observation was the expression of a 24 kDa (Irep-24) in organisms grown with 0.02 to 8 µg Fe / mL (lanes 1-7) and a 26 kDa (Irep-26) in organisms grown with 12 µg Fe / mL (Fig. 3.2 b). This pattern of expression of the two proteins was reversed in the aqueous phase of cell membrane proteins (Fig. 3.2 d), with the Irep-24 seen as a major band at 12 µg Fe / mL (lane 8) and the Irep-26 seen in all the lower concentrations of iron (lanes 1-7).

All subsequent studies were done with 0.02 µg Fe / mL and 8 µg Fe / mL for representing low and high iron growth respectively.

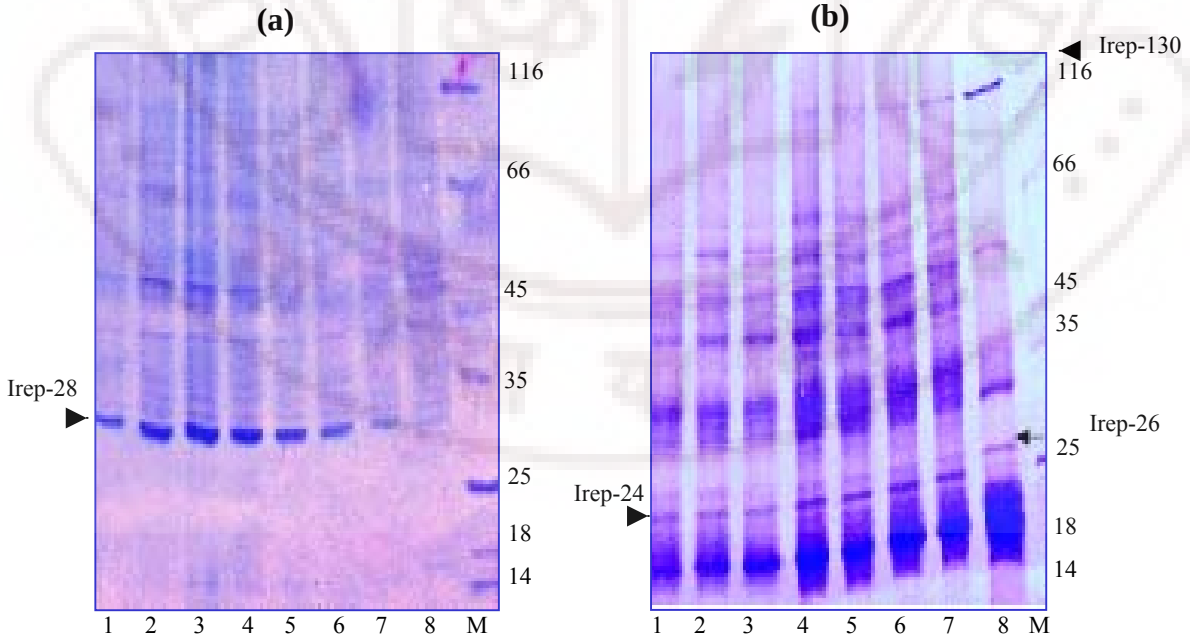

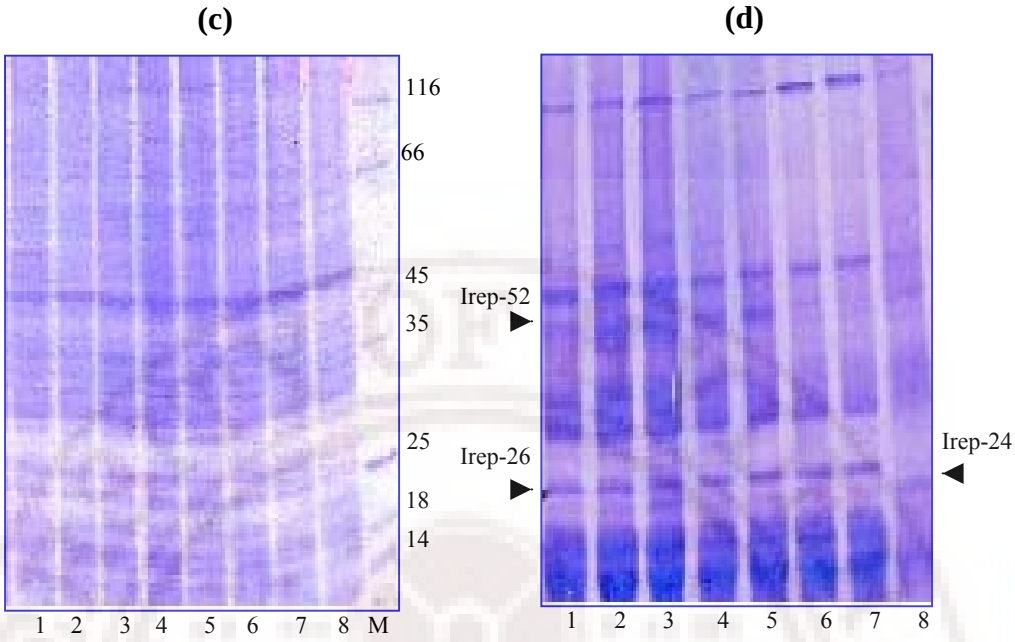

Fig. 3.2. Protein profile of cell wall and membrane fractions of *M. tuberculosis* grown under various iron concentrations. The proteins in the detergent and aqueous phase of the Triton X-114 solubilized cell wall (a and b respectively) and cell membrane (c and d respectively) were separated on a 5 - 20% gradient SDS-PAGE with lanes 1 to 8 corresponding to cells grown with iron 0.02, 0.05, 0.1, 0.4, 1, 4, 8, and 12 µg Fe / mL respectively. Arrows indicate the different iron-regulated envelope proteins.

3.1.3. Time-course studies

Six sets of flasks with iron added at 8 µg Fe / mL (high) and 0.02 µg Fe / mL (low) respectively were inoculated with 1 mL of McFarland 4 equivalent of cell suspension grown under low iron conditions. The cells were harvested on days 8, 12, 16, 20 and 25 respectively. Both Mb and CMb were assayed and the time course of expression of the Irep-28 was analyzed. Figure 3.3 a & b show the variations in the levels of Mb and CMb with increasing periods of growth. In four-day-old cultures, the spent growth medium showed high levels of CMb in both high and low iron organisms. However, since the cell growth was low, Mb and Irep-28 were not analyzed. From day 8, there was a steady increase in the levels of both Mb and CMb in low iron organisms, with a six-fold increase on day 20. High iron organisms showed low levels of both the siderophores, until on day 20; the CMb began to increase, reflecting the onset of iron

limitation in these cells that were originally iron sufficient. Mb was slower to increase as seen on day 25.

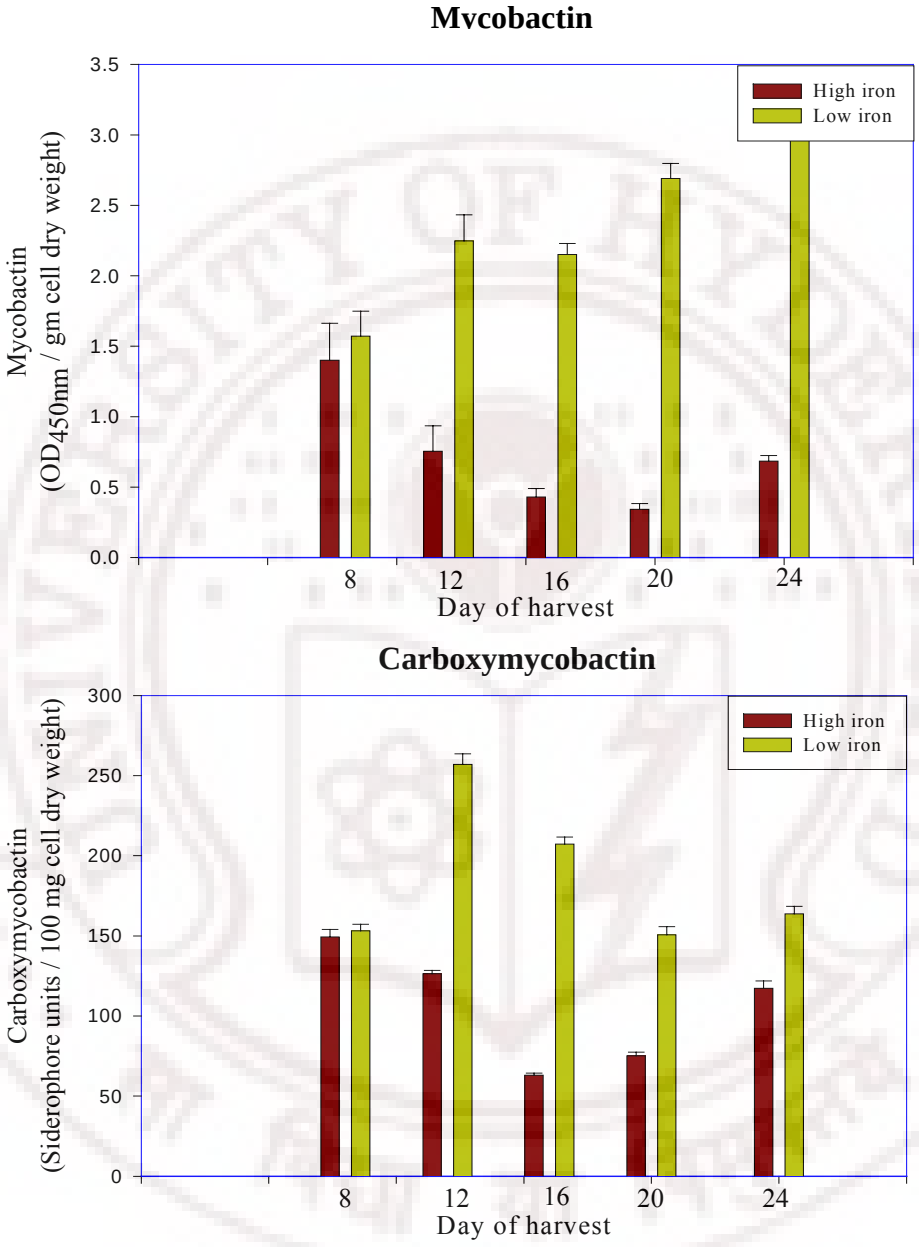

Fig.3.3. Time-course studies: expression of Mb and CMb. *Mycobacterium tuberculosis*, grown under high iron (8 µg Fe / mL) and low iron (0.02 µg Fe / mL) conditions were harvested on days 8, 12, 16, 20 and 24 respectively. Mb is expressed as OD450 nm units / gm cell dry weight and CMb is expressed as SU / 100 mg cell dry weight. The vertical bars represent the standard deviation of the mean from three independent experiments.

The expression of Irep-28 coincided with the siderophore profile. As the inoculum was from low iron culture, a faint band was detected in both low and high iron cultures on day 8. With increase in growth, on days 12 and 16, negligible expression was noted in the high iron cultures (Fig. 3.4), with significant levels in the corresponding low iron organisms. In the 20-day old high iron cultures, simultaneous with the expression of CMb, there was up-regulation of Irep-28 (Fig. 3.3 b), though mycobactin was still low.

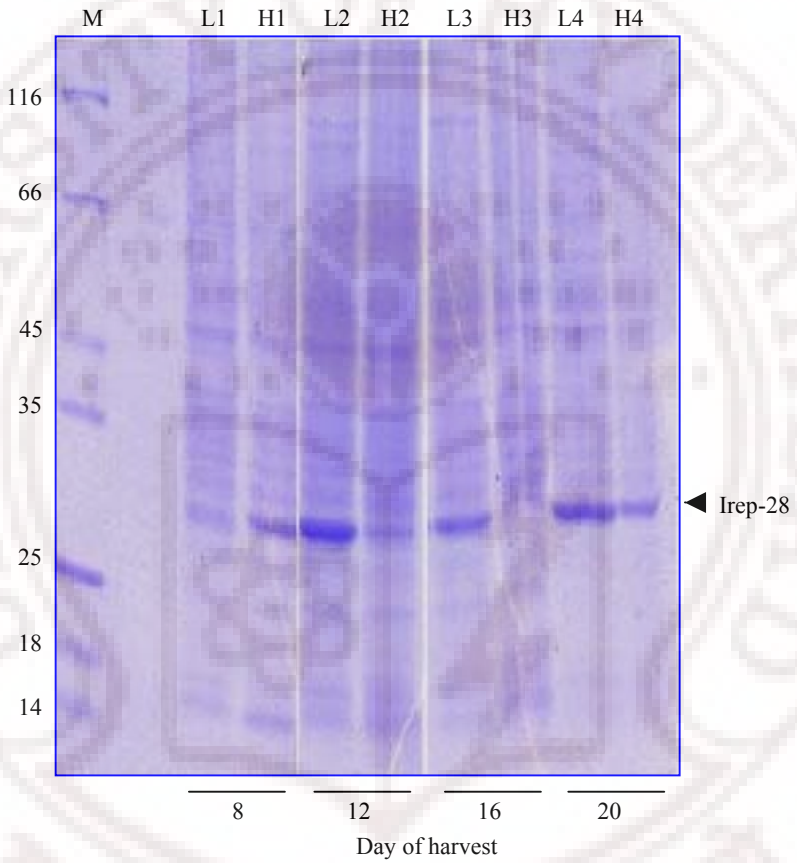

Fig. 3.4. Time course studies: expression of Irep-28. The detergent fraction of the Triton X-114 solubilised cell wall pellet was subjected to SDS-PAGE on 5 - 20% gradient gel. Lanes H and L represent the samples from high (8 µg Fe / mL) and low iron (0.02 µg Fe / mL) grown cells harvested on days 8, 12, 16 and 20 respectively.

3.1.4. Purification, sequencing and identification of the IREPs

3.1.4.1. Irep-28: DNA-binding protein HupB

Irep-28 was purified by preparative gel electrophoresis and shown as a single band in SDS-PAGE (Fig. 3.5). The purified protein was sequenced by tandem mass spectrometry after subjecting to tryptic digestion. Three distinctive peptides, comprising of residues 20 to 34, 87 to 94, and 95 to 103 were obtained (Fig. 3.6a). The amino acid sequence of these three peptides identified it as the DNA binding HU homologue HupB / histone-like protein, *hlp* (Accession No. Rv2986c, Swiss-Prot P95109).

The purified protein was also used to raise polyclonal mono-specific antibodies in rabbit.

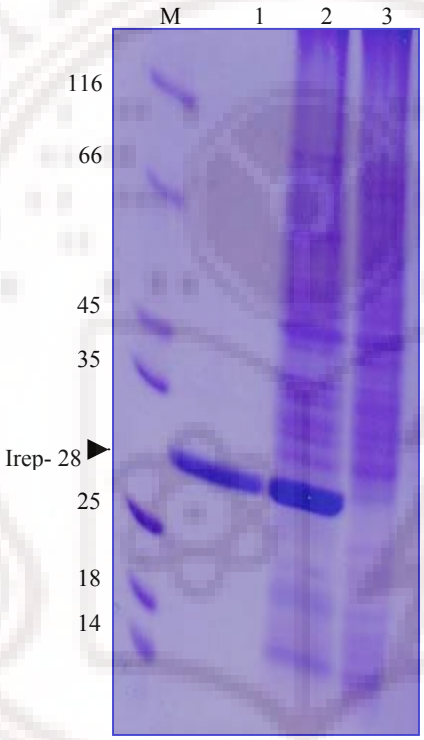

Fig. 3.5. Purification of Irep-28. The purified Irep-28 is represented in lane 1 with lanes 2 and 3 showing the unfractionated cell wall detergent proteins from cells grown with 0.02 µg Fe / mL and 12 µg Fe / mL respectively and. Lane M represents the molecular weight marker.

(a)

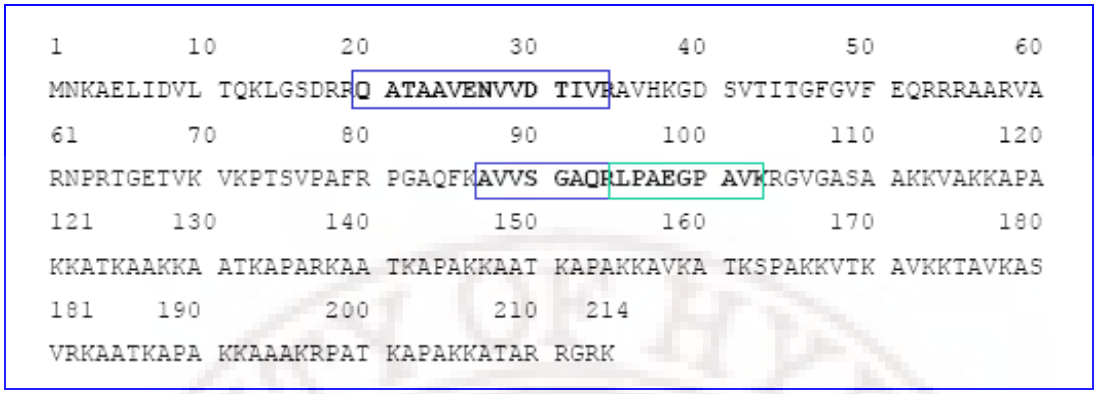

(b)

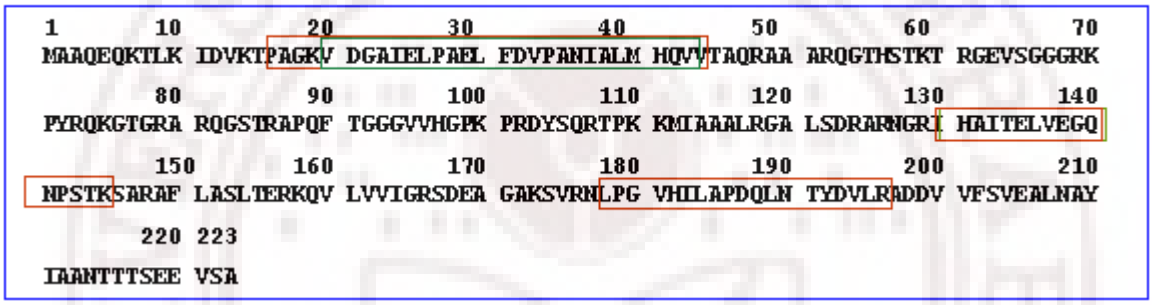

Fig. 3.6. Sequencing analysis. Panel (a) shows Irep-28 that was identified as Histone-like DNA binding protein, HupB (Swiss-Prot P95109); the three tryptic peptides sequenced by MS/MS are represented in boxes. In Panel (b), both Irep-26 and Irep-54 were identified as the 50S ribosomal protein L4 (Swiss-Prot P60729); the red boxes represent the tryptic peptides of Irep-26, while the green boxes represent the tryptic peptides that overlapped between Irep-26 and Irep-54.

3.1.4.2. Irep-54 and Irep-26: 50S ribosomal protein L4

Irep-54 and Irep-26, purified and sequenced in a similar manner to Irep-28 were identified as the 50S ribosomal protein L4. The three peptides of Irep-26 comprised of residues 15 to 44, 130 to 145 and 177 to 196; the sequences of the overlapping peptides in Irep-54 comprised of residues 15 to 44 and 20 to 48 (Fig. 3.6b), unambiguously identified the two proteins as the 50S ribosomal protein L4 from *M. tuberculosis*. The overlapping peptide sequences between the two proteins can be seen from the sequence information listed in Table.3.1.

Table.3.1. Peptide residues identified by sequencing Irep-54 and Irep-26

Sample	MS / MS identified peptides	Protein identified as
Irep-54	• VDGAIELPAELFDVPANIALMHQVVTAQR • TPAGKVDGAIELPAELFDVPANIALMHQVVTAQR	P60729|RL4_MYCTU 50S ribosomal protein L4 - *Mycobacterium tuberculosis*
Irep-26	• IHAITELVEGQNPSTK • NLPGVHILAPDQLNTYDVLR • TPAGKVDGAIELPAELFDVPANIALMHQVVTAQR	P60729|RL4_MYCTU 50S ribosomal protein L4 - *Mycobacterium tuberculosis*

3.1.5. Studies on the characterization of HupB

3.1.5.1. Bioinformatic analysis

The N-terminal 90 amino acids of the 214 amino acids long HupB of *M. tuberculosis* showed homology with the corresponding homologue expressed by other bacteria. The C-terminal end of HupB was found to be unique to mycobacteria, as seen from the multiple sequence alignment of the HupB from *M. tuberculosis* with that of other bacteria (Fig. 3.9). This stretch of the protein, rich in the basic amino acid lysine was composed of several repeats comprising of lysine and alanine residues. This, in addition to the helix-turn-helix repeats predicted by the Scratch protein structure program implied the DNA binding property of the protein (Fig. 3.7). The presence of lysine residues conferred a high pI value of 12.5 to the protein and resulted in the faster migration of the 22 kDa protein as a 28 kDa protein.

Fig. 3.7. Secondary structure prediction of HupB. Using Scratch protein prediction software, the secondary structure of HupB predicted is hypothesized to be helix-turn helix without disulfide bonds. The red coloured letter H represents alpha helix, the black E is the extended strand and C represents structures other than these.

Comparison of the amino acid sequence of HupB among the members of the *M. tuberculosis* complex (Fig. 3.10) revealed that the protein from the vaccine strain BCG Pasteur and the *M. bovis* AN5, used in the lab for production of bovine PPD showed deletion of 9 amino acids (137-146 amino acids) while *M. marinum* showed a relatively higher number of amino acids residues (220) when compared to the HupB protein from *M. tuberculosis*. Extension of the comparison of the primary sequence of the protein with other mycobacterial species showed several differences, as seen from multiple sequence alignment (Fig. 3.8). Phylogenetic tree construction revealed that the ancestral mycobacteria such as *M. ulcerans*, *M. marinum* and *M. kansasii* formed a distinct well-separated cluster; *M. avium*, *M. paratuberculosis* and *M. intracellulare* came together from a single branch while *M. leprae* deviated to form a separate branch. The closely related *M. bovis* AF2122/ 97 and *M. tuberculosis* grouped together; BCG Pasteur, derived from *M. bovis* and the laboratory grown *M. bovis* AN5, both of which expressed HupB

with 9 amino acid deletion separated out from *M. tuberculosis* (Fig. 3.11). The relatedness of the mycobacteria with *Nocardia*, *Rhodococci* and *Streptomyces* is evident from Fig. 3.6 Further, from the phylogenetic analysis of HupB performed across members of different genera of bacteria, it is evident that other bacteria form a separate cluster, with little relatedness to the mycobacterial HupB (Fig. 3.12).

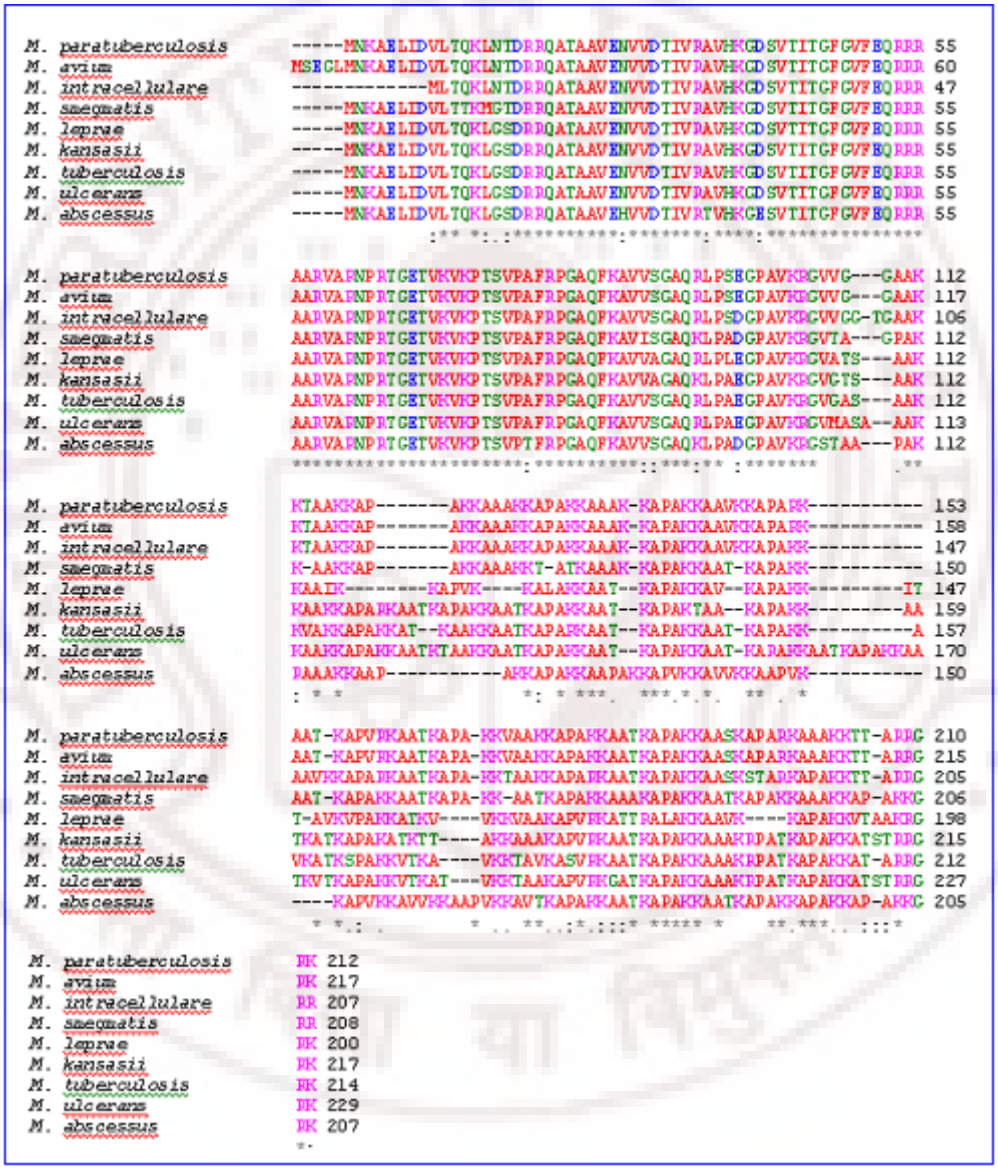

Fig. 3.8. HupB comparison of among different mycobacterial species. EBI CLUSTALW multiple sequence alignment of *Mycobacterial spp* indicating variable deletions in the C-terminal region among the members

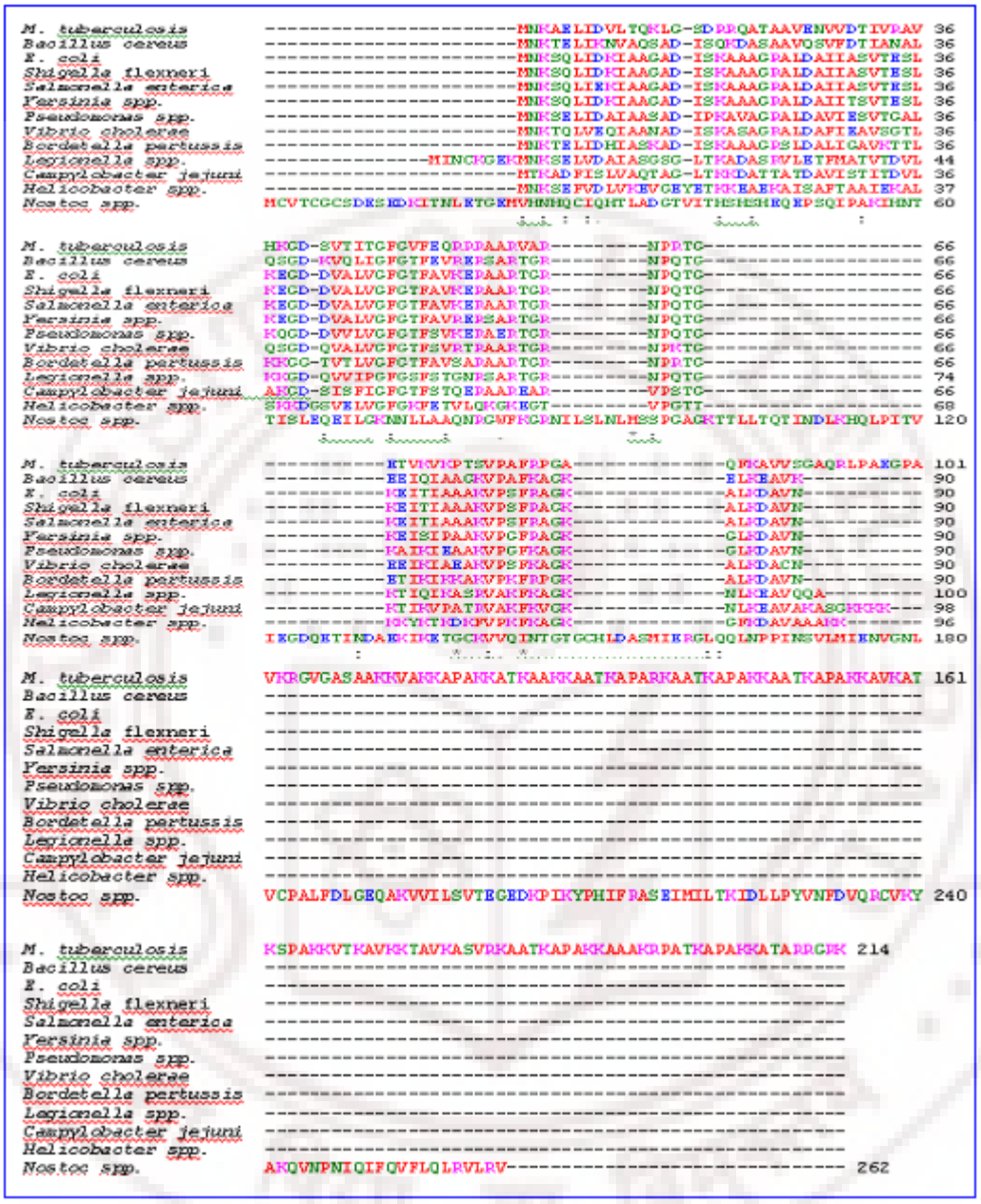

Fig. 3.9. Comparison of HupB among the different bacterial species. EBI CLUSTALW multiple sequence alignment of bacterial spp. indicates the significant deletions in the C-terminal region in comparison with *M. tuberculosis.*

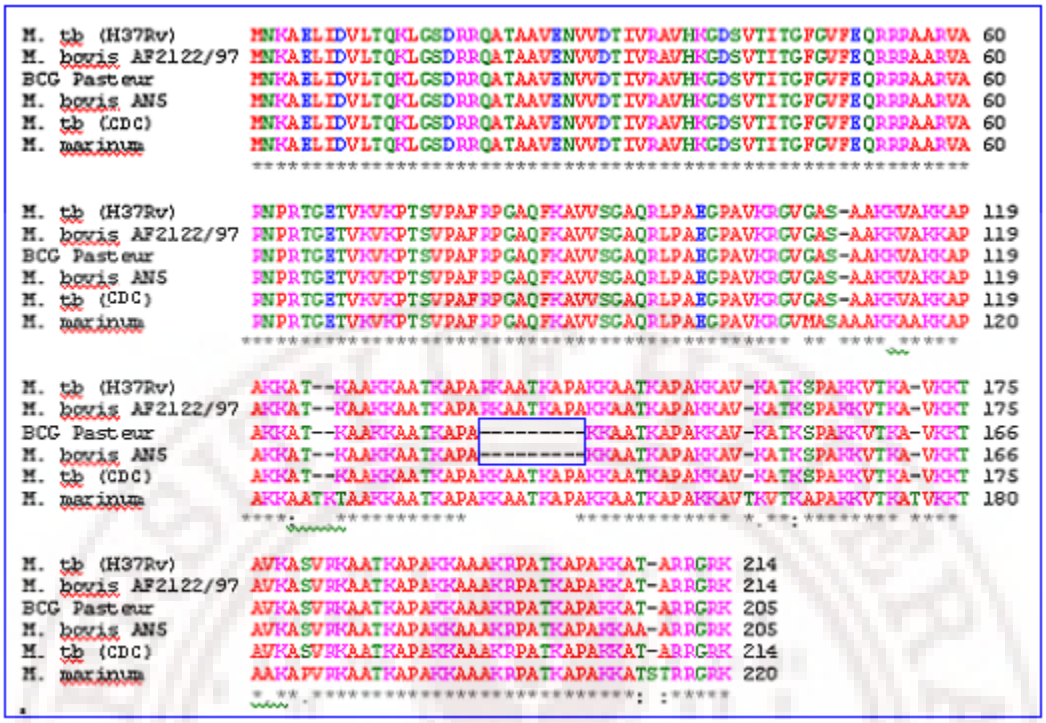

Fig. 3.10. Heterogeneity of HupB among the members of *M. tuberculosis* complex (MTBC). EBI CLUSTALW multiple sequence alignment of MTBC members. The boxed region indicates the region (amino acids 137-146) of deletion in *M. bovis* BCG Pasteur and *M. bovis* AN5

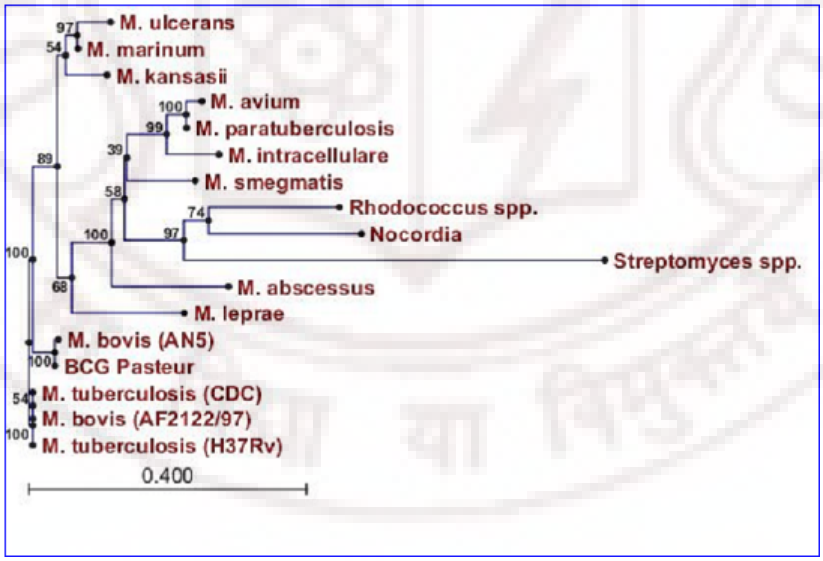

Fig. 3.11. Phylogenetic analysis of HupB among different mycobacterial spp. The phylogenetic tree generated by neighbor joining analysis using 100 bootstrap replicates, rooted at midpoint and bootstrap values. The numbers shown as a percentage refers to the divergence between the sequences.

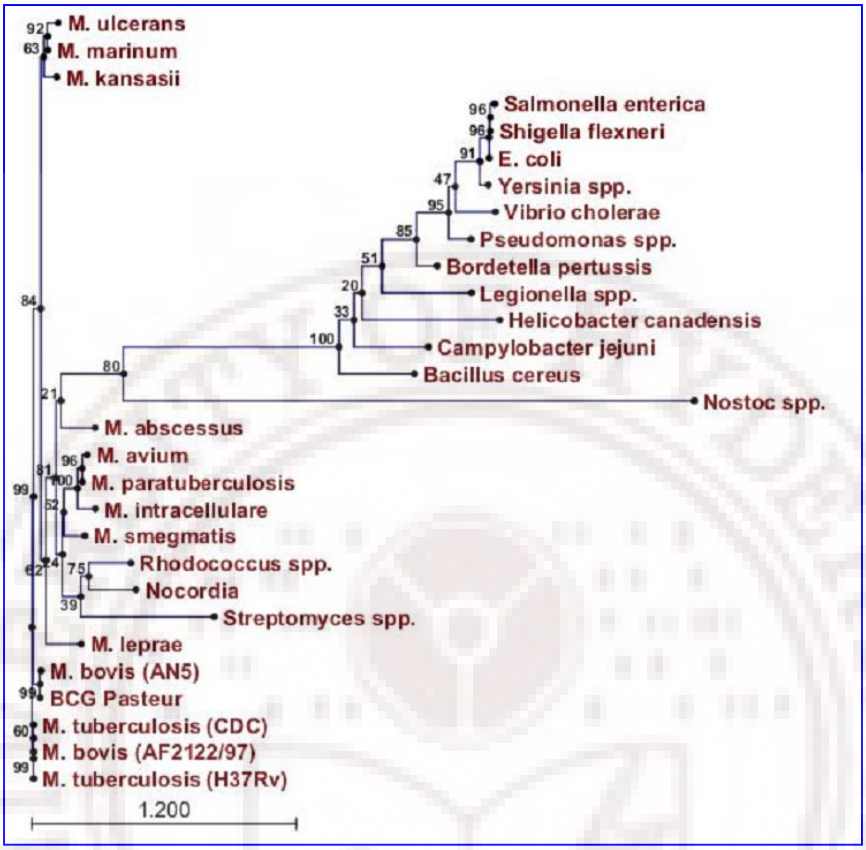

Fig. 3.12. Phylogenetic analysis of HupB from all bacteria. The phylogenetic tree was generated with neighbor joining analysis using 100 bootstrap replicates, rooted at midpoint and bootstrap values. The numbers were shown as percentages refer to the divergence between the sequences.

Role of HupB in *M. tuberculosis*

As the expression of HupB was regulated by iron and shown to be associated with that of the two siderophores mycobactin and carboxymycobactin, studies were done to see if HupB played a role as ferric siderophore receptor. The ligand binding studies, described below were done to assay the association of the protein with mycobactin / carboxymycobactin.

In silico analysis of the functional partners of HupB (Fig. 3.13), predicted by SMART software revealed that the smaller and larger subunits of isopropylmalate

isomerase (encoded by *leuC* and *leuD* respectively) and a 233 amino acid protein encoded by Rv2989 annotated as a probable transcriptional regulator occurred as neighborhood genes and *mfd*, a transcriptional repair coupling factor and *rplR*, coding for 50S ribosomal subunit L18 were predicted to be co-occurrence genes.

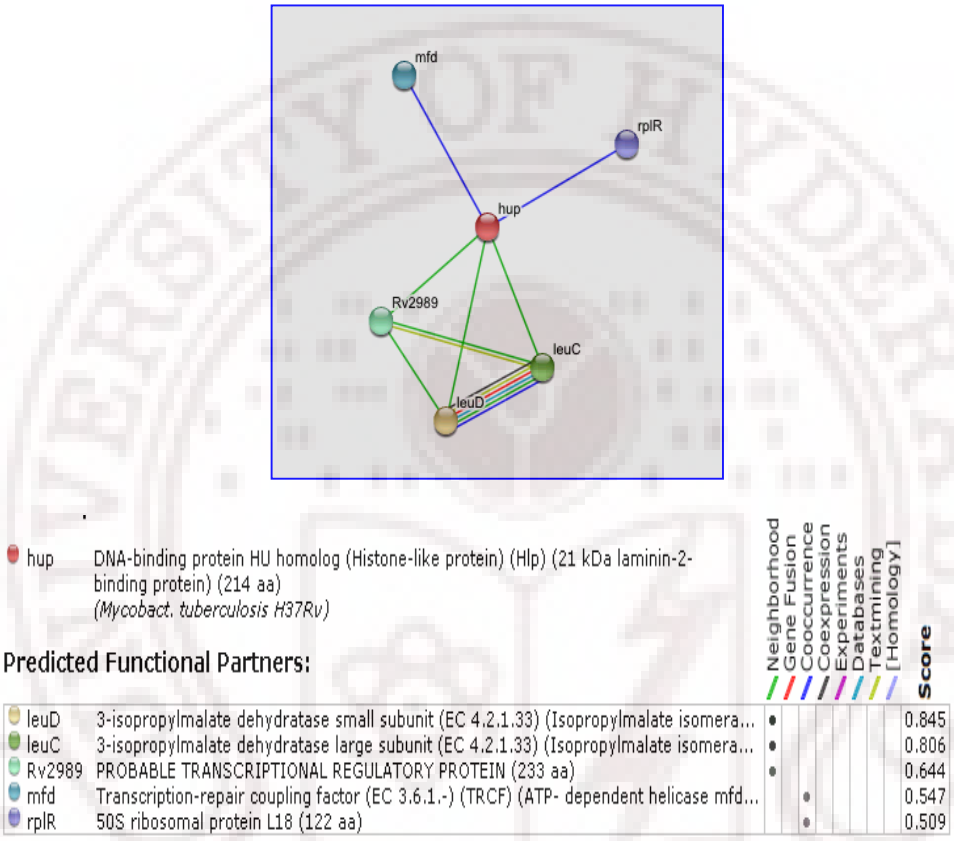

Fig. 3.13. Functional partners of *hupB*, as identified by SMART soft ware.

3.1.5.2. Surface localization of HupB

(a). *In silico* analysis

Using TB PRED software, HupB was predicted to be a membrane protein anchored to the membrane by lipid.

(b). Confocal microscopy

The surface localization of HupB was evident in the low iron organisms of *M. bovis* BCG Moreau subjected to immunoreactivity with anti-HupB antibodies. Propidium Iodide used as a counter stain showed equal number of high iron organisms that however

did not express HupB as deduced from the lack of the green fluorescence in Panel B1 (Fig. 3.14).

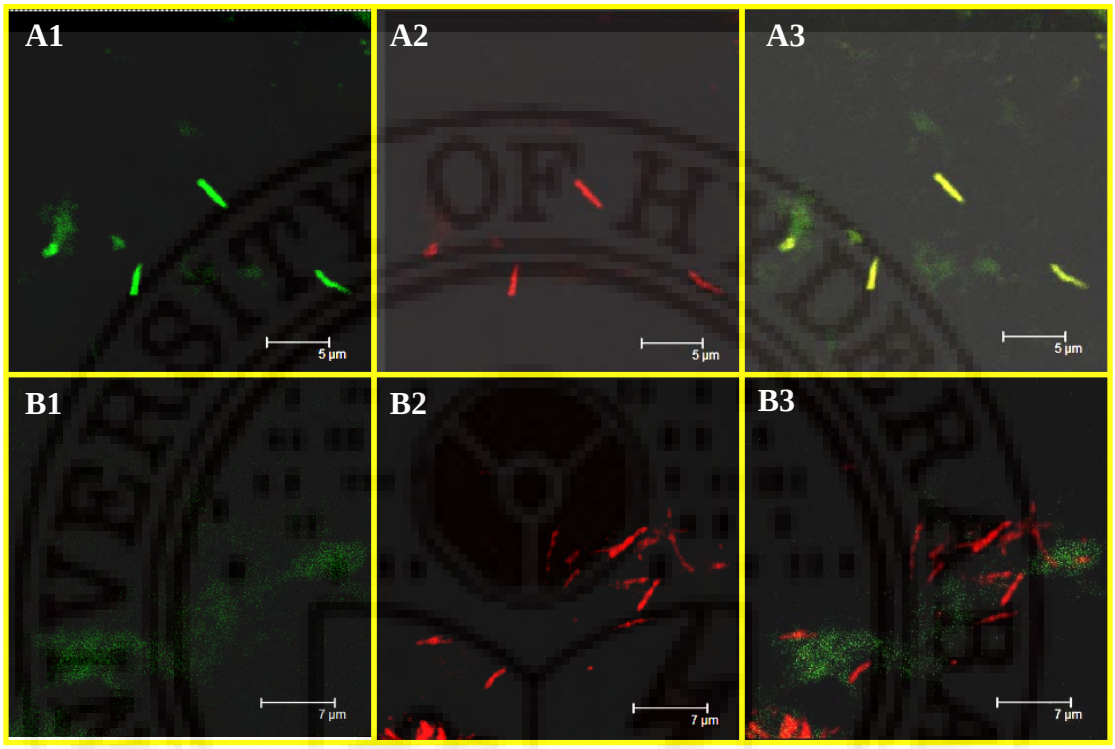

Fig. 3.14. Surface expression of iron-regulated HupB in *M. bovis* BCG Moreau by confocal microscopy. Low-iron (A1 to A3) and high-iron (B1 to B3) organisms were incubated with anti-HupB antibodies and detected using FITC-conjugated secondary antibody. The bacteria were counter stained with the DNA stain propidium iodide.

3.1.5.3. Variation in the expression of HupB among *M. bovis* BCG strains

Eight *M. bovis* BCG strains including Denmark, Birkhaug, Pasteur, Moreau, Connaught, Phipps, Russia and Sweden were subjected to growth under high (8 µg Fe / mL) and low (0.02 µg Fe / mL) iron conditions. All the strains showed a 3-15 fold increase in the levels of Mb and CMb, when compared to high iron conditions (Fig. 3.15 a & b). While the levels of CMb among the BCG strains were almost identical, notably high level of Mb was expressed by the Denmark strain, with low levels of expression in BCG Russia.

Mycobactin

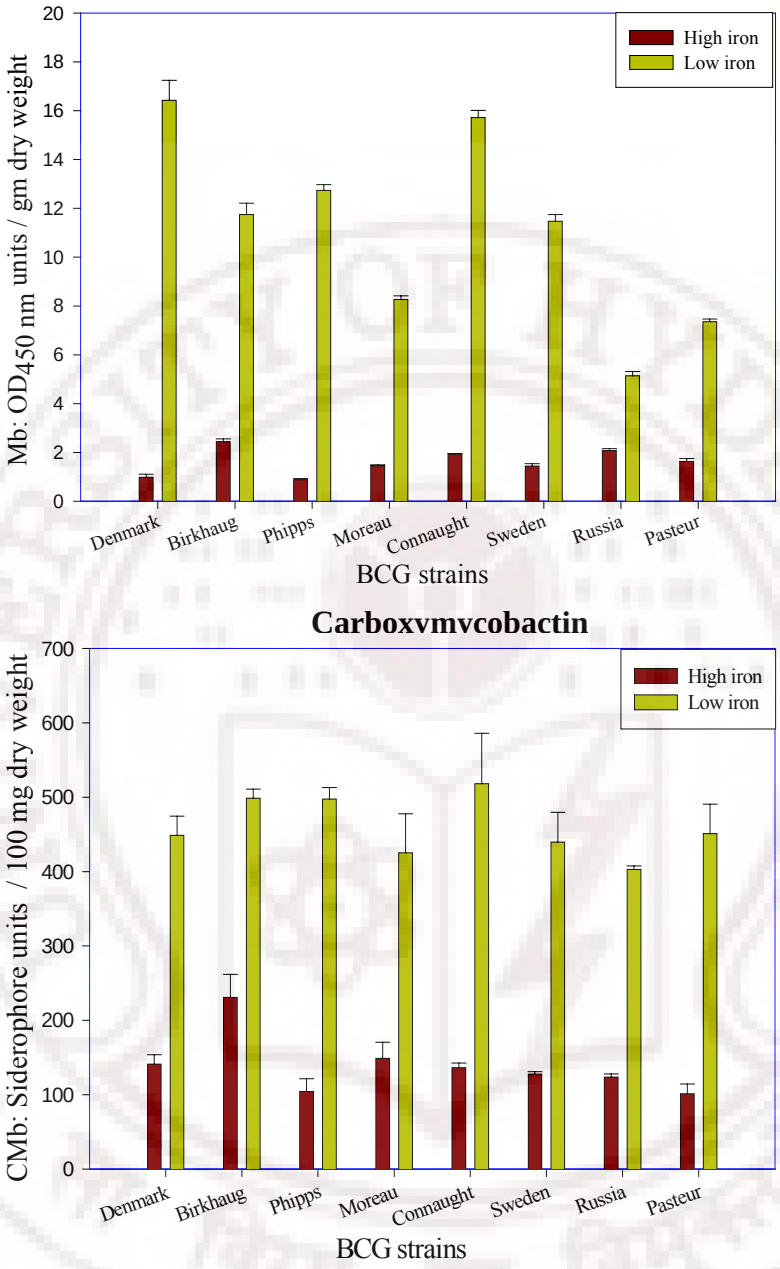

Fig. 3.15. Expression of Mb and CMb in *M. bovis* BCG strains. *M. bovis* BCG strains were grown under high iron (8 µg Fe / mL) and low iron (0.02 µg Fe / mL) conditions respectively. Mb and CMb were assayed and were found up regulated upon iron limitation in all the strains. The vertical bars represent the standard deviation of three independent experiments.

These BCG strains also showed variations in HupB. (Fig. 3.16 & Table 3.2). Low levels of the protein, irrespective of iron levels were noted in the strains Pasteur, Phipps

and Sweden. Iron limitation induced HupB in Denmark, Birkhaug, and Connaught similar to that seen in *M. tuberculosis*. Under the conditions in this study, HupB could not be detected in BCG Russia. The HupB protein profile observation in SDS-PAGE was reflected in the immunoblots developed with anti-HupB antibodies.

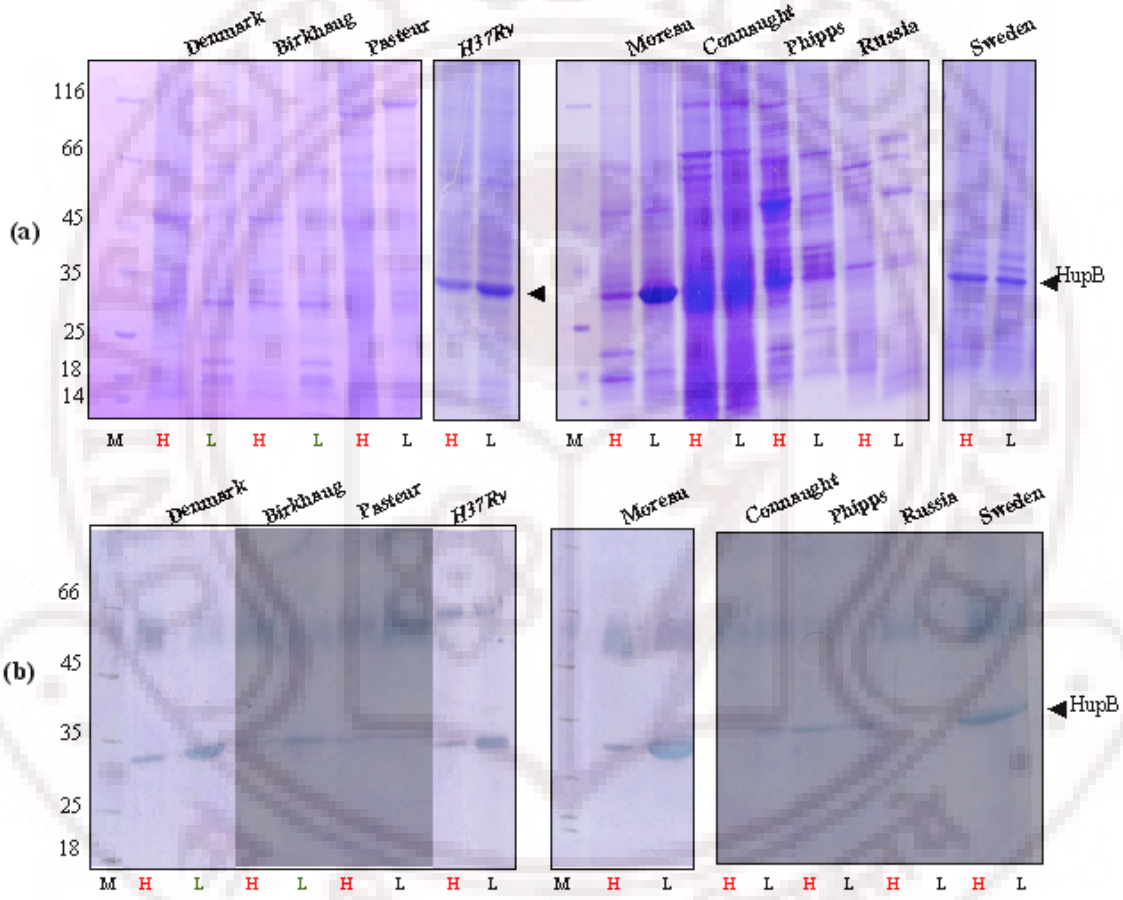

Fig. 3.16. Expression of HupB in *M. bovis* BCG strains. The cell wall detergent phase was subjected to SDS-PAGE (Panel a) and immunoblotting with rabbit anti-HupB antibodies (Panel b). Lanes H and L represent high iron (8 µg Fe / mL) and low iron (0.02 µg Fe / mL) samples.

Table.3.2. Influence of iron levels on the expression of HupB in the different *M. bovis* BCG strains.

BCG strains	Denmark	Birkhaug	Pasteur	Moreau	Connaught	Phipps	Russia	Sweden	*H37Rv*
Level of HupB expression	++	+	++	+++	+	++	Not detected	++	++
Influence of iron levels on expression	I*	I*	C**	I*	I*	C**		C**	I*

* Induced under low iron conditions, **Constitutively expressed

3.1.5.4. Ligand binding studies

In order to study the interaction of HupB with Mb and CMb, the protein and the respective siderophores were first purified as shown below.

(a) Purification of HupB protein

HupB protein was obtained both from the cell wall fraction and as a recombinant protein by cloning of the full-length gene.

- **Purification of the native HupB protein.** HupB was purified from the Triton X-114 solubilized cell wall detergent fraction of *M. tuberculosis* (as described in the Materials and Methods 2.10).
- **Cloning, expression and purification of recombinant HupB**

The cloning and expression of rHupB is represented in Fig. 3.17 & Fig. 3.18. The full-length 645 bp *hupB* amplicon and the vector pET-28a (+), subjected to double digestion with *NdeI* and *HindIII* were ligated and initially transformed into *E. coli* DH5α. Positive clones were selected by colony PCR. The recombinant plasmid pUH-hupB was isolated and transformed into the expression host *E. coli* BL21 (DE3). One of the positive clones, identified by colony PCR was used for preparation of rHupB (Fig. 3.17).

The transformants were small and the growth rate was relatively low as compared to the host organism. The rHupB was expressed as insoluble protein in inclusion bodies upon induction with 1 mM IPTG for 2 h at 37ºC (Fig. 3.18). The insoluble pellet, obtained by centrifugation was solubilised in sample buffer and subjected to SDS-PAGE. The rHupB, purified by gel elution was re-run and shown to be a single band.

The mobility of the rHupB was slightly retarded as compared to the HupB from cell wall fraction. This is evident from the immuno blot of the two preparations developed with anti-HupB antibody (Fig. 3.18).

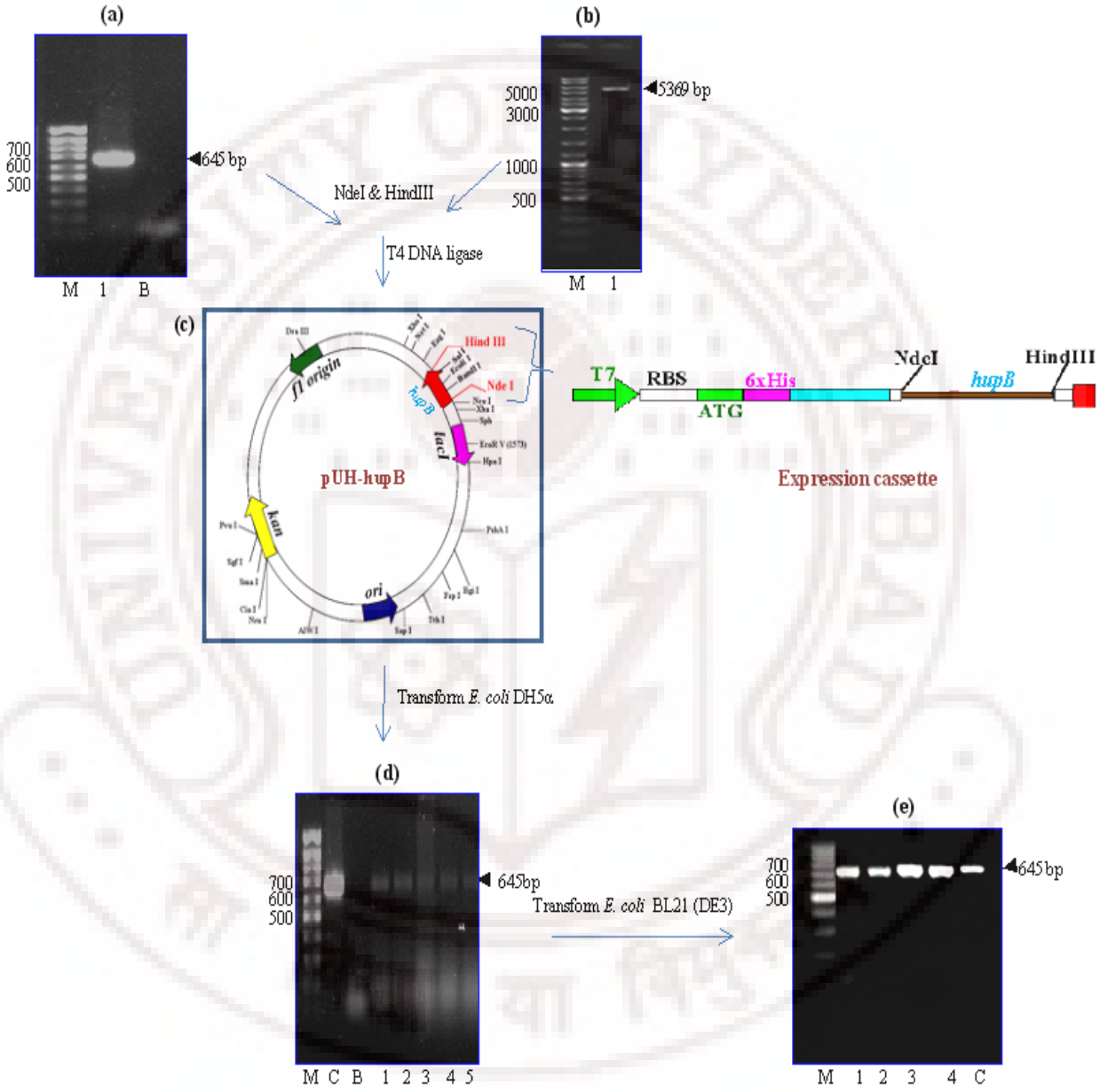

Fig. 3.17. Cloning of *hupB* gene (645bp) from *M. tuberculosis.* Panel (a) represents the 645 bp *hupB* amplicon (lane 1) and Panel (b) shows the pET-28a (+) plasmid (lane 1) were digested and ligated to generate the recombinant plasmid pUH-hupB (Panel c). The *hupB* amplicon was detected in several *E. coli* DH5α transformants (Panel (d), lanes 1-5, c and d representing positive control and blank respectively). Panel (e) shows the 645 bp insert in the *E. coli* BL21 (DE3) transformants (lanes 1-4) in which lane C represents the positive control. Lane M is the 100 bp ladder used as molecular marker.

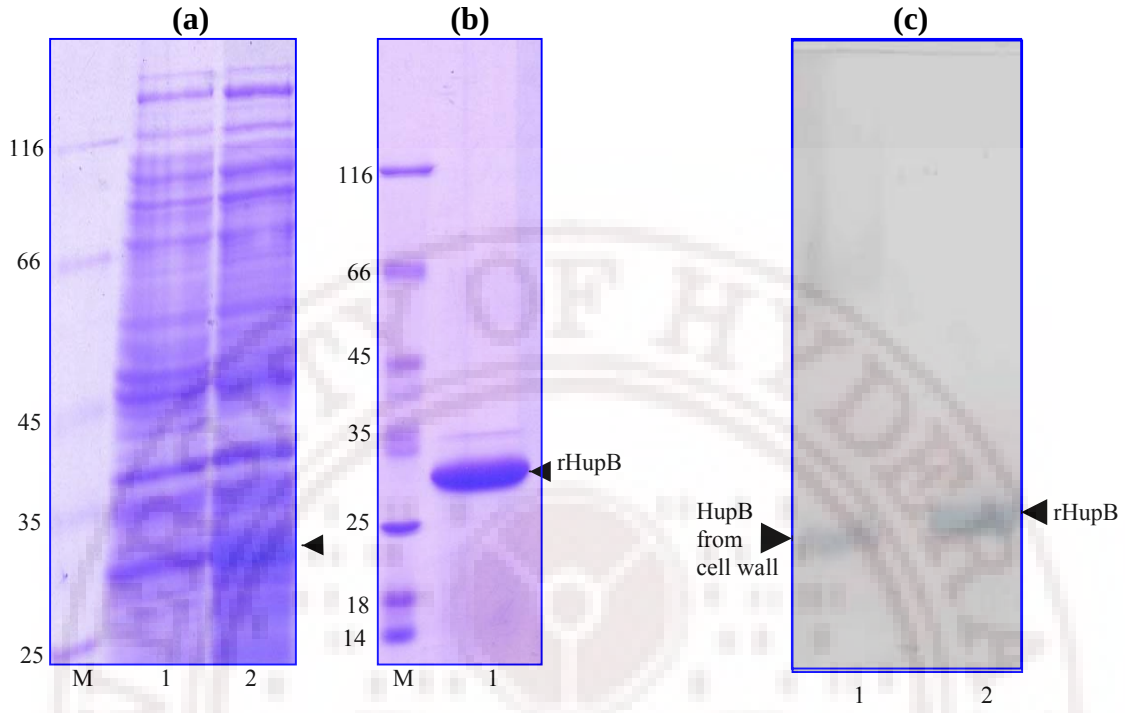

Fig. 3.18. Expression and purification of rHupB. SDS-PAGE analysis of the lysate of un-induced (lane 1) and IPTG induced (lane 2) *E. coli* BL21 (DE3). Panel (b) shows the purified rHupB protein (lane 1). Lane M represents the molecular weight marker. The mobility shift of the rHupB (lane 2) showing slower migration than the cell wall associated HupB (lane 1) is shown in the immunoblot of the respective proteins with anti-HupB antibody

(b) Purification of Mb and CMb

Using reverse phase HPLC, the hydrophobic Mb was separated with a gradient of methanol, acetonitrile and water, while the relatively more hydrophilic CMb was separated with acetonitrile and water gradient. As reported earlier (Barclay *et al*., 1986) both the siderophores separated out as a mixture of almost identical compounds with maximal absorbance at 450 nm. Mb resolved into 9 peaks with retention time between 12-28 min (Fig. 3.19a), while CMb resolved into 15 compounds with retention time between 15-23 min (Fig. 3.19b).

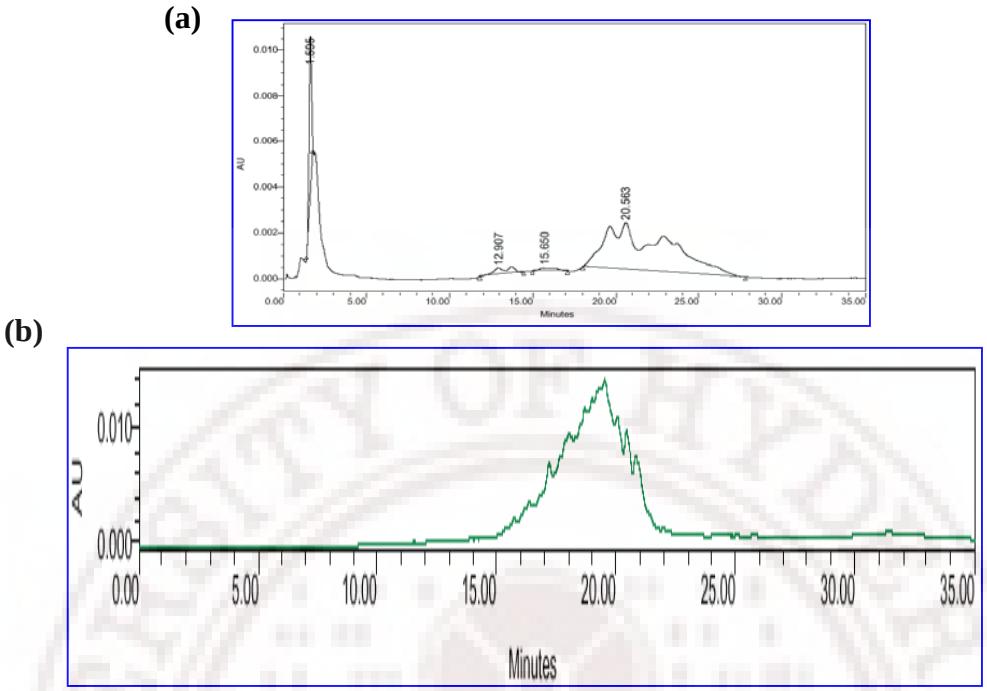

Fig. 3.19. Purification of Mb and CMb by HPLC. The chloroform extracts of Mb and CMb were subjected to reverse phase HPLC on Water's C18 column (150 mm x 4.6 mm id, 5 µm). The eluate, monitored at 450 nm shows the mixture of compounds representing Mb and CMb respectively in Panels (a) and (b).

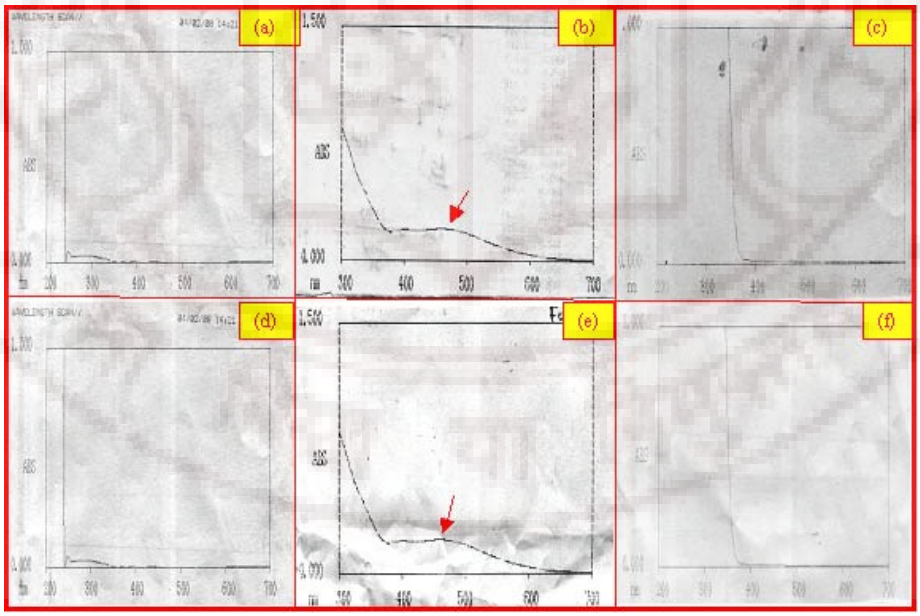

Fig. 3.20. UV-Visible Spectral scan of Mb and CMb. Panels (b) and (e) show the absorption maximum of ferric-Mb and ferric-CMb respectively at 450 nm. The corresponding peak was not observed in the desferri forms of Mb and CMb (Panels (c) and (f)) and the chloroform blank (Panels (a) and (d)).

3.1.5.4.1. Preparation of ^{59}Fe- Mb and ^{59}Fe- CMb

Prior to the preparation of the radiolabelled ferric siderophores, the amount of Fe^{3+} required to bind a known concentration of the siderophore was determined. Desferri Mb and CMb do not absorb at 450 nm while the ferric forms showed absorption maximum at 450 nm (Fig. 3. 20).

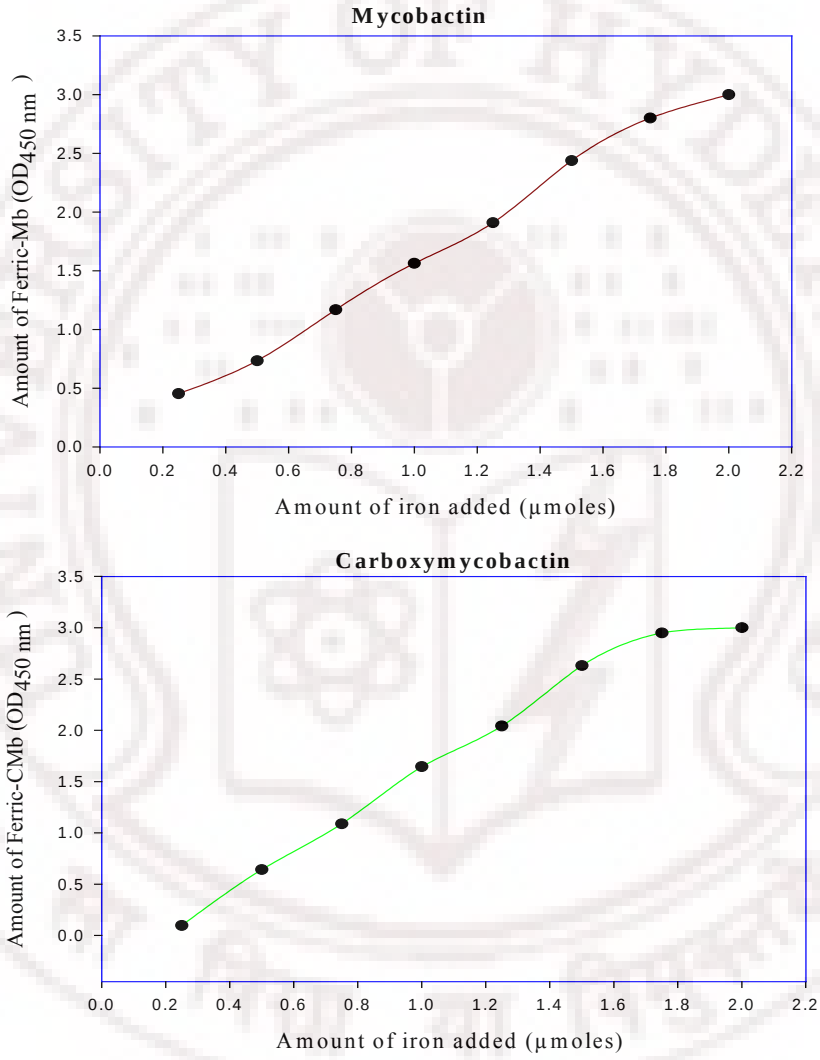

Fig. 3.21. Determination of iron-binding capacity of Mb and CMb. Increasing amounts of ferric chloride from a stock solution of 250 mM was added to 16 µg of Mb / CMb respectively. The amount of the ferric-Mb and ferric-CMb formed was measured by reading at OD450 nm. The saturation value was determined as the point where further addition of iron did not result in the further increase in OD450 nm.

Hence titration of known concentration of Mb and CMb with increasing amount of Fe^{3+} was done. It was determined that 16 µg of Mb / CMb bound 2 µmoles of Fe^{3+} (Fig. 3.21). Radioactive Fe^{3+} (specific activity 5.77 Ci / gm) was suitably diluted with cold iron and 2 µmoles of $^{59}Fe^{3+}$ was added to 16 µg Mb / CMb respectively to prepare ^{59}Fe- Mb and ^{59}Fe- CMb respectively.

3.1.5.4.2. Binding studies

(a). Radiolabeled studies

25 µg of HupB protein purified from the cell wall fraction was immobilized on nitrocellulose membrane and several such individual strips were incubated with increasing concentrations of ^{59}Fe-Mb / ^{59}Fe-CMb respectively (Fig. 3.22). The amount of radioactivity associated with each strip was measured and plotted to show the dose-dependent binding of the ferric-siderophores to HupB. With increasing concentrations of the ferric-siderophore, it was observed that both Fe-Mb and Fe-CMb bound HupB in a dose-dependent manner until it reached a plateau indicating the saturation value that was almost similar for both the siderophores.

The specificity of the binding of ^{59}Fe-Mb / ^{59}Fe-CMb to HupB was demonstrated by the inhibition of binding of the ferric-siderophores by anti-HupB antibodies; more than 50% inhibition was achieved with both ferric-Mb and ferric-CMb (Fig. 3.23). The specificity of this binding was evident from the relatively low level of binding to a non-specific protein BSA used as control. Non-specific binding of the ferric-siderophore to the nitrocellulose membrane was almost negligible.

From the displacement studies (Fig. 3.24), it was evident that addition of cold ferric-siderophore(s) displaced the bound label from HupB. With increasing addition of the cold ferric-siderophore(s), there was a corresponding displacement of the bound ^{59}Fe-Mb / ^{59}Fe-CMb.

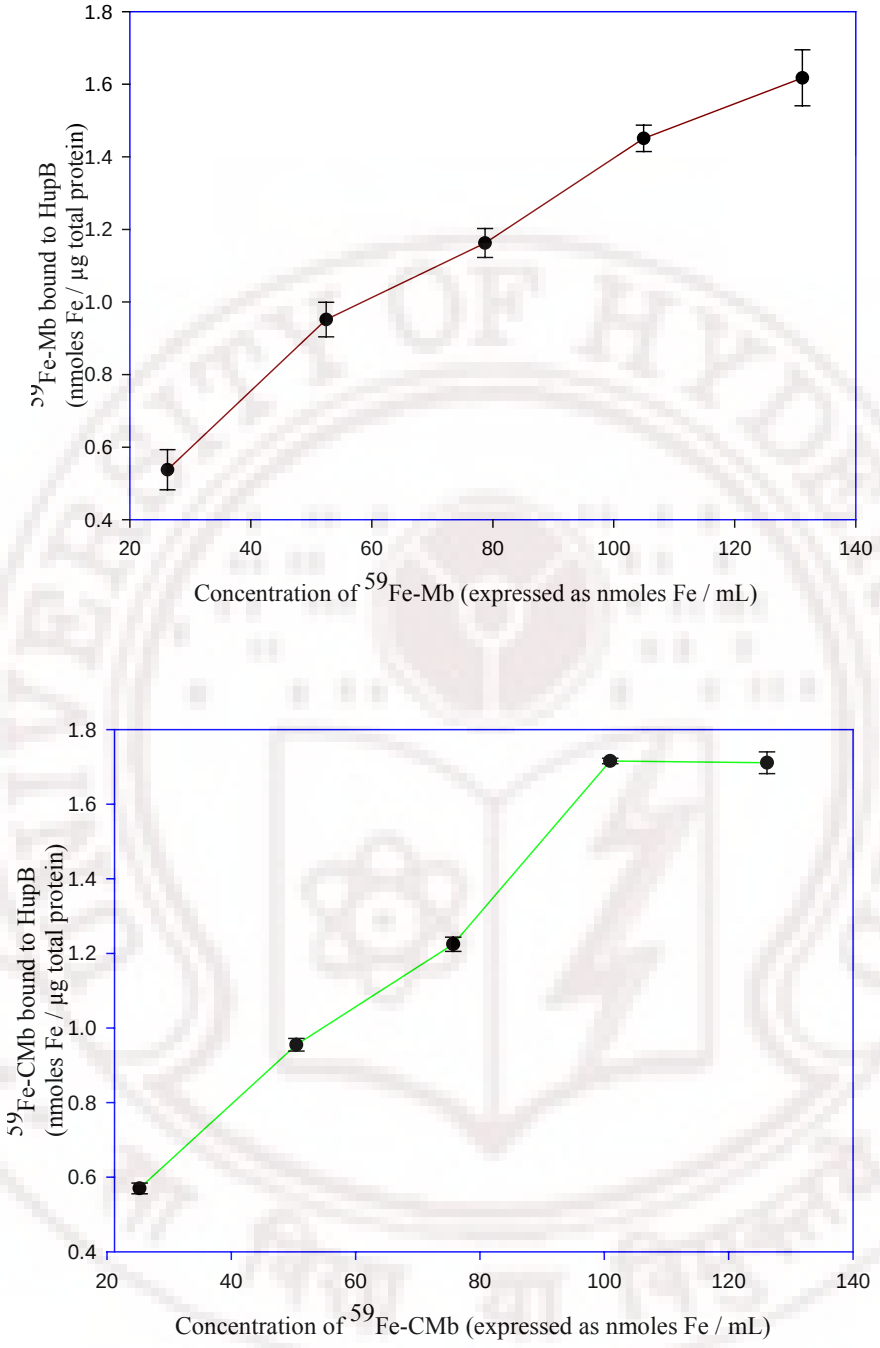

Fig. 3.22. Dose-dependent binding of Mb and CMb to HupB. Increasing amounts of ^{59}Fe-Mb (Panel a) and ^{59}Fe-CMb (Panel b) was incubated with 25 µg HupB and after suitable washes, the amount of bound radioactivity was measured. The vertical bars represent the standard deviation of the mean from three independent experiments.

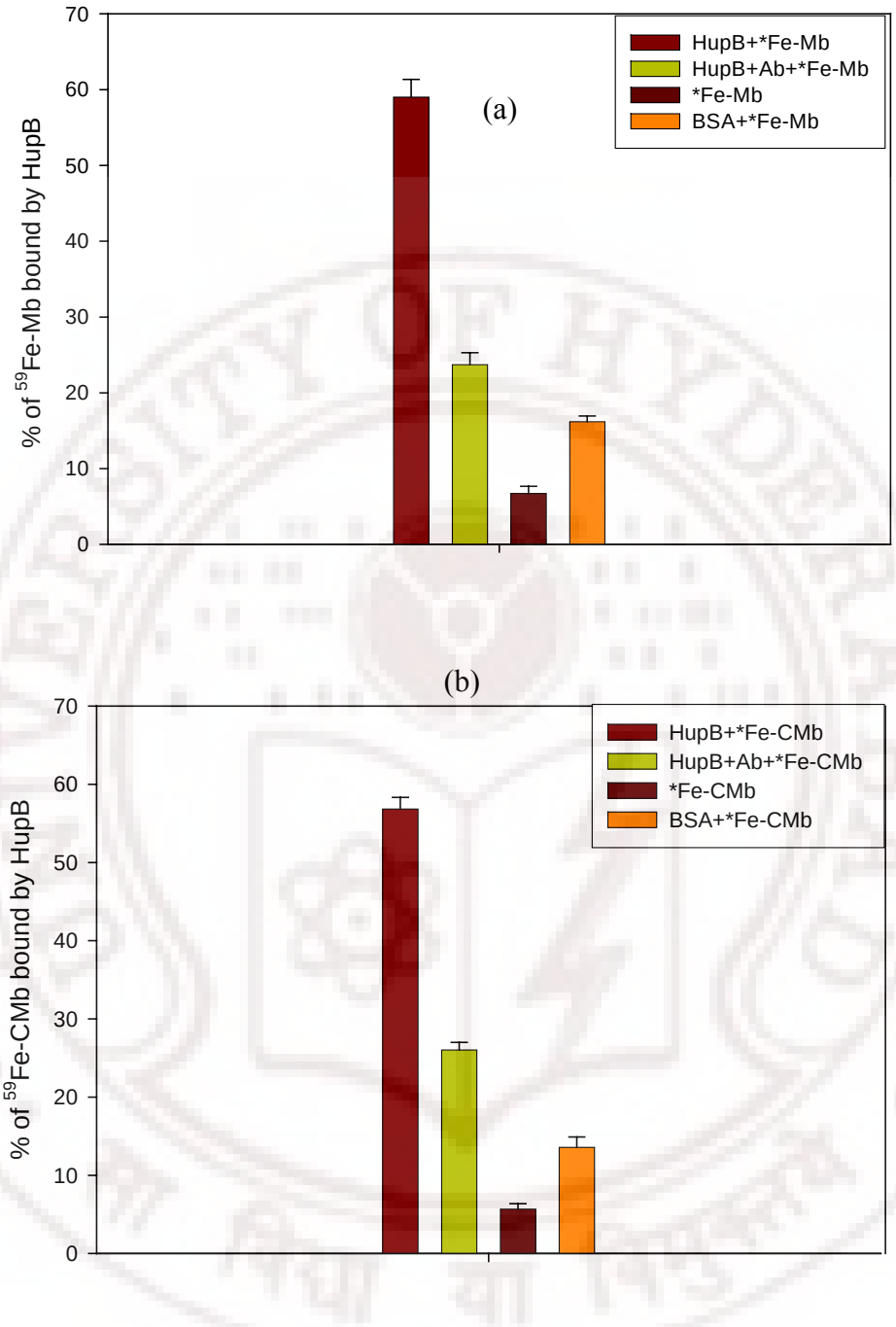

Fig. 3.23. Specificity of binding of Mb and CMb to HupB: Inhibition of binding by anti-HupB antibodies. Panels (a) and (b) show the inhibition of binding of ^{59}Fe Mb and ^{59}Fe CMb to HupB by anti-HupB antibodies. The non-specific binding of the ferric-siderophores to the nitrocellulose membrane was almost negligible. BSA was used as a control protein to which the ferric-siderophores showed a low level of binding. The amount of the ^{59}Fe-Mb / ^{59}Fe –CMb bound is represented as percentage of the ratio of bound versus added radioactivity. The vertical bars represent the standard deviation of the mean from three independent experiments.

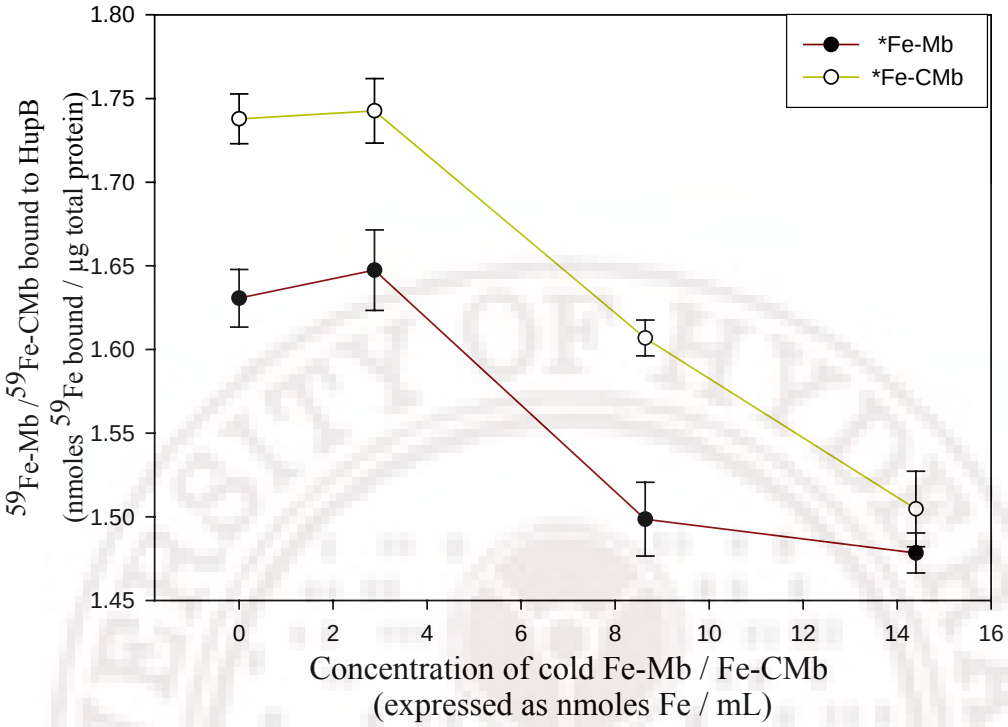

Fig. 3.24. Displacement of bound ^{59}Fe-siderophores using cold ferric-siderophore. The dose-dependent decrease in the bound radioactivity with increasing addition of cold ferric-siderophore was observed with both ^{59}Fe-Mb / ^{59}Fe-CMb. The vertical bars represent the standard deviation of the mean from three independent experiments.

(B). Spectrofluorimetric analysis

The association of both Mb and CMb to the iron-regulated HupB protein was strengthened by spectrofluorimetric analysis (Fig. 3.25 & Fig. 3.26). The rHupB protein, excited at a wavelength of 280 nm showed an emission peak at 384 nm. Upon addition of Fe-Mb to the protein sample, the intensity of the emitted light decreased; increasing aliquots of the ligand resulted in the steady decrease in the intensity of the emitted light (Fig. 3.25 b). A similar observation was observed upon addition of Fe-CMb (Fig. 3.26). Both the siderophores and the buffer used in the reaction, serving as negative controls showed negligible baseline fluorescence.

From the Scatchard plot, the binding capacity (B_{max}) of Fe-Mb (Fig. 3.25c) / Fe-CMb (Fig. 3.26c) was calculated as 1.045 mM and 0.551 mM respectively. The association constant (K_b) values, derived from the ratio of the slope to intercept were determined as 0.247 μM^{-1} and 0.122 μM^{-1} respectively for Fe-Mb and Fe-CMb.

(a)

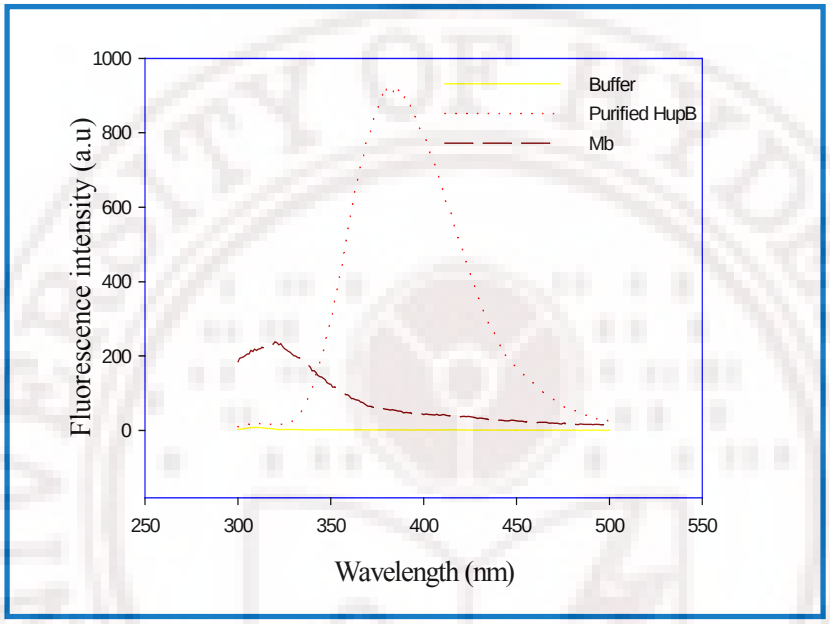

(b)

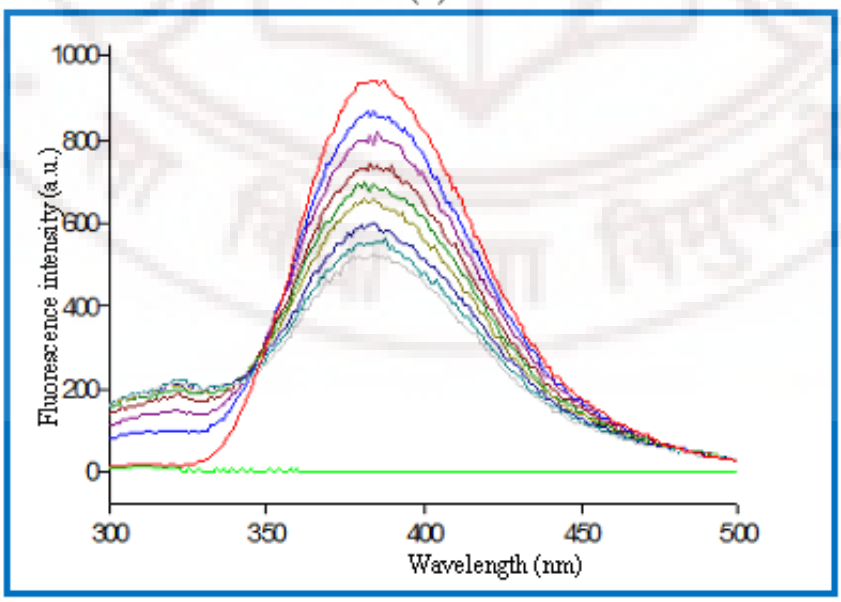

(c)

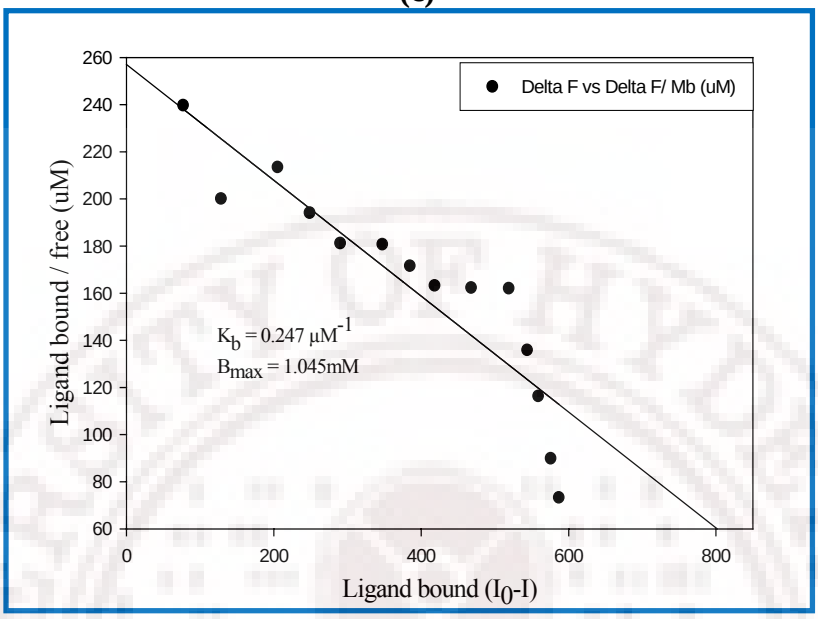

Fig. 3.25. Spectrofluorimetric analysis: Association of Fe-Mb to HupB. The peak intensity of the emitted spectrum of the purified HupB (µg total protein), with base line fluorescence of buffer and Fe-Mb is represented in Panel (a). The decrease in the intensity of the emitted light upon addition of increasing aliquots of Fe-Mb (stock concentration of 160 µM) can be seen in Panel (b). From the Scatchard plot (Panel c), the binding and the dissociation constants were obtained.

(a)

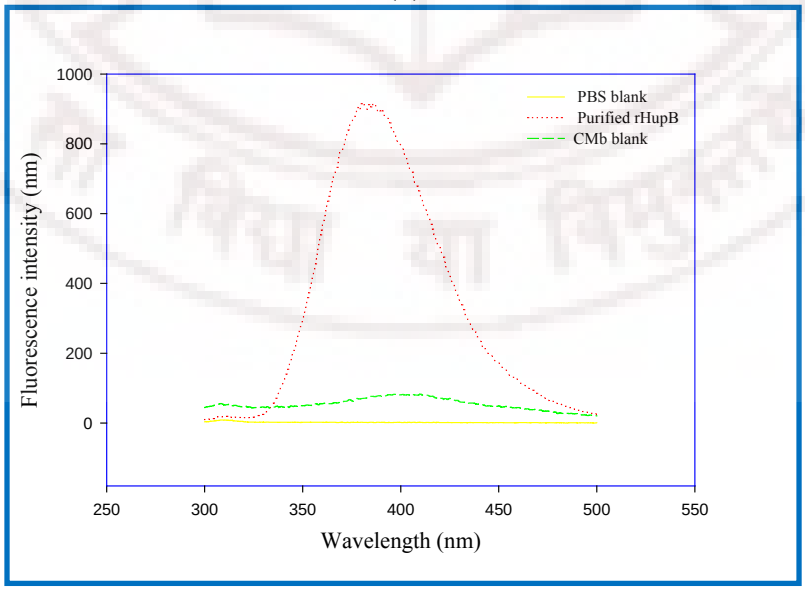

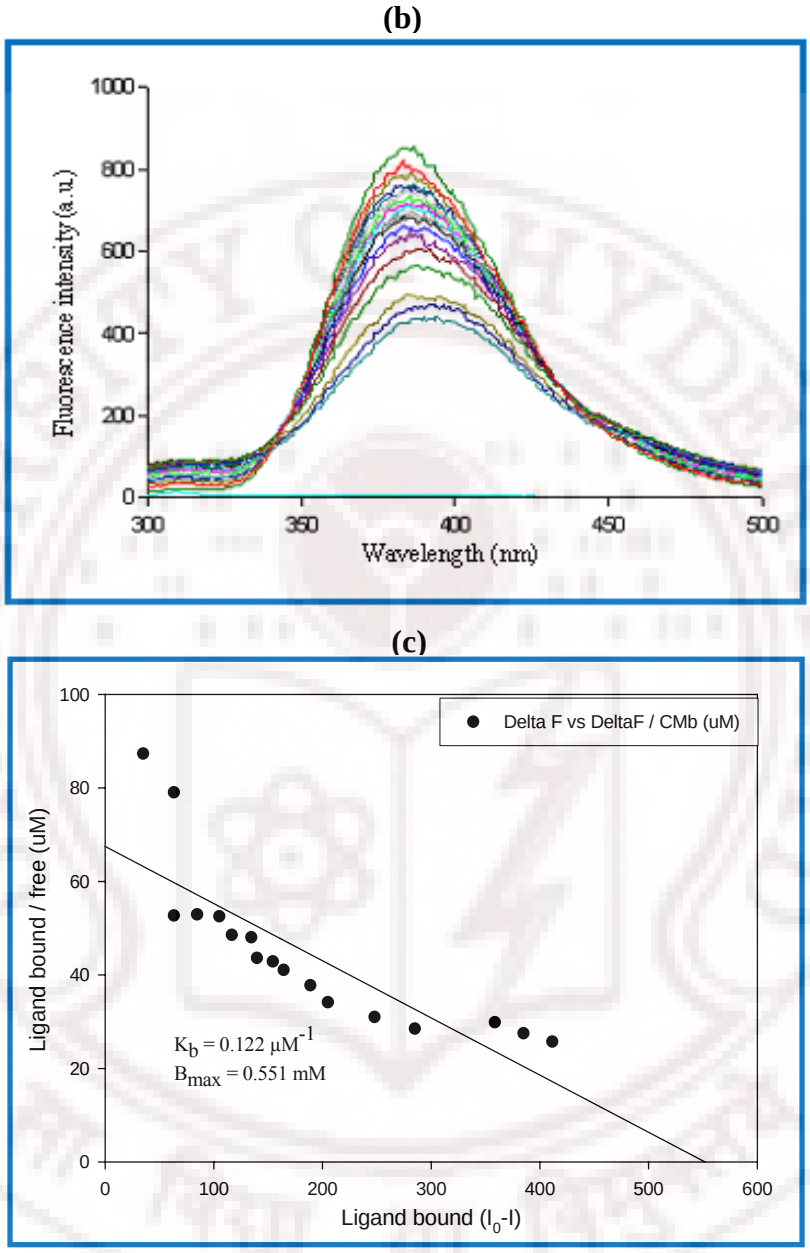

Fig. 3.26. Spectrofluorimetric analysis: Association of Fe-CMb to HupB. The peak intensity of the emitted spectrum of the purified HupB (µg total protein), with base line fluorescence of buffer and Fe-CMb is represented in Panel (a). The decrease in the intensity of the emitted light upon addition of increasing aliquots of Fe-CMb (stock concentration of 200 µM) can be seen in Panel (b). From the Scatchard plot (Panel c), the binding and the dissociation constants were obtained.

3.1.5.5. Clinical Significance of HupB expression in *M. tuberculosis*: Detection of anti-HupB antibodies in the serum of patients with tuberculosis

Serum from tuberculosis patients, with clinical and culture confirmation of the disease were analysed for the presence of antibodies against the HupB protein. The cell wall detergent phase proteins of *M. tuberculosis*, subjected to growth under varying concentrations of iron showed HupB expression under low iron conditions with repression of synthesis at 8 and 12 µg Fe / ml (section 3.1.2). One of the serum samples, incubated with the above cell wall detergent phase proteins reacted with the HupB protein, the immunoblot profile reflecting the iron-regulated expression of this protein (Fig. 3.27).

Subsequent dot blot analysis was done using cell wall-purified HupB (2.5 µg) antigen and the detection of anti-HupB antibody was compared with culture, radiological examination and a commercial screening device Mycotest. Of the 44 patients in the study, culture by BACTEC was done in 40 cases, chest X-ray examination was performed for 41 cases, and 42 of the serum samples were tested by using the Mycotest device (Fig. 3.28 a,b & c). A total of 28 of the 33 culture-positive cases and 33 of 39 chest X-ray positive cases showed antibodies to HupB. The commercial Mycotest (with a sensitivity of 87% and a specificity of 90%) identified only 22 cases versus the 36 cases identified by immuno-reactivity with HupB. Figure 3.29 shows the comparison of the immuno-reactivity of HupB with the mycotest.

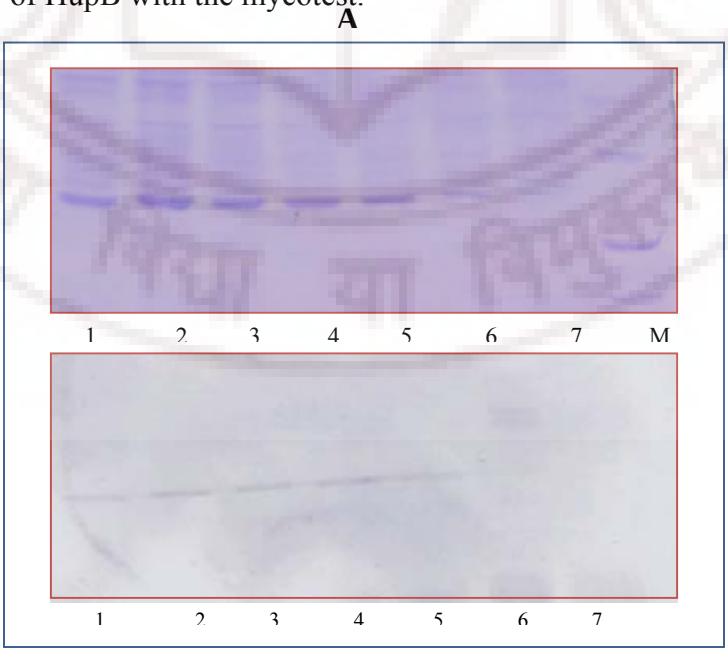

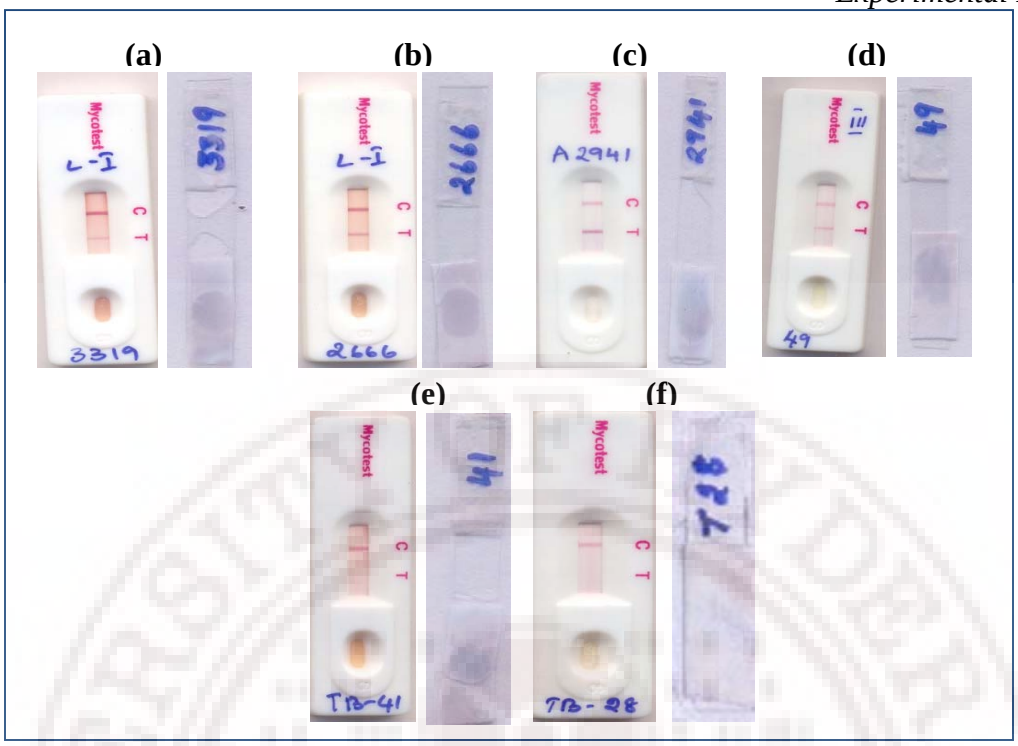

Fig.3.27. Detection of anti-HupB antibodies in the serum of patients with tuberculosis.

A. HupB protein expressed under low iron concentrations (section 3.1.2) reacted with anti-HupB antibodies in the serum of a tuberculosis patient. Panel A shows the proteins separated by SDS-PAGE and stained with Coomassie blue (i) while (ii) represents the corresponding immunoblot. Lanes 1 to 7 in both panels A and B represent cells grown with iron added at 12, 8, 4, 1, 0.1, 0.05, and 0.02 µg of Fe / mL, respectively.

B. Dot blot analysis of serum samples from tuberculosis patient's *vs* Mycotest. Samples (a), (b), (c) and (d) represents the serum samples positive for both HupB and Mycotest. Panel (e) represents the serum sample positive HupB but negative for Mycotest and Panel (f) represents the negative control.

(A). Immuno-reactivity of HupB in relation to the clinical investigation *i. e* Chest X-ray

		Chest X- ray		
		+	-	Total
HupB	+	33	6	39
	-	2	0	2
Total		35	6	41

(B). Immuno-reactivity of HupB in relation to BACTEC culture

		BACTEC culture		
		+	-	Total
HupB	+	28	5	33
	-	5	2	7
Total		33	7	40

(C). Immuno-reactivity of HupB in relation to Mycotest

		Mycotest		
		+	-	Total
HupB	+	20	16	36
	-	2	4	6
Total		22	20	42

Fig. 3.28. *In vivo* expression of HupB. Panels A, B and C represents the analysis of 44 serum samples from confirmed tuberculosis patients are presented. The detection of antibodies to HupB is compared to conventional diagnostic tests including culture, chest X-ray, and the commercial antibody-detection lateral flow device Mycotest. The results show the high degree of correlation of the detection of anti-HupB with culture and chest X-ray compared to the Mycotest.

3.2. Effect of iron levels on mycobacterial catalase-peroxidases

3.2.1. Establishment of iron limitation in different mycobacterial species

Mycobacterium tuberculosis, M. bovis, M. bovis BCG Denmark, *M. fortuitum, M. kansasii, M. smegmatis and M. vaccae* were grown in Proskauer and Beck medium with iron added at 4 µg Fe / mL (high) and 0.02 µg Fe / mL (low) respectively. The extracellular siderophore CMb / exochelin showed 3-4 fold increase under low iron conditions in all the mycobacterial species (Fig. 3.29) except *M. vaccae*, in which low levels of exochelin were observed.

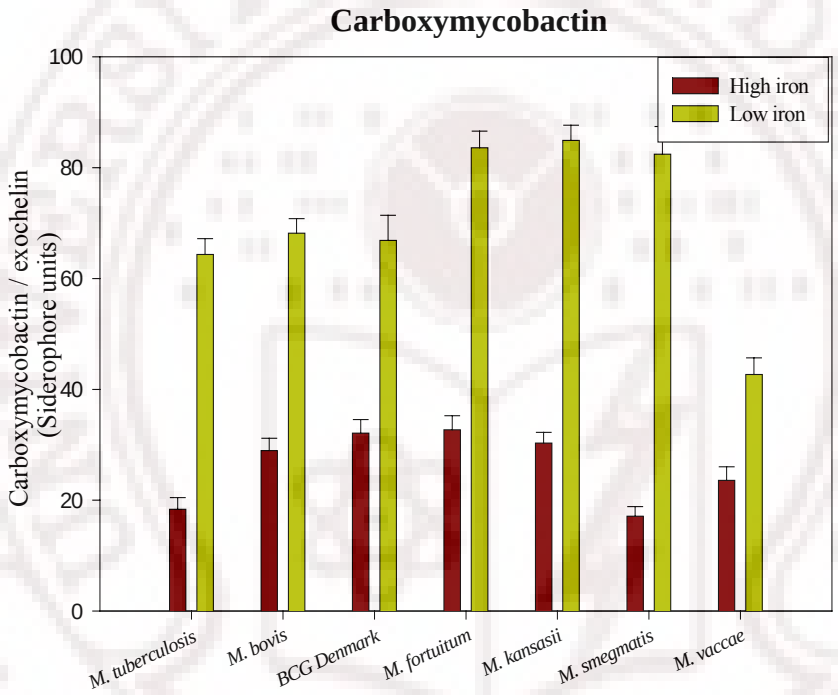

Fig. 3.29. Influence of iron levels of expression of CMb / exochelin in different mycobacterial species. Iron-limited organisms of *M. tuberculosis*, *M. bovis*, *M. bovis* BCG (Denmark), *M. kansasii*, *M. smegmatis* and *M. vaccae* showed increased levels of the extracellular siderophore CMb / exochelin upon iron limitation (0.02 µg Fe / mL) as compared to high iron conditions (4 µg Fe / mL). It is expressed as siderophore units (SU) and the vertical bars represent the standard deviation of the mean from three independent experiments.

3.2.1.1 Spectrophotometric assay of catalase and peroxidase activities: Demonstration of low levels in iron-limited organisms

Peroxidase activity was seen in all the mycobacterial species when grown under high iron conditions (Fig. 3.30a), the levels being 3 - 4 fold higher in *M. bovis* BCG, *M. fortuitum* and *M. kansasii* when compared to *M. tuberculosis* and *M. bovis*; low levels of activity were seen in *M. smegmatis* and *M. vaccae*.

Iron limitation resulted in a dramatic decrease in the peroxidase activity (10-13 folds) in all the mycobacterial species tested except in *M. vaccae*. In the latter, both peroxidase and catalase activities were unaffected by iron levels, though the relative activity of catalase was high comparable to that of *M. kansasii* and *M. fortuitum* grown under high iron conditions. Catalase activity also showed a significant reduction in all the mycobacterial species except *M. vaccae* (Fig. 3.30b).

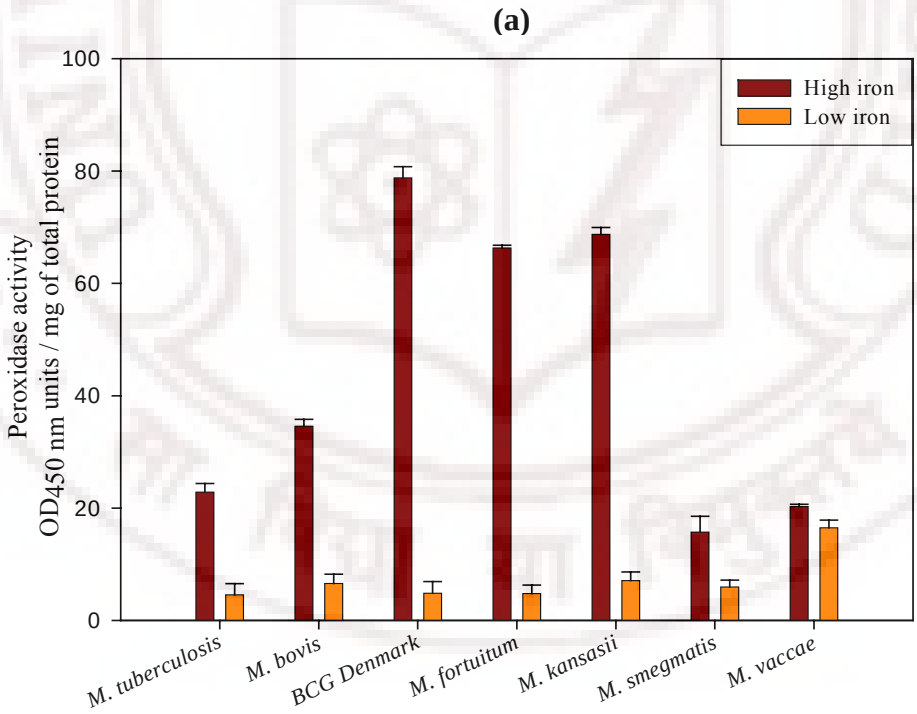

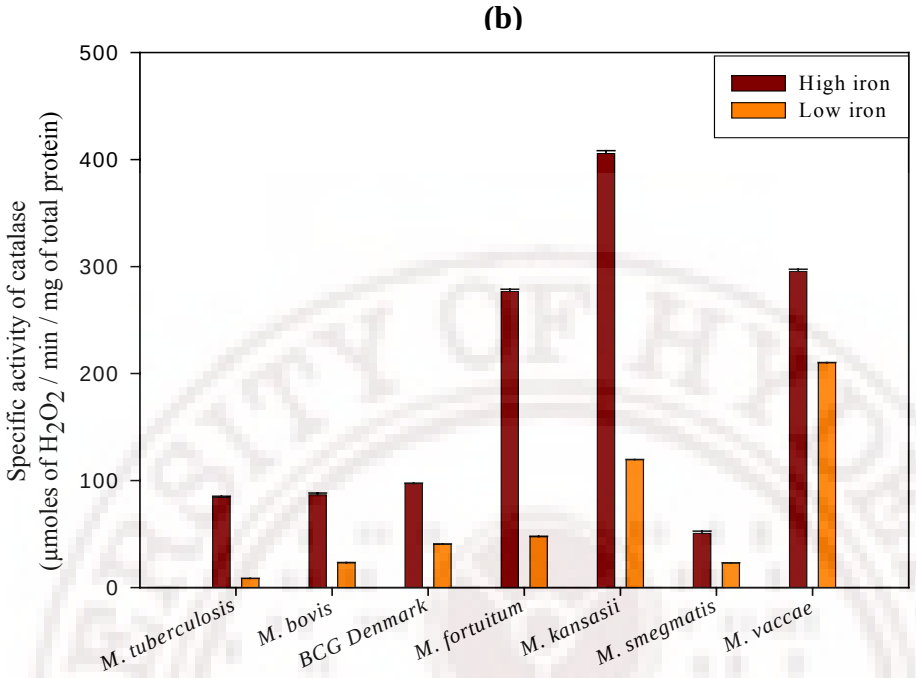

Fig. 3.30. Spectrophotometric assay of peroxidase and catalase activities. The cell-free sonicates of *M. tuberculosis*, *M. bovis*, *M. bovis* BCG Denmark, *M. kansasii*, *M. smegmatis* and *M. vaccae* grown in high iron (4 µg Fe / mL) and low iron (0.02 µg Fe / mL) conditions were assayed for peroxidase (a) and catalase (b) activities. Peroxidase activity was measured using TMB / H_2O_2 as substrate and catalase was measured by the decrease in the H_2O_2 concentration per min at 240 nm. The vertical bars represent the standard deviation of three independent experiments.

3.2.1.2 Activity staining of the isoforms of catalase and peroxidase in polyacrylamide gels

Dual staining for the activity of catalase and peroxidase revealed several isoforms in the different mycobacterial species, with variation seen in the number, enzymatic activity and heat inactivation among these isoforms.

Two isoforms with dual activity were seen in high iron cells of *M. tuberculosis, M. bovis* and *M. bovis* BCG; of the two isoforms, one of them is a major band with significant activity, which is completely lost and cannot be detected in low iron organisms (Fig. 3.31). Heat treatment of the cell sonicates from high iron cells of all the above species resulted in a marked loss of the peroxidase activity. The catalase activity

was also much lower in low iron organisms, the difference being apparent in *M. tuberculosis* and *M. bovis* while it was relatively more stable in *M. bovis* BCG, even upon heat treatment.

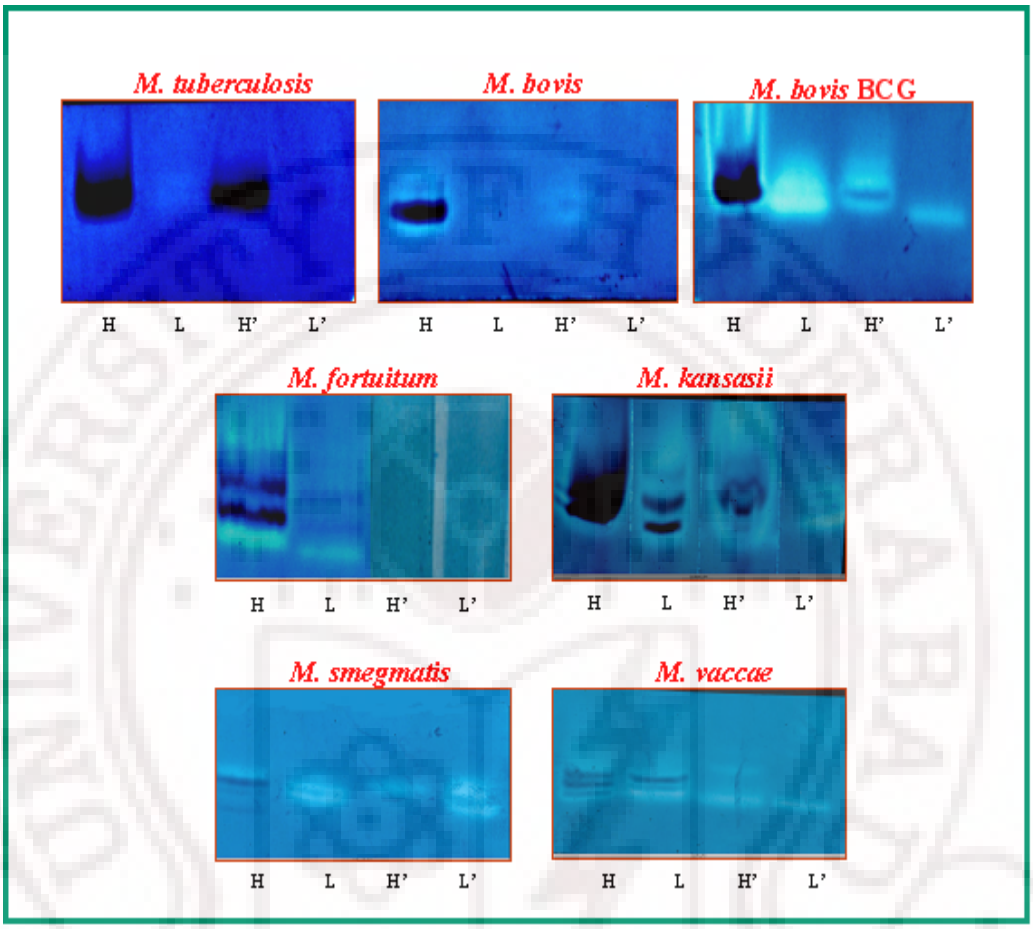

Fig. 3.31. In-gel activity staining for catalase and peroxidase activities. Dual staining method of Wayne and Diaz (1986) was employed for the demonstration of catalase and peroxidase activities. Cell-free extracts of *M. tuberculosis, M. bovis, M. bovis* BCG Denmark, *M. fortuitum, M. kansasii, M. smegmatis and M. vaccae* grown in high iron (4 µg Fe / mL, lanes H) and low iron (0.02 µg Fe / mL, lanes L) conditions. The lanes H' and L' represent the activity of an identical aliquot subjected to heat treatment at 55ºC for 10 min. The dark coloured bands represent peroxidase and the hollow represents catalase activity.

Both *M. fortuitum* and *M. kansasii* showed four isoforms; however differences were observed among the isoforms in the two species. Of the four isoforms in *M. fortuitum,* two of them showed dual activity with high levels of peroxidase; the other two isoforms showed only catalase activity. The former was seen only in high iron organisms

with faint bands of activity in low iron cells (Fig. 3.31). All the four isoforms were completely lost upon heat treatment. In *M. kansasii*, three isoforms showed dual activity while the fourth possessed only catalase activity that was found to be both heat stable and unaffected by iron levels (Fig. 3.32c). In the former three isoforms, both peroxidase and catalase activities were drastically reduced in low iron organisms; there was complete loss of peroxidase activity at 60°C in all of them (Fig. 3.32a & c), while the catalase activity was unaffected in one of the isoforms (Fig. 3.32c).

Similarly, the non-pathogenic mycobacteria *M. smegmatis* and *M. vaccae* showed differences in the number and activities among the isoforms (Fig. 3.31). In the former, a unique band with heat resistant catalase activity was seen in low iron organisms. Low level of peroxidase activity was seen in this isoform that was also heat resistant. On the other hand, the peroxidase activity of the high iron organisms was lost upon heat treatment. Four isoforms expressed by *M. vaccae* possessed dual activity in three of them; there was relatively less influence by iron on the peroxidase activity, which however was heat sensitive. As seen in some of the above mycobacteria, catalase activity (indicated in Fig. 3.32) remained unaffected by iron levels and heat in one of the isoforms.

(a)

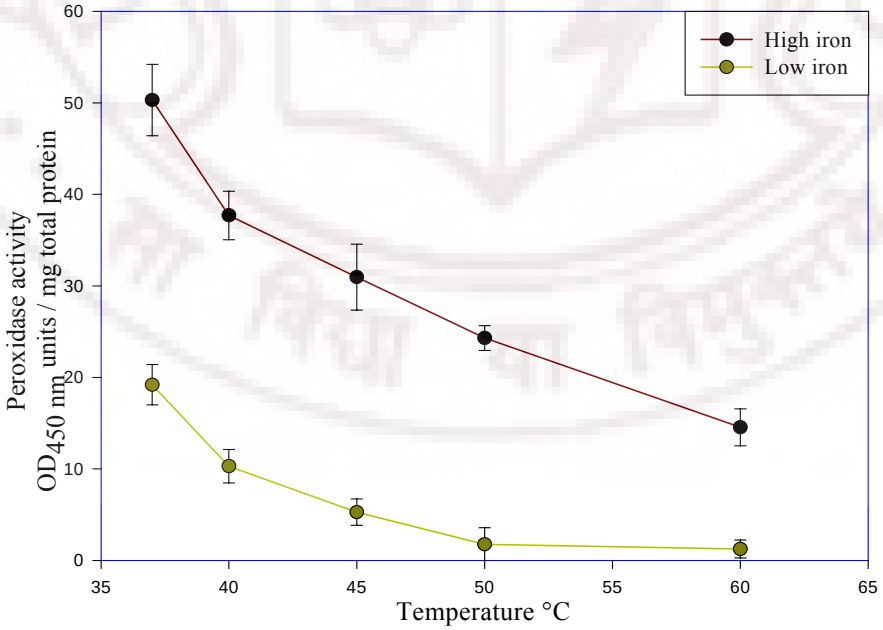

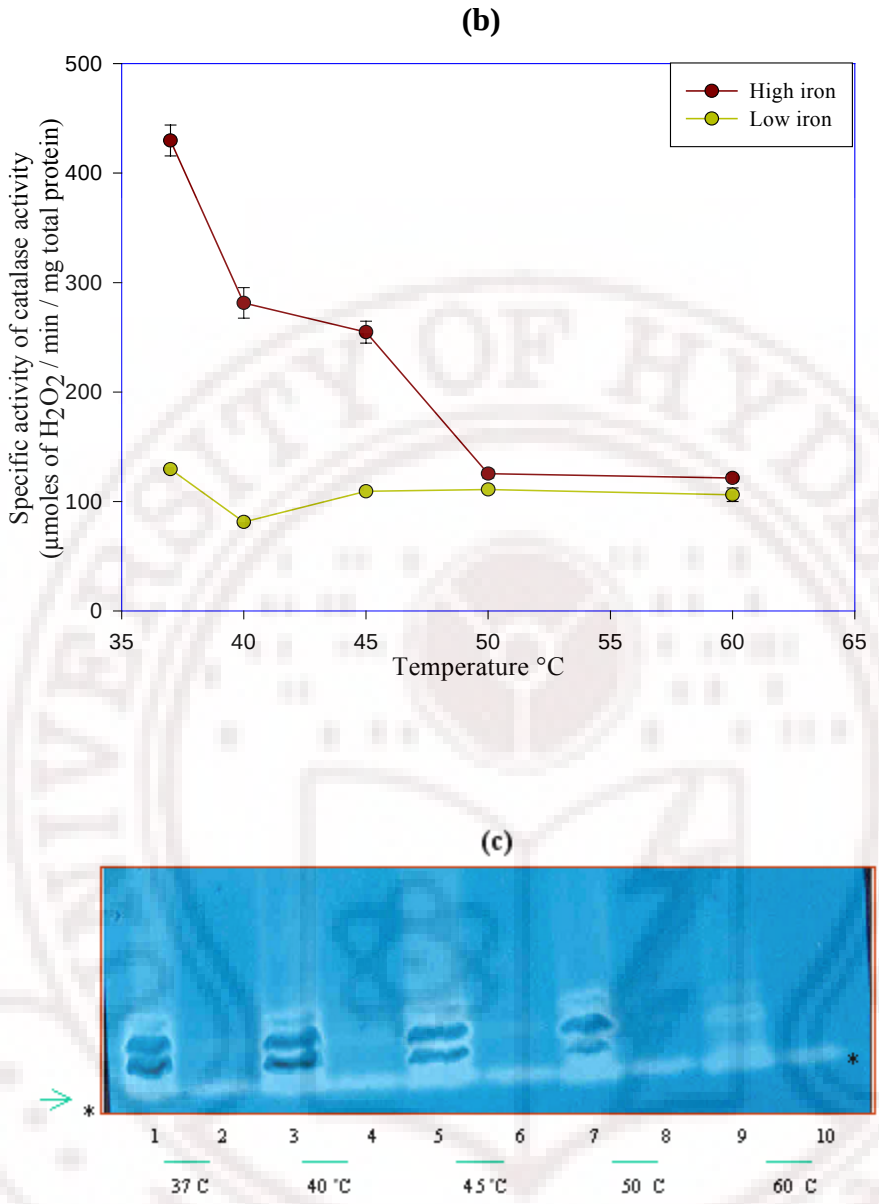

Fig.3.32. Influence of temperature on peroxidase and catalase activities in *M. kansasii*. Identical aliquots of the cell-free sonicate of *M. kansasii* grown in high iron (4 µg Fe / mL) and low iron (0.02 µg Fe / mL) conditions were heat treated at different temperatures of 37, 40, 45, 50 and 60°C and assayed spectrophometrically for peroxidase (a) and catalase (b). The vertical bars represent the standard deviation of three independent experiments. Activity staining of the same extracts is represented in (c). Lanes 1, 3, 5, 7 and 9 represent high iron organisms while lanes 2, 4, 6, 8 and 10 represent low iron organisms.

3.2.2. Role of peroxidase in the activation of anti-tubercular drug isoniazid (INH): studies with high and low organisms of *M. tuberculosis*

Spectrophotometric assay and activity staining were done to demonstrate the role of peroxidase in the activation of INH; cell free sonicates of high and low iron grown mycobacteria were used as the latter failed to express peroxidase activity. Further, the viability of high and low iron grown organisms were studied by the Microplate Alamar Blue assay that showed that high iron organisms, expressing the peroxidase were susceptible to INH while low iron organisms were unaffected. *Mycobacterium fortuitum*, which has a relatively much higher MIC to INH, was used as a control.

3.2.2.1. Spectrophotometric assay and activity staining in polyacrylamide gels.

The cell free sonicates of high iron organisms of *M. tuberculosis*, *M. bovis* and *M. bovis* BCG catalysed the INH-mediated NBT reduction, as assayed by the spectrophotometric assay (Fig. 3.33); relatively insignificant reduction of NBT was seen by extracts of *M. fortuitum.*

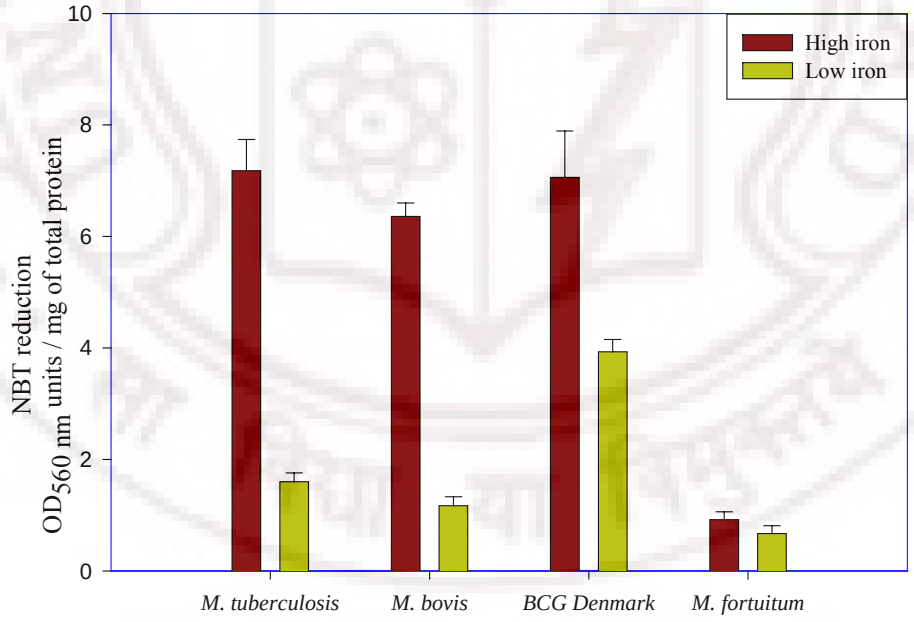

Fig. 3.33. Spectrophotometric assay of INH-mediated NBT reduction. The peroxidase mediated INH activation was assayed by the reduction of NBT using the cell-free extracts of *M. tuberculosis, M. bovis,* BCG and *M. fortuitum* grown in high iron (4 µg Fe / mL) and low iron (0.02 µg Fe / mL) conditions.. The vertical bars represent the standard deviation of the mean from three independent experiments

Activity staining for peroxidase and NBT reduction in native polyacrylamide gels provided concrete evidence for the role of peroxidase in INH activation. The cell free sonicates of high iron organisms of *M. tuberculosis*, *M. bovis* and *M. bovis* BCG showed clear reddish brown bands of peroxidase with diaminobenzidine while low iron organisms completely lacked the peroxidase bands (Fig. 3.34b). This pattern coincided exactly with the purple-colored bands in the identical gel subjected to INH-mediated NBT reduction (Fig. 3.34a). While sonicates of high iron organisms showed the purple bands, none could be detected in low iron organisms.

Interestingly, despite the high peroxidase activity in two of the isoforms *M. fortuitum*, no NBT reduction was seen, which correlated with the above spectrophotometric observations. In confirmation with these observations, viability assay (discussed below) showed that *M. fortuitum*, irrespective of the iron status was unaffected by the drug.

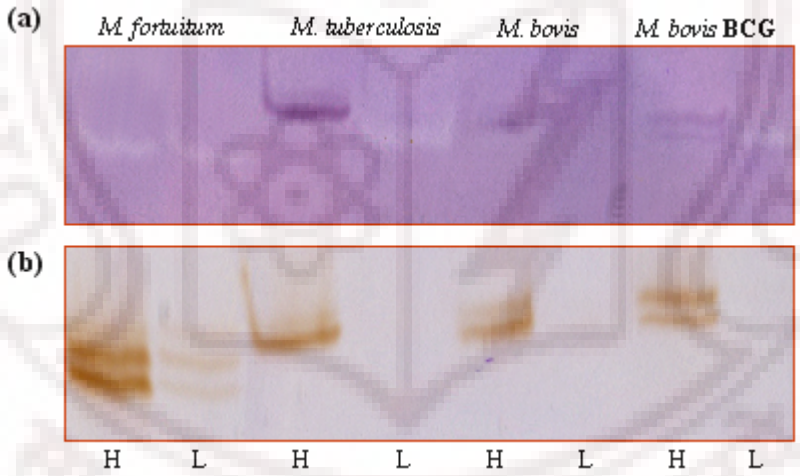

Fig. 3.34. Activity staining of peroxidase-mediated INH activation. Panel a & b represents the activity staining to show the direct relation between peroxidase activity and INH-mediated NBT reduction. (Panel a)- Activity gels developed with INH and NBT and (Panel b) - Activity staining of peroxidase by diaminobenzidine. Lanes H and L in panels a & b corresponds to the cell-free extracts of high iron (4 µg Fe / mL) and low iron (0.02 µg Fe / mL) conditions of *M. fortuitum*, *M. tuberculosis*, *M. bovis* and BCG Denmark respectively.

3.2.2.2. Viability testing by Microplate Alamar Blue Assay (MABA)

High and low iron organisms of *M. fortuitum*, *M. tuberculosis*, *M. bovis* and *M. bovis* BCG were grown in the presence of increasing concentrations of INH. The findings, presented in Table clearly showed that *M. fortuitum*, irrespective of the iron status was unaffected by the drug at all concentrations while in the three members of the *M. tuberculosis* complex, the high iron cells were susceptible to the drug even at the least concentration of 0.125 µg /mL while the low iron cells were unaffected even at high concentrations.

Table.3.3: Iron levels and the effect of INH on the viability of *M. tuberculosis*, *M. bovis* and *M. bovis* BCG and *M. fortuitum* (MABA)

INH (µg / mL)	High iron (4 µg Fe / mL) cells				Low iron (0.02 µg Fe / mL) cells			
	M. tuberculosis	*M. bovis*	*M. bovis* BCG	*M. fortuitum*	*M. tuberculosis*	*M. bovis*	*M. bovis* BCG	*M. fortuitum*
0.125	-	-	-	+++	+++	++	++	+++
0.25	-	-	-	+++	+++	++	++	+++
0.5	-	-	-	+++	+++	++	++	+++
1	-	-	-	+++	+++	++	++	+++
2	-	-	-	+++	+++	++	++	+++
4	-	-	-	+++	+++	++	++	+++

The results were scored visually as follows: dark purple (-), light purple (+), pink (++), completely yellow (+++). The experiment was performed thrice and identical results were obtained.

3.2.3. Studies on catalase-peroxidase activities in clinical isolates of *M. tuberculosis*

Clinical isolates of *M. tuberculosis* obtained from BACTEC culture of sputum samples from patients with tuberculosis (a total of 40 samples) were categorized as drug sensitive isolates (SIRE samples sensitive to Streptomycin, Isoniazid, Rifampicin and Ethambutol) and INH-resistant isolates. These clinical isolates were subjected to growth under high and low iron conditions and the profile of the catalase and peroxidase activities analysed by spectrophotometeric analysis and by activity staining in native polyacrylamide gels.

3.2.3.1. Expression of Mb and CMb upon iron limitation

All the clinical isolates in the two categories, expressed both CMb (Fig. 3.35) and Mb (Fig. 3.36) at significant levels when grown in Proskauer and Beck medium with 0.02 µg Fe / mL (low iron) as compared to growth under high iron conditions (8 µg Fe / mL). The increase in expression of CMb and Mb varied widely (2 - 18 fold) among the different isolates.

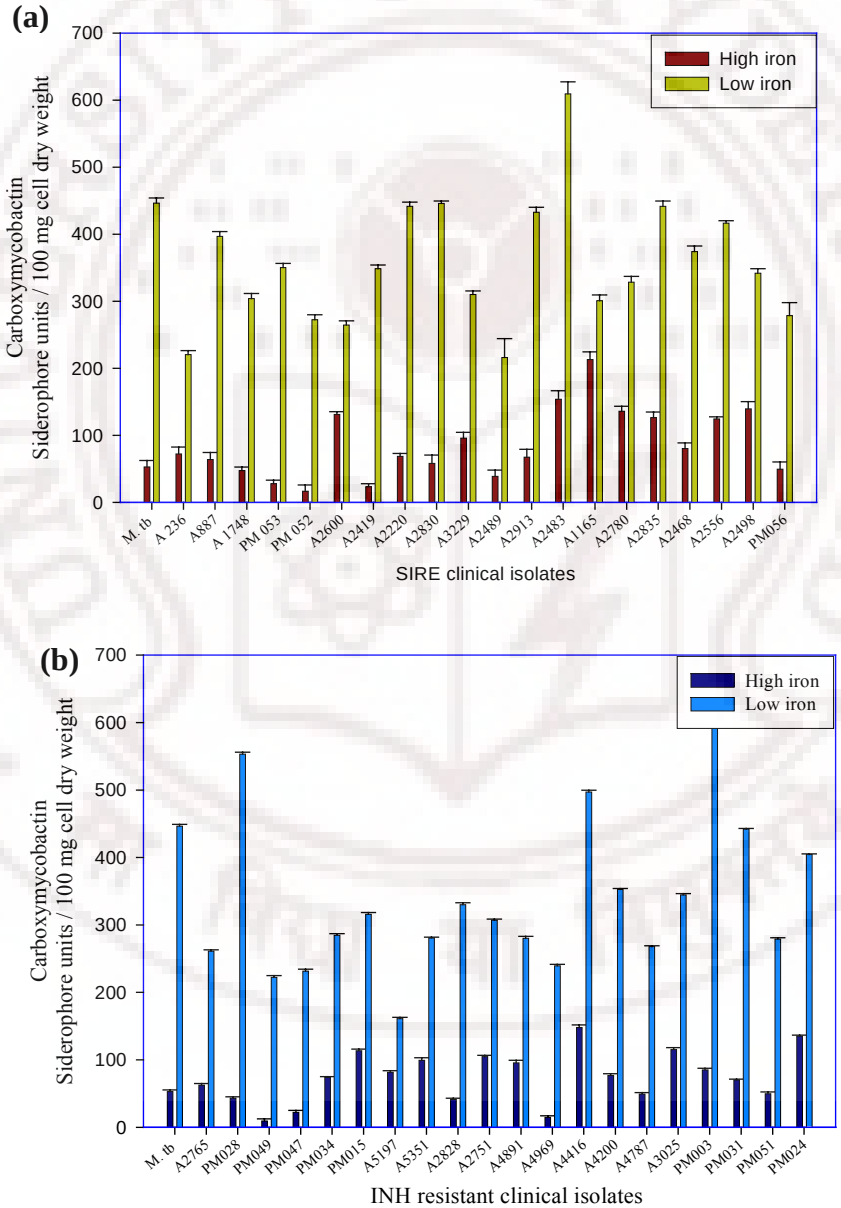

Fig. 3.35. Influence of iron levels on the expression of CMb in clinical isolates. Panel (a) represents drug sensitive clinical isolates and Panel (b) represents INH resistant

clinical isolates grown under high iron (8 µg Fe / mL) and low iron (0.02 µg Fe / mL) conditions respectively. The extracellular CMb was assayed as described in Methods and expressed as SU / 100 mg cell dry weight. The vertical bars represent the standard deviation of the mean from three independent experiments.

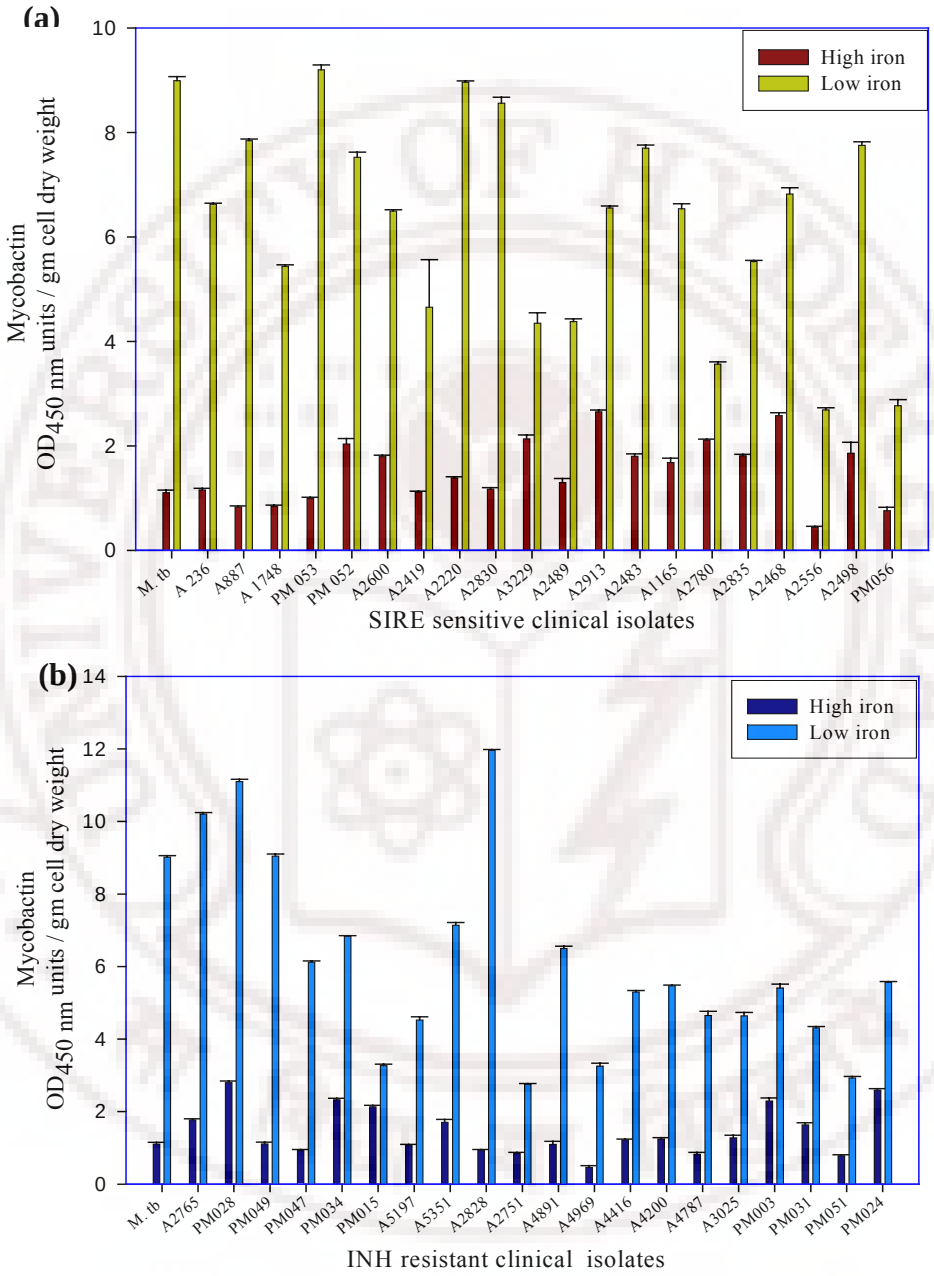

Fig. 3.36. Influence of iron levels on the expression of Mb in clinical isolates. Panel (a) represents drug sensitive clinical isolates and Panel (b) represents INH resistant clinical isolates grown under high iron (8 µg Fe / mL) and low iron (0.02 µg Fe / mL) conditions respectively. The Mb was assayed as described in Methods and expressed as OD450 nm units / gm cell dry weight. The vertical bars represent the standard deviation of the mean from three independent experiments.

3.2.3.2. Influence of iron levels on peroxidase and catalase activities

The cell-free sonicates of drug sensitive and INH resistant isolates were analysed for peroxidase and catalase activity by in-gel activity staining. Fig. 3.37 & 3.38 shows three panels, Panel A, B and C representing peroxidase staining by diaminobenzidine, dual staining for catalase & peroxidase and INH mediated NBT reduction. In the drug sensitive samples (Fig. 3.37), it was seen that in most of the samples (Table3.4), the peroxidase and the catalase activity was not affected by iron levels in the growth medium, showing similar activity in both high and low iron grown organisms, however in clinical isolate A236 the molecular size of the isoforms differs from the other clinical isolates. Further, the peroxidase activity correlated with the purple coloured band representing INH-mediated NBT reduction. The laboratory grown *M. tuberculosis* used as a control showed peroxidase activity and subsequent activation of INH in high iron organisms; no peroxidase activity was observed in low iron organisms.

In the INH resistant organisms (Fig. 3.38), notable was the influence of iron levels on the peroxidase activity; iron limitation resulted in the loss of activity in a majority of the isolates, whereas loss of catalase activity was observed in majority of the isolates irrespective of the iron status. Compared to the control *M. tuberculosis*, no INH activation was evident in the clinical isolates, as seen by the absence of the purple coloured band upon NBT reduction. (Table.3.5)

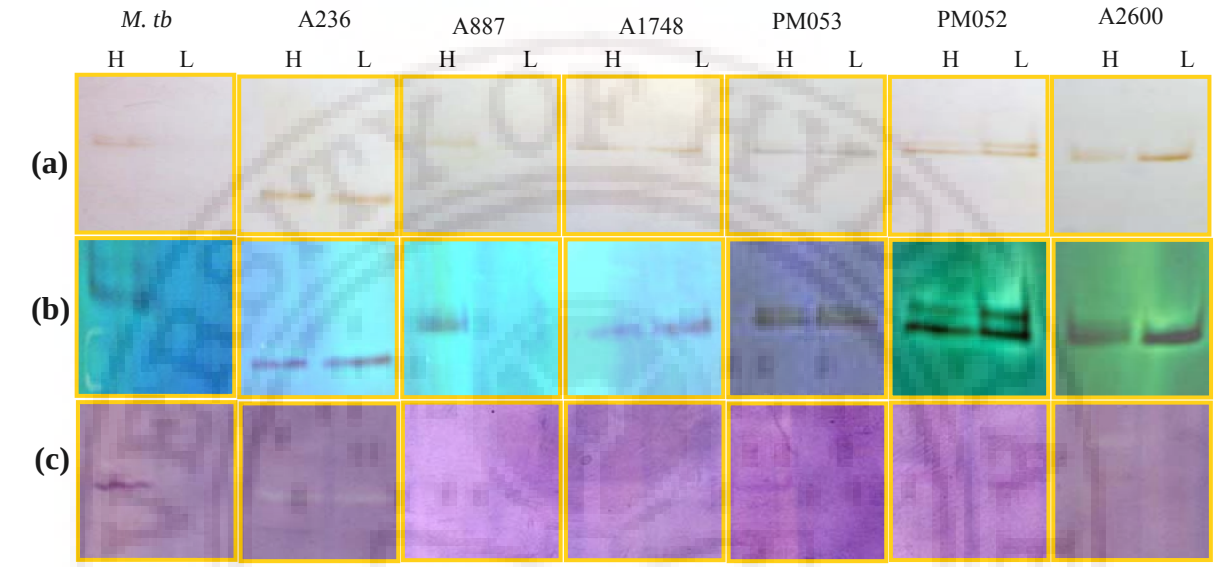
M. tb
A236
A887
A1748
PM053
PM052
A2600
H L
(a)
(b)
(c)

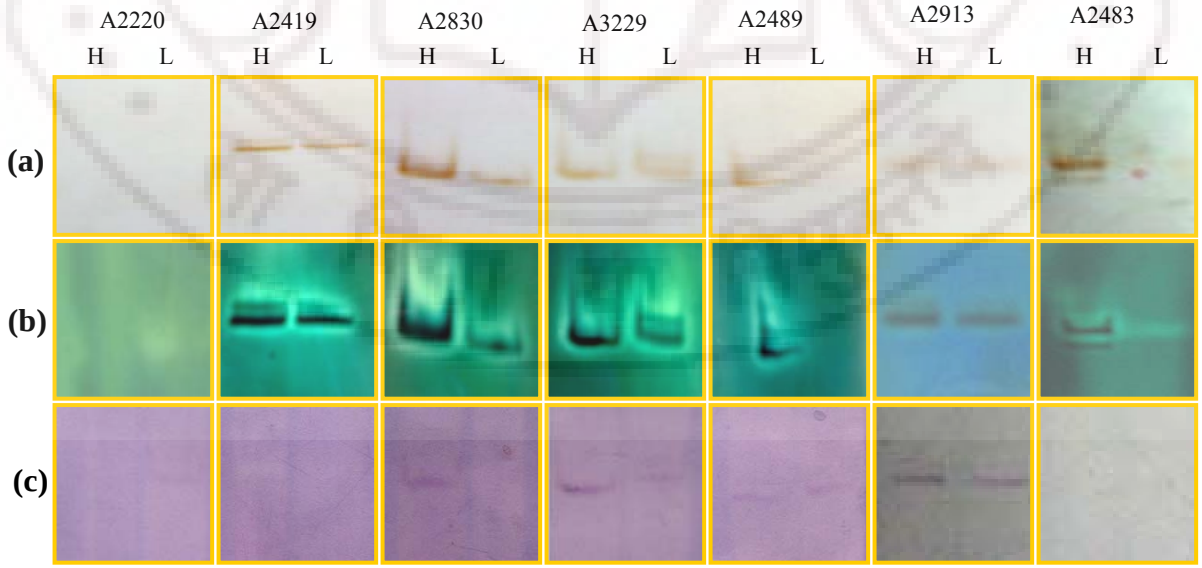
A2220
A2419
A2830
A3229
A2489
A2913
A2483
H L
(a)
(b)
(c)

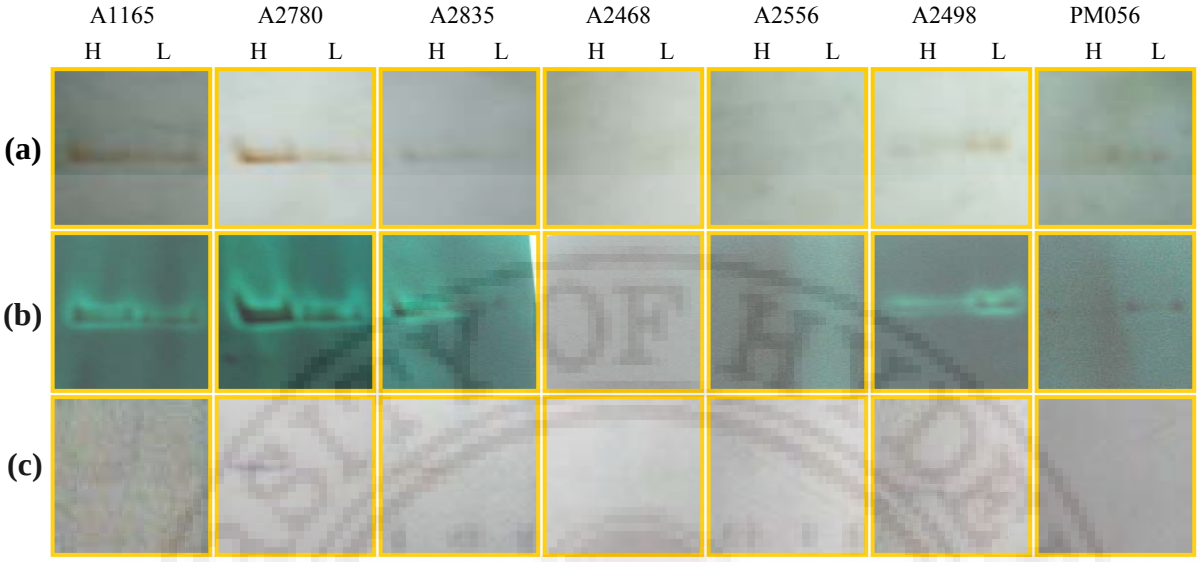

Fig. 3.37. In-gel assay for catalase and peroxidase in drug sensitive clinical isolates. The cell- free sonicates of drug sensitive isolates grown in high iron (8 µg Fe / mL) and low iron (0.02 µg Fe / mL) conditions were used for the analysis of peroxidase (Panel a), dual staining (Panel b) and INH mediated NBT reduction activity (Panel c) from the native gels. *M. tuberculosis* grown under the similar conditions was used as a positive control.

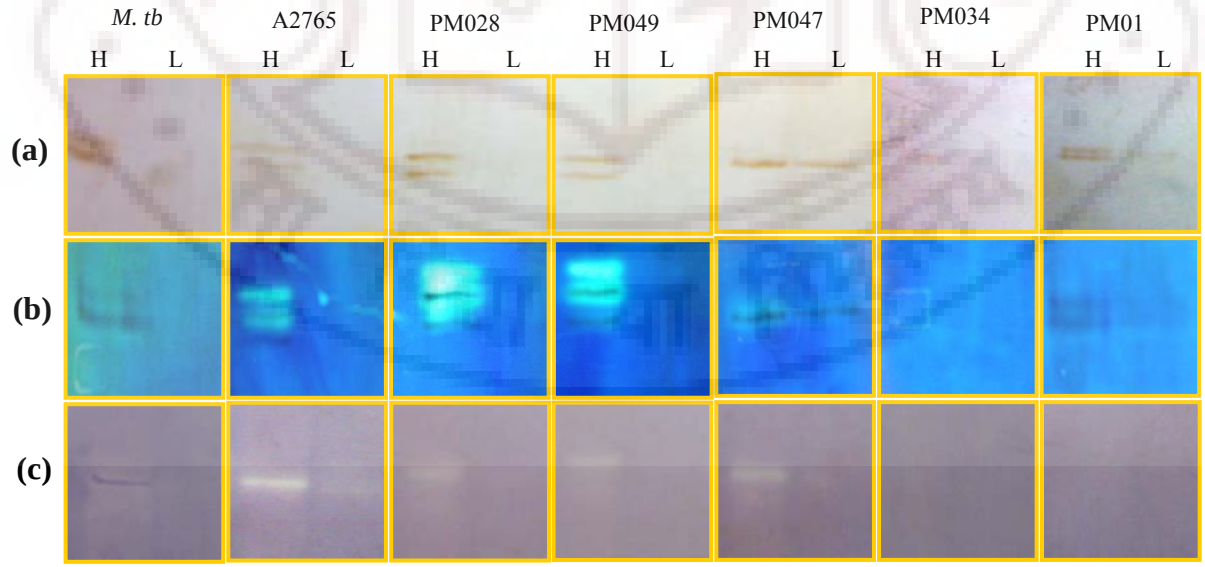

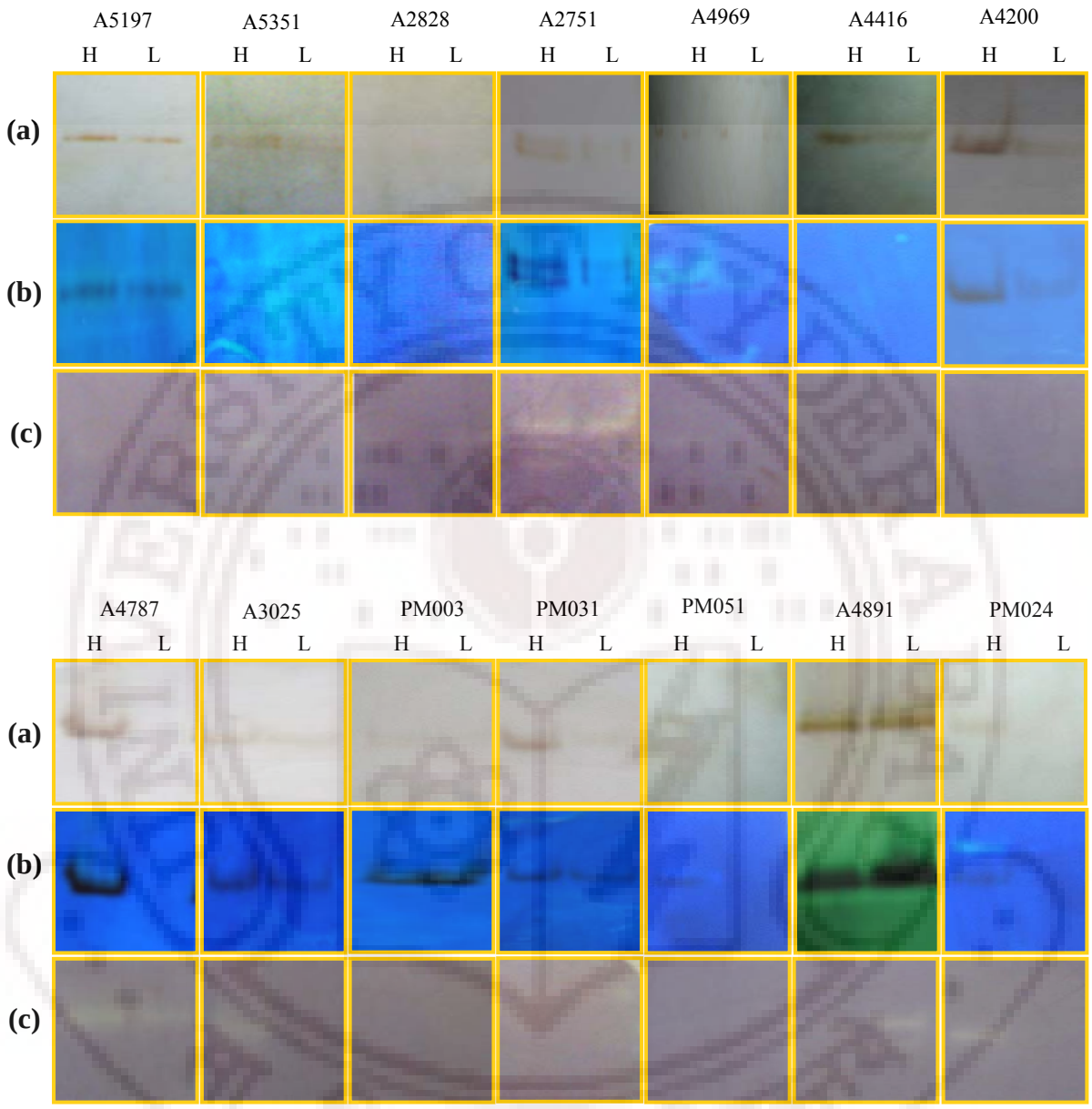

Fig. 3.38. In-gel assay for catalase and peroxidase in INH resistant clinical isolates. The cell- free sonicates of INH resistant clinical isolates grown in high iron (8 µg Fe / mL) and low iron (0.02 µg Fe / mL) conditions were used for the analysis of peroxidase (Panel a), dual staining (Panel b) and INH mediated NBT reduction activity (Panel c) from the native gels. *M. tuberculosis* grown under the similar conditions was used as a positive control.

Table.3.4. Peroxidase activity and the INH mediated NBT reduction in the SIRE sensitive clinical isolates

No.	***Strain M. tuberculosis***	**Peroxidase activity**		**INH-mediated NBT reduction (Correlation with peroxidase activity)**
		High Iron	Low Iron	
1.	H37Rv	+	-	+
2.	A236	+	+	+
3	A887	+	-	-
4	A 1748	+	+	+
5	PM053	+	+	+
6	PM 052	+	+	+
7	A2600	+	+	+
8	A2200	-*	-*	-*
9	A 2419	+	+	-
10	A 2830	+	+	+
11	A 3229	+	+	+
12	A 2489	+	-	+
13	A 2913	+	+	+
14	A 2483	+	-	-
15	A 1165	+	+	+
16	A 2780	+	+	+
17	A 2835	+	+	+
18	A 2468	-*	-*	-*
19	A 2556	-*	-*	-*
20	A 2498	+	+	+
21	PM 056	+	+	-

- No activity could be detected for peroxidase / catalase

Table 3.5 Peroxidase activity and the INH mediated NBT reduction in the INH resistant clinical isolates

No.	***Strain M. tuberculosis***	**Peroxidase activity**		**INH-mediated NBT reduction (correlation with peroxidase activity**
		High Iron	Low Iron	
1	H37Rv (control)	+	-	+
2	A2765	+	-	-
3	PM 028	+	-	-
4	PM049	+	-	-
5	PM047	+	+	-
6	PM034	+	-	-
7	PM015	+	-	-
8	A5197	+	+	-
9	A5351	+	+	-
10	A2828	-*	-*	-*
11	A2751	+	-	-
12	A4969	+	-	-
13	A4416	+	-	-
14	A4200	+	-	-
15	A4787	+	-	-
16	A3025	+	+	-
17	PM003	+	+	-
18	PM031	+	-	-
19	PM051	+	-	-
20	A4891	+	+	-
21	PM024	+	-	-

* No activity could be detected for peroxidase / catalase

CHAPTER 4

DISCUSSION

4.1. Iron and mycobacteria

Tuberculosis still remains a major killer among infectious diseases, despite the worldwide use of a live attenuated vaccine and several antibiotics (WHO report, 2009). New vaccines and drugs are needed to stem the worldwide epidemic of the disease that kills two million people each year. The problem is compounded due to the development of drug-resistant organisms, co-occurrence of the disease in HIV patients and the increase in the number of opportunistic mycobacterial pathogens causing disease (WHO report, 2008). There is a need to identify novel candidates for vaccines, diagnosis and as drug targets. To rationally do this, it is essential to understand the *M. tuberculosis*-host interactions, more so at the molecular level to learn how these bacteria circumvent host defenses and cause disease. Iron acquisition is an important aspect of host-pathogen interactions that contributes to the pathogenicity of several bacteria, as described in Review of Literature. The aim of this study was to understand the influence of iron limitation on mycobacteria, specifically *M. tuberculosis*. First aspect of the study focused on the effect of iron limitation on the iron acquisition machinery; we report the identification and characterization of an iron-regulated envelope protein Irep-28 in *M. tuberculosis* as HupB protein, which showed coordinate regulation with the two siderophores Mb and CMb. Secondly, we present our findings on the effect of iron deprivation on mycobacterial catalase-peroxidases and the ensuing effects on the efficacy of the anti-tubercular drug isoniazid.

There is increasing evidence to show that pathogenic mycobacteria face conditions of iron deprivation *in vivo* (Ratledge, 2004; Gold *et al.,* 2001). Iron, at physiological pH has a solubility of approximately 1.4 x 10^{-9} M. The solubility of Fe^{3+} increases by 10^{-3} M for every unit that the pH drops so that, for example, at pH 5 the solubility of Fe^{3+} is 10^{-3} M, making it biologically available; however, this concentration will be further lowered within the mammalian system, where iron-withholding proteins like transferrin and lactoferrin come into play (Griffiths & Chart, 1999). The intracellular *M. tuberculosis* and other pathogenic mycobacteria, growing within the phagocytic vacuoles of the macrophages, where the pH is between 6.1 and 6.5 face a maximum concentration of free Fe^{3+} between 1 and 10 ng / mL, a value which is further lowered due to the lactoferrin in the macrophages that can hold the iron efficiently even at acidic

pH (Aisen & Leibman, 1972). Therefore, these pathogens, in order to grow and cause disease within a host, must compete against the host for its supply of iron. Addition of exogenous iron favoured bacterial multiplication, as shown by Douvas *et al.* (1993) on *M. avium* -infected macrophages.

4.2. HupB as an iron-regulated protein in *M. tuberculosis*

Mycobacteria respond to iron limitation in *in vitro* cultures by the expression of significant levels of both the intracellular and extracellular siderophores Mb and CMb / exochelins respectively. Today, there is considerable information on the biosynthesis of these molecules (detailed earlier in Review of Literature), though their exact role in iron uptake remains unclear. Unlike in other bacterial systems, like *E. coli*, in which specific cell-surface receptors to the ferric-siderophores have been systematically characterized and structurally elucidated, much remains to be done in mycobacteria. Though the 29 kDa iron-regulated envelope protein in *M. smegmatis* has been proved to be ferri-exochelin receptor (Hall *et al.,* 1987, Dover & Ratledge, 1996), structural elucidation as a receptor protein has not been done. Though several IREPs have been reported in other mycobacteria (Sritharan & Ratledge 1989, 1990), including *in vivo* grown mycobacteria, none of them have been shown to be ferric-siderophore receptors. In *M. tuberculosis*, iron-regulated proteins are reported (Rodriguez *et al.,* 2002); however, they did not show much promise as ferric-siderophore receptors, except the IrtA and IrtB, encoded by *irtAB* as part of the *mbt-2* operon that was implicated in CMb uptake and transport across the membrane (Rodriguez & Smith 2006).

The slow progress in the analysis of ferric-siderophore receptors could perhaps be due to the difficulty of analysis of the lipid-rich cell envelope of mycobacteria that causes poor resolution of the cell wall / membrane proteins. Mycobacterial proteins have been detected by techniques that include single dimension denaturing gel electrophoresis and two-dimensional gel electrophoresis; these, along with a combination of sophisticated mass spectrometry techniques and comparison with the genome sequence to analyze protein patterns have made possible the identification of several cytoplasmic and excretory-secretory proteins (Rosenkrands *et al.,* 2000). However, envelope proteins analysed by these methods are not satisfactory. Sinha *et al*. (2000, 2005) used Triton X-

114 to extract the envelope proteins before subjecting them to denaturing gel electrophoresis. Further they observed that single dimension gel electrophoresis was better in the identification of mycobacterial envelope proteins. We adopted the method of Sinha *et al*. (2000) for our studies (discussed below).

Our studies on the influence of iron levels on the cell envelope proteins of *M. tuberculosis* were done as reported for *M. smegmatis* (Hall *et al.,* 1987). However, solubilisation of the cell wall and membrane proteins by SDS did not result in a good resolution of the proteins, possibly due to the interference by the lipids present in these sample preparations. Hence, the method of Sinha *et al.* (2002), using Triton X-114 was adopted for the analysis of the cell envelope proteins. *Mycobacterium tuberculosis* responded to iron deprivation by increased synthesis of both Mb and CMb (Yeruva *et al*., 2006). Four preparations of envelope proteins, comprising the detergent and aqueous phases of cell wall and membrane were analysed; a 28 kDa protein, referred to as Irep-28 was identified as an iron-regulated protein in the cell wall detergent fraction. Use of the Triton X-114 extraction protocol allowed complete solubilization of the lipid-rich wall and membrane samples and allowed for the relatively easier detection of Irep-28. When the added iron ranged between 0.02 to 12 µg Fe / mL, maximal expression of both these siderophores was seen when iron level is below 0.4 µg Fe / mL. The levels of both these siderophores decreased with increasing iron levels. Earlier studies in several mycobacterial species showed that concentrations of 0.02 and 4 µg Fe / mL, respectively, indicated low-iron and high-iron conditions (Sritharan & Ratledge, 1990; Hall *et al*., 1987). However, we did not find appreciable differences in the protein pattern in *M. tuberculosis* under similar growth conditions, although differences in the siderophore levels were seen. Here, in a detailed analysis, we found detectable levels of Mb, CMb, and Irep-28 even at 4 µg Fe / mL; at 8 µg Fe / mL none of them were expressed. It is possible that a relatively higher level of the intracellular iron is required to repress the iron acquisition machinery in *M. tuberculosis* as compared to other mycobacteria. Since the iron status of the organism is reflected directly by the induction of siderophore expression, Irep-28 showing coordinated expression with both Mb and CMb is indeed an iron-regulated protein. Time-course analysis of the expression of Mb, CMb and Irep-28 showed that Irep-28 and CMb were the first indicators of iron limitation due to nutrient

depletion; Mb was slower to increase, an observation that is in accordance with the view of Ratledge (2004) that this siderophore is an intra-envelope iron storage molecule, holding the excess iron temporarily as ferric-Mb and releasing it slowly into the cytoplasm for immediate utilization and / or storage in the iron storage molecule bacterioferritin (BfrA and BfrB).

Irep-28 is perhaps similar to the Irp28 reported by Calder and Horwitz (1998) in their initial study using single dimension electrophoresis, but these authors did not emphasize it as an iron-regulated protein. They did not detect Irp28 protein in their subsequent analysis by two-dimensional gel electrophoresis (Wong *et al*., 1999) indicating that not all proteins are resolved by the latter technique. We used preparative gel single dimension electrophoresis for the separation and purification of not only Irep-28 but also other iron-regulated envelope proteins. They include two proteins, seen upon iron limitation, namely Irep-52 and Irep-26, both of which are seen in the cell membrane detergent phase upon extraction with Triton X-114. Both Irep-52 and Irep-26 proved to be 50S ribosomal protein L4 upon sequence analysis. Under high iron conditions, two proteins were up regulated, namely Irep-130 and Irep-24, the former probably representing bacterioferritin; however sequencing of the protein was not done in this study.

Irep-28 was identified as the DNA-binding HU homologue HupB protein (Rv2986c) and will be the focus of further analysis in this study. Information on HupB from the *M. tuberculosis* genome annotation (Cole *et al*., 1998) showed it to be 214 amino acids in length, rich in amino acids lysine, alanine, arginine and proline, with an exceptionally high isoelectric point of 12.4 that could have been responsible for the failure to detect in the 2D gels. HupB probably does not conform to the predicted size of 21.8 kDa and migrates as a 28 kDa protein due to the high content of positively charged lysine residues. Comparison of the HupB sequence with the corresponding homologues in other bacteria showed that the N-terminal 90 amino acids of the protein is homologous to HupB of *E. coli* (and several other bacterial species) while the C-terminal region is unique to mycobacteria. Phylogenetic analysis of HupB from different genera representing *Enterobacteria*, *Mycobacterium*, *Rhodococcus* and *Streptomyces* groups the ancestral mycobacteria such as *M. ulcerans*, *M. marinum* and *M. kansasii* as a distinct

well-separated cluster. This indicates the presence of an ancestral copy of the *hupB* gene that would have subsequently rearranged in more contemporary forms such as *M. leprae*, *M. bovis* AN5 and BCG Pasteur. The latter two formed a separate branch when only the members of the genus *Mycobacterium* were analysed. This segregation may be due to 'artificial' rearrangement, as the deletion was observed in *M. bovis* AN5 and BCG Pasteur that have been passaged and sub-cultured for vaccine production. This could be a random deletion introduced during subculturing, as frequent deletions and duplications have been reported during the production of BCG vaccines (Brosch *et al*., 2007). Prabhakar *et al.* (2004) made of the use of this deletion in *M. bovis* AN5 by the development of a PCR-based diagnostic test. They developed a nested PCR to amplify segments of *hupB* gene that helped in the differentiation of the field strains of *M. bovis* in India from *M. tuberculosis*, with which it shares similarities in growth characteristics and very close homology at the genomic level. The relevance of the deletion may be worth further analysis, instead of just attributing the deletion due to simple growth conditions as mentioned above, as these authors performed PCR with *in vivo* derived *M. bovis* from cattle samples from India.

Phylogenetic analysis of HupB also showed that the free-living saprophytic mycobacteria (*M. avium* complex and *M. smegmatis*) are clustered together due to the genetic relatedness of these organisms. It is thus highly likely that this protein is widely conserved and maintained in the genome of different bacteria. Though there are no reports to know how the plasticity of this gene regulated its functionality, the presence of various homologues hints at the possibility that the gene may be dispensable under *in vitro* and free-living conditions, indicating that it may not be absolutely essential for the survival of these bacteria. It is possible that it has a role *in vivo*, as can be speculated from the presence of a functional HupB in *M. leprae* that forms a distinct separate branch in the tree. Though this could indicate rearrangement of the gene due to the dominant trend of pseudogenisation in the *M. leprae* genome, the functionality of the protein probably reflects its importance *in vivo*; support for this presumption comes from the demonstration of the protein (referred to as laminin-binding protein LBP in *M. leprae*) as an adhesion molecule that is necessary for binding to Schwann cells (described below).

A detailed analysis of the different strains of the *M. bovis* BCG revealed that the *hupB* gene was under the control of the intracellular iron concentration in only some of the strains, though all of them responded to iron limitation by the expression of siderophores. All the eight strains of BCG expressed almost similar levels of CMb, while Mb levels were relatively higher in BCG Denmark with low levels in BCG Russia. The HupB profile, as analysed by SDS-PAGE and western blotting with anti-HupB antibodies showed marked up-regulation in BCG Moreau, similar to that seen in *M. tuberculosis* H37Rv upon iron limitation. Appreciable increase in expression was seen in BCG Denmark with a marginal increase in expression in Birkhaug and Connaught. A low level of the protein was seen in both high and low iron organisms of BCG Pasteur, Phipps and Sweden. Under the conditions of the study, we could not detect the protein in BCG Russia. It is becoming increasingly evident that there are several changes among the BCG strains at the molecular level (Behr & Small, 1997), possibly due to the differences in the growth and maintenance conditions that were adopted before standard protocols of cryopreservation were adopted. From the genealogy of the BCG strains, BCG Russia, seen as an early strain after the first BCG strain in 1921, showed maximal expression of HupB upon iron limitation, while the late strain BCG Pasteur showed constitutive expression of HupB. The protein is probably not required for growth under *in vitro* conditions as the strain was repeatedly passaged *in vitro,* so in iron-sufficient growth medium it would be interesting to see if BCG Pasteur, repeatedly grown in low iron medium would show an increase in the expression of the HupB protein. These studies would perhaps help in the assessing the role of the protein in iron acquisition.

To summarize our findings, HupB protein in *M. tuberculosis* is a cell wall-associated, surface-exposed protein, whose expression is coordinately regulated with that of the siderophores Mb and CMb that are proven indicators of iron acquisition. Based on our observations and published reports on HupB by other researchers, we hypothesize two possible roles for HupB. First, by virtue of the positively charged amino acid residues present in the C-terminal region and the helix-turn-helix repeats in the protein, HupB is a DNA-binding protein and perhaps plays a regulatory role. Evidence to this DNA-binding property has reported by other researchers (discussed below). Second, the surface localization and the iron-regulated expression of the protein led us to propose a

role of the protein as a putative ferric-siderophore receptor for the extracellular carboxymycobactin. In this study, the latter was addressed by performing ligand-binding studies of the purified protein with both the siderophores.

Ligand-binding studies demonstrated the ability of the purified HupB protein to bind both Mb and CMb. The chloroform extracts of the cell pellet and spent growth medium of low iron *M. tuberculosis*, containing ferric-Mb and ferric-CMb were subjected to HPLC to purify these siderophores. Both Mb and CMb eluted out as a mixture of closely related compounds due to varying levels of esterification and were thus seen as mixture of peaks (9 for Mb; 16 for CMb) instead of a single peak (also reported by earlier researchers, including Barclay *et al.,* 1986). Cell wall-associated HupB, purified by preparative gel electrophoresis was used to study the binding of ^{59}Fe-labelled Mb / CMb. Both ferric-Mb and ferric-CMb bound HupB, the specificity of which was demonstrated by inhibition of the binding upon pre-incubation of HupB with anti-HupB antibodies. Additionally, displacement of ^{59}Fe-labelled Mb / CMb bound by the purified protein by the addition of cold ferric-siderophore provided additional evidence. We did not observe any difference in the binding of the two siderophores to HupB. However, from the spectrofluorimetric studies performed with rHupB, the binding affinity of the ferric-Mb was found to be relatively higher than that of ferric-CMb, calculated as 1.045 mM and 0.551 mM respectively. Though the intensity of the emitted light decreased with increasing addition of the ferric-Mb / ferric-CMb, no spectral shift was observed. Spectral shift has been reported in the emitted light when ferric-siderophore (Meyer *et al.,* 1990) / hemin receptors (Asuthkar *et al.,* 2007) bind with ligand.

In *M. smegmatis,* the 29 kDa protein IREP, shown to be the ferri-exochelin receptor (Hall *et al.*, 1987; Dover & Ratledge, 1996) was recognized by the anti-HupB antibody (results not shown), showing the similarity between HupB and the ferri-exochelin receptor. As antibodies against the 29 kDa protein significantly inhibited the uptake of ferri-exochelin by *M. smegmatis*, it was presumed that HupB was a possible receptor to ferric-CMB. Contrary to the expectation of specific binding of the extracellular ferric-CMb to HupB, both ferric-Mb and ferric-CMb bound the protein, with the former showing higher affinity. Whether this binding is specific or occurs non-

specifically due to the hydrophobicity of the protein needs to be addressed. Further work, preferably uptake studies with ferric-carboxymycobactin using live organisms in the presence and absence of anti-HupB antibodies probably would help to understand the role of HupB as a receptor.

Reports on HupB by other researchers attribute varied roles to the protein in the mycobacterial system. Incidentally, HupB is referred by several synonyms, including histone-like protein Hlp in *M. smegmatis* (Lee *et al*., 1998), Hlp protein in *M. tuberculosis* with DNA-binding property (Prabhakar *et al*., 1998), laminin binding protein LBP21 in *M. leprae* by Brennan & group (Marques *et al*., 2000; Soares *et al*., 2005), mycobacterial DNA-binding protein 1 (MDP1) in *M. smegmatis* and BCG (Katsube *et al.,* 2007). In *M. smegmatis*, Hlp was shown to express under dormancy; disruption of the gene however did not affect the viability of the dormant culture proving that it was not an essential gene (Lee *et al*., 1998). In *M. leprae*, LBP is a 200-amino acid protein and was demonstrated as a surface-exposed cell wall-associated protein in organisms isolated from infected armadillo tissues (Shimoji *et al*., 1999). The protein has been implicated as an adhesion molecule used by *M. leprae* for the invasion of Schwann cells and thought to initiate nerve damage in leprosy. It has been experimentally proved that the protein can bind laminin, heparin and heparan sulfate. Interestingly, it was shown that the interaction of Hlp / LBP with laminin and heparin was mainly mediated by the C-terminal domain of the protein (Marques *et al.,* 2000; Soares *et al.,* 2005). Matsumoto *et al.* (1999) showed that MDP1 bound DNA and RNA and localized not only in the nucleoid but also at the 50S ribosomal subunits and cell surface. The same group (Katsube *et al.,* 2007) provided experimental evidence to prove that it is necessary for the cell wall biogenesis in *M. smegmatis* and BCG. Their observations indicate that the protein interacts with both Ag85 complex proteins (mycolyltransferases) and trehalose-6-monomycolate, thereby controlling the transfer of mycolic acids to sugars by Ag85 complex. A recent report by Lewin *et al.* (2008) using recombinant *M. bovis* BCG expressing the MDP1-antisense gene re-iterated the role of the protein as an adhesion molecule and its association with cell wall assembly. They showed that the MDP1 protein in the recombinant *M. bovis* BCG containing the MDP1-antisense plasmid was reduced by about 50% compared to the reference strain *M. bovis* BCG containing the empty

vector. They showed that the antisense strain grew faster than the reference strain and also reached a much higher cell mass in stationary phase. There was less aggregation in the recombinant strain and it was suggested that HupB plays a role in aggregation similar to heparin-binding hemagglutinin HBPA that was thought to be mainly responsible for mycobacterial aggregation (Verbelen *et al.,* 2007). Aggregation and clumping, more pronounced in virulent strains of mycobacteria (Zhang *et al*., 1998) not only complicates many experimental procedures like determination of growth but also influences other important features like accessibility of antibiotics into the bacteria. Studies by Lewin *et al* (2008) also showed that the protein played an important role in the adaptation of the bacteria to hypoxic conditions, which is a prerequisite for the survival in the granuloma.

HupB and HBPA are found to be closely related proteins. These two proteins share several common features. Both proteins produce a band at MW 28 kDa in SDS gels, are surface exposed and promote binding to epithelial cells (Menozzi *et al.,* 1996). They are both post-translationally methylated and show cross-reactivity due to the presence of copies of the motif APAKKAA (Soares *et al.,* 2005). Knock out mutants of *hupB* gene in *M. smegmatis* probably did not show the anticipated effect due to the compensatory role by the closely related HBHA.

A possible *in vivo* role of HupB gains strength from the detection of anti-HupB antibodies in the serum of patients with tuberculosis (Yeruva *et al*. 2006; Cohavy *et al*., 1999; Prabhakar *et al*., 1998) (indicates a possible role in the survival within the mammalian host). In our studies with tuberculosis patients, we detected anti-HupB antibodies that showed good correlation with BACTEC culture, radiological examination and clinical history. Though antibody-based detection methods are not useful in diagnosis of tuberculosis, detection of anti-HupB antibodies correlated well, not only with standard testing protocols but also with a commercial lateral flow device that was based on the *M. tuberculosis*-specific ESAT proteins. It is likely that HupB expression reflected active infection, and was expressed only upon iron limitation *in vivo*, though direct evidence for the iron-regulated expression *in vivo* is warranted. HupB probably plays an important role in the survival of the organism within the mammalian host; a presumption that needs to be experimentally verified.

4.3. Iron, mycobacterial catalase-peroxidases and INH activation

Iron limitation influences not only the components of the iron acquisition machinery in bacterial systems but also several genes, notably virulence / toxin genes that are associated with the survival of the organism, particularly *in vivo* within the mammalian host (Salyers & Whitt, 1994; Sritharan, 2000). In mycobacteria, despite a wealth of knowledge on the mycobacterial iron acquisition machinery, there are lacunae, particularly on the role and interplay, if any, among the iron regulators, not only on the iron acquisition machinery but also on the expression of other genes required for the survival of the organism. In the second half of our study, our objective was to analyze the association of iron levels with oxidative stress, mainly the effect of iron limitation on the known virulence determinant catalase-peroxidase KatG of *M. tuberculosis* H37Rv and other mycobacteria. Oxidative stress response and protection against reactive oxygen intermediates and reactive nitrogen intermediates have been implicated in the intracellular survival of pathogenic mycobacteria and their persistence in the host. We then extended the study to understand the influence of catalase-peroxidase on the activation of the front-line drug isoniazid INH, not only in *M. tuberculosis* H37Rv but also in clinical isolates of *M. tuberculosis* that were resistant to the drug and compared the findings with drug-sensitive clinical isolates.

As reviewed earlier in Chapter I, different classes of mycobacterial catalases are seen, with different isoforms among them. Wayne and Diaz (1986) demonstrated both catalatic and peroxidatic activities in polyacrylamide gels. In our study, we extended the influence of iron levels analysis of the enzyme activities, as catalase-peroxidase contain iron in the heme centre of the molecule. Our initial studies focused on the catalase-peroxidases in different mycobacteria. Selected mycobacterial spp. including *M. tuberculosis, M. bovis, M. bovis* BCG, *M. fortuitum, M. kansasii, M. smegmatis and M. vaccae* were grown under high and low iron conditions: they responded to iron limitation by the production of extracellular CMb / exochelins, thereby reflecting the iron status of the organisms. The cell sonicates of these mycobacteria, assayed for catalase and peroxidase activities both by spectrophotometric and by in-gel assays clearly indicated that iron limitation drastically influenced these enzyme activities. When sufficient iron is present in the growth medium, significant levels of both catalase and peroxidase were

seen; however, iron limitation during growth of the organisms resulted in a dramatic 10-13 fold decrease in the peroxidase activity in all the mycobacterial species tested. *Mycobacterium vaccae* was exceptional in that low levels of peroxidase and catalase were seen even under high iron conditions though the relative activity of catalase was high comparable to that of *M. kansasii* and *M. fortuitum* grown under high iron conditions. Catalase activity also showed reduction in all the mycobacterial species except *M. vaccae*.

The total enzymatic activities, distributed among the various isoforms were detected by the dual staining method of Wayne & Diaz (1986); variations were seen in the number, enzymatic activity and heat inactivation among these isoforms, with iron availability contributing further to this variability. Two isoforms of T- catalase with both catalase and peroxidase activities were seen in high iron cells of *M. tuberculosis, M. bovis* and *M. bovis* BCG; of the two isoforms, one of them is a major band with significant activity which is completely lost and could not be detected in low iron organisms. Heat treatment of the cell sonicates from high iron cells of all the above species resulted in a marked loss of both the enzyme activities. Notable feature was that in low iron *M. bovis* BCG, a prominent band of catalase activity that was unaffected by heat was seen; this was clearly absent in *M. tuberculosis* and *M. bovis*. It is likely that this is M-catalase expressed by the vaccine strain. It is not clear if this is present in high iron organisms, as it is likely that it is masked by the T-catalase isoform that was co-migrating with it. However, in *M. kansasii*, the band of M-catalase was evident in both high and low iron organisms, due to the distinct mobility of the band and it was seen that this band remained unaffected by the iron status and heat treatment. M-catalases were also seen in *M. smegmatis* and *M. vaccae*; they were unaffected by iron and heat unlike the T-catalase bands which lost the peroxidase activity upon iron limitation and was also heat-sensitive. In conclusion, it was evident that the peroxidase activity (and to a relatively lesser extent, the catalase) in most of the mycobacterial species, except *M. vaccae* was found to be highly sensitive to iron limitation and increase in temperature (Yeruva *et al*., 2005).

Although *katG* is a known virulence factor, the regulation of expression is not completely understood. OxyR, product of the *oxyR* gene, known to be the central regulator of oxidative stress response in *E. coli* is inactivated in *M. tuberculosis* due to

multiple mutations (Deretic *et al.,* 1995; Sherman *et al.,* 1995). The changes in oxyR are seen in all members of the *M. tuberculosis* complex. The loss of *M. tuberculosis oxyR* appears to be related to the altered expression of the closely linked and divergently transcribed *ahpC* gene encoding a homolog of alkyl hydroperoxide reductase and *katG*, both of which are up-regulated by OxyR in *E. coli* and several other bacteria, where this antioxidant system plays a role in reducing organic peroxides and detoxifies targets particularly sensitive to peroxide-mediated damage, such as lipids and nucleic acids. However, it is now proved that in *M. smegmatis* (Zahrt *et al*., 2001) and *M. tuberculosis* (Pym *et al.,* 2001), *katG* is negatively regulated by the FurA protein, encoded by *furA* located directly upstream of *katG*. Milano *et al*. (2001) identified two more regions called the *pfurA* and *pkatG* that controlled the expression of katG. Our observations clearly show the role of iron in the regulation of expression of the catalase-peroxidase in *M. tuberculosis*; however, the role-played by FurA and IdeR need to be addressed. The exact role of IdeR in *katG* expression in *M. tuberculosis* is not clear though both IdeR mutants of *M. smegmatis* and *M. tuberculosis* are more sensitive to hydrogen peroxide and superoxide (Dussurget *et al.,* 1996; Rodriguez *et al.,* 2002). Though no IdeR binding regions are identified upstream of the *katG* and *sodA* genes, IdeR is required for the full expression of catalase and superoxide dismutase in *M. smegmatis* (Dussurget & Smith 1998), while in *M. tuberculosis* there is no increase in their expression. This effect was shown to be iron-independent in *M. smegmatis* (Pym *et al.,* 2001).

The activity of catalase-peroxidase is closely associated with the efficacy of isoniazid as an anti-tubercular drug. Isoniazid and rifampicin comprise the backbone of the current chemotherapy program for tuberculosis and resistance to one or both of them results in the therapeutic failure and worse, the development of drug resistance, with the subsequent risk of the spread of these resistant organisms that contributes to the success of the pathogen and has made human efforts to combat this disease more difficult. Rifampicin resistance has been studied extensively (Telenti *et al*., 1993). Resistance to INH (discussed in detail in Chapter I) has involved one or more genes, the more common of which involves the inactivation or mutation of the *katG* gene (Heym *et al.*, 1994; Zhang *et al*., 1993). The other mutations that are seen in INH-resistant strains occur in dispersed gene loci including *inhA* (enoyl-acyl reductase) (Banerjee *et al*., 1994), *kasA*

(β-ketoacyl ACP synthase) (Mdluli *et al*., 1998a), *mabA* (3-ketoacyl reductase) (Ducasse-Cabanot *et al*., 2004), and *ndh* (NADH dehydrogenase) (Lee *et al*., 2001); mutation in the promoter region of *ahpC* (alkyl hydroperoxidase) resulting in an increased production of AhpC was also found to be associated with INH resistance (Kelley *et al*., 1997).

In this study, we demonstrated how a simple, yet essential micronutrient like iron can influence the catalase-peroxidase activity and hence the activation of INH. The loss of catalase-peroxidase activity and the failure of activation of isoniazid were evident both by NBT reduction assay and by viability studies. Two main points emerged from our study; first, the peroxidase activity of *M. tuberculosis* was associated with the activation of the drug and second, there was species specificity of the enzyme for the drug, as the peroxidase of *M. fortuitum* failed to act on the drug. The direct effect of the peroxidase on INH activation was evident from the coinciding banding pattern for the peroxidase and INH-mediated NBT reduction (See Results, Fig. 3.34). This is in accordance with the strong evidence provided by Shoeb *et al*. (1985 a and b) who demonstrated that the toxicity of the drug is potentiated by the peroxidase activity of the catalase-peroxidase; experimentally induced mutations in the N-terminal heme-containing domain of KatG in *M. tuberculosis* resulted in the abolishing of peroxidase activity and subsequent failure to act on INH. Most strains of *M. tuberculosis* are sensitive to INH with the reported minimal inhibitory concentration of the drug being 0.02 μg / mL. Other species of mycobacteria show a range of sensitivities to INH, for example *M. smegmatis* is highly resistant with minimal inhibitory concentrations being as high as 32 μg / mL (Zhang *et al.,* 1992). This refractoriness to INH is perhaps due to the lack of specificity of the peroxidase for the substrate. In our study, we have directly demonstrated the refractoriness of *M. fortuitum* to INH to be due to the ineffectiveness of the peroxidase; though it is expressed at high levels, it does not act on INH. Both our observations were further reiterated in the viability assay; high iron *M. tuberculosis* as susceptible to INH while *M. fortuitum*, irrespective of the iron status was unaffected by the drug even at high concentrations. Sequence differences of KatG among the different mycobacterial species (Zámocký *et al*., 2001) could influence heme coordination number and spin state as studied in *M. tuberculosis* (Chouchane *et al.,* 2003), which could contribute to the target specificity of the peroxidase for INH by influencing the binding to the drug and the

catalytic activity. Multiple sequence alignment reveals notable differences in the protein sequence of the enzyme from *M. fortuitum* (Fig.4.1) as compared to that of *M. tuberculosis*, and *M. bovis*, which share perfect homology between them (Yeruva *et al*., 2006). Further studies are needed to prove if these differences in the amino acid residues contribute directly to the binding of INH or indirectly alter the folding of the molecule resulting in altered affinity of binding to the drug.

There are several reports on the association of INH resistance with mutations in the *katG* gene (Ramaswamy *et al*., 2003; Marttila *et al*., 1996; Heym *et al*., 1994). Though deletion of the gene with no functional protein has been seen in some isolates, single point mutations have been noted in several isolates, notably the two mutations seen in INH-resistant *M. tuberculosis*, Thr-275 to Pro and Ser 315 to Thr in the N-terminal

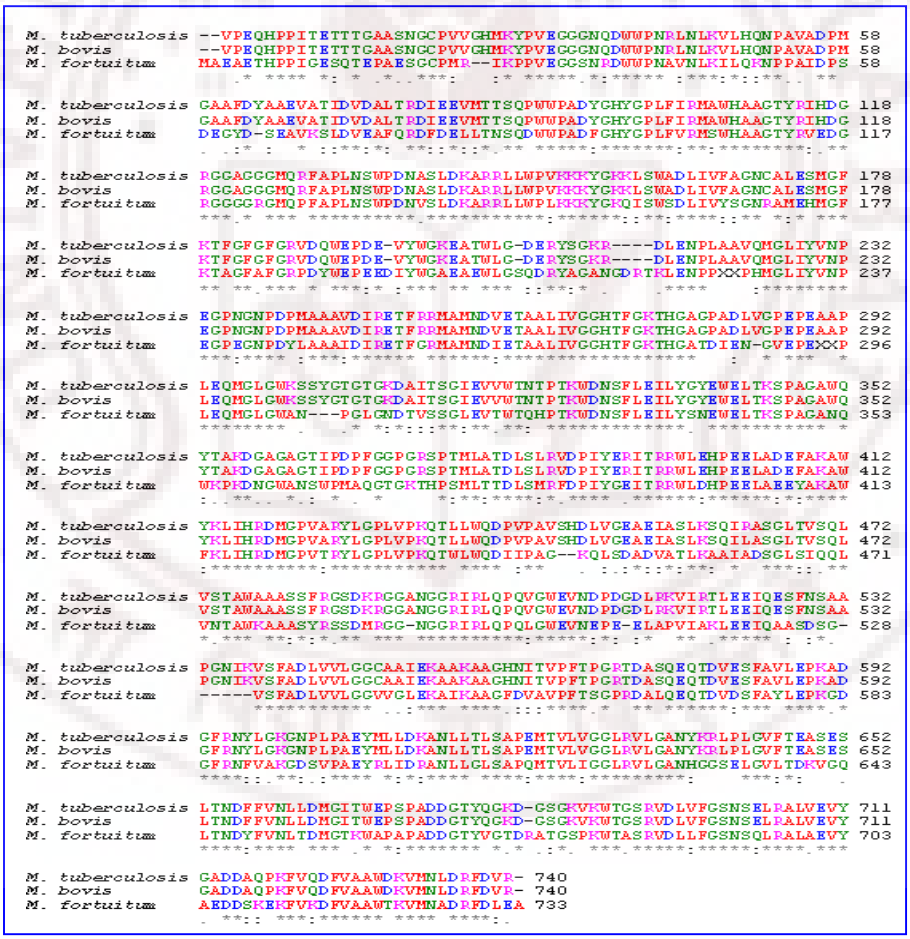

Fig. 4.1. Multiple sequence alignment (CLUSTAL W2) of *M. tuberculosis*, *M. bovis* and *M. fortuitum*. Identical amino acid residues are marked with (*) and similar residues are marked with (:, .).

domain of the molecule that are proved to affect the functioning of the enzyme. However, all INH-resistant isolates do not show these mutations and strains with these changes do not always result in INH resistance. In the context of the findings on INH resistance with reference to functional *katG*, it is our hypothesis that a simple alteration of the level of the micronutrient iron is an additional contributing factor towards ineffective INH activation (Fig. 4.2). As there is now increasing evidence to show that these pathogens face conditions of iron limitation within the phagocytes (Sritharan *et al*., 2006; Ratledge, 2004; Gold *et al*., 2001) and anemia is frequently encountered in tuberculosis patients, the serum iron levels in these patients may be monitored during the chemotherapy.

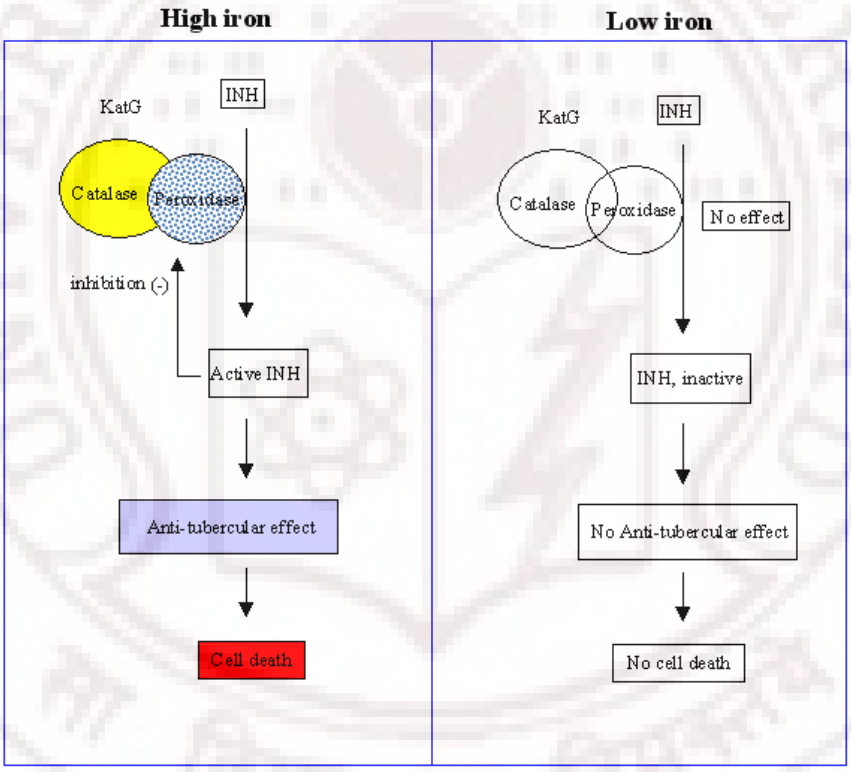

Fig. 4.2. Iron enhances the susceptibility of pathogenic mycobacteria to isoniazid

In strains with *katG* mutation, there is usually an up-regulation of AhpC. *M. tuberculosis* being facultative intracellular pathogen needs to overcome the reactive oxygen and reactive nitrogen intermediates generated within the environment of the phagolysosome where it resides. The regular strain of *M. tuberculosis* has a high resistance to killing by up to millimolar concentrations of hydrogen peroxide (Dussurget

et al., 1996), due to the enzymatic activity of KatG and by AhpC. In INH-sensitive strains, when the KatG is active, usually the levels of AhpC are low. But in some INH-resistant strains, it was observed that the level of AhpC increases considerably (Sherman *et al*., 1996). This is due to a mutation upstream of *ahpC* that results in an up-regulation of the protein. This probably helps to overcome the low or no activity of KatG, as *M. tuberculosis* cannot survive the high concentrations of hydrogen peroxide in the absence of both KatG and AhpC.

We extended our observations on *M. tuberculosis* H37Rv to clinical isolates. The catalase and peroxidase activities of twenty drug sensitive and twenty INH-resistant clinical isolates were assayed in the cell-free sonicates of these organisms grown under high and low iron conditions. All of them responded to iron levels by the production of the siderophores Mb and CMb, though there was some variation in their levels, as assayed by our methods. A notable feature in these isolates was the peroxidase activity; both high and low iron organisms showed peroxidase activity in a majority of the drug sensitive organisms, with no inhibition of the peroxidase activity in low iron organisms. This was reflected in the ability of these cell sonicates to activate INH in the NBT reduction assay. On the contrary, the low iron organisms of the majority of the INH-resistant isolates (few exceptions were seen) did not show peroxidase activity, some of which did not show the enzymatic activity even under high iron conditions. INH activation was thus ineffective, as noted by the negative NBT reduction assay. In all these assays, the cell sonicate of *M. tuberculosis* H37Rv functioned as a positive control, showing clearly the peroxidase activity and NBT reduction in high iron organisms. Our observations would have gained strength with viability assays and AhpC levels, which were not done in this study. Exposure of high and low iron drug-sensitive and INH-resistant clinical isolates to varying concentrations of the drug will help to confirm our above observations with the cell sonicates.

Conclusions & Future Perspectives

Our studies on the influence of iron limitation in mycobacteria, specifically *M. tuberculosis* focused on the identification of novel cell envelope proteins, whose expression was regulated by iron. We identified and characterized a 28 kDa cell wall

associated protein, localized on the cell surface as HupB protein (Rv2986c). The features of the protein, as annotated in the mycobacterial genome and deduced from the amino acid sequence showed it to be a protein rich in the positively charged lysine that was present as part of repeat sequences with alanine at the C-terminal end, unique to mycobacteria. The helix-turn-helix and positively charged lysine residues, similar to the eukaryotic histone proteins was indicative of DNA-binding ability of the protein. However, due to its co-expression with the mycobacterial siderophores Mb and CMb and its surface localization, we performed ligand-binding studies to see if it was a receptor for the extracellular CMb. Contrary to the expectation that HupB may serve as a specific receptor to CMb, the affinity for Mb appeared to be higher. Since both these siderophores share similarity in structure, it is perhaps not surprising that both the molecules interacted with the protein. Uptake studies with whole organisms in the presence of antibodies against HupB would help to understand further its role. Our ongoing studies include transcriptional profiling of a *hupB* mutant of *M. tuberculosis* that will help us to unravel the role of the protein. The protein is likely to play to role *in vivo*, as serum from patients with tuberculosis showed the presence of antibodies against the protein.

A second important aspect of this study focused on the effect of iron limitation on the virulence determinant catalase-peroxidase. Iron limitation drastically abolished the peroxidatic activity of the catalase-peroxidase activity in *M. tuberculosis* that was shown to influence directly the activation of the anti-tubercular drug INH, as shown by the NBT reduction assays and viability of the pathogen in the presence of the drug. Peroxidase of *M. fortuitum* failed to activate INH, proving the substrate specificity of the enzyme for INH. We extended the studies to clinical isolates of *M. tuberculosis* that were resistant to INH. Iron limitation resulted in the loss of peroxidase activity in a majority of the INH resistant strains, unlike in the drug sensitive strains that did not show any influence of iron. Further work, including screening of the isolates for *katG* deletions, AhpC activity can be done to understand the mechanism of INH resistance in these strains.

Our studies show how a simple micronutrient could have considerable implications in the outcome of an infection by *M. tuberculosis* within the mammalian host During the regular monitoring of tuberculosis patients during chemotherapy, an additional parameter of the iron profile may be included; supplements of iron, given to

correct anemia in these patients must be done with careful monitoring to prevent aggravation of the disease. Unlike *in vitro* conditions where it is possible to maintain the organisms under defined iron levels, the *in vivo* organisms must be continually exposed to varying concentrations of the metal ion and the successful mycobacterial pathogen must have adapted to these fluctuations and is probably continuously altering its profile to suit the immediate iron status. Hence, the *in vivo* organisms must be on the "cusp", the word put forth by Ratledge (2004) indicating the easy switch on and off of the different genes, both for iron acquisition and for successful survival in the hostile intracellular environment of the macrophage. Ours has been a small effort in the long journey towards the understanding of the iron metabolism in this human pathogen.

CHAPTER 5

SUMMARY

Summary

- Iron acquisition machinery is the focus of research in our lab. Though the mycobacterial siderophores are well studied, little is known about ferric-siderophore receptors in mycobacteria. Iron limitation in pathogenic *M. tuberculosis* was established with increased expression of the siderophores. Coordinated expression of a cell wall associated 28 kDa protein (Irep-28) with both Mb and CMb was demonstrated.Irep-28 was purified and sequenced by tandem mass spectrometry and identified as HupB (Rv2986c). It is annotated as histone- like DNA- binding protein.*In silico* analysis and confocal microscopy showed the protein to be surface associated, probably anchored via lipid molecule to the membrane.
- Ligand-binding studies with both Mb and CMb were done to see the role of the protein as a putative ferri-siderophore receptor. However, both the siderophores bound the protein in a dose-dependant manner. With spectrofluorimetric studies, though quenching of the emitted light was observed upon ligand binding, the results were not conclusive about the role of HupB as a receptor.
- Heterogeneity of HupB was seen among the members of *M. tuberculosis* complex. Deletions were observed in *M. bovis* AN5 and *M. bovis* BCG.
- Considerable variations in HupB expression among the different strains of *M. bovis* BCG were observed, with low levels of expression in the recent strains BCG Pasteur, that was not induced by iron limitation; iron limitation resulted in up regulation of the protein in the old strains like BCG Moreau.
- Anti-HupB antibodies in the serum of tuberculosis patients indicate the expression of the protein *in vivo*. The detection of antibodies against HupB showed good correlation with clinical examination, culture and radiological examination, thus making possible the use of HupB as a diagnostic antigen. However, larger samples need to be screened to validate the potential as a diagnostic antigen.
- Iron limitation was demonstrated to influence the activity of catalase-peroxidase (KatG) that was proved to be a virulence determinant necessary for the survival of the pathogenic *M. tuberculosis* within the hostile environment of the macrophages in the mammalian host.

- Mycobacteria express both catalase-peroxidase (KatG, T catalases) and catalase alone (M catalase). The influence of iron limitation on these enzymes from different mycobacterial species were studied and it was observed that iron limitation drastically abolished the peroxidase activity and to a lesser extent the catalase activity of T catalases with little or no effect on the M catalases. The observations were also demonstrated among the different isoforms in polyacrylamide gels.
- *Mycobacterium tuberculosis* expresses only KatG that was demonstrated to affect by iron deprivation. The loss of peroxidase activity was correlated with the failure to activate the anti-tubercular drug INH.
- It was also observed that there was substrate specificity of the peroxidase for the drug, as the peroxidase of *M. fortuitum* failed to act on INH.
- Our studies were extended to INH resistant clinical isolates and compared with that of drug sensitive isolates; in the former, iron regulated the activity of the KatG with almost negligible effect in the latter.
- Iron is an important factor that is not only required for the growth of the organism but is also used at the molecular level to regulate genes that influence the survival of the organism as a whole. There is increasing evidence to show that *M. tuberculosis* is growing under conditions of iron deprivation in vivo and our observations are discussed with reference to the in vivo status of the pathogen.

CHAPTER 6

REFERENCES

1. Adilakshmi T, Ayling PD, and Ratledge C. (2000). Mutational analysis of a role for salicylic acid in iron metabolism of *Mycobacterium smegmati*s. *Journal of Bacteriology,* **182:** 264–271.
2. Aisen P & Leibman A. (1972). Lactoferrin and transferrin: a comparative study. Biochimica et Biophysica Acta, **257**: 314±323.
3. Andrews SC, Robinson AK & Rodriguez-Quinones F. (2003). Bacterial iron homeostatis. *FEMS Microbiology Reviews,* **27**: 215 - 37.
4. Arounaguiri S, Easwaramoorthy D, Ashok kumar A, Aparna Datta Gupta & Maiya BG. (2000). Cobalt(III), nickel(II), and ruthenium(II) complexes of 1,10-phenanthroline family of ligands: DNA binding photocleavagestudies. *Proceedings of Indian Academy Sciences (Chemical sciences),* **112,** 1-17.
5. Arruda S, Bomfim G, Knights R, Huima-Byron T & Riley LW. (1993). Cloning of an *M. tuberculosis* DNA fragment associated with entry and survival inside cells. *Science,* **261:** 1454-1457.
6. Asuthkar S, Velineni S, Stadlmann J, Altmann F & Sritharan M. (2007). Expression and characterization of an iron-regulated hemin binding protein, HbpA, from *Leptospira interrogans* serovar Lai. *Infection and Immunity*, **75** (9): 4582 – 4591.
7. Banerjee A, Dubnau E, Quemard A, Balasubramanian V, UM KS, Wilson T, Collins D, de Lisle G, and Jacobs WR, Jr. (1994). *inhA*, a gene encoding a target for isoniazid and ethionamide in *Mycobacterium tuberculosis*. *Science,* **263**: 227 –230.
8. Barclay R, Ewing DF. & Ratledge C. (1986). Isolation, identification and strucural analysis of the Mycobactins of *M. avium*, *M. intracellulare*, *M. scrofuloceum* and *M. paratuberculosis*. *Journal of Bacteriology*, **164**: 896- 903.
9. Bartos M, Falkinham III JO & Pavlik I (2004). Mycobacterial catalases, peroxidases, and superoxide dismutases and their effects on virulence and isoniazid-susceptibility in mycobacteria. *Veternary Medicine– Czech*, **49** (5): 161 –170.
10. Beers RF & Sizer IW. (1952). A spectrophotometric method for measuring the breakdown of hydrogen peroxide by catalase. *Journal of Biological Chemistry,* **195**: 133–140.
11. Behr MA & Small PM. (1997). Has BCG attenuated to impotence? *Nature,* **389**: 133-4.
12. Behr MA. (2002). BCG- different strains, different vaccines? *Lancet Infectious Diseases,* **2**: 86 –92.
13. Bernstein J, Lott WA, Steinberg BA, Yale HL. (1952). Chemotherapy of experimental tuberculosis. V. Isonicotinic acid hydrazide (nydrazid) and related compounds. *American Reviews in Tuberculosis*, **65**: 357-64.
14. Bertrand T, Eady NAJ, Jones JN, Jesmin JM, Nagy B, Jamart-Gregoire EL, Raven KA & Brown. (2004). Crystal Structure of *Mycobacterium tuberculosis* Catalase-Peroxidase. *Journal of Biological Chemistry*, **279**: 38991–38999.
15. Bloom BR and Murray CJ. (1992). Tuberculosis: commentary on a re-emergent killer. *Science*, **257**: 1055-1064.

16. Boyd J, Oza MN & Murphy JR. (1990). Molecular cloning and DNA sequence analysis of a diphtheria toxin iron dependent regulatory element (*dtxR*) from *Corynebacterium diphtheriae*. *Proceeding of National Academy of Sciences,* USA, **87**: 5968 - 5972.

17. Braun V & Killmann H. (1999). Bacterial solutions to the iron-supply problem. *Trends in Biochemical Sciences,* **24**: 104 - 109.

18. Braun V, Hantke K & Koster W. (1998). Bacterial iron transport: mechanisms, genetics and regulation. In Metal Ions in Biological systems. Iron transport and storage in Microorganisms, Ed. Sigel, A & Sigel, H. New York, Marcel Dekker. ISBN 0-8247-9984-4. *Plants and Animals*, 67- 145.

19. Brennan PJ & Crick DC. (2007). The cell-wall core of *Mycobacterium tuberculosis* in the context of drug discovery. *Current Topics on Medical Chemistry*, **7**: 475-488.

20. Brennan PJ & Nikaido H. (1995). The envelope of mycobacteria. *Annual Reviews of Biochemistry*, **64**: 29-63.

21. Brickmann TJ & Armstrong SK. (1999). Essential Role of the Iron-Regulated Outer Membrane Receptor FauA in Alcaligin Siderophore-Mediated Iron Uptake in *Bordetella* Species. *Journal of Bacteriology*, **181** (19): 5958-5966.

22. Brosch R & Cole ST. (2002). A new evolutionary scenario for the *M. tb* complex. *Proceedings of National Academy of science.* USA, **99**: 3684-3689.

23. Brosch R, Gordon SU, Garnier T, EiglmeierK, Frigui W, Valenti P, Dos Santos S, Duthoys S, Lacroix C, Garcia-Pelayo C, In wald JK, Golby P, Garcia JN, Hewinson RG, Behr MA, Quail MA, Churcher C, Barrell BG, Park hill J & Cole ST. (2007). Genomic plasticity of BCG and impact on vaccine efficacy. *Proceedings of National Academy of science*. USA, **104**: 5596-601.

24. Brosch R, Gordon SV, Buchrieser C, Pym AS, Garnier T & Cole ST. (2000a). Comparative genomics uncovers large tandem chromosomal duplications in *M. bovis* BCG Pasteur. *Yeast*, **17:** 111-123.

25. Brosch R, Gordon SV, Eiglmeier K, Garnier T & Cole ST. (2000). Comparative genomics of the leprosy and tubercle bacilli. *Research inMicrobiology*, **151:** 135-142.

26. Brosch R, Pym AS, Gordon SV & Cole ST. (2001). The evolution of mycobacterial pathogenicity: clues from comparative genomics. *Trends in Microbiology*, **9**: 452-458.

27. Bullen JJ & Griffiths E. editors. (1999). Iron and infection: molecular, physiological and clinical aspects, 2nd ed. Chichester, UK: Wiley.

28. Butterton JR, Stoebner JA, Payne SM & Calderwood SB. (1992). Cloning, sequencing, and transcriptional regulation of viuA, the gene encoding the ferric vibriobactin receptor of *Vibrio cholerae*. *Journal of Bacteriology*, **174**: 3729 - 3738.

29. Cade CE, Medzihradszky KF, Salas-Castillo SP & Ghiladi RA. (2010). Isoniazid-Resistance Conferring Mutations in *Mycobacterium tuberculosis* KatG: Catalase, Peroxidase, and INH-NADH Adduct Formation Activities. *Protein Science*, 324.

30. Calder KM & Horwitz MA. (1998). Identification of iron-regulated proteins of *Mycobacterium tuberculosis* and cloning of tandem genes encoding a low-

induced protein and a metal transporting ATPase with similarities to two-component metal transport systems. *Microbial Pathogenisis*, **24**:133–143.

31. Camacho, L. R., D. Ensergueix, E. Perez, B. Gicquel, & C. Guilhot. 1999. Identification of a virulence gene cluster of *Mycobacterium tuberculosis* by signature-tagged transposon mutagenesis. *Molecular Microbiology*, **34**: 257–267.
32. Canueto-Quintero J, Caballero-Granado FJ, Herrero-Romero M, Dominguez-Castellano A, Martin–Rico A, Verdu EV, Santamaria DS, Cerquera RC & Torres-Tortosa M. (2003). Epidemiological, clinical, and prognostic differences between the diseases caused by *M. kansasii* and *M. tuberculosis* in patients infected with Human immunodeficiency virus: a multi-center study. *Clinical Infectious diseases*, **37:** 584-590.
33. Card GL, Peterson NA, Smith CA, Rupp B, Schick BM & Baker EN. (2005). The crystal structure of Rv1347c, a putative antibiotic resistance protein from *Mycobacterium tuberculosis*, reveals a gcn5-related fold and suggests an alternative function in siderophore biosynthesis. *The journal of Biological Chemistry*, **280**: 13978–13986.
34. Chauhan DR. (2003). Epidemiology of tuberculosis. Chapter 1. Tuberculosis control in India.
35. Chen XY, Li CY, Ma Y, Liu C, Wang JH, Zhang XF & Chang ZY. (2004). Study on gene knockout in Mycobacterium BCG. *Zhonghua Jie He He Hu Xi Za Zhi.*, **27**: 183-187.
36. Chikata Y, Kusunose E, Ichihara K & Kusunose M. (1975). Purification of superoxide dismutases from *Mycobacterium phlei*. *Osaka City Med. J.*, **21**: 127 – 136.
37. Chipperfield JR & Ratledge C. (2000). Salicylate is not a bacterial siderophore: A theoretical study. *Biometals.*, **13**: 165-168.
38. Chouchane S, Girotto S, Kapetanaki S, Schelvis JP, Yu S, Magliozzo RSJ. (2003). Analysis of Heme Structural Heterogeneity of *Mycobacterium tuberculosis* in Catalase-Peroxidase (KatG). *The journal of Biological Chemistry*, **278**: 8154-8162.
39. Cohavy O, Harth G, Horwitz M, Eggena M, Landers C, Sutton C, Targan SR & Braun J. (1999). Identification of a novel mycobacterial histone H1 homologue (HupB) as an antigenic target of pANCA monoclonal antibody and serum immunoglobulin A from patients with Crohn's disease. *Infection & Immunity*, **67**: 6510-6517.
40. Colangeli R, Helb D, Sridharan S, Sun J, Varma-Basil M, Hazbon MH, Harbacheuski R, Megjugorac NJ, Jacobs Jr WR, Holzenburg A, Sacchettini JC, and Alland D. (2005). The *Mycobacterium tuberculosis inhA* gene is essential for activity of an efflux pump that confers drug tolerance to both isoniazid and ethambutol. *Molecular Microbiology,* **55**: 1829–1840.
41. Cole ST, Brosch R, Parkhill J, Garnier T, Churcher C, Harris D, Gordon SV, Eiglmeier K, Gas S, Barry CE 3rd, Tekaia F, Badcock K, Basham D, Brown D, Chillingworth T, Connor R, Davies R, Devlin K, Feltwell T, Gentles S, Hamlin N, Holroyd S, Hornsby T, Jagels K, Barrell BG & *et al*., (1998). Deciphering the

biology of *Mycobacterium tuberculosis* from the complete genome sequence. *Nature*, **393**: 537-544.

42. Cole ST, Eiglmeier K, Parkhill J, James KD, Thomson NR, Wheeler PR, Honore N, Garnier T, Churcher C, Harris D, Mungall K, Basham D Brown, D, Chillingworth T, Connor R, Davies RM, Devlin K, Duthoy S, Feltwell T, Fraser A, Hamlin N, Holroyd S, Hornsby T, Jagels K, Lacroix C, Maclean J, Moule S, Murphy L, Oliver K, Quail MA, Rajandream MA, Rutherford KM, Rutter S, Seeger K, Simon S, Simmonds M, Skelton J, Squares R, Squares S, Stevens K, Taylor K, Whitehead S, Woodward JR. & Barrell BG. (2001). Massive gene decay in the leprosy bacillus. *Nature*, **409:** 1007- 011.
43. Cole ST. (1999). Learning from the genome sequence of *Mycobacterium tuberculosis* H37Rv. *FEBS letters*, **452:** 7-10.
44. Collins HL & Kaufmann SH. (2001). Prospects for better tuberculosis vaccines. *Lancet Infection & Disease*, **1**: 21-28.
45. Coulton JW, Mason P & Du Bow MS. (1983). Molecular cloning of the ferrichrome-iron receptor of *Escherichia coli* K-12. *Journal of Bacteriology*, **156** (3): 1315 – 1321.
46. Crooksey RC, Morlock GP, McQueen A, Glickman SE & Crawford JT. (1996). Characterisation of streptomycin resistance mechanisms among *Mycobacterium tuberculosis* isolates from patients in New York City. *Antimicrobial Agents and Chemotherapy*, **40**: 1186 –1188.
47. Crowle, AJ, Dahl R, Ross E & May MH. (1991). Evidence that vesicles containing living, virulent *Mycobacterium tuberculosis* or *Mycobacterium avium* in cultured human macrophages are not acidic. *Infection & Immunity*, **59:** 1823–1831.
48. Curtis NAC, Eisenstadt RL, East SJ, Cornford RJ, Walker LA & White AJ. (1988). Iron-regulated outer membrane proteins of *Escherichia coli* K-12 and mechanism of action of catechol-substituted cephalosporins. *Anti-microbial agents and Chemotherapy*, **32** (12): 1879 - 1886.
49. Dannenberg AM, Jr & Rook JA. (1994). Pathogenesis of pulmonary tuberculosis: an interplay of tissue-damaging and macrophage-activating immune responses. Dual mechanisms that control bacillary multiplication, p. 459–483. *In* B. R. Bloom (ed.), Tuberculosis: pathogenesis, protection, and control. *American Society for Microbiology*, Washington, D.C. **141:**1239–1245.
50. De Voss JJ, Rutter K, Schroeder BG, Su H, Znu Y. & Barry CE. (2000). The salicylate-derived mycobactin siderophores of *Mycobacterium tuberculosis* are essential for growth in macrophages. *Proceedings of National Academy of Science.* USA, **97**: 1252-1257.
51. De Voss JJ, Rutter K, Schroeder BG. & Barry III, C.E. (1999). Iron acquisition and metabolism by mycobacteria. *Journal of Bacteriology*, **181**: 4443-4451.
52. Deres KH, Schild H, Weismuller KH, Jung G & Rammesee HG. (1989). *In vivo* priming of virus-specific cytotoxic T lymphocytes with synthetic lipopeptide vaccine. *Nature*, **342**: 561–564.
53. Deretic V, Philipp W, Dhandayuthapani S, Mudd M.H, Curcic R, Garbe T, Heym B, Via LE & Cole ST. (1995). *Mycobacterium tuberculosis* is a natural

mutant with an inactivated oxidative-stress regulatory gene: implications for sensitivity to isoniazid. *Molecular Microbiology*, **17**: 889 –900.

54. Douvas GS, May MH & Crowle AJ. (1993). Transferrin, iron and serum lipids enhance or inhibit *M. avium* replication in human macrophages. *Journal of Infectious diseases*, **167**: 857-864.

55. Dover LG, & Ratledge C. (1996). Identification of a 29 kDa protein in the envelope of *Mycobacterium smegmatis* as a putative ferri-exochelin receptor. *Microbiology*, **142**: 1521-1530.

56. Ducasse-Cabanot S, Cohen-Gonsaud M, Marrakchi H, Nguyen M, Zerbid D, Bernadou J, Daffe M, Labesse G & Quemard A. (2004). *Antimicrobial agents and Chemotherapy*, **48:** 242-49

57. Dussurget O, Rodriguez M & Smith I. (1996). An *ideR* mutant of *Mycobacterium smegmatis* has derepressed siderophore production and an altered oxidative stress response. *Molecular Microbiology*, **22**: 535-544.

58. Dussurget, O. & Smith, I. (1998). Interdependence of mycobacterial iron regulation, oxidative-stress response and isoniazid resistance. *Trends in Microbiology*, **6:** 354±358.

59. Dussurget_O, Timm J, Gomez M, Gold B, Yu S, Sabol ZS, Holmes RK, Jacobs WR Jr & Smith I. (1999)**.** Transcriptional control of the iron-responsive *fxbA* gene by the mycobacterial regulator IdeR. *Journal of Bacteriology*, **181**: 3402-3408.

60. Edwards KM, Cynamon MH, Voladri RK, Hager CC, DeStefano MS, Tham KT, Lakey DL, Bochan MR & D. S. Kernodle. (2001). Iron-cofactored superoxide dismutase inhibits host responses to *Mycobacterium tuberculosis. American Journal of Respiration and Critical Care Medicine*, **164**: 2213–2219.

61. Escalante P, Ramaswamy S, Sanabria H, Soini H, Pan X, Valiente-Castillo O & Musser JM. (1998). Genotypic characterization of drug-resistant *Mycobacterium tuberculosis* isolates from Peru. *Tubercular Lung Disease*, **79**: 111 –118.

62. Feese MD, Ingason BP, Goranson-Siekierke J, Holmes RK and Hol WG. (2001). Crystal structure of the iron-dependent regulator from *Mycobacterium tuberculosis* at 2.0-A resolution reveals the Src homology domain 3-like fold and metal binding function of the third domain. *Journal of Biological Chemistry*, **276:** 5959–5966.

63. Finken M, Kirschner P, Meier A, Wrede A & Bottger EC. (1993). Molecular basis of streptomycin resistance in *Mycobacterium tuberculosis*: alterations of the ribosomal protein S12 gene and point mutations within a functional 16S ribosomal RNA pseudoknot. *Molecular Microbiology*, **9**: 1239 –1246.

64. Fiss EH, Yu S & Jacobs WR. (1994). Identification of genes involved in the sequestration of iron in mycobacteria: the ferric exochelin biosynthetic and uptake pathways. *Molecular microbiology*, **14**: 557-569.

65. Ford A & Hayhoe PV. (1976). An investigation of alternatives to hog gastric mucin as virulence-enhancing agents in the cholera vaccine potency assay. *Journal of Biological Standardization*, **4** (4): 353 – 366.

66. Franzblau SG, Witzig RS, McLaughlin JC, Torres P, Madico G, Hernandez A, Degnan MT, Cook MB, Quenzer VK, Ferguson RM & Gilman RH. (1998). Rapid, low-technology MIC determination with clinical *Mycobacterium tuberculosis* isolates by using the microplate Alamar Blue assay. *Journal of Clinical Microbiology*, **36**: 362–366.

67. Garnier T, Eiglmeier K, Camus JC, Medina N, Mansoor H, Pryor M, Duthoy S, Grondin S, Lacroix C, Monsempe C, Simon S, Harris B, Atkin R, Doggett J, Mayes R, Keating L, Wheeler PR, Parkhill J, Barrell BG, Cole ST, Gordon SV & Hewinson RG (2003). The complete genome sequence of *M. bovis. Proceedings of the National Academy of Sciences*, **100:** 7877- 7882.

68. Gary E. Kaiser. (2008). Structure of an acid-fast cell wall. Biol. 230-*lecture guide*. (Student.ccbcmd.edu/images/afcw_illus.jpg).

69. Genco CA & Desai PJ. (1996). Iron acquisition in the pathogenic Neisseria. *Trends in Microbiology*, **4**: 179.

70. Ghiladi RA, Knudsen, GM, Medzihradszky KF & Ortiz de Montellano PR (2005). The Met-Tyr-Trp crosslink in *Mycobacterium tuberculosis* catalase-peroxidase (KatG): Autocatalytic formation and effect on enzyme catalysis and spectroscopic properties. *Journal of Biological Chemistry*, **280**: 22651-22663.

71. Girard MP, Fruth U & Kieny MP. (2005). A review of vaccine research and development. *Vaccine*, **23**: 5725-5731.

72. Gladstone GP & Walton E. 1970. Effect of iron on the bactericidal proteins from rabbit polymorphonuclear leukocytes. *Nature*, **227** (5260): 849 – 851.

73. Glassroth J. (2005). Tuberculosis 2004: challenges and opportunities. *Trans Am Clin Climatol Assoc*., **116**: 293-308.

74. Gobin J, Moore CH, Reeve Jr JR, Wong DK, Gibson BW & Horwitz MA. (1995). Iron acquisition by *Mycobacterium tuberculosis*: isolation and characterization of a family of iron-binding exochelins. *Proceedings of National Academy of Sciences* USA, **92**: 5189-93.

75. Gobin J, Wong DK, Gibson BW & Horwitz MA. (1999). Characterisation of exochelins of the *M. bovis* strain and BCG substrains. *Infection and Immunity*, **67**: 2035-2039.

76. Gobin J. & Horwitz M. (1996). Exochelins of *Mycobacterium tuberculosis* remove iron from human iron-binding proteins and donate iron to mycobactins in the *M. tuberculosis* cell wall. *Journal of Experimental Medicine*, **183**: 1527–1532.

77. Gold B, Rodriguez GM, Marras SA, Pentecost M & Smith I. (2001). The Mycobacterium tuberculosis IdeR is a dual functional regulator that controls transcription of genes involved in iron acquisition, iron storage and survival in macrophages. *Molecular Microbiology*, **42**: 851-865.

78. Gordon RE. (1966). Some strains in search of Genus-*Corynebacterium, Mycobacterium, Nocardia* or What? *Journal of general Microbiology*, **43**: 329-343.

79. Gordon SV, Brosch R, Billault A, Garnier T, Eiglmeier K & Cole ST. (1999). Identification of variable regions in the genomes of tubercle bacilli using bacterial artificial chromosome arrays. *Molecular Microbiology*, **3**2: 643-655.

80. Grange JM. (1996). Mycobacteria and human disease, 2nd ed. Oxford University Press, New York, NY.

81. Gray-Owen SD & Schryvers AB. (1996). Bacterial transferrin and lactoferrin receptors. *Trends in Microbiology*, **4**: 185–191.

82. Griffiths E & Chart H. (1999). Iron as a regulatory signal. In iron and Infection 2nd Edition: *Molecular, physiological and clinical aspects*. Editors Bullen JJ and E. Griffiths John Wiley & Sons. 213 - 254.

83. Hall RM, Sritharan M, Messenger AJ & Ratledge C. (1987). Iron transport in *Mycobacterium smegmatis*: occurrence of iron-regulated envelope proteins as potential receptors for iron uptake. *Journal of General Microbiology*, **133**: 2107-2114.

84. Harrison AJ, Yu M, Gardenborg Middleditch M, Ramsay RJ, Baker EN & Lott JS. (2006). The Structure of MbtI from *Mycobacterium tuberculosi*s, the First Enzyme in the Biosynthesis of the Siderophore Mycobactin, Reveals It To Be a Salicylate Synthase. *Journal of Bacteriology*, **181** (17): 6081-6091

85. Heifets LB. (1994). Anti tubercular drugs. *Seminars on Respiratory Infections*. **9**: 84-103.

86. Henderson RA, Watkins SC & Flynn JL. (1997). Activation of human dendritic cells following infection with *Mycobacterium tuberculosis*. *Journal of Immunology*, **159**: 635-643.

87. Herrington DA & Sparling PF. (1985). *Haemophilus influenzae* can use human transferrin as a sole source for required iron. *Infection & Immunity*, **48**: 248–251.

88. Heym B, Honore N, Truffot-Pernot C, Banerjee A, Schurra C, Jacobs Jr. WR, van Embden JDA, Grosset JH & Cole ST. (1994). The implications of multi-drug resistance for the future of short course chemotherapy of tuberculosis: a molecular study. *Lancet,* **344**: 293–298.

89. Husson MO, Legrand D, Spik G & Leclerc H. (1993). Iron acquisition by *Helicobacter pylor*i: importance of human lactoferrin. *Infection & Immunity,* **61**: 2694–2697.

90. Ichihara K, Kusunose E, Kusunose M, Mori T. (1977). Superoxide dismutase from *Mycobacterium lepraemurium*, *Journal of Biochemistry*. (Tokyo), **81**:1427 –1433.

91. Katsube T, Matsumoto S, Takatsuka M, Okuyama M, Ozeki Y, Naito M, Nishiuchi Y, Fujiwara N, Yoshimura M, Tsuboi T, Torii M, Oshitani N, Arakawa T & Kobayashi K. (2007). Control of cell wall assembly by a histone-like protein in mycobacteria. *Journal of Bacteriology*, **189**: 8241-8249.

92. Kelley CL, Rouse DA & Morris. (1997). Analysis of ahpC gene mutations in isoniazid-resistant clinical isolates of *Mycobacterium tuberculosis*. *Antimicrobial agents and Chemotherapy*, **41**(9): 2057-2058.

93. Knight SAB, Vilaire G, Lesuisse E & Dancis A. (2005). Iron acquisition from transferrin by *Candida albicans* depends on the reductive pathway. *Infection & Immunity*, **73**: 5482–5492.

94. Kochan I. (1976). Role of iron in the regulation of nutritional immunity. *Bioorganic Chemistry*, **2**: 55 - 57.

95. Krithika R, Uttara Marathe, Priti Saxena, Mohd. Zeeshan Ansari, Debasisa Mohanty & Gokhale RS. (2005). A genetic locus required for iron acquisition in *Mycobacterium tuberculosis*. *Proceedings of National Academy of Sciences*, **103** (7): 2069-2074.

96. Kushner S, Dalalian H, Sanjurjo JL, Bash JL, Jr Safir SR, Smith VK, Jr & Williams JH. (1952). *Journal of American Chemical Society*, **74**: 3617.

97. Kusunose M, Noda Y, Ichihara K & Kusunose E. (1976b). Superoxide dismutase from *Mycobacterium species*, strain Tokyo. *Archives in Microbiol*ogy, **108**: 65 –73.

98. Laemmli UK. 1970. Cleavage of structural proteins during the assembly of the head of bacteriophage T4. *Nature,* **227**: 680 - 685.

99. Lane SJ, Marshall PS, Upton RJ & Ratledge C (1998). Isolation and characterization of carboxymycobactins as the second extracellular siderophores in *Mycobacterium smegmatis. Biometals*, **11**: 13-20.

100. Lane SJ, Marshall PS, Upton RJ, Ratledge C, Ewing M. (1995). Novel extracellular mycobactins, the carboxymycobactins from *Mycobacterium avium*. *Tetrahedron Letters*, **36**: 4129-32.

101. Lee ASG, Teo ASM & wong SY. (2001). Novel Mutations in *ndh* in Isoniazid-Resistant *Mycobacterium tuberculosis* Isolates. *Antimicrobial Agents and Chemotherapy*, **45** (7): 2157-2159

102. Lee BH, Murugasu-Oei B & Dick T. (1998). Up-regulation of a histone-like protein in dormant *Mycobacterium smegmatis*. *Molecular General Genetics*, **260**: 475-479.

103. Lehmann KB & Neumann R. (1896). Atlas und Grundriss der Bakteriologie und Lehrbuch der speciellen bakteriologischen. Munich.

104. Lei B, Wei CJ & Tu SC. (2000). Action mechanism of anti-tubercular isoniazid: Activation by *Mycobacterium tuberculosis* KatG, Isolation, and Characterization of *inhA* inhibitor. *Journal of Biological Chemistry*, **275**: 2520–2526.

105. Lewin A, Baus D, Kamal E, Bon F, Kunisch R, Maurischat S, Adonopoulou M and Eich K. (2008). The mycobacterial DNA-binding protein 1 (MDP1) from *Mycobacterium bovis* BCG influences various growth characteristics. *BMC Microbiology*, **8**: 91.

106. Litwin CM. & Calderwood SB. (1993). Role of iron in regulation of virulence genes. *Clinical Microbiology Reviews*, **6** (2): 137 – 149.

107. Lucarelli D, Russo S, Garman E, Milano A, Meyer-Klaucke W & Pohl E. (2007). Crystal structure and function of the zinc uptake regulator FurB from *Mycobacterium tuberculosis*. *Journal Biological Chemistry*, **282**: 9914-9922.

108. Macham LP & Ratledge C. (1975). A new group of water-soluble iron-binding compounds from mycobacteria: the exochelins. *Journal of General Microbiology*, **89**: 379-82.

109. Macham LP, Stephenson MC & Ratledge C. (1977). Iron transport in *M. smegmatis*: The isolation, purification and function of Exochelin MS. *Journal of General Microbiology*, **101**: 41-49.

110. Mahairas GG, Sabo PJ, Hickey MJ, Singh DC & Stover CK. (1996). Molecular analysis of genetic differences between *M. bovis* BCG and virulent *M. bovis*. *Journal of Bacteriology*, **178**: 1274-1282.

111. Manabe YC, Saviola BJ, Sun L, Murphy JR & Bishai WR. (1999). Attenuation of virulence in *M. tuberculosis* expressing a constitutively active iron repressor. *Proceedings of National Academy of Sciences*, **96**: 12844-12848.

112. Manca C, Tsenova L, Barry III. Bergtold CEA, Freeman S, Haslett PA, Musser JM, Freedman VH & Kaplan G. (1999). *Mycobacterium tuberculosis* CDC1551 induces a more vigorous host response *in vivo* and *in vitro*, but is not more virulent than other clinical isolates. *Journal of Immunology*. **162**: 6740–6746.

113. Marahiel MA, Stachelhaus T & Mootz HD. (1997). Modular peptide synthetases involved in non-ribosomal peptide synthesis. *Chem. Rev*., **97**: 2651-2673.

114. Marcinkeviciene JA, RS Magliozzo & JS Blanchard. (1995). Purification and characterization of the *Mycobacterium smegmatis* catalase-peroxidase involved in isoniazid activation. *Journal of Biological Chemistry*, **270**: 22290–22295.

115. Marques MAM, Mahapatra S, Sarno EN, Santos S, Spencer JS, Brennan PJ, Pessolani MCV. (2001). Further biochemical characterization of *Mycobacterium leprae* laminin-binding proteins. *Braz. J. Med. Biol. Res*, **34**: 463–470.

116. Marttila HJ, Soini H, Huovinen P & Viljanen MK (1996). *katG* mutations in isoniazid-resistant *Mycobacterium tuberculosis* isolates recovered from Finnish patients. *Antimicrobial Agents and Chemotherapy*, **40**: 2187–9.

117. Master SS, Springer B, Sander P, Boettger EC, Deretic V & Timmins GS. (2002). Oxidative stress response genes in *Mycobacterium tuberculosi*s: role of *ahpC* in resistance to peroxynitrite and stage-specific survival in macrophages. *Microbiology*, **148**: 3139-3144.

118. Mayer BK & Falkinham JO, III (1986). Superoxide dismutase activity of *Mycobacterium avium*, *M. intracellulare* and *M. scrofulaceum*. *Infection & Immunity*, **53**: 631–635.

119. McIntosh MA & Earhart CF. (1977). Coordinate regulation by iron of the synthesis of phenolate compounds and three outer membrane proteins in *Escherichia coli*. *Journal of Bacteriology*, **131** (1): 331 - 9.

120. Mdluli K, Slayden RA, Zhu Y, Ramaswamy S, Pan X, Mead D, Crane DD, Musser JM & Barry CE III (1998a). Inhibition of a *Mycobacterium tuberculosis* beta-ketoacyl ACP synthase by isoniazid. *Science*, **280**: 1607 –1610.

121. Menozzi FD, Rouse JH, Alavi M, Laude-Sharp M, Muller J, Bischoff R, Brennan MJ & Locht C. (1996). Identification of a heparin-binding hemagglutinin present in mycobacteria. *Journal of Experimental Medicine*, **184**: 993-1001.

122. Meyer JM, Hohnadel D, Khan A & Cornelis P. (1990). Pyoverdin-facilitated iron uptake in *Pseudomonas aeruginosa*: immunological characterization of the ferripyoverdin receptor. *Molecular Microbiology*, **4** (8): 1401 - 5.

123. Middlebrook G & Cohn ML. (1953). Some observations on the pathogenicity of isoniazid resistant variants of tubercle bacilli. *Science*; **118**: 297–99.

124. Middlebrook G. (1952). *American Reviews on Tuberculosis*, **65**: 765-67.

125. Milano A, Forti F, Sala C, Riccardi G, Ghisotti D. (2001). Transcriptional regulation of furA and katG upon oxidative stress in *M. smegmatis. Journal of Bacteriology*, **183** (23): 6801-6806.

126. Mitchison DA. (1985). *Tubercle*, **66**: 219-26.

127. Moody DB, Young DC, Cheng TY, Rosat JP, Roura Mirc, O'Connor PB, Zajonc DM, Walz A, Miller M, Levery SB, Wilson LA, Costello CE & Brenner MB (2004). T- cell activation by lymphopeptide antigens. *Science*, **303**: 527-531.

128. Mostowy S, Tsolaki AG, Small PM & Behr MA. (2003). The *in vitro* evolution of BCG vaccines. *Vaccine*, **21**: 4270–4274

129. Nguyen M, Quemard A, Broussy S, Bernadou J & Meunier B. (2002). Mn (III) Pyrophosphate as an Efficient Tool for Studying the Mode of Action of Isoniazid on the InhA Protein of *Mycobacterium tuberculosis Antimicrobial Agents & Chemotherapy*, **46**: 2137–2144.

130. Ohara N & Yamada T. (2001). Recombinant BCG vaccines. *Vaccine.*, **19**: 4089-98.

131. Olsen AW & Andersen P. (2003). A novel TB vaccine; strategies to combat a complex pathogen. *Immunology Letters*, **85**: 207-211.

132. Osborn TW. (1983). Changes in BCG strains. *Tubercle*, **64**: 1-13.

133. Park RY, Sun HY, Choi MH, Bai YH & Shin SH. (2005). *Staphylococcus aureus* siderophore-mediated iron-acquisition system plays a dominant and essential role in the utilization of transferrin-bound iron. *Journal of Microbiology*, **43**: 183–190.

134. Pavelka Jr. MS. (2000). Genetics of mycobacterial metabolism. In: Hatfull GF, Jacobs Jr WR, editors. Molecular genetics of mycobacteria. Washington, DC: *American Society for Microbiology*, 221-34.

135. Pohl E, Holmes RK & Hol WG. (1999). Crystal structure of the Iron dependent regulator (IdeR) from *M. tuberculosis* shows both metal binding sites fully occupied. *Journal of Molecular Biology*, **285:** 1145-1156.

136. Prabhakar S, Annapurna PS, Jain NK, Dey AB, Tyagi JS & Prasad HK. (1998). Identification of an immunogenic histone-like protein (HLPMt) of *Mycobacterium tuberculosis*. *Tuber Lung Dis*, **79**: 43-53.Prabhakar S, Mishra A, Singhal A, Katoch VM, Thakral SS, Tyagi JS & Prasad HK. (2004). Use of the hupB gene encoding a histone-like protein of *Mycobacterium tuberculosis* as a target for detection and differentiation of *M. tuberculosis* and *M. bovis*. *Journal of Clinical Microbiology*, **42**: 2724-2732.

138. Pym AS, Domenech P, Honoré N, Song J, Deretic V & Cole ST. (2001). Regulation of catalase-peroxidase (KatG) expression, isoniazid sensitivity and

virulence by *furA* of *Mycobacterium tuberculosis*. *Molecular Microbiology*, **40**: 879-889.

139. Qiu X, Verlinde CLMJ, Zhang L, Schmitt MP, Holmes RK and Hol WGJ. (1995). Three-dimensional structure of the diphtheria toxin repressor in complex with divalent cation co-repressors. *Structure*, **3:** 87–100.

140. Quadri LE, Sello J, Keating TA, Weinreb PH & Walsh CT. (1998). Identification of a *M. tuberculosis* gene cluster encoding the biosynthetic enzymes for the assembly of the virulence conferring siderophores mycobactin. *Chemical Biology*, **5**: 631-645.

141. Quadri LEN, (2008). Iron uptake in mycobacteria, Pg. 167-184. In M Daffee, JM Reyrat (ed.), *The mycobacterial cell envelope*. ASM Press, Washington, DC.

142. Quemard A, Lacave C & Laneelle G. (1991). Isoniazid inhibition of mycolic acid synthesis by cell extracts of sensitive and resistant strains of *Mycobacterium aurum*. *Antimicrobial Agents & Chemotherapy*, **35:**1035 –1039.

143. Rakin A, Saken E, Harmsen D & Heesemann J. (1994). The pesticin receptor of *Yersinia enterocolitica*: a novel virulence factor with dual function. *Molecular Microbiology*, **13**: 253 – 263.

144. Ramaswamy SV, Reich R, Dou SJ, Jasperse L, Pan X, Wanger A, Quitugua T & Graviss EA. (2003). Single nucleotide polymorphisms in genes associated with isoniazid resistance in *Mycobacterium tuberculosis*. *Antimicrobial Agents & Chemotherapy*, **47**: 1241–50.

145. Ratledge C & Dover LG. (2000). Iron metabolism in pathogenic mycobacteria. *Annual Reviews in Microbiology*, **54**: 881-941.

146. Ratledge C & Ewing DF. (1978). The separation of the mycobactins from *Mycobacterium smegmatis* by using high-pressure liquid chromatography. *Journal of Biochemistry*, **175**: 853–857.

147. Ratledge C. & Ewing M. (1996). The occurrence of carboxymycobactin, the siderophore of pathogenic mycobacteria, as a second extracellular siderophore in *Mycobacterium smegmatis*. *Microbiology*, **142**: 2207–2212.

148. Ratledge C. (2004). Iron, mycobacteria and tuberculosis. *Tuberculosis* (Edinb), **84**: 110-130.

149. Ratledge, C. (1999). Iron Metabolism. In Mycobacteria: Molecular Biology and Virulence. (Ratledge, C. and Dale, J., eds). *Blackwell Science*, 260–286.

150. Redhead K, Hill T & Chart H. (1987). Interaction of lactoferrin and transferrins with the outer membrane of *Bordetella pertussis*. *Journal of General Microbiology*, **133**: 891–898.

151. Rhoades ER & Ullrich HJ. (2000). How to establish a lasting relationship with your host: lessons learned from *Mycobacterium* spp. *Immunology and Cell Biology*, **78:** 301 –310.

152. RNTCP report. TB India (2009),168.

153. Robins-Browne RM & Prpic JK. (1985). Effects of iron and desferrioxamine on infections with *Yersinia enterocolitica*. *Infection & Immunity*, **47**: 774 - 779.

154. Rodriguez GM & Smith I. (2003). Mechanisms of iron regulation in mycobacteria: role in physiology and virulence. *Molecular Microbiology*, **47**: 1485-1494.

155. Rodriguez GM & Smith I. (2006). Identification of an ABC transporter required for iron acquisition and virulence in *M. tuberculosis*. *Journal of Bacteriology*, **188**: 424-430.

156. Rodriguez GM, Voskuil MI, Gold B, Schoolnik GK & Smith I. (2002). *ideR*, An essential gene in *Mycobacterium tuberculosis*: role of IdeR in iron-dependent gene expression, iron metabolism, and oxidative stress response. *Infection & Immunity*, **70**: 3371-3381.

157. Rodriguez, G.M. (2006). Control of iron metabolism in *Mycobacterium tuberculosis*. *Trends in microbiology*, **14** (7): 320-327.

158. Rosenkrands I, Weldingh K, Jacobsen S, Hansen CV, Florio W, Gianetri I & Andersen P. (2000). Mapping and identification of *Mycobacterium tuberculosis proteins* by two-dimensional gel electrophoresis, micro sequencing and immunodetection. *Electrophoresis*, **21:** 935-48.

159. Russell DG. (2007). Who puts the tubercle in tuberculosis? *Nature Reviews on Microbiology*, **5**: 39-47.

160. Saint-Joanis B, Souchon H, Wilming M, Johnsson K, Alzar PM & Cole ST. (1999). Use of site-directed mutagenesis to probe the structure, function and isoniazid activation of the catalase / peroxidase, KatG from *Mycobacterium tuberculosis*. *Journal of Biochemistry*, **338**:753–760.

161. Sala C, Forti F, Di Florio E, Canneva F, Milano A, Riccardi G & Ghisotti D. (2003). *Mycobacterium tuberculosis* FurA autoregulates its own expression. *Journal of Bacteriology*, **185**: 5357-5362.

162. Salyers AA & Whitt DD. (1994). In Bacterial Pathogenesis: A Molecular Approach. New York: ASM Press. ISBN 1-55581-070-5.

163. Sambrook J, Fristsch EF & Maniatis T. 1989. Molecular cloning: a laboratory manual, 2nd ed. Cold Spring Harbor Laboratory, Cold Spring Harbor, NY.

164. Sassetti C & Rubin EJ. (2002). Genomic analysis of microbial virulence. *Current Opinion in Microbiology*, **5:** 27-32.

165. Schmitt MP, Predich M, Doukhan L, Smith I & Holmes RK. (1995). Characterization of an iron-dependent regulatory protein (IdeR) of *Mycobacterium tuberculosis* as a functional homolog of the diphtheria toxin repressor (DtxR) from *Corynebacterium diphtheriae*. *Infection & Immunology*, **63**: 4284-4289.

166. Schmitt MP, Talley BG and Holmes RK. (1997). Characterization of lipoprotein IRP1 from *Corynebacterium diphtheriae*, which is regulated by the diphtheria toxin repressor (DtxR) and iron. *Infection & Immunity*, **65:** 5364–5367.

167. Schryvers AB & Stojiljkovic I. (1999). Iron acquisition systems in the pathogenic Neisseria. *Molecular Microbiology*. **32**: 1117 - 1123.

168. Schwyn B & Neilland JB. (1987). Universal chemical assay for the detection and characterization determination of siderophore. *Analytical Biochemistry*, **160:** 47-56.

169. Sharman GJ, Williams DH, Ewing DF & Ratledge C. (1995 a). Isolation, purification and structure of exochelin MS, the extracellular siderophore from *Mycobacterium smegmatis*. *Journal of Biochemistry,* **1**: 187-196.

170. Sharman GJ, Williams DH, Ewing DF & Ratledge C. (1995 b). Determination of the structure of exochelin MN, the extracellular siderophore from *Mycobacterium neoaurum. Chemical Biology,* **2**: 553-561.

171. Sherman DR, Mdluli K, Hickey MJ, Barry CE & Stover CK. (1999). AhpC, oxidative stress and drug resistance in *Mycobacterium tuberculosis*. *Biofactors,* **10**: 211–7.

172. Shimoji Y, Ng V, Matsumura K, Fischetti VA & Rambukkana A. (1999). A 21-kDa surface protein of *Mycobacterium leprae* binds peripheral nerve laminin-2 and mediates Schwann cell invasion. *Proceedings of the National Academy of Sciences. USA*, **96**: 9857-9862.

173. Shoeb HA, Bowman BUJr, O olenghi AC & Merola AJ. (1985a). Peroxidase-mediated oxidation of isoniazid. *Antimicrobial Agents & Chemotherapy,* **27**: 399 –403.

174. Shoeb, HA, BU Bowman Jr, AC Ottolenghi & AJ Merola. (1985b). Evidence for the generation of active oxygen by isoniazid treatment of extracts of *Mycobacterium tuberculosis* H37Ra. *Antimicrobial Agents & Chemotherapy*, **27**: 404–407.

175. Sinha S, Arora S, Kosalai K, Namane A, Pym AS, & Cole ST. (2002). Proteome analysis of the plasma membrane of *M. tuberculosis*. *Computational Functional Genomics*, **3**: 470-483.

176. Sinha S, Kosalai K, Arora S, Namane A, Sharma P, Gaikwad AN, Brodin P & Cole ST. (2005). Immunogenic membrane-associated proteins of *Mycobacterium tuberculosis* revealed by proteomics. *Microbiology*, **151**: 2411-2419.

177. Slayden RA & Barry CE, III (2000). The genetics and biochemistry of isoniazid resistance in *Mycobacterium tuberculosis*. *Microbes & Infection*, **2**: 659 –669.

178. Snow GA. (1970). Mycobactins: iron chelating growth factors from mycobacteria. *Bacteriology Reviews*, **34**: 99-125.

179. Soares de Lima C, Zulianello L, Marques MA, Kim H, Portugal MI, Antunes SL, Menozzi FD, Ottenhoff TH, Brennan PJ & Pessolani MC. (2005). Mapping the laminin-binding and adhesive domain of the cell surface-associated Hlp / LBP protein from *Mycobacterium leprae*. *Microbes & Infection,* **2** (7): 1097-1109.

180. Sokol PA & Woods DE. (1983). Demonstration of an iron-siderophore binding protein in the outer membrane of *Pseudomonas aeruginosa*. *Infection & Immunity*, **40** (2): 665 – 669.

181. Somoskovi A, Parsons LM & Salfinger M. (2001). The molecular basis of resistance to isoniazid, rifampin, and pyrazinamide in *Mycobacterium tuberculosis. Respiratory Reviews*, **2**:164 –168.

182. Spigelman M & Gillespie S. (2006). Tuberculosis drug development pipeline: progress and hope. *Lancet,* **367**: 945-947.

183. Sreevatsan S, Pan X, Zhang Y, Deretic V & Musser JM. (1997). Analysis of the oxyR-ahpC region in isoniazid-resistant and -susceptible *Mycobacterium tuberculosis* complex organisms recovered from diseased humans and animals in diverse localities. *Antimicrobes Agents & Chemotherapy*, **41**: 600–6.

184. Sritharan M & Ratledge C. (1990). Iron regulated envelope proteins of mycobacteria grown in vitro and their occurrence in *M. avium* and *M. leprae* grown *in vivo*. *Biometals*, **2**: 203-208.

185. Sritharan M & Sritharan V (2002) Microbial pathogenesis: an in-sight into Mycobacterium tuberculosis. *Indian Journal of Medical Microbiology*, **20**: 61–68.

186. Sritharan M, Yeruva VC, Sivasailappan SC & Duggirala S. (2006). Iron enhances the susceptibility of pathogenic mycobacteria to isoniazid, an antitubercular drug. *World Journal of Microbiology and Biotechnology*, **22**: 1357-1364.

187. Sritharan M. (2000). Iron as a candidate in virulence and pathogenesis in mycobacteria and other microorganisms. *World Journal of Microbiology and Biotechnology*, **16**: 769-780.

188. Sritharan, M. & Ratledge, C. (1989). Coordinated expression of the components of iron transport (mycobactin, exochelin and envelope proteins) in *Mycobacterium neoaurum*. *FEMS Microbiology Letters*, **60**: 183±186.

189. Sriyosachati S & Cox CD. (1986). Siderophore-mediated iron acquisition from transferrin by *Pseudomonas aeruginos*a. *Infection & Immunity*. **52**: 885–891.

190. Stephenson MC & Ratledge C. (1979). Iron transport in *Mycobacterium smegmatis*: uptake of iron from ferriexochelin. *Journal of General Microbiology*, **110**: 193-202.

191. Stephenson MC & Ratledge C. (1980). Specificity of exochelins for iron transport in three species of mycobacteria. *Journal of General Microbiology*, **116**: 521-3.

192. Stoebner JA, Butterton JR, Calderwood SB & Payne SM. (1992). Identification of the vibriobactin receptor of *Vibrio cholerae*. *Journal of Bacteriology*. **174**: 3270 - 3274.

193. Stoeckle MY, Guan L, Riegler N, Weitzman I, Kreiswirth B, Kornblum J, Laraque F & Riley LW. (1993). Catalase–peroxidase gene sequences in isoniazid sensitive and resistant strains of *Mycobacterium tuberculosis* from New York City. *Jounal of Infectious Disease*, **168**: 1063–5.

194. Takayama K, Wang L & Merkal RS. (1973). Scanning electron microscopy of the H37Ra strain of *Mycobacterium tuberculosis* exposed to isoniazid. *Antimicrobial Agents & Chemotherapy*. **4**: 62–65.

195. Takayama K & Kilburn JO. (1989). Inhibition of synthesis of arabinogalactan by ethambutol in *Mycobacterium smegmatis*. *Antimicrobial Agents and Chemotherapy*, **33**: 1493 –1499.

196. Tekaia F, Gordon SV, Garnier T, Brosch R, Barrell BG & Cole ST. (1999). Analysis of the proteome of *Mycobacterium tuberculosis in silico*. *Tuberculosis Lung Disease*, **79**: 329-342.

197. Telenti A, Imboden P, Marchesi F, Lowrie D, Cole S, Colston MT, Matter L, Schopfer K & Bodmer T. (1993). Detection of rifampicin-resistance mutations in *Mycobacterium tuberculosis*. *Lancet,* **41**: 647 –650.

198. Towbin H, Staehelin T & Gordon J. (1979). Electrophoretic transfer of proteins from polyacrylamide gels to nitrocellulose sheets: procedure and some applications. *Proceedings of the National Academy of Sciences. USA*, **76:** 4350 - 4354.

199. Trias J & Benz R. (1992). Porins in the cell wall of Mycobacteria. *Science*, **258**: 1479-1481.

200. Tuberculosis Research Centre (ICMR), Chennai. (1999). Fifteen-year follow-up of trial of BCG vaccines in south India for tuberculosis prevention. *Indian Journal of Respiratory Medicine,* **110**: 56–69.

201. Van Crevel R, Ottenhoff TH & Van Der Meer JW. (2002). Innate immunity to *Mycobacterium tuberculosis*. *Clinical Microbiology Reviews*, **15**: 294-309.

202. Verbelen C, Raze D, Dewitte F, Locht C & Dufrene YF. (2007): Single-molecule force spectroscopy of mycobacterial adhesin-adhesin interactions. *Journal of Bacteriology,* **189**: 8801-8806.

203. Vergne I, Chua J, Singh SB & Deretic V. (2004). Cell biology of *Mycobacterium tuberculosis* phagosome. *Annual Reviews on Cell Division & Biology*, **20**: 367-394.

204. Via, LE, Deretic D, Ulmer RJ, Hibler NS, Huber LA & Deretic V. (1997). Arrest of mycobacterial phagosome maturation is caused by a block in vesicle fusion between stages controlled by *rab5* and *rab7*. *Journal of Biological Chemistry*, **272**:13326–13331.

205. Vordermeier HM, Chambers MA, Buddle BM, Pollock JM & Hewinson RG. (2006). Progress in the development of vaccines and diagnostic reagents to control tuberculosis in cattle. *The Veterinary Journal*, **171**: 229- 244.

206. Wagegg W & Braun V. (1981). Ferric citrate transport in *Escherichia coli* requires outer membrane receptor protein *fecA*. *Journal of Bacteriology*, **145** (1): 156 – 163.

207. Wayne LG & Diaz G.A. (1982). Serological, taxonomic, and kinetics studies of the T and M classes of mycobacterial catalase. *International Journal of Systematic Bacteriology,* **32**: 296 –304.

208. Wayne LG & Diaz G.A. (1988). Detection of a novel catalase in extracts of *Mycobacterium avium* and *Mycobacterium intracellulare*. *Infection & Immunity*, **56**: 936 –941.

209. Wayne LG & Diaz GA. (1986). A double staining method for differentiating between two classes of mycobacterial catalase in polyacrylamide electrophoresis gels. *Analytical Biochemistry*, **157**: 89–92.

210. Wheeler PR & Gregory D. (1980). Superoxide dismutase, peroxidatic activity and catalase in *Mycobacterium leprae* purified from armadillo liver. *Journal of General Microbiology*, **121**: 457 –464.

211. WHO. (2006). Global tuberculosis control: Surveillance, planning, financing. Geneva: World Health Organisation, 242.

212. Wilson TM, de Lisle GW & Collins DM. (1995). Effect of *inhA* and *katG* on isoniazid resistance and virulence of *Mycobacterium bovis*. *Molecular Microbiology*, **15**: 1009 –1015.

213. Wong DK, Gobin J, Horwitz MA & Gibson BW. (1996). Characterisation of exochelins of *M. avium*: evidence for saturated and unsaturated and for acid and ester forms. *Journal of Bacteriology*, **178**: 6394-6398.

214. Wong DK, Lee BY, Horwitz MA & Gibson BW. (1999). Identification of fur, aconitase, and other proteins expressed by *Mycobacterium tuberculosis* under conditions of low and high concentrations of iron by combined two-dimensional gel electrophoresis and mass spectrometry. *Infection & Immunity*, **67**: 327-336.

215. Woodley CL, Kilburn JO, David HL, Silcox VA. (1972). Susceptibility of mycobacteria to Rifampicin. *Antimicrobial Agents & Chemotherapy*, **2**: 245-49.

216. World Health Organisation, WHO. (1993). Tuberculosis on the increase. World Health Forum, **14**: 1-94.

217. World Health Organization (2008). Anti-tuberculosis Drug Resistance in the World. Report No. 4. Geneva: WHO/HTM/TB/ 2008, 394.

218. World Health Organization (2009). Global tuberculosis control: epidemiology, strategy, financing. Report No. 5. Geneva: WHO/HTM/TB/ 2009, 411.

219. Yeruva VC, Duggirala S, Lakshmi V, Kolarich D, Altmann F & Sritharan M. (2006). Identification and characterisation of a major cell wall associated iron regulated envelope protein (Irep-28) in *M. tuberculosis*. *Clinical Vaccine Immunology*, **13**: 1137-1142.

220. Yeruva VC, Sivagami sundaram CAS & Sritharan M. (2005). Influence of iron concentration on the expression and activity of catalases-peroxidases in mycobacteria. *Indian Journal of Biochemistry and Biophysics*, **42:** 28-33.

221. Youatt J. (1969). A Review of the action of isoniazid. *American Reviews of Respiratory Diseases*, **99**: 729-49.

222. Yu S, Fiss E & Jacobs WR Jr. (1998). Analysis of exochelin locus in *M. smegmatis*: biosynthesis genes have homology with genes of the peptide synthetic family. *Journal of Bacteriology*, **180**: 4676-4685.

223. Zahrt TC, Song J, Siple J & Deretic V. (2001). Mycobacterial FurA is a negative regulator of catalase-peroxidase gene *katG*. *Molecular Microbiology*, **39**:1174–1185.

224. Zamocky M, Regelsberger G, Jakopitsch C & Obinger C. (2001). The molecular peculiarities of catalase-peroxidases. *FEBS Lett*ers, **492**:177–182.

225. Zhang M, Gong J, Lin Y & Barnes PF. (1998). Growth of virulent and avirulent *Mycobacterium tuberculosis* strains in human macrophages. *Infection & Immunology*, **66**: 794-799.

226. Zhang Y, Garbe T & Young D. (1993). Transformation with katG restores isoniazid-sensitivity in *Mycobacterium tuberculosis* isolates resistant to a range of drug concentrations. *Molecular Microbiology*, **8**: 521 –524.

227. Zhang Y, Heym B, Allen B, Young D & Cole S. (1992). The catalase-peroxidase gene and isoniazid resistance of *Mycobacterium tuberculosis*. *Nature*, **358**: 591–593.

228. Zhang Y. & Mitchison D. (2003). The curious characteristics of pyrazinamide: a review. *International Journal of Tubercular Lung Disease*, **7**: 6 –21.

229. Zhu W, Arceneaux JEL, Beggs ML, Byers BR, Eisenach KD & Lundrigan MD. (1998). Exochelin genes from *M. smegmatis*: identification of an ABC transporter and two nonribosomal peptide synthetase genes. *Molecular microbiology*, **29**: 629-639.

LIST OF PUBLICATIONS

1. **Yeruva, V.C**, Duggirala, S, Lakshmi, V, Kolarich, D Altmann, F and Sritharan, M. (2006). Identification and characterization of a cell wall - associated iron-regulated envelope protein (Irep-28) in *Mycobacterium tuberculosis*. *Clinical and Vaccine Immunology*, **13**, 1137-1142.

2. Sritharan M, **Yeruva VC**, Sivagami Sundaram CAS & Sridevi D. (2006). Iron enhances the susceptibility of pathogenic mycobacteria to isoniazid, an anti-tubercular drug. *World journal of Microbial Biotechnology*, **22**: 1357-1364.

3. **Yeruva VC**, Sivagami Sundaram CAS and Sritharan M. (2005). Effect of iron concentration on the expression and activity of catalase-peroxidase in mycobacteria. *Indian Journal of Biochemistry and Biophysics*, **42**: 28-33.

4. Duggirala Sridevi**, Yeruva YC**, Venu K, Subhakar K & Manjula Sritharan. Immune response of peripheral blood mononuclear cells (PBMCs) of tuberculosis patients to culture filtrate proteins of *Mycobacterium tuberculosis* grown under high and low iron conditions (Manuscript under preparation).